STRUCTURAL STYLES AND SEDIMENTATION AT THE SOUTHERN TERMINATION OF THE HIKURANGI SUBDUCTION ZONE, OFFSHORE NORTH CANTERBURY, NEW ZEALAND

A thesis

submitted in partial fulfilment

of the requirements for the degree

of

Doctor of Philosophy

at the

University of Canterbury

by

PHILIP M. BARNES

University of Canterbury

1993

(maps)

ABSTRACT

In the northern region of South Island, New Zealand, a major tectonic transition occurs in the obliquely convergent Australia-Pacific plate boundary. The southern end of the Hikurangi subduction zone terminates against the Chatham Rise, a submerged continental plateau on the Pacific Plate, which is too buoyant to be subducted. Relative plate motion that is accommodated along the Hikurangi margin is transferred by a complex arrangement of faults, to a zone of transpressive, continental collision across the Southern Alps. A detailed study of offshore seismic-reflection profiles, sediment cores and bathymetry from the north Canterbury continental margin and northwestern Chatham Rise reveals the complex interactions between late Cenozoic sedimentation and tectonics at the southern termination of the Hikurangi subduction zone.

The north Canterbury shelf and the NW Chatham Rise slope are separated by major submarine canyons that link the shelf with the 3000 m-deep Hikurangi Trough. The sedimentary succession beneath the shelf and slope attains a maximum thickness of about 2 km and is inferred to be underlain by Torlesse terrane basement of Mesozoic age. The late Cenozoic stratigraphy of both regions has been established by correlating unconformity-bounded sedimentary units between seismic-reflection profiles, sampling the units in cores from exposures at the seabed, and dating the sediments by foraminifera and nannoflora biostratigraphy. Tectonic structures have been mapped from seismic profiles and the stratigraphy has been used to constrain the structural and sedimentary evolution of each area. The north Canterbury shelf and the NW Chatham slope exhibit contrasting tectonic and sedimentation styles, which reflect differences in proximity to sediment sources, bathymetry, physical oceanography, sedimentation response to global climate cycles and relative sea-level changes, and different stresses imposed on the basement rocks within the plate-boundary zone.

Late Quaternary sedimentation patterns on the NW Chatham slope and in the southern Hikurangi Trough have been studied using 3.5 kHz echo-character mapping. The slope is dominated by current-controlled sedimentary processes, whereas turbidite processes characterise the adjacent part of the southern Hikurangi Trough. On the slope north of Mernoo Saddle (a 580 m-deep depression between the South Island shelf and the Chatham Rise) a 160 x 30 km zone of current erosion occurs between 700 m and 2300 m water depths. Within this region are several northeast trending channels, 5–20 km wide and up to 105 km long, scoured obliquely down slope. These scours are inferred to have been formed by a northward flowing current of Antarctic Intermediate Water passing through the Mernoo Saddle, then braiding as it cascaded down and across the mid-slope before merging again further east into a contour current on the unstable lower slope of the northern Chatham Rise. The lower slope between and below the scours comprises a complex of coalescing sediment drifts. The adjacent Hikurangi Trough is characterised by a canyon and levee-channel system that guide turbidites from the eastern South Island margin and Cook Strait. On the trough floor is a meandering axial channel up to 10 km wide, with a left-bank dominated levee off Cook Strait where the trough widens.

Within the down-slope thickening, late Cenozoic succession on the NW Chatham slope there is a stratigraphic change in acoustic impedance that is inferred to mark a change from predominantly carbonate to terrigenous sedimentation in the Late Miocene (c. 9–10 Ma). This change might reflect an increase in uplift and erosion of the Southern Alps at this time. Analysis of 13 unconformity-bounded seismic units of Pliocene-Recent age indicates an episodic history of mid-bathyal (c. 700–2300 m) current erosion and deposition on the NW Chatham slope. Erosion began in the mid-Pliocene and was most widespread in the Late Pleistocene, when several regional-scale erosion surfaces developed. The regional extent of the older surfaces differ from the pattern of oblique-to-slope, *en echelon*, scour channels and associated sediment drifts which are related only to the five youngest depositional units (< 0.25 Ma). All erosional or non-depositional unconformities between the 13 Plio-Pleistocene seismic units resulted from major velocity changes in the northward, mid-bathyal flow over the Mernoo Saddle. Therefore, the sedimentary units and their intervening unconformities have a different origin to sea-level-controlled sequences in the Vail/ Exxon stratigraphic model. The eight youngest seismic units are Late Pleistocene and have a cyclicity of about 57–75 ka, which is similar to high-order (40 and 100 ka) glacio-eustatic sea-level cycles. The older units, deposited between Early Pliocene and Late Pleistocene, have a longer frequency of about 750 ka. The similarity of the Late Pleistocene sequence cyclicity to that of high-order glacio-eustatic cycles, together with consideration of the physical oceanography, a recent phase of reduced erosion during the Holocene, and the inferred subsidence history of the region collectively suggest that the paleoceanographic fluctuations causing the sequences are related to high-amplitude Plio-Pleistocene glacial-interglacial climatic oscillations superimposed on the late Cenozoic subsidence of Mernoo Saddle.

The north Canterbury inner-middle shelf is underlain by twelve unconformity-bounded seismic units of Late Pliocene-Early Pleistocene to Recent age. The units consist predominantly of terrigenous silty mud and thin layers of gravel, which are inferred to have been deposited in c. < 70–80 m water depth predominantly during transgressions and relative highstands of high amplitude, glacio-eustatic sea-level cycles. Erosional unconformities of middle Pleistocene to Recent age have been progressively tilted seaward as a result of contemporaneous coastal uplift and outer shelf subsidence.

The northwestern corner of the Chatham Rise has been extending by normal faulting since the Late Miocene (c. 8–6 Ma). The North Mernoo Fault Zone (NMFZ) is a 100 x 300 km extensional province that evolved contemporaneously with offshore sedimentation and with the plate-boundary zone in northern South Island. Growth faults are characteristic, but the distribution of faulting has varied temporally. The fault zone is seismically active and consists of a domino-style array of overlapping, southward dipping normal faults which are typically 2–5 km apart and trend roughly east-west at a high angle to the plate-boundary zone. Late Quaternary surface traces are widely distributed on the mid-upper continental slope but many surface scarps are poorly preserved due to extensive erosion of the seafloor. Despite the wide distribution of faulting, late Cenozoic extensional strain is < 2%. The geometry of the NMFZ is partially inherited from older basement structures. Many of the late Cenozoic faults are reactivated Late Cretaceous and Eocene normal faults which developed during periods of widespread extension of the New Zealand region, in

tectonic settings different from now. Two possible models for extension of the edge of continental Pacific Plate are considered: (1) lateral buckling of the upper continental crust across the southern termination of the Hikurangi subduction zone; and (2) flexure of the NW Chatham Rise as the region is bent downward into the southern end of the Hikurangi subduction zone.

The extensional NMFZ is one of three offshore fault systems that almost merge together over the southern end of the Hikurangi subduction zone. The western end of the NMFZ crosses submarine canyons at the southern end of the Hikurangi Trough and extends to within 20 km of two opposite-verging, NE-trending fold and thrust fault systems on the northeastern South Island continental margin. One fold and thrust system verges eastward and represents the southern part of the Hikurangi margin imbricated frontal wedge that is deforming the Marlborough continental slope above the southern part of the Hikurangi subduction zone. The other fold and thrust fault system verges northwestward and is deforming the north Canterbury shelf to the west of the NMFZ.

In addition to tilting of the north Canterbury shelf, the inner edges of the Plio-Pleistocene units have been progressively deformed since the middle Pleistocene. Gentle, asymmetric folds up to 35 km long are inferred to be developing above the propagating tips of SE-dipping thrust faults. Some structural elements of the fold and thrust system may be reactivated Late Cretaceous extensional faults. The fold and thrust region extends 20 km offshore between central Pegasus Bay and Kaikoura. The northeastern end of the zone extends to within 20 km of the extensional NMFZ, but these two fault systems are not linked kinematically. Two possible tectonic models for the north Canterbury coastal region are considered. The preferred model involves NW-SE oriented, upper-crustal shortening of much of the north Canterbury region, which is required to accommodate a component of the relative plate motion in northern South Island.

A comparison with other obliquely convergent plate boundaries and with other tectonic settings where continental extensional faulting is occurring today, suggests that the style of tectonic interactions at the southern termination of the Hikurangi subduction zone is rare in the world.

TABLE OF CONTENTS

Page

CHAPTER 8 SYNTHESIS AND CONCLUSIONS

LIST OF FIGURES

ACKNOWLEDGMENTS

This Ph.D programme was undertaken whilst I was employed on permanent staff at New Zealand Oceanographic Institute (NZOI), which is now part of the National Institute of Water and Atmospheric Research and was formerly part of DSIR. Commencement of the programme at the University of Canterbury in March 1990 became possible only after changes to the university regulations were made. These changes were brought about partly as a result of the persistent efforts of Jim Cole, Chairman of the Geology Department. Many thanks to Jim for making this thesis possible and for his willingness and flexibility to take on a student working mostly off campus. This study also would not have been possible without the financial support of NZOI management, which went through several changes during the 3.5-year course of the study. Thanks to Ron Heath, my Director/General Manager throughout the study, to former NZOI managers Janet Bradford and Dick Pickrill, and to Lionel Carter, my NZOI section leader. The study was funded by grants to NZOI from the Foundation for Research Science and Technology.

I am grateful to my supervisors, Jarg Pettinga and Keith Lewis, for their guidance throughout the study and for advice with planning, methodology, data analysis and interpretation. Their relaxed style, encouragement, and apparent faith in me (which I could never understand!) certainly helped to ease the stress that goes with any Ph.D study.

Chris Morris, the captain of R.V. *Rapuhia,* and his officers and crew assisted with operations on NZOI cruises 2019, 2022, 2030, 2034 and 2046. The data would never have been successfully acquired were it not for the expertise of the technical science staff on the cruises, who managed to keep most of the equipment up and running most of the time. Special thanks to Ed Arron for participating in all surveys and putting up with my technical incompetence. Thanks also to John Hunt, Steve Wilcox, Nicola Blackmore, John Mitchell, Ruth Baldwin, Kim Rose and Martin Burrows for their help on the cruises and with post-cruise bathymetric and navigation data reduction, photography and laboratory analyses of cores. Ruth Baldwin and I collaborated to produce and publish the 2nd edition of the Mernoo Coastal Bathymetry chart 1:200 000 (Appendix 4). It was a pleasure to have the company and local knowledge of Hugh Cowan and Andy Nicol on cruises 2034 and 2046 off the north Canterbury coast. Thanks to Keith Lewis for his advice on cruise 2034.

Many people assisted me in various ways with my interpretation of the data and in developing ideas presented in this thesis. Of course, I remain responsible for any misconceptions and errors in the interpretation. After myself, the person who probably knows the data set used in this thesis better than anyone else is Scott Nodder. Scott and I have shared a steep learning curve and had many useful discussions on most aspects of both my work and his offshore Taranaki data. Thanks also to other NZOI colleagues Lionel Carter and Ian Wright for their assistance with cruise planning, data analysis and interpretations. My understanding of late Cenozoic tectonics in north Canterbury and Marlborough developed partly from discussions and field trips with the University of Canterbury team of Hugh Cowan, Andy Nicol,

Jocelyn Campbell and Jarg Pettinga. For similar discussions on various aspects of the study I thank Dick Walcott, James Jackson, Helen Anderson, Martin Reyners, Russell Robinson, and Terry Webb. Thanks also to Sara Beanland, Alan Hull, Kelvin Berryman, Tim Little, Stuart Henrys and John Crowell who made useful suggestions regarding methods of data analysis and interpretation. Rick Herzer freely discussed his knowledge of oil industry seismic-reflection data, stratigraphy and structure off northeastern South Island. Ray Wood provided unpublished seismic refraction analyses of the NW Chatham Rise. Geoff Rait assisted with the Anomaly 18 plate tectonic reconstruction in Chapter 5. Discussions with John Bradshaw, Peter King, Mac Beggs, Bill Leask and Chris Uruski improved my understanding of Late Cretaceous and Cenozoic basin evolution in New Zealand. Len Brown provided me with an unpublished log and interpretation of the Bexley Bore in New Brighton. Tony Edwards and George Scott completed the foraminifera and nannoflora analyses of core samples. Philip Shane analysed the chemistry and mineralogy of tuffaceous horizons in NW Chatham Rise cores and also attempted to obtain a paleomagnetic stratigraphy. Phil and I collaborated to produce a joint publication manuscript discussing the composition and stratigraphy of the cores.

Many people considerably improved the rigor and conciseness of the text by their careful reviews of various chapters and publication manuscripts derived from the text. Jarg Pettinga and Keith Lewis read all sections more than once and sometimes at short notice. Thanks also to the following for their reviews: Bob Carter and Lionel Carter (chapters 3 and 4), E. Hamilton and Peter Ballance (chapter 3), G. Mountain, L. Jansa, John Damuth, Hevre Chamley and three anonymous reviewers (chapter 4), Paul Froggatt, George Scott, Norcot Hornibrook and James Kennett (chapter 4, appendix 3), Ray Wood and John Bradshaw (chapter 5), Dick Walcott, James Jackson and Russell Korsch (chapters 5, 6 and 8 (or part of 8 by RK and JJ)), Hugh Cowan (chapter 6 and part of 8) and Jocelyn Campbell (chapters 7 and 8).

The production of figures, particularly the various maps, was an arduous task. Most of the figures were drawn by Peter Bennett and Karl Majorhazi, and some in chapter 7 and 8 were drawn by Lee Leonard. Kerry Swanson and Albert Downing produced the final photographic plates. Rose-Marie Thompson kindly assisted with typing, final editing and type setting of this thesis.

Finally, but certainly not least, I thank my wife Annette, who supported and encouraged me throughout this thesis (even after having been through a thesis with me once before!).

CHAPTER 1

INTRODUCTION

1.1 BACKGROUND TO THIS STUDY

The New Zealand region straddles the convergent boundary between the Pacific and Australian plates (Fig. 1.1). The plate boundary includes by a wide zone of deformation characterised by subduction-related volcanic eruptions, active faulting, folding, frequent moderate and large earthquakes, and high rates of shear strain (e.g., Walcott, 1978, 1987). Mountain ranges are being rapidly uplifted and eroded (e.g., Wellman, 1979; Adams, 1980). A major structural transition occurs in the northern region of South Island where the two plates converge obliquely at about 42 mm/yr on an azimuth of 075° (De Mets *et al.,* 1990). The Hikurangi subduction zone terminates against the Chatham Rise, a submerged continental plateau on the Pacific Plate, that is too buoyant to be subducted (Walcott, 1978; Lewis and Pettinga, in press; Reyners and Cowan, in press). Relative plate motion accommodated by the Hikurangi subduction zone and associated deformation in the over-riding forearc, is transferred to the Southern Alps collision zone, mainly through distributed strike-slip faulting in the Marlborough fault system (Freund, 1971; Campbell, 1973, 1991; Arabasz and Robinson, 1976; Bibby, 1981; Cowan, 1990; Van Dissen and Yeats, 1991). Relative plate motion across the Southern Alps is expressed at the surface by oblique-slip thrusting on the Alpine Fault system and rapid uplift of the Southern Alps (e.g., Wellman, 1979; Norris *et al.,* 1990). The width of the deformation zone in central New Zealand is several hundred kilometres, encompassing the full width of northern South Island, including the northwestern corner of the Chatham Rise.

Two major research programmes were established in the late 1980s to increase our understanding of the tectonics of the complex structural transition zone in northern South Island. One programme is the "North Canterbury Active Tectonics Programme" at the University of Canterbury and the other is the "Active Seabed Processes Programme" within the geological section of the New Zealand Oceanographic Institute. As part of both of these research programmes, the study presented in this thesis was established with the broad aim of documenting the interactions between late Cenozoic tectonic deformation and sedimentation at the southern end of the Hikurangi subduction zone (Fig. 1.1).

Previous reconnaissance geophysical studies of the Marlborough continental margin and western Chatham Rise region (Davey, 1977; Lewis *et al.*, 1986; Herzer and Wood, 1988; Wood *et al.,* 1989) indicated that the NW Chatham Rise continental

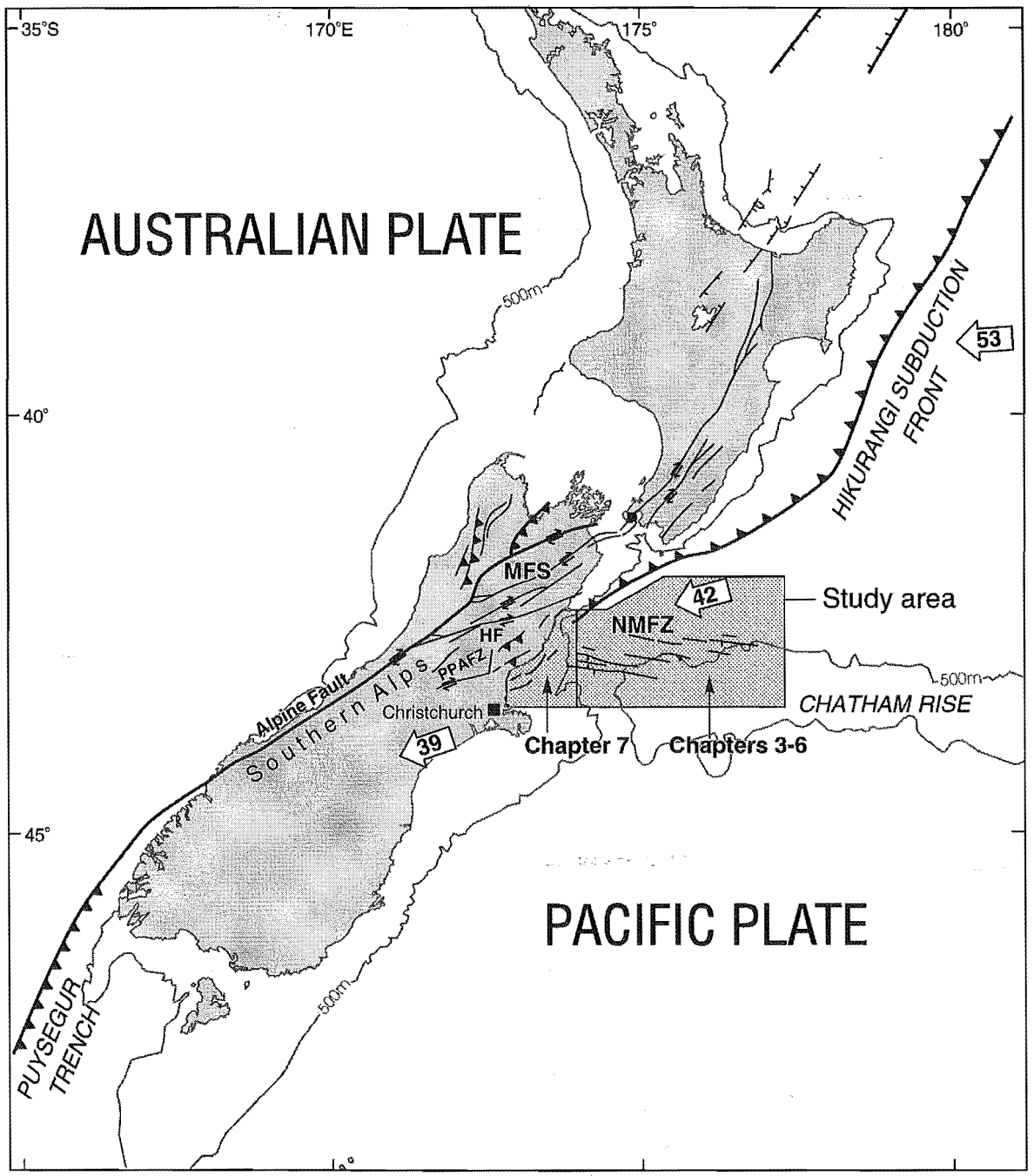

Fig. 1.1. Major structural elements of the plate boundary through New Zealand. The major features are (i) the west-facing Hikurangi subduction zone, axial strike-slip belt and back-arc extension in the North Island; (ii) the strike-slip Marlborough fault system (MFS) and transpressional Alpine Fault in the South Island; and (iii) the east-facing Puysegur subduction zone south of New Zealand. The offshore study area (shaded) lies at the southern termination of the Hikurangi subduction zone. NMFZ, North Mernoo Fault Zone; PPAFZ, Porter's Pass-Amberley Fault Zone; HF, Hope Fault. The 500 m isobath defines the continental shelf and upper slope of New Zealand and the Chatham Rise. Large arrows with numbers are the vectors, in mm/yr, of relative motion between the Pacific and Australian plates (De Mets *et al.*, 1990).

slope is characterised by widespread normal faults of late Cenozoic age. The normal faults were referred to by Lewis *et al.* (1986) as the North Mernoo Fault Zone (NMFZ) (Fig. 1.2). It was noted by previous workers that the apparent extensional style of deformation in the NMFZ contrasted with the fold and thrust-faulted and strike-slip-faulted styles of deformation onshore in northern South Island and beneath the Marlborough continental margin. Furthermore, it was noted by Davey (1977) and Lewis *et al.* (1986) that the morphology of the NW Chatham Rise slope has been significantly modified by currents or slumping. Reconnaissance structural studies of the north Canterbury continental margin indicated the presence of growing folds and possibly a deep-seated zone of NE-trending dextral shear beneath the coast and continental shelf (Carter and Carter, 1982; Carter, R.M. and Carter, 1985; Herzer and Bradshaw, 1985). Prior to the present study, however, there was insufficient data to map and analyse in detail the late Cenozoic structural styles and sedimentation on the NW Chatham Rise and north Canterbury margins. Consequently, the tectonics of the southern termination of the Hikurangi subduction zone was not well understood and the total width of the deformation zone associated with the plate boundary in northern South Island has commonly been under-estimated.

1.2 SCOPE AND OBJECTIVES OF THIS THESIS

It became apparent early in this study that in order to understand the complex structure and sedimentation at the southern end of the Hikurangi subduction zone, a substantial amount of new data was required. The new data was obtained with consideration to the following primary objectives of this study:

(1) Document and analyse the regional patterns of Quaternary sedimentation on the NW Chatham Rise slope and the adjacent part of the southern Hikurangi Trough.

(2) Establish and interpret the late Cenozoic sedimentary stratigraphy beneath the NW Chatham Rise slope.

(3) Map the structural elements of the extensional North Mernoo Fault Zone and integrate with the available historical seismicity data from the region to help constrain the kinematics of deformation.

(4) Examine the previous episodes of basement faulting that have occurred in the NW Chatham Rise region so that their influence on the style and kinematics of active deformation in the NMFZ can be resolved. At least two separate phases (Cretaceous and early Cenozoic) of normal faulting, generated in plate tectonic

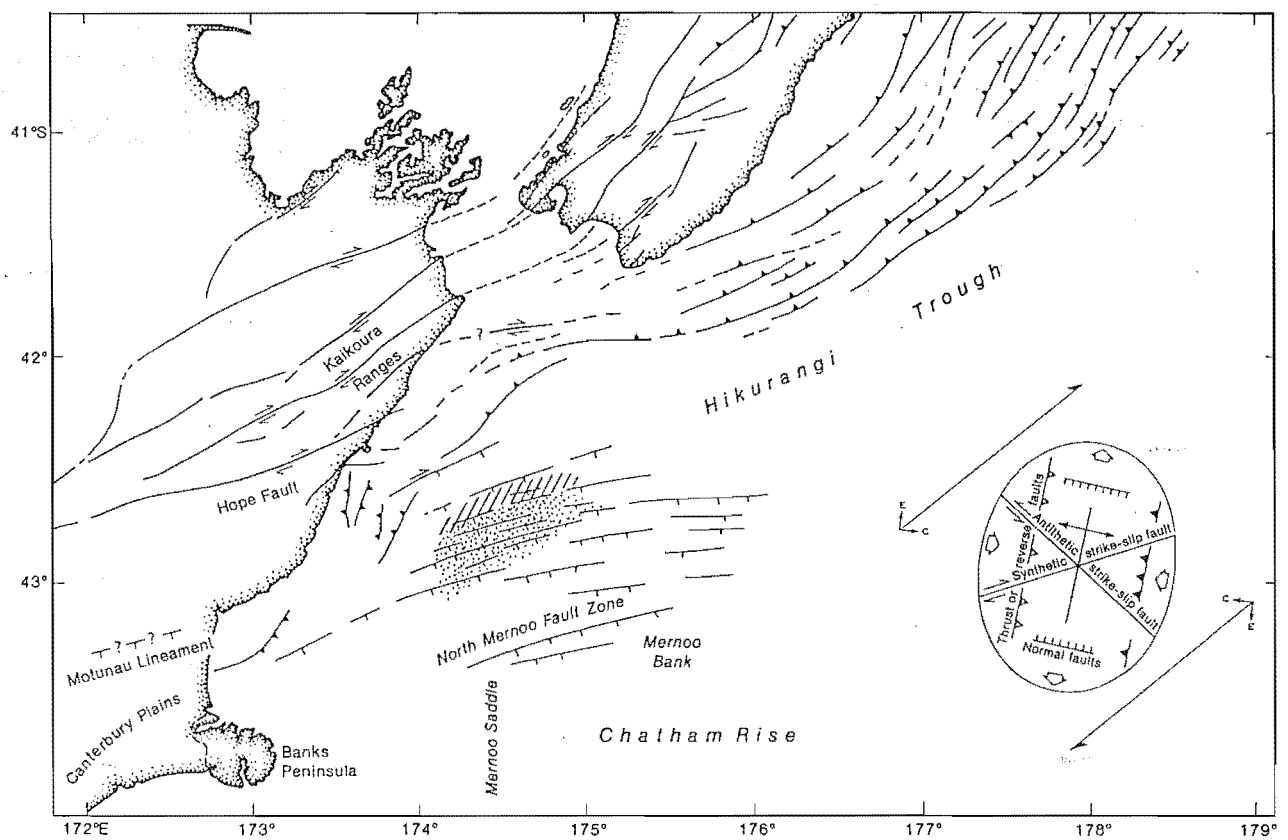

Fig. 1.2. A previous tectonic interpretation of the major structural elements in the plate boundary zone in central New Zealand (after Lewis *et al.*, 1986). Structural models by Lewis *et al.* are discussed in section. 8.3. The stippled and cross-hatched zones on the NW Chatham Rise were recognised as areas of seabed scour and sediment drift deposition respectively.

settings different from present day, were known to have occurred in the western Chatham Rise region prior to the late Cenozoic development of the NMFZ (Herzer and Wood, 1988; Wood *et al.*, 1989).

(5) Analyse the late Cenozoic tectonic evolution of the NMFZ by examing the evolving interactions between contemporaneous sedimentation and faulting. Fortuitously, it was discovered in this study of the stratigraphy that late Cenozoic fluctuations in sedimentation and erosion on the NW Chatham Rise slope generated numerous, regionally extensive stratigraphic markers and sedimentary units which have been used here to constrain the late Cenozoic history of the extensional deformation.

(6) Establish the geometric relationship between the extensional NMFZ and the tectonic provinces in north Canterbury, by mapping in detail the major structures in the sedimentary cover succession beneath the north Canterbury continental shelf and southern Marlborough continental slope.

(7) Establish a preliminary, late Cenozoic seismic stratigraphy within the deformation zone beneath the north Canterbury shelf to help constrain: (i) the timing and evolution of deformation; and (ii) the interactions between contemporaneous sedimentation and tectonic folding.

(8) To compile offshore and onshore data, and interpret the regional tectonic processes at the southern termination of the Hikurangi subduction zone.

1.3 THESIS ORGANISATION

This study was undertaken in several overlapping phases, each involving planning, data collection, analysis, interpretation and writing. This thesis has been constructed partly from a series of publication manuscripts which evolved from several phases of the study. Manuscripts which have now been published or submitted for publication have been restructured, however, in such a way as to minimise repetition between chapters. Chapter 2 describes the regional tectonic, sedimentary and physical oceanographic setting of the study area. Chapters 3 to 6 deal with sedimentary and tectonic aspects in the NW Chatham Rise region and the adjacent southern Hikurangi Trough. Chapter 3 deals with the late Quaternary sedimentation patterns; Chapter 4 presents a detailed seismic-stratigraphic analysis of the late Cenozoic sedimentary units in the NMFZ; and Chapters 5 and 6 discuss the tectonic evolution and kinematics of the extensional NMFZ. Chapter 7 presents a summary of previous work and a preliminary interpretation of the late Cenozoic stratigraphy and tectonics

of the north Canterbury continental shelf. Chapter 8 compares and contrasts the offshore and onshore data in the north Canterbury and NW Chatham Rise regions and discusses the major implications of the data to our understanding of the sedimentary and tectonic processes at the southern termination of the Hikurangi subduction zone. Chapter 8 also includes a comparison of the regional tectonics with other obliquely convergent plate boundaries and with other tectonic settings where active continental extensional faulting is occurring. Finally, recommendations for future research are made.

Although all mapping of data was carried out at a scale of 1: 200 000, various maps are presented in Chapters 3 to 7 at reduced scales appropriate for journal publication.

Chapters 3 to 7 also present a number of seismic-reflection profiles and some profiles, or parts thereof, are shown in more than one chapter to illustrate different aspects of the study. Because several of these chapters are based on discrete publication manuscripts that were prepared prior to thesis compilation, some profiles or parts of profiles used in more than one chapter have different reference numbers in different chapters. However, this should not confuse the reader because there is no cross-referencing of these figures between chapters. A complete list of the seismic profiles illustrated in each chapter are presented in Appendix 1, together with the NZOI cruise number, the dates and times when the profiles were obtained, and the working line numbers used by the author during the data analysis.

During the course of the study some work on volcanic ash deposits was undertaken jointly with Philip Shane (Victoria University of Wellington). Some of the conclusions of this joint work are referred to in the main body of the thesis. Full results of the work and appropriate responsibilities appear in Appendix 3.

1.4 DATA BASE: ACQUISITION, REDUCTION, INTERPRETATION AND STORAGE

The majority of the data utilised in this study was obtained on five research surveys undertaken by New Zealand Oceanographic Institute (NZOI), on the Department of Scientific and Industrial Research's (DSIR) survey vessel R.V. *Rapuhia*. The surveys were led by the author and were carried out between June 1988 and July 1991. The surveys are referenced as the following NZOI cruises: Cr. 2019 (June 1988), Cr. 2022 (November 1988), Cr. 2030 (September 1989), Cr. 2034 (April 1990) and Cr. 2046 (July 1991). Navigational positioning for each survey was provided by Global Positioning System and Transit Satellite data. At the time of the surveys positional

'fixes' from Global Positioning System were accurate to c. ± 100 m and Transit Satellite to ± 500 m.

1.4.1 SEISMIC-REFLECTION DATA

The above cruises obtained about 2800 km of unprocessed, single-channel airgun seismic-reflection data from within the study area (Figs 1.3 and 1.4). The profiles were shot with 20, 40 and 120 cubic-inch airguns. Incoming signals were received through SECO, Benthos and EG&G hydrophone arrays and filtered using a high-frequency bandwidth, providing high resolution of the uppermost 0.5–1.5 s two-way-travel time (TWT). The analogue data was recorded both on EPC 4600 and 4800 graphic recorders and on hi-fi VHS video tapes.

The airgun profiles are complemented with over 8000 km of newly-acquired 3.5 kHz seismic-reflection profiles obtained on the same *Rapuhia* cruises listed above (Figs 1.3 and 1.4). These profiles were acquired using a hull-mounted Ferranti ORE 16 transducer array. The incoming signals were recorded in analogue form on EPC 4600 and 4800 graphic recorders. The seismic penetration on the 3.5 kHz profiles is up to 100 ms (c. 80 m) and, depending on recorder settings, resolution is typically about 1–2 m.

In addition to the above newly-acquired seismic-reflection profiles, about 3500 km of variable quality single-channel and multi-channel airgun and watergun seismic-reflection data shot during several previous DSIR surveys on R.V. *Tangaroa*, by Glomar Challenger (Kennett and von der Borch, 1986), and by several oil companies (Northward, 1966; Davies and Ferrett, 1969; Magellan, 1969; Hunt, 1971; Mobil, 1972; Australian Gulf, 1973) were also available for this study. Approximately 1600 km of additional, mixed-quality 3.5 kHz profiles obtained by DSIR on R.V. *Tangaroa* (NZOI Cruises 1002, 1012, 1034, 1096 and 1116) were also utilised. The full set of seismic-reflection profiles have vertical exaggerations that range from about 5:1 to nearly 50:1. Limited sonobuoy refraction data obtained from the region and modelled by Dr D. Bennett (formerly of DSIR) complement the seismic-reflection profiles.

The seismic-reflection line spacings vary from < 1 to 5 km at the western end of the Chatham Rise-southern Hikurangi Trough region (the western end of the NMFZ) and increase to 10–18 km in places at the eastern end of the survey area (Fig. 1.3). The line spacings on the north Canterbury continental shelf are typically 1–4 km throughout most of the deformation zone in the coastal region, and 5–6 km in the southeastern part of the shelf, outside of the deformation zone (Fig. 1.4). The

Fig. 1.3. Seismic-reflection profiles and sonobuoy refraction locations from the NW Chatham Rise and southern Hikurangi Trough. The airgun profiles include all government research and oil company data. The details of profiles referred to and illustrated in various figures throughout this thesis are listed in Appendix 1.

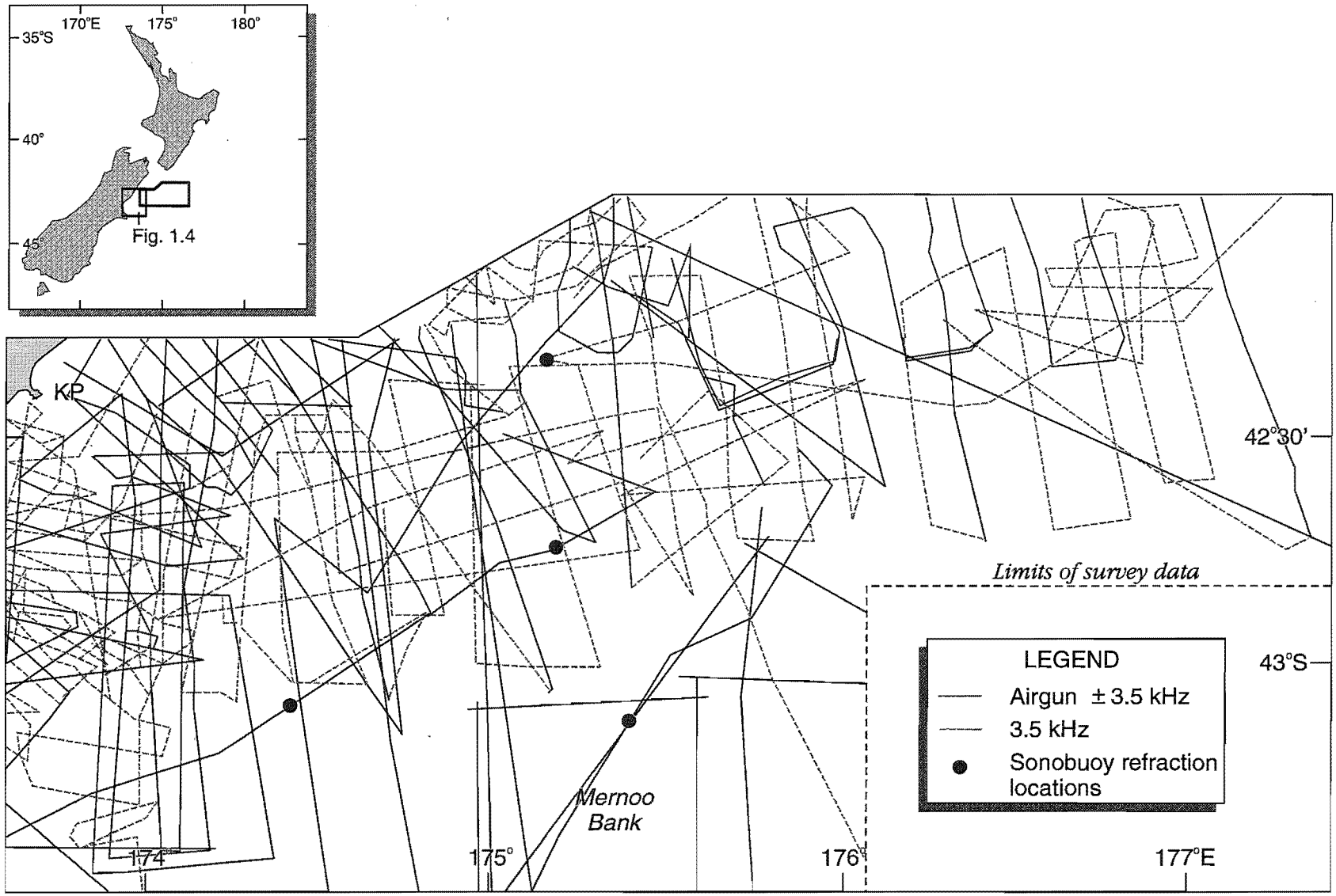
170°E
175°
180°
35°S
40°
45°
Fig. 1.4
KP
42°30'
Limits of survey data
LEGEND
Airgun ±3.5 kHz
3.5 kHz
Sonobuoy refraction locations
43°S
Mernoo Bank
174
175°
176°
177°E

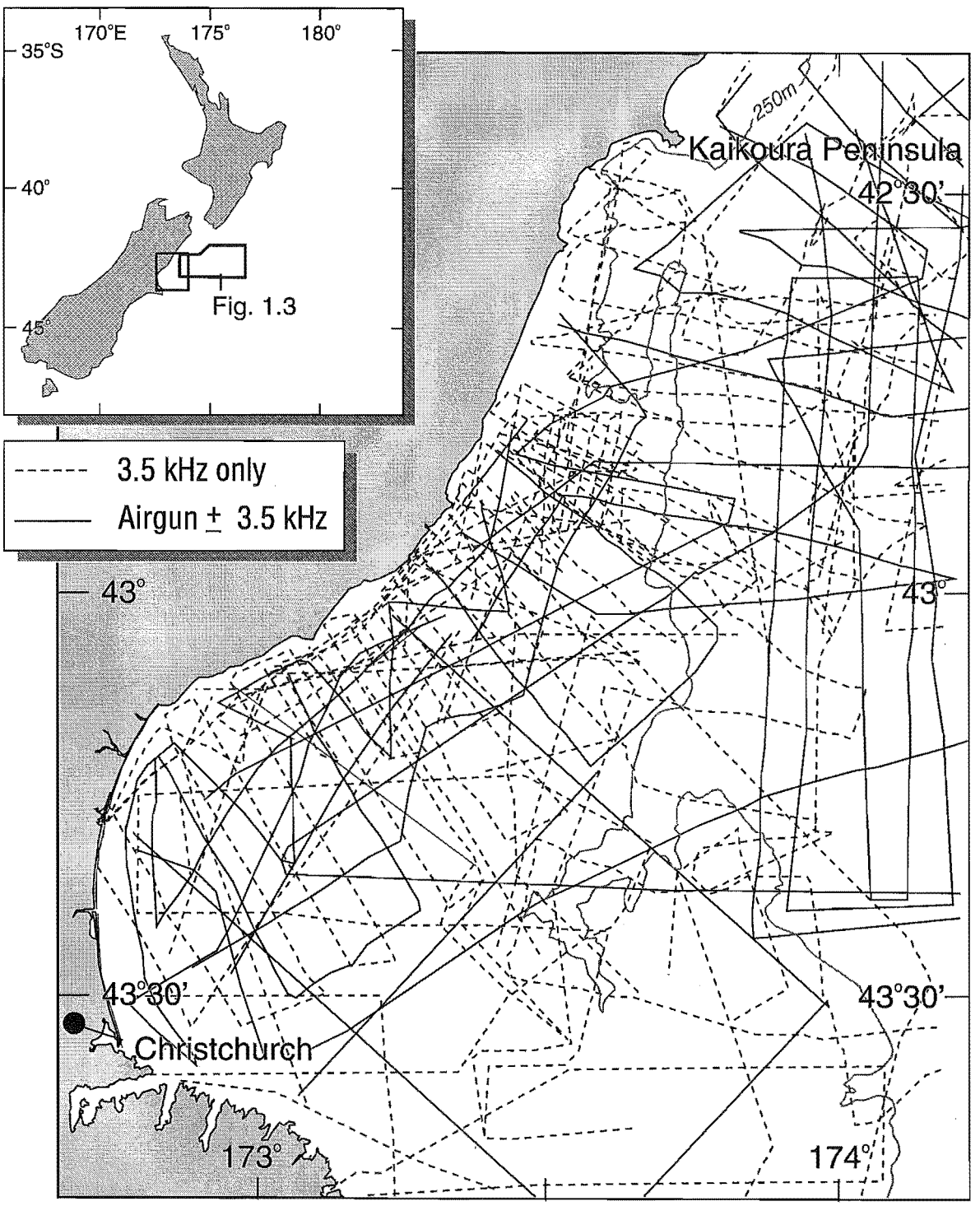

Fig. 1.4. Airgun and 3.5 kHz seismic-reflection profiles from the north Canterbury continental margin. The airgun profiles include all government research and oil company data. The details of profiles referred to and illustrated in various figures throughout this thesis are listed in Appendix 1.

seismic-reflection profiles shot during the *Rapuhia* surveys were positioned with consideration of the expected structural trends and complexity, the positions of existing seismic-reflection profiles and on-board interpretations of incoming data during the surveys. Follow-up surveys, after preliminary interpretations ashore, targeted specific areas requiring additional structural and stratigraphic data.

1.4.2 BATHYMETRIC DATA

Routine echo-soundings were recorded continuously on and between all seismic-reflection survey lines and core locations on the R.V. *Rapuhia* surveys. The 30 kHz, gyro-stabilised narrow-beam soundings were recorded on paper rolls and were automatically logged to computer. At NZOI, the depths were merged with satellite navigation data, compiled with existing depth files from previous surveys and, where necessary, sounding and seismic-reflection profiles were digitised. From the compiled set of echo-soundings a bathymetric map of the NW Chatham Rise and southern Hikurangi Trough region was constructed at a scale of 1:200 000. The full map is presented as Figure 3.1 and part of it was used to produce a revised edition of Mernoo Bathymetry 1:200 000 (NZOI Coastal Bathymetry chart series) (Barnes and Baldwin, 1993; Appendix 4). The new bathymetry provides considerably more detail than previous charts of the NW Chatham Rise region (Krause and Cullen, 1970; Herzer, 1977a). The existing Pegasus Coastal Bathymetry 1:200 000 chart of the north Canterbury margin (Herzer and Carter, 1983) is sufficiently accurate for this study.

1.4.3 SEDIMENT CORES

As part of this study, 38 piston cores, 69 mm in diameter and up to 4.5 m long, were recovered from the NW Chatham Rise continental slope and the southern part of the Hikurangi Trough using a modified Kullenberg piston corer on R.V. *Rapuhia* (Fig. 1.5). The cores were obtained from water depths ranging from 411 to 2904 m. In addition, 22 samples were recovered from the north Canterbury shelf (Fig. 1.5). A Shipek Grab sample was collected also from each site. Sampling sites were chosen after ship-board and on-shore interpretations of seismic profiles. The fortuitous outcrop of many different sedimentary sequences at the seabed on both the NW Chatham Rise slope and the north Canterbury shelf enabled sampling of sequences using conventional coring equipment. On Figure 1.5 all of the new sample locations are shown together with the locations of previously existing samples archived at NZOI. Samples discussed in the text are annotated on relevant figures throughout the thesis and specific data from these stations are presented in Appendix 2.

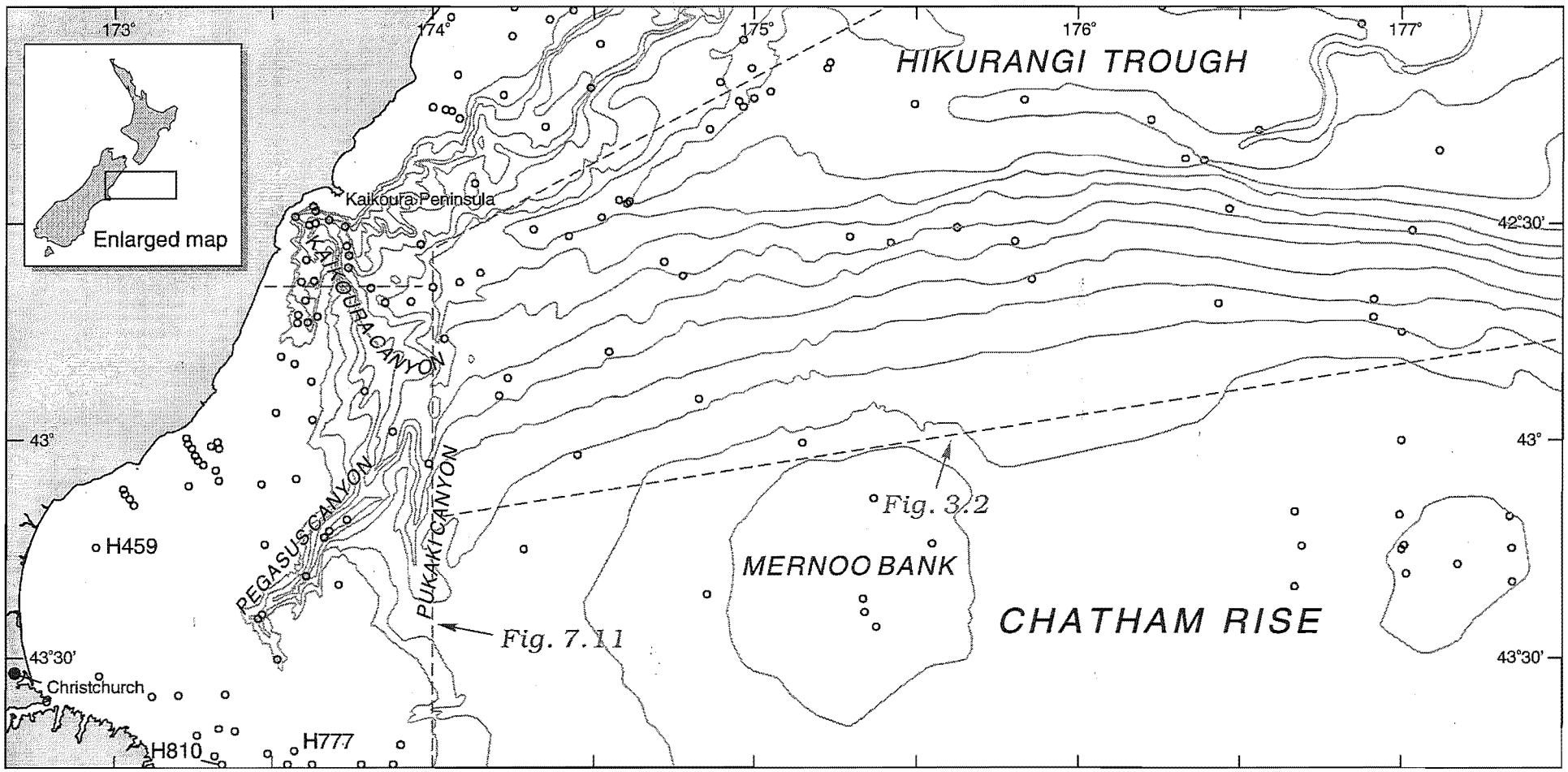

Fig. 1.5. Locations of piston cores from the southern Hikurangi Trough, NW Chatham Rise and north Canterbury margin. Analysis of some of these cores have been used to constrain the stratigraphic and structural evolution of the region. Specific cores referred to in this thesis, excluding cores H777, H459 and H810 shown here, are located on Figs 3.2, 4.7, 6.5 and 7.11. Details of the cores are listed in Appendix 2.

In the laboratory, cores were split, photographed, and described wet. One half was retained unaltered as a reference. Ten mm-thick slices of representative lithologies were X-ray radiographed for examination of fine-scale sedimentary structure. Thirty-eight samples (2–4 representative samples from each core) were taken from 15 cores from the NW Chatham Rise continental slope, together with 25 samples from 13 cores from the north Canterbury shelf, for grainsize and carbonate analyses. Grainsize was determined by the pipette method, and $CaCO_3$ by vacuum gasometric analysis. In addition, sand fractions were extracted at 100–300 mm intervals from the same 15 cores from the Chatham Rise continental slope so that microscopic tuffaceous horizons could be identified for analysis. Analytical methods and results of microprobe analyses of volcanic glass shards from the cores are presented in Appendix 3.

To determine ages of sedimentary units within the NMFZ, the foraminiferal fauna of 14 cores were analysed, together with the calcareous nannofossil flora of six cores. In addition, the calcareous nannofossil flora of 13 cores from the north Canterbury shelf were analysed. An attempt was made at Victoria University of Wellington to establish a magnetostratigraphy of the cores from within the NMFZ using a Molspin Spinner Magnetometer. However, the natural remnant magnetisation intensities of pilot samples from five cores were too low to provide reliable data after stepwise cleaning by standard alternating field methods.

1.4.4 DATA STORAGE AND RETRIEVAL

All of the original data obtained during the five *Rapuhia* cruises undertaken as part of this study are stored at NZOI, Wellington. The data can be retrieved by searching files under the relevant NZOI cruise number. Computer files contain the satellite navigation and digitised echosounding data, together with locations and brief descriptions of station operations. Various cases and cabinets house the cruise plans and reports, original seismic-reflection profiles and tapes, interpreted copies of all profiles, working copies of all map foils at 1:200 000, analogue records of echo-soundings, core logs, sediment analyses and X-ray radiographs. Both halves of each split sediment core are sealed in plastic and stored in the NZOI core store. The foraminifera microfossil data are archived on the New Zealand Fossil Record File (SE42174/f1, f3-8; SE42175/f3-6; SE42176/f2-3). Lists of nannofossil flora identified are archived on NZOI file 12/2/3. The original copies of Mobil Corporation oil company seismic-reflection profiles from the study area are also stored at NZOI, whereas all other oil company data are archived at the Institute of Geological and Nuclear Sciences, Lower Hutt.

CHAPTER 2

REGIONAL SETTING

2.1 BATHYMETRY

The Chatham Rise is a submerged continental plateau that extends eastward off central New Zealand, for over 1000 km (Figs 1.1 and 2.1). The rise crest has an average water depth of about 400 m, although locally the crest shoals to continental shelf depths at several locations including Mernoo Bank at the western end and the Chatham Islands near the eastern end. Basement rocks of Mesozoic Torlesse terrane are exposed at Mernoo Bank and correlative schists crop out at the Chatham Islands. The southern margin of the rise is bounded by the Bounty Trough, a Cretaceous failed rift and a major Plio-Pleistocene sedimentary conduit to the 4000 m-deep Bounty fan system in the southwest Pacific basin (Carter and Carter, 1988; Carter *et al.*, 1990). To the north of the rise is the Hikurangi Trough, a 3000 m-deep structural trench formed at the southern end of the Tonga-Kermadec-Hikurangi subduction system (Lewis, 1980; Lewis and Pettinga, in press). Bathymetrically, the Chatham Rise is separated from the north Canterbury continental shelf by the 580 m-deep Mernoo Saddle and by major submarine canyons that funnel sediment northward from the eastern South Island shelf to the Hikurangi Trough (Fig. 1.5; see also Fig. 4.1).

2.2 STRUCTURAL AND STRATIGRAPHIC EVOLUTION OF THE CHATHAM RISE

The Cretaceous and Cenozoic structural and stratigraphic evolution of the Chatham Rise has been discussed by several workers (Davey, 1977; Cullen, 1980; Lewis *et al.*, 1986; Herzer and Wood, 1988; Wood *et al.*, 1989). However, these studies were based on seismic lines typically c. 10–40 km apart, and they lacked the high-resolution seismic-reflection data necessary for understanding the late Cenozoic stratigraphy and tectonics in the northwestern part of the rise. The block-faulted basement was covered during the Late Cretaceous and early Cenozoic by a blanket of transgressive clastic sediments and pelagic carbonates (see Fig. 5.1). Throughout the late Cenozoic most of the rise crest comprised a tectonically stable platform starved of terrigenous sediment, with greensand and carbonate deposition punctuated by intermittent phases of erosion, phosphorite accumulation or non-deposition (Cullen, 1980). The late Cenozoic succession is thin over most of the rise crest but the succession typically thickens down the flanks of the rise (Lewis *et al.*, 1986; Herzer and Wood, 1988;

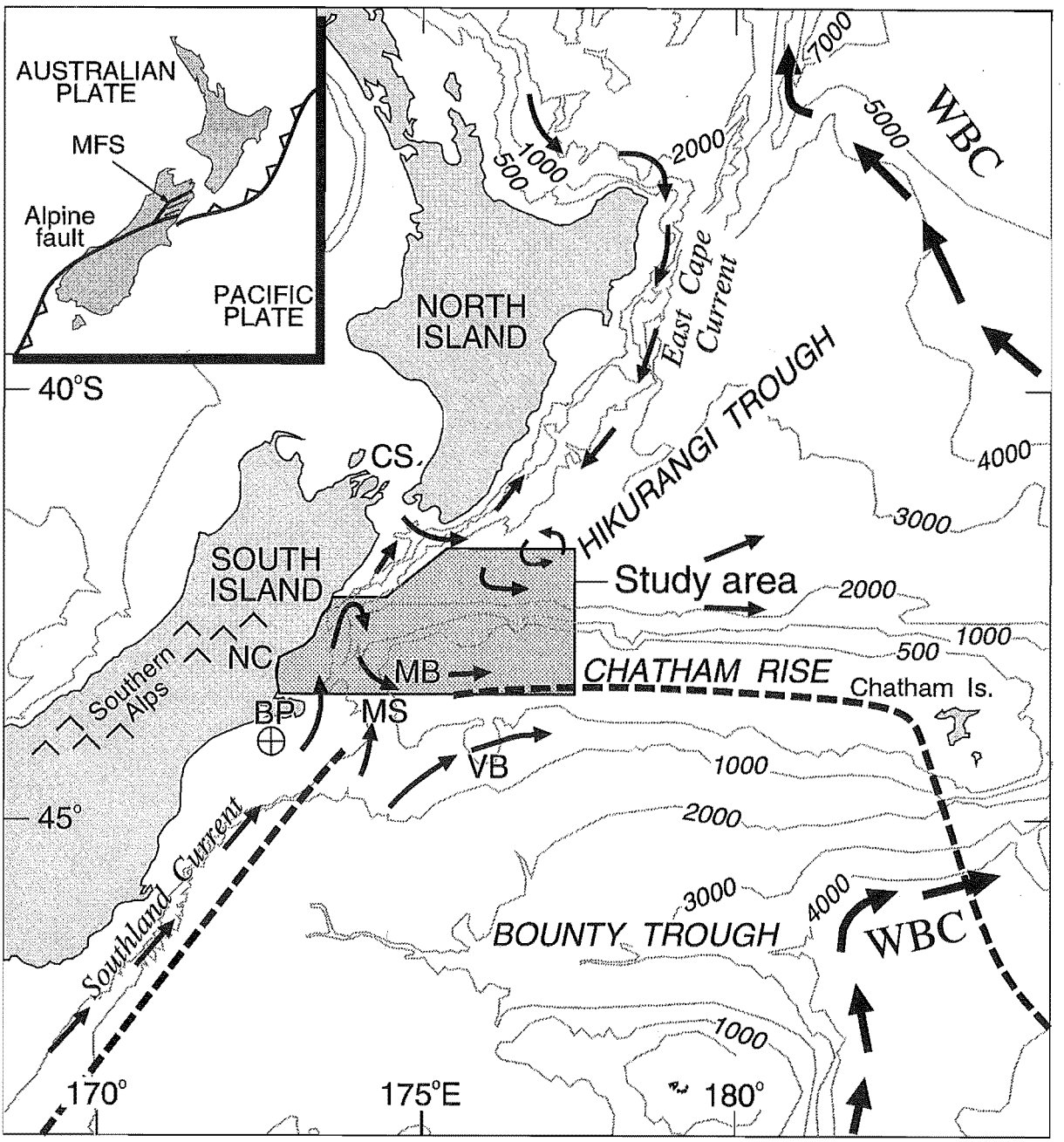

Fig. 2.1. Summary of physical oceanography and regional bathymetry east of New Zealand. Location of the investigated area is shaded. Small arrows indicate surface circulation; large arrows, deep circulation Western Boundary Current; dashed line, Subtropical Convergence Zone.(contours are in metres). MS, Mernoo Saddle; NC, North Canterbury; BP, Banks Peninsula; MB, Mernoo Bank; VB, Veryan Bank; CS, Cook Strait. Circle with cross inside, south of Banks Peninsula, is Resolution-1 well. Inset figure shows plate tectonic configuration. MFS, Marlborough fault system.

Wood *et al.*, 1989). Rapid uplift and erosion of the Southern Alps since the Late Miocene built a wide, eastward-prograding, Canterbury continental shelf and led to accumulation of terrigenous sediment on the gently dipping (1–6°) flanks of the western end of the Chatham Rise (Nelson *et al.*, 1986b; Field *et al.*, 1989; Fulthorpe and Carter, 1989; Wood and Herzer, in press). Late Cenozoic intraplate volcanic centres are widespread in the southwest Chatham Rise region, including Banks Peninsula and Veryan Banks (Fig. 2.1) (Wood *et al.*, 1989).

2.3 LATE QUATERNARY SEDIMENTATION

With the exception of relict, glacial-age sediments on the South Island continental shelf and along the crest of the Chatham Rise, the regional distribution of surface sediments reflects mainly the post-glacial sedimentation patterns (e.g., McDougall, 1982; Griggs *et al.*, 1983; Carter and Mitchell, 1987). Reconnaissance surface sediment sampling indicates a predominance of Holocene terrigenous mud over the South Island continental shelf and slope, Hikurangi Trough, Mernoo Saddle, and in a lobe on the southern flank of the rise extending as far south as 45°30'S and eastwards to 179°E (see Fig. 4.1) (McDougall, 1982). In contrast, sampling indicates a predominance of benthic carbonate sand and gravel on Mernoo Bank (Fleming and Reed, 1951; Reed and Hornibrook, 1952), authigenic greensand and planktonic carbonate sand and mud on the rise crest east of Mernoo Bank, and predominantly planktonic carbonate mud in the Bounty Trough.

2.4 PHYSICAL OCEANOGRAPHY

The crest of the Chatham Rise coincides with a major physical oceanographic feature, the Subtropical Convergence Zone, which separates the subtropical surface-water mass north of the rise from subantarctic surface water to the south (Fig. 2.1) (Heath, 1976, 1985). At Mernoo Saddle the Subtropical Convergence Zone is poorly defined and variable, depending on short-term surface circulation and intermittently upwelling, cool, Antarctic Intermediate Water flowing northward through the saddle. Subtropical water flows southward down the east coast of North Island as the East Cape Current and through Cook Strait as the D'Urville Current. In contrast, from southeastern South Island a mixture of subtropical and subantarctic water flows northeast as the Southland Current (e.g., Heath, 1972a). The boundary between the Southland Current and subantarctic water further offshore forms the Southland Front, which in this region represents the Subtropical Convergence Zone. At Mernoo Saddle this northeast-flowing current of mixed water diverges with a component flowing eastward along the Chatham Rise crest, and a branch of cool water continuing northward through the saddle to mix with subtropical water in complex eddies over the southern Hikurangi Trough (Fig. 2.1) (Heath, 1976; Barnes, 1985).

The deeper parts of Mernoo Saddle are characterised by strong tidal flows that periodically exceed 0.6 m/s (Greig and Gilmour, 1992). Superimposed on the tidal flows, there is a very slow (<0.1 m/s) net water drift, usually to the north, that entrains Antarctic Intermediate Water upwelling south of Mernoo Saddle (Heath, 1972a, 1976). In contrast to these currents a Deep Western Boundary Current enters the south Pacific Ocean well to the east of Mernoo Saddle, flowing along the > 4000 m deep edge of the New Zealand continental plateau, across the mouth of the Bounty Trough and around the end of the Chatham Rise (e.g., Carter and Mitchell, 1987).

2.5 REGIONAL TECTONICS OF THE HIKURANGI MARGIN-TO-ALPINE FAULT TRANSITION

Beneath North Island and northeastern South Island the subducted oceanic Pacific Plate is well defined by seismicity data (Reyners 1983, 1989; Robinson, 1986, 1991). In this region the Pacific Plate crust appears to be anomalously thick (c. 15 km thick beneath Cook Strait; Robinson, 1986) and, hence, buoyant, resulting in an anomalously shallow-dipping and seismically active slab in contrast to the more typical oceanic crust subducted north of New Zealand (Davy, 1992). This thicker oceanic crust appears to dip also beneath the northern margin of the continental Chatham Rise, reflecting not late Cenozoic subduction along the Australia-Pacific plate boundary, but presently-inactive, Mesozoic-age subduction at the edge of Gondwana prior to its breakup and isolation of the New Zealand continental block in the Cretaceous (Davy, 1992).

The NMFZ represents a very large region on the northwestern corner of the Chatham Rise plateau that has been undergoing continental extension during the late Cenozoic (see Fig. 1.1). Prominent fault scarps on the seabed and scattered, instrumentally-recorded shallow earthquakes attest to the continuing deformation. The position of the fault zone on the edge of the Pacific Plate and at the southern end of the Hikurangi subduction zone, appears to be related, somehow, to the transfer of relative plate motion from the subduction zone to the transpressive Alpine Fault system in the South Island. The crust at the western end of the Chatham Rise is inferred to be about 27 km thick (Reyners and Cowan, in press). Herzer and Wood (1988) and Wood *et al.* (1989) mapped with reconnaissance seismic-reflection data, numerous west-east trending fault-bounded sedimentary basins of Late Cretaceous age beneath the Chatham Rise, including Mernoo Bank and the northwestern upper continental slope. They inferred that some of the faults were reactivated as normal faults in the early Cenozoic. Furthermore, they noted the occurrence of late Quaternary faults in the NMFZ, but did not have the data to map and analyse the late Cenozoic deformation. It is shown in Chapters 5 and 6 of this thesis that NMFZ has a west-

east structural grain and extends for about 100 km down slope from Mernoo Bank. The fault zone extends along slope about 300 km from the head of the Hikurangi Trough, 60 km off the northeastern South Island coast, to at least 177°30'E (see Figs 1.1 and 6.5).

The Marlborough continental slope forms the northwestern flank of the southern Hikurangi Trough. Beneath the slope are thrust faults that represent the southern end of the imbricated frontal wedge which has developed above the leading edge of the Hikurangi subduction zone (Lewis, 1980; Lewis *et al.*, 1986; Davey *et al.*, 1986; Lewis and Pettinga, in press). The frontal wedge in the Marlborough region is considered by Lewis and Pettinga (in press) to comprise a deformed sequence of prograded shelf-slope strata, with minimal frontally-accreted trench fill. The north-easterly-trending thrust-fault deformation front lies at the base of the Marlborough slope and its southern extent appears to be close to the northwestern corner of the extensional NMFZ (Figs 1.1 and 1.2).

Onshore, between the Alpine Fault and the southern Hikurangi subduction system, a large component of the total relative plate motion is accommodated by the Marlborough fault system. The Marlborough fault system consists of several northeasterly-trending, active right-lateral strike-slip faults, typically 5–20 km apart and > 200 km in length (Fig. 1.1). Presently, the most active element is the Hope Fault in the southern part of the system, where Late Pleistocene horizontal slip rates range typically from 15 to 30 mm/yr (e.g., Cowan, 1990; Van Dissen and Yeats, 1991; Knuepfer, 1992). The northeastern end of the Marlborough fault system appears to merge with the imbricate frontal wedge beneath the Marlborough slope. Although the detailed geological structure and fault kinematics off the Marlborough coast have yet to be resolved, the strike-slip faults appear to terminate in coastal and offshore, seaward-verging thrust faults and folds, which in places form prominent, slope-parallel bathymetric ridges and troughs (Lewis and Pettinga, in press; author's unpublished data).

South of the Hope Fault and west of the NMFZ, in north Canterbury, deformation is dominated by thrust faulting and folding of the basement and its sedimentary cover (Nicol, 1991). In places there are two orthogonal sets of contemporary faults; one west-east-trending set includes reactivated Cretaceous normal faults. The southeastern margin of the plate-boundary zone onshore is the Porter's Pass-Amberley Fault Zone (Cowan, 1992), which extends northeast from Porters Pass in the eastern Southern Alps, across the north Canterbury range front to the coastal hills north of Christchurch City (Fig. 1.1). Early workers interpreted this range front as an evolving strike-slip fault system (Carter and Carter, 1982; Herzer and Bradshaw, 1985) and recent field mapping indicates a complex transition from strike-slip faulting

in the Porters Pass region to thrust faulting nearer the coast (Cowan, 1992). Prior to this thesis study, there was limited seismic-reflection data available from the north Canterbury shelf and to date there has not been agreement as to the geological structure and tectonics in that area (Carter and Carter, 1982; Carter, R.M. and Carter, 1985; Herzer and Bradshaw, 1985). Previous interpretations of the structure beneath the shelf are outlined in Chapter 7, together with a new interpretation of the late Cenozoic tectonics and stratigraphy based on analysis of a substantial amount of new seismic-reflection data.

The above review of regional data suggests that late Cenozoic sedimentation on the north Canterbury margin and NW Chatham Rise is likely to reflect, among other things, the paleoceanography, bathymetry and proximity to sediment sources. The tectonics and sediment-tectonic interactions in the region are likely to be complex and varied, in response to the transition from oceanic subduction to continental collision.

CHAPTER 3

LATE QUATERNARY SEDIMENTATION PATTERNS: NORTHWESTERN CHATHAM RISE AND SOUTHERN HIKURANGI TROUGH

3.1 INTRODUCTION

The use of high frequency (3.5 and 12 kHz) echo characteristics for the study of deep-sea sedimentary processes is well established (e.g., see review by Damuth, 1980). Echo-character mapping of large areas of the ocean floor may be combined with additional data such as cores, bottom photographs and nephelometer records to enable distinction between down-slope mass wasting processes (turbidity currents, slumps and debris flows) and strong, deep circulation thermohaline flows such as Western Boundary Undercurrents (Heezen and Johnson, 1969; Damuth, 1975; Damuth and Kumar, 1975; Damuth and Hayes, 1977; Johnson and Damuth, 1979; Kolla *et al.*, 1980; Klaus and Ledbetter, 1988; Pratson and Laine, 1989; among others). The methodology is most appropriate for studying erosional and depositional processes of late Quaternary age.

In this study 3.5 kHz echo-character mapping has been utilised to examine the late Quaternary sedimentary processes on the NW Chatham Rise continental slope, and in the adjacent part of the southern Hikurangi Trough. The Hikurangi Trough has been identified as a significant sink for vast quantities of terrigenous sediment derived from mountains in the South Island (e.g., Katz, 1974; Lewis, 1980; Carter *et al.*, 1982); however, the acoustic characteristics and geomorphology of this major dispersal system had never been mapped prior to this study. Similarly, although several tentative seismic-stratigraphic interpretations have been made on the NW Chatham Rise slope using widely spaced airgun profiles (Davey, 1977; Lewis *et al.*, 1986; Wood *et al.*, 1989), these studies lacked sufficient high-frequency seismic data for echo-character mapping of the late Quaternary sedimentary processes. Irregular seabed morphology seen in reconnaissance airgun profiles of the slope was first thought by Davey (1977) to be the product of large-scale slumping but was later interpreted by Lewis *et al.* (1986) to have formed by some type of mid-bathyal current erosion, perhaps related to flow through Mernoo Saddle. Thus, the late Quaternary sedimentation patterns in the region are likely to reflect both the proximity to the plate-boundary zone, and the physical oceanography pertaining to the region.

3.2 BATHYMETRY

A new interpretation of the bathymetry is presented here for the area extending from Mernoo Bank on the crest of the Chatham Rise, to the Hikurangi Channel on the floor of the Hikurangi Trough (Fig. 3.1). Mernoo Bank is a prominent bathymetric high including a large region at continental shelf depths (< 150 m), and with a minimum water depth of 49 m. On the upper northern slope there are several smaller, isolated bathymetric highs where probable volcanic rocks crop out (Fig. 3.1). Deeper than the 700 m isobath, the slope descends to the Hikurangi Trough at a gentle average gradient of about 2°. The most surprising feature of the new contours is that on the mid slope between 700 m and 2300 m, there are several broad *en echelon* channels up to 20 km wide and with up to 100 m relief, that are oriented northeast, obliquely down slope. East of 175°E the lower slope below 1500 m is steeper (4–5°) and exhibits irregular microtopography. Beyond the toe of the slope the axis of the Hikurangi Channel descends from 2500 m deep in the west to 3100 m deep in the east of the investigated area (Fig. 3.1). The channel floor (between the dashed lines on Fig. 3.2) is 4–5 km wide between the Chatham Rise and South Island slopes, up to 10 km wide at its confluence with Cook Strait Canyon, and then narrows to 1–3 km wide in the east of the mapped region where it begins to meander and deepens so that it lies up to 250 m below its levees.

3.3 ECHO-CHARACTER, MICROBATHYMETRY AND SEDIMENTARY PROCESSES

A 3.5 kHz echo-character map was constructed following the general guidelines of Damuth (1980) (Fig. 3.2). Airgun profiles were not used for echo-character mapping, although they provide additional information for interpreting the late Quaternary sedimentary processes. Thirteen echo types were classified on the basis of the acoustic character of the seafloor including echo distinction, seismic penetration and subbottom reflection characteristics, and both the microtopography and medium-scale morphology of the seafloor (Fig. 3.2). They are essentially acoustic facies, and are illustrated in Figures 3.3 to 3.5. The classification scheme includes echo types similar to those reported elsewhere on continental slopes and basin floors (e.g., Damuth, 1975; Pratson and Laine, 1989); however, it has been tailored specifically for this region. For simplicity of description the echo types have been grouped into three broad classes based on seafloor morphology: these are (I) irregular echoes, (II) smooth echoes, and (III) wavy echoes.

The lithological characteristics of sediment cores are shown in Figures 3.6 to 3.8. The cores typically consist of unconsolidated to well compacted, greyish olive to

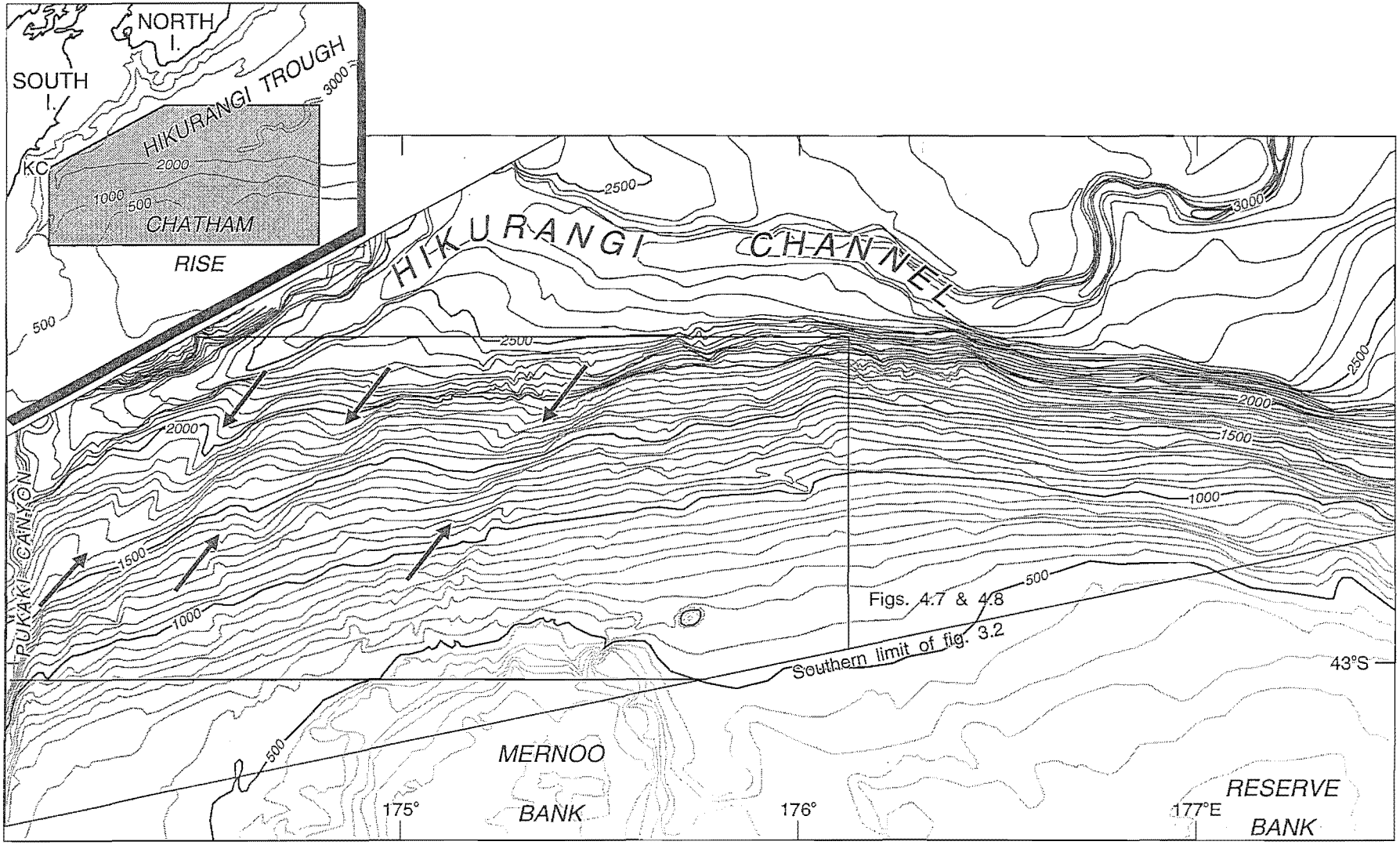

Fig. 3.1. Bathymetry of the NW Chatham Rise and southern Hikurangi Trough. Arrows indicate positions of oblique-to-slope scoured depressions. KC, Kaikoura Canyon (top left).

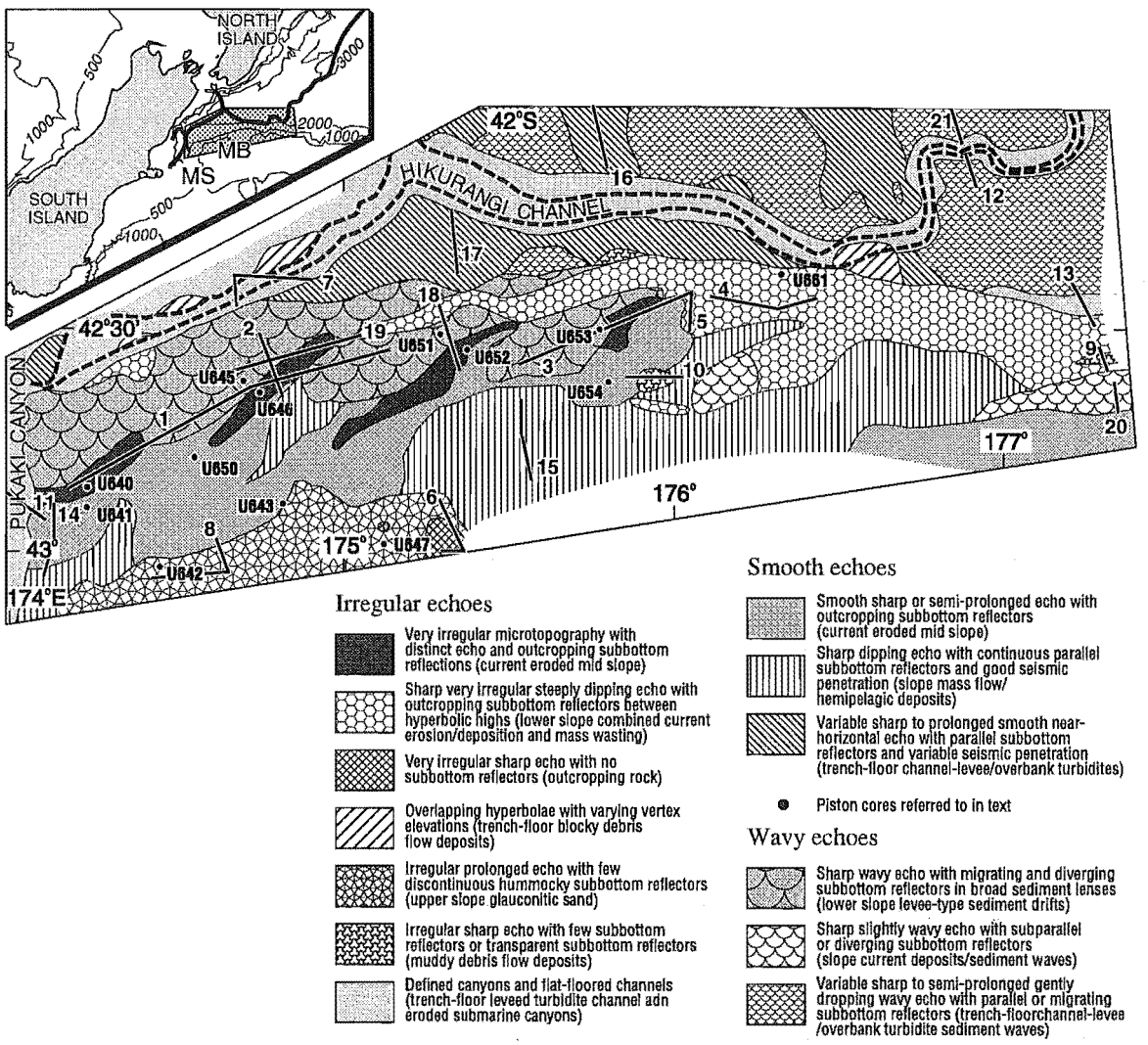

Fig. 3.2. 3.5 kHz echo-character map of the NW Chatham Rise slope and the adjacent southern Hikurangi Trough. Solid lines with numbers are seismic profiles illustrated in Figs 3.3 to 3.5. Legend includes echo-type interpretation in brackets. MS, Mernoo Saddle; MB, Mernoo Bank.

Fig. 3.3. Examples of class I irregular 3.5 kHz echo types (continued on following page). Profile positions and echo type distribution are shown on Fig. 3.2. **A.** Along-slope profile of type IA very irregular microtopography with distinct echo and outcropping subbottom reflectors, merging into type IIIA (see Figs 3.5A and B); faults arrowed. **B.** Down-slope profile 2 of types IA and IIIA echo types. **C.** Oblique-to-slope profile of type IA, along with IIIA, IIA (Fig. 3.4A) and IB. **D.** Along-slope profile 4 of type IB sharp, very irregular, steeply dipping echo with outcropping subbottom reflectors between hyperbolic highs. **E.** Down-slope profile 5 of type IB. **F.** Profile 6 of type IC very irregular, sharp echo with no subbottom reflectors. **G.** Profile 7 of type ID overlapping hyperbolae with varying vertex elevations, along with type IG. **H.** Along-slope and down-slope profile 8 of type IE irregular, prolonged echo with few discontinuous hummocky subbottom reflectors. **I.** Down-slope profile 9 of type IF irregular, sharp echo with few subbottom reflectors or transparent subbottom. **J.** Along-slope profile 10 of type IF along with type IIA (see Fig. 3.4A). **K.** Profile 11 of type IG defined canyons (Pukaki C). **L.** Profile 12 of type IG, flat-floored channels (Hikurangi C), along with type IIIC (see Fig. 3.5D). **M.** Profile 13 of type IG.

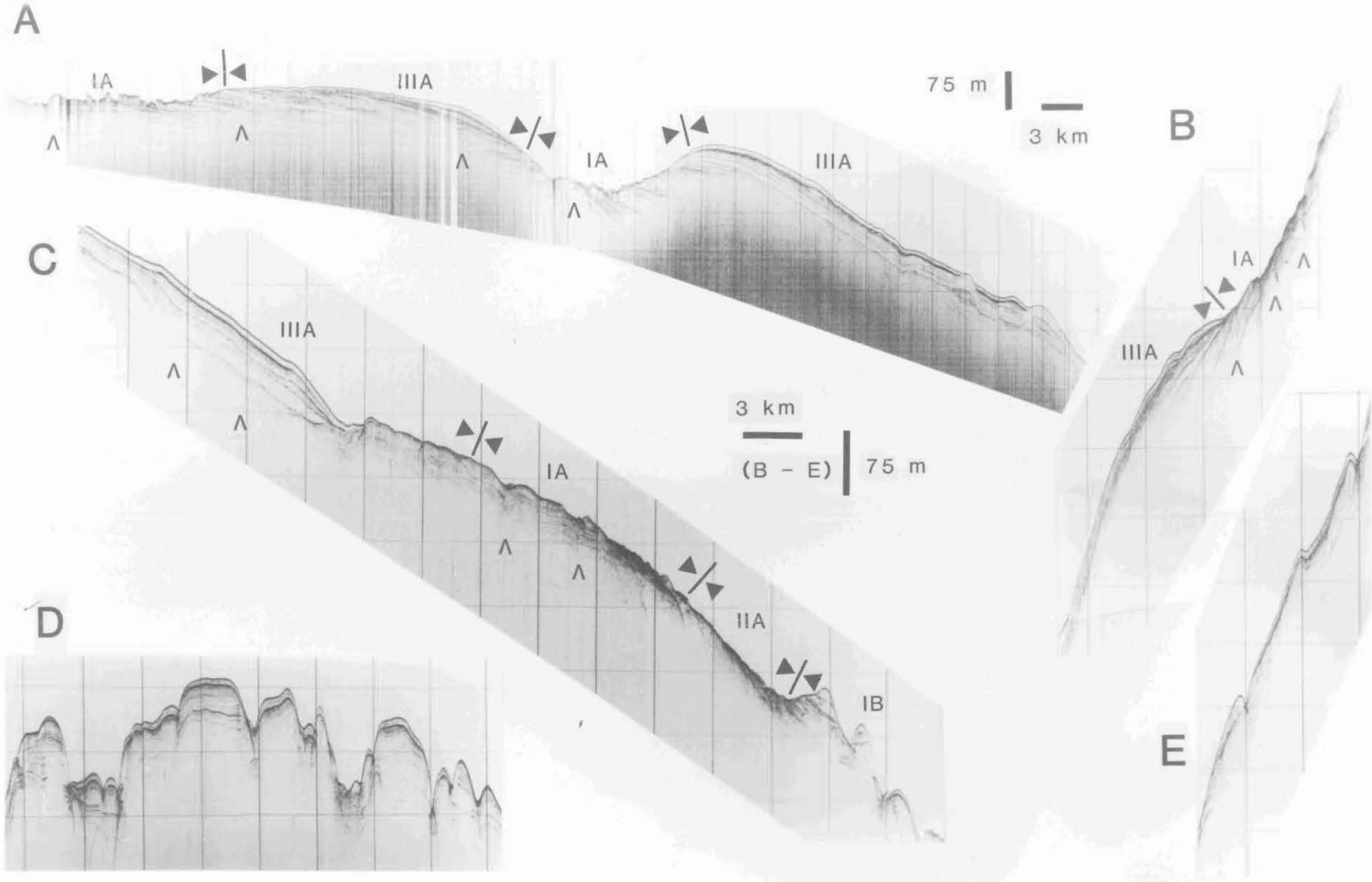
A
IA
IIIA
IA
IIIA
75 m
3 km
B
C
IIIA
IA
IIIA
3 km
(B - E)
75 m
IA
IIA
IB
D
E

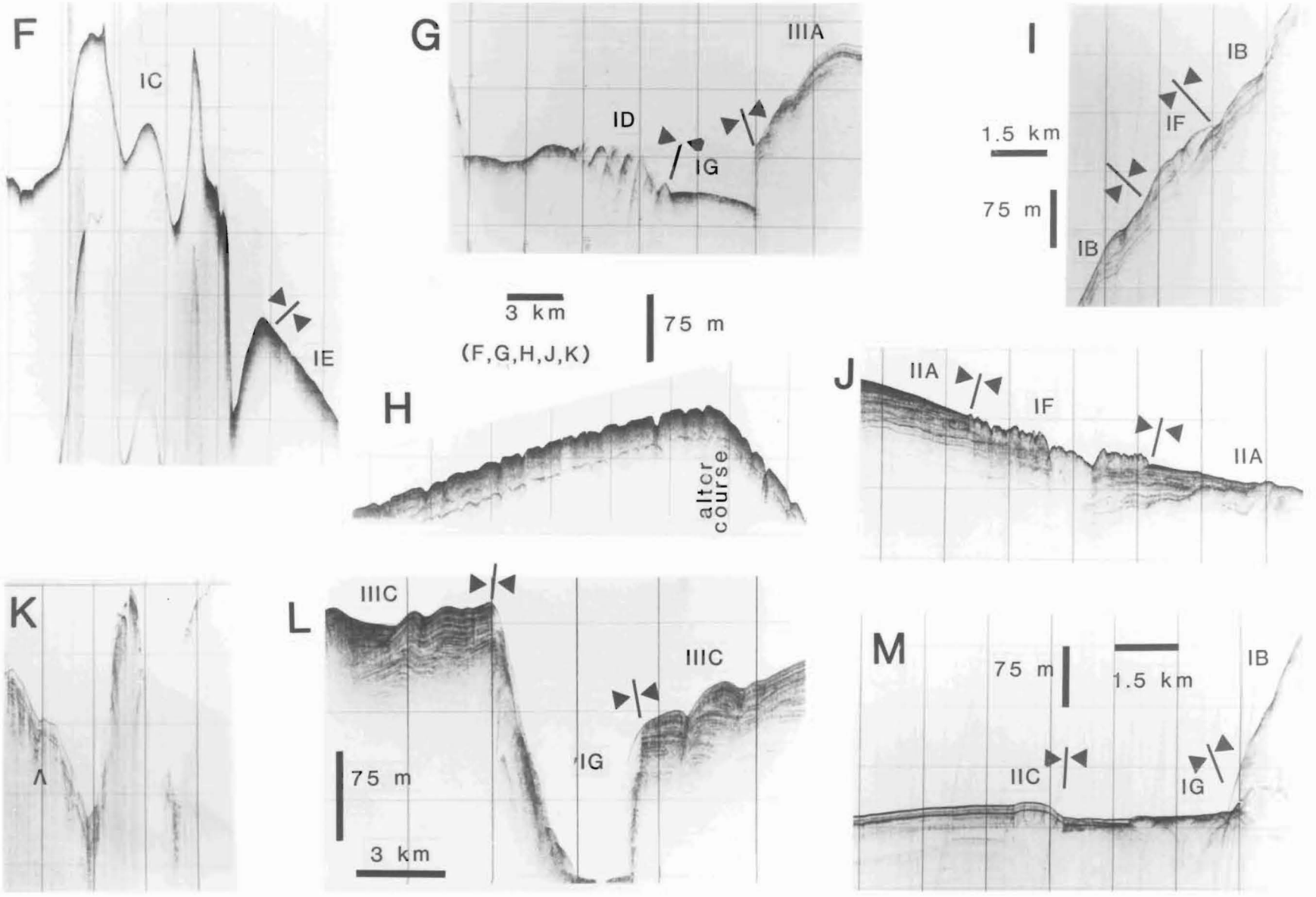
F
IC
IE
G
IIIA
ID
IG
I
IB
1.5 km
75 m
IF
IB
3 km
(F,G,H,J,K)
75 m
H
alter course
J
IIA
IF
IIA
K
L
IIIC
IIIC
IG
75 m
3 km
M
75 m
1.5 km
IB
IIC
IG

Fig. 3.4. Examples of class II smooth 3.5 kHz echo types in down-slope profiles. Profile positions and echo type distribution are shown on Fig. 3.2. **A.** Profile 14 of type IIA smooth, sharp or semi-prolonged echo with outcropping subbottom reflectors. Faults arrowed. **B.** Profile 15 of type IIB sharp, dipping echo with continuous parallel subbottom reflectors and good seismic penetration. **C.** Profile 17 of type IIC sharp, smooth near-horizontal echo with parallel subbottom reflectors. **D.** Profile 16 of type IIC prolonged, smooth near-horizontal echo with few discontinuous parallel subbottom reflectors.

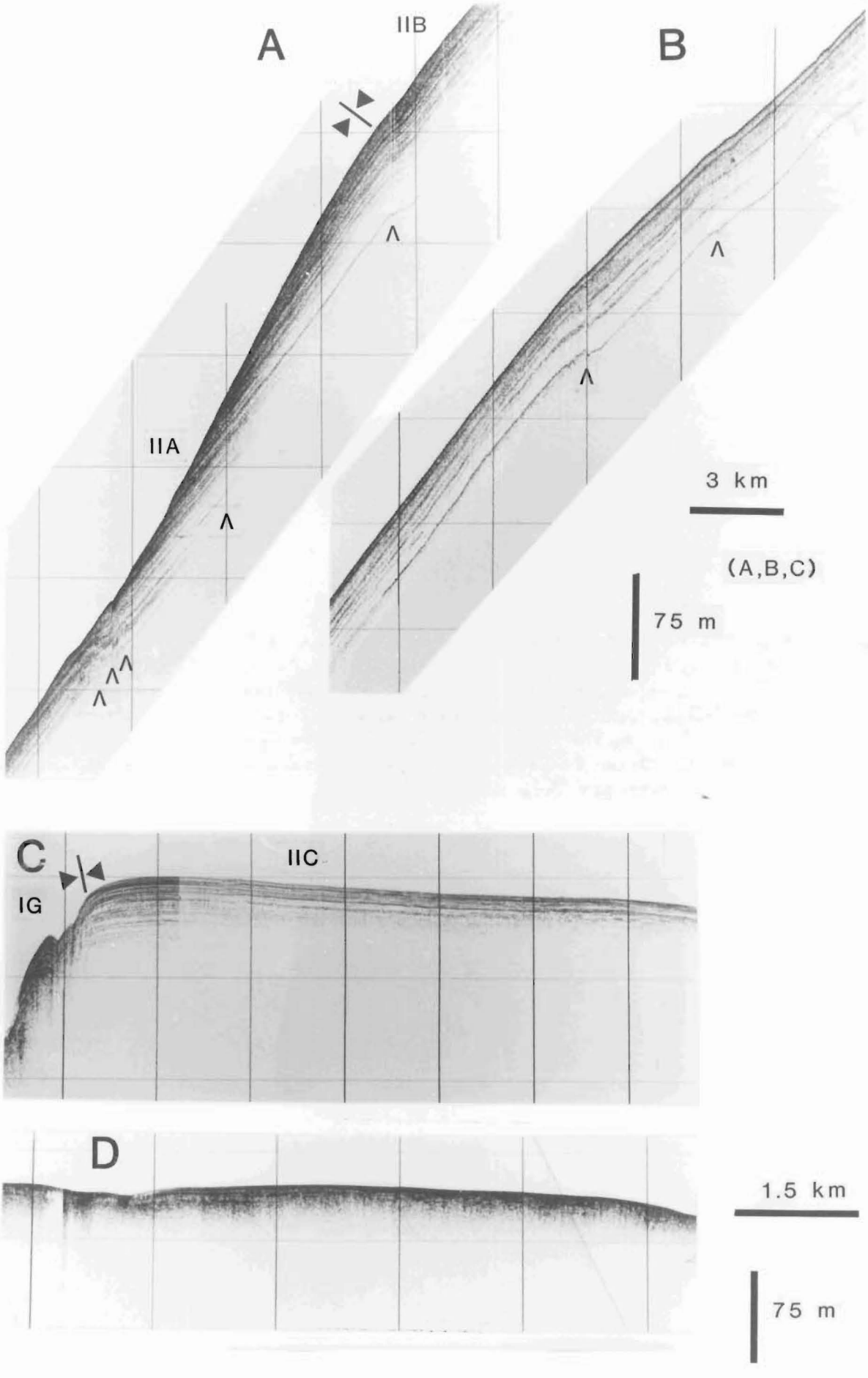
A
IIB
IIA
B
3 km
(A,B,C)
75 m
C
IG
IIC
D
1.5 km
75 m

Fig. 3.5. Examples of class III wavy 3.5 kHz echo types. Profile positions and echo type distribution are shown on Fig. 3.2. **A.** Down-slope profile 18 of type IIIA sharp wavy echo with migrating and diverging subbottom reflectors in broad sediment lenses, along with type IA. Faults arrowed. **B.** Along-slope profile 19 of type IIIA, along with type IA. Dashed reflector is a buried erosion surface. **C.** Down-slope profile 20 of type IIIB sharp slightly wavy echo with subparallel or diverging subbottom reflectors. **D.** Down-slope profile 21 of type IIIC variable sharp to semi-prolonged gently dipping wavy echo with parallel or migrating subbottom reflectors.

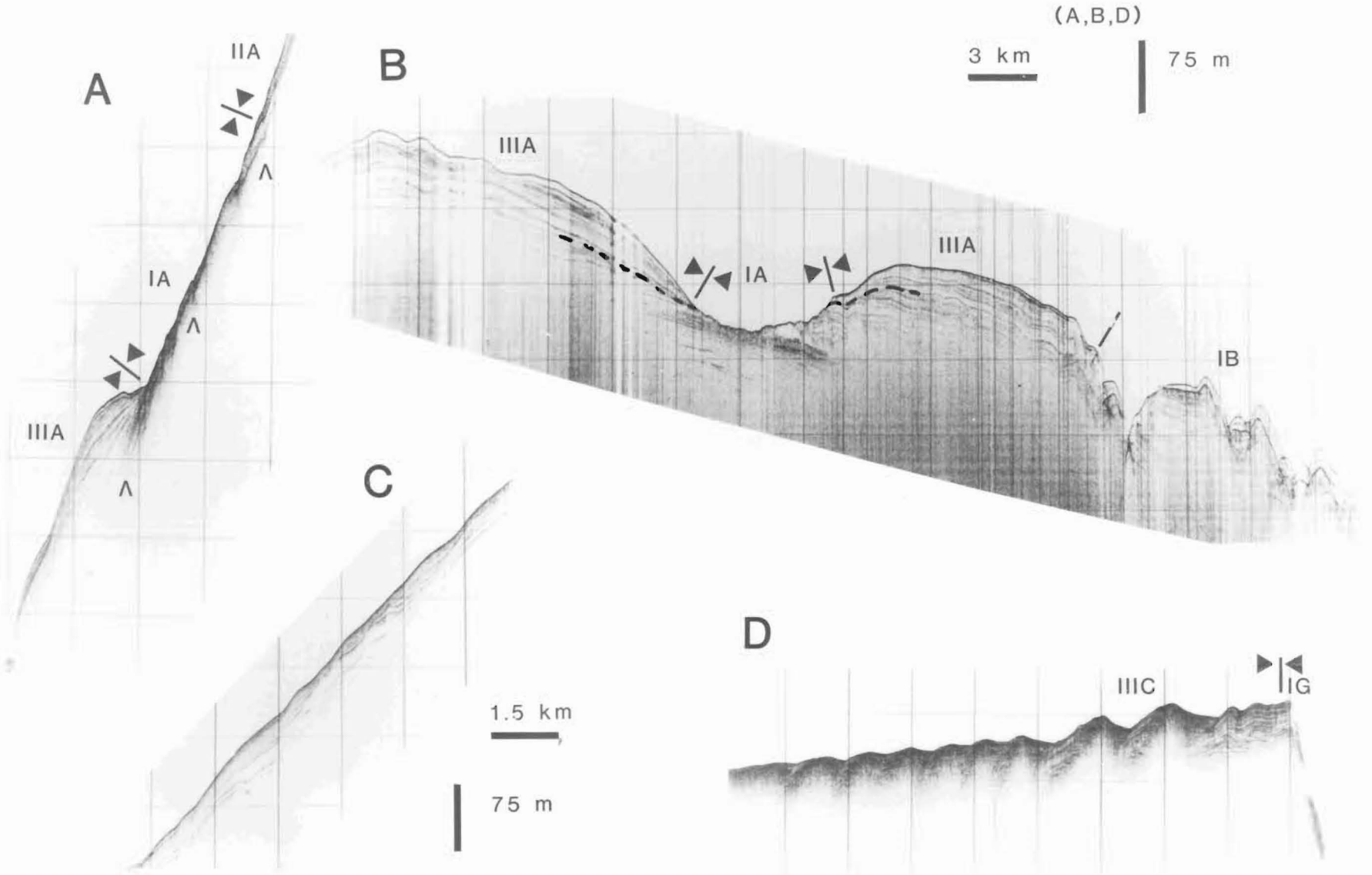
A
IIA
IA
IIIA
B
(A,B,D)
3 km
75 m
IIIA
IA
IIIA
IB
C
1.5 km
75 m
D
IIIC
IG

Fig. 3.6. Sedimentary lithofacies, relative volcanic glass distribution, and glass shard chemical population characteristics in cores from the north Chatham slope. For localities, see Fig. 3.2. Cores are grouped according to New Zealand Stage ages (Wo = Opoitian, Wp = Waipipian, Wn = Nukumaruan, Wc = Castlecliffian, Wq = Haweran; see summary in Fig. 4.2). Major sedimentary environments are indicated, along with sample positions analysed for biostratigraphy and glass chemistry. Glass shard percentages are concentrations in the sand fractions. Sediment colour codes : a, 10Y4/2 greyish olive; b, 5Y5/2 light olive grey; c, 5Y7/2 yellowish grey; d, 5GY5/2 dusky yellow green; e, 5GY3/2 greyish olive green; f, 5GY4/1 dark greenish grey.

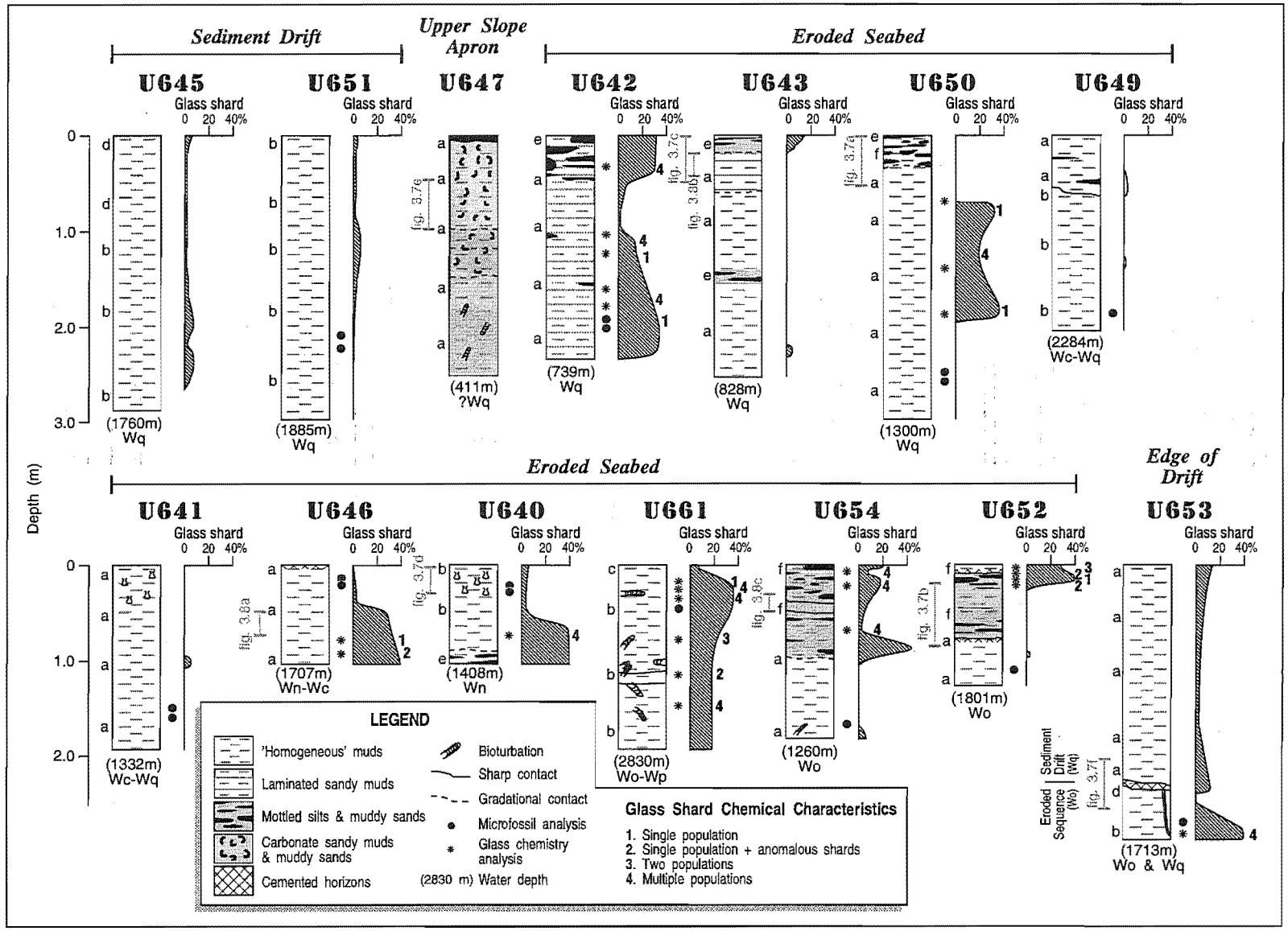
Sediment Drift
Upper Slope Apron
Eroded Seabed
Eroded Seabed
Edge of Drift
U645
U651
U647
U642
U643
U650
U649
U641
U646
U640
U661
U654
U652
U653
Glass shard
0 20 40%
Depth (m)
0
1.0
2.0
3.0
(1760m) Wq
(1885m) Wq
(411m) ?Wq
(739m) Wq
(828m) Wq
(1300m) Wq
(2284m) Wc-Wq
(1332m) Wc-Wq
(1707m) Wn-Wc
(1408m) Wn
(2830m) Wo-Wp
(1260m) Wo
(1801m) Wo
(1713m) Wo & Wq
fig. 3.7e
fig. 3.7c
fig. 3.8b
fig. 3.7a
fig. 3.6a
fig. 3.7d
fig. 3.8c
fig. 3.7b
fig. 3.7f
Eroded Sequence (Wo)
Sediment Drift (Wq)
LEGEND
'Homogeneous' muds
Laminated sandy muds
Mottled silts & muddy sands
Carbonate sandy muds & muddy sands
Cemented horizons
Bioturbation
Sharp contact
Gradational contact
Microfossil analysis
Glass chemistry analysis
(2830 m) Water depth
Glass Shard Chemical Characteristics
1. Single population
2. Single population + anomalous shards
3. Two populations
4. Multiple populations

Fig. 3.7. Examples of lithofacies in cores. For localities, see Fig. 3.2. Positions of illustrated sections are shown on core logs in Fig. 3.6. HM, homogeneous mud; Mz & mS, mottled silt and muddy sand; LsM, laminated sandy mud; CsM & mS, carbonate sandy mud and muddy sand; CH, cemented horizons.

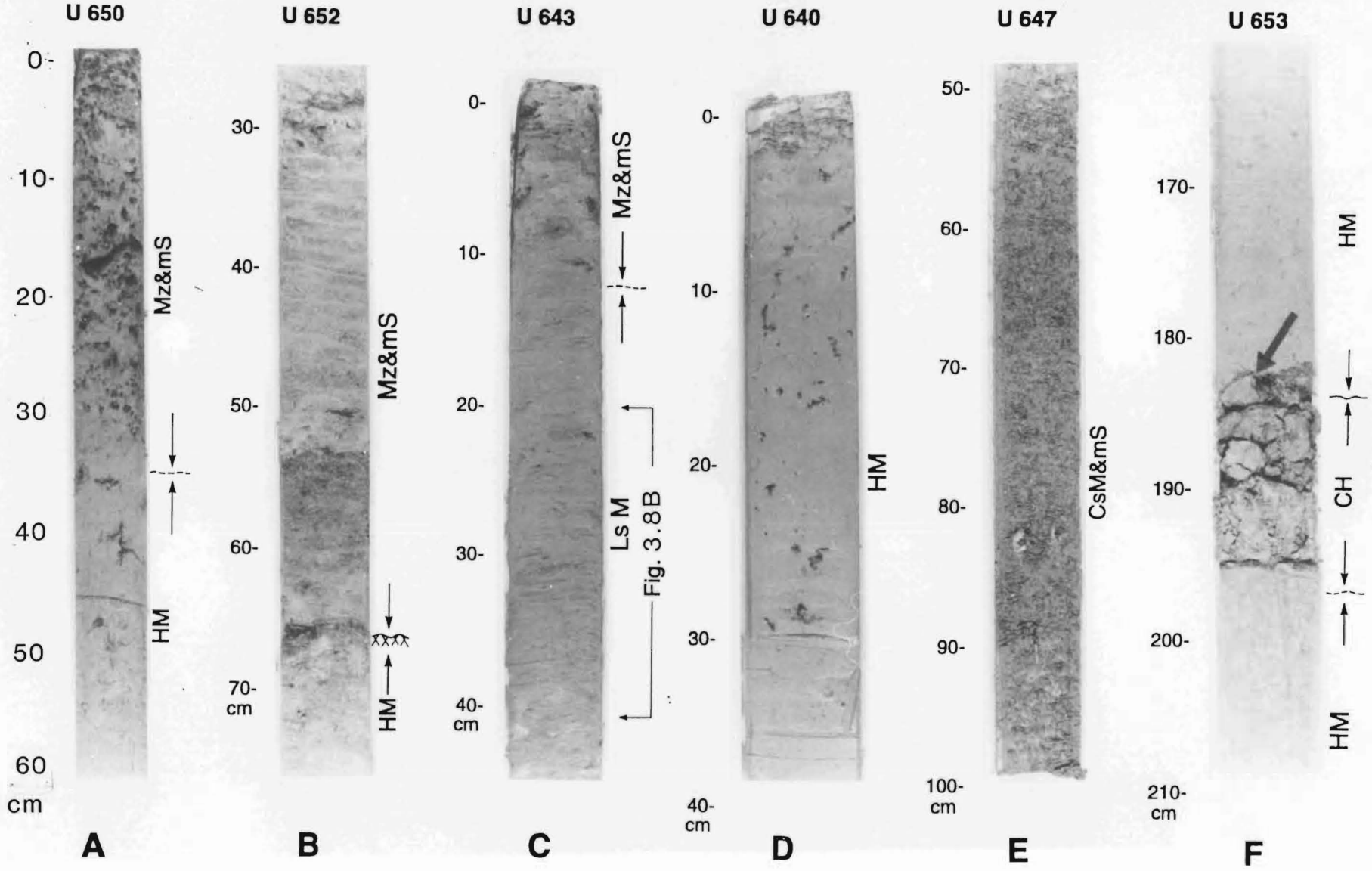
U 650
U 652
U 643
U 640
U 647
U 653
Mz&mS
HM
Ls M
Fig. 3.8B
CsM&mS
CH
cm
A
B
C
D
E
F

Fig. 3.8. X-ray radiographs of 10 mm thick slices of cores illustrating the three main lithofacies. Large irregular white areas are fractures in the core slices. **A.** Early Pleistocene, bioturbated, homogeneous mud with abundant sulphide-filled worm tubes. **B.** Late Pleistocene, laminated sandy mud with discontinuous stratification. **C.** Early Pliocene, mottled silts and sandy muds. See Fig. 3.6 for section positions and Fig. 3.2 for core locations.

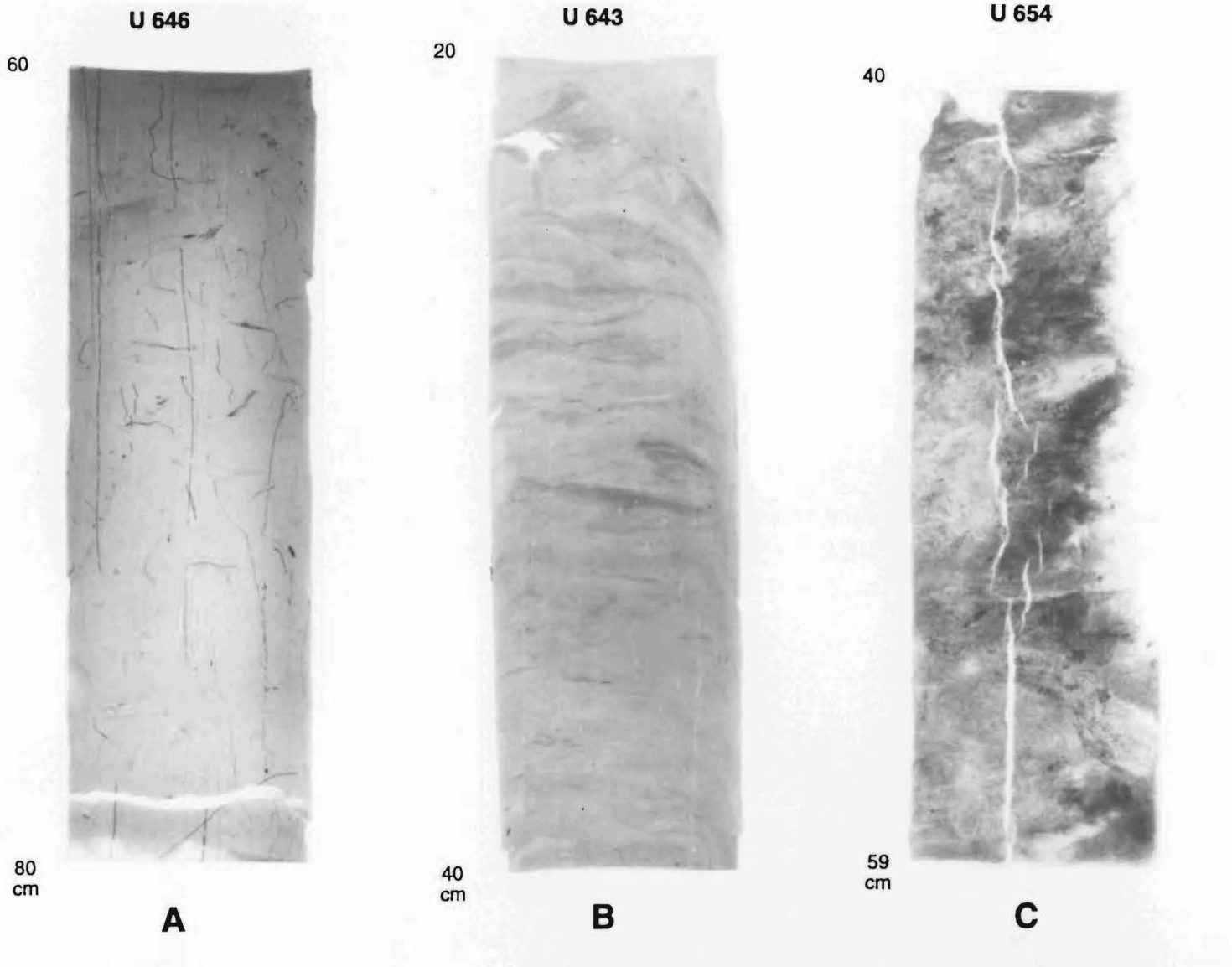
U 646
60
80
cm
A
U 643
20
40
cm
B
U 654
40
59
cm
C

greyish green mud with minor amounts of sand. Sand fractions consist of variable amounts of glauconite, clear glass shards, foraminiferans, radiolarians, iron sulphides, and terrigenous detritals. For ease of description of the sediments four lithofacies, which are independent of age and echo type, are distinguished on the basis of texture and sedimentary structure (Fig. 3.6): (1) homogeneous mud; (2) laminated sandy mud; (3) mottled silts and muddy sands; and (4) carbonate sandy muds and muddy sands. In addition, cemented horizons that characterise some buried erosion surfaces are distinguished (Fig. 3.6). Contacts between lithofacies are mostly gradational but some are sharp. The sediment lithologies are discussed below together with the descriptions and interpretations of echo types.

3.3.1 IRREGULAR ECHOES

Type IA: Irregular microtopography with distinct, sharp echoes and outcropping subbottom reflectors occurs in four areas on the mid slope and is indicative of deep erosion. The areas coincide with the axes of oblique-to-slope *en echelon* current scour channels that are also expressed in the bathymetry (Fig. 3.1), and exhibit up to 20 m microtopographic relief (Fig. 3.3A-C; 3.5A, B). In places, relict type IA echoes with up to 35 m relief have been draped by a thin muddy sequence (Fig. 3.3A) and they now form the thin, up-slope extent of lower slope sediment drifts (type IIIA). Cores from this echo type (U640, U646, U652; Fig. 3.2) consist predominantly of homogeneous mud together with mottled silt and sandy mud of Late Pliocene and Early Pleistocene age (Fig. 3.6).

Type IB: Sharp, very irregular, steeply dipping (4–5°) echo with localised outcropping subbottom reflectors between hyperbolic highs of varying vertex elevation (Fig. 3.3D, E) is a widespread echo type (Fig. 3.2). It extends as a 3–20 km wide belt for over 180 km along the lower Chatham Slope east of 175°E, between about 1000 m and 2600 m water depth. Channels between the quasi-hyperbolic highs are prominent on slope-parallel profiles where they exhibit up to 120 m relief (Fig. 3.3D), and are less prominent on slope-normal profiles (Fig. 3.3E) indicating that their orientation is predominantly down-slope rather than along-slope. The hyperbolae and some of the intervening channels are draped by a seismically transparent (probably muddy) veneer, up to 15 m thick, with a sharp echo and few internal reflectors.

Type IB echo exhibits both erosional and depositional characteristics. Slope-normal profiles resemble the smooth, steeply dipping type IC echo of Pratson and Laine (1989) whereas slope-parallel profiles appear similar to their type VC, large irregular wavy echoes that characterise the sediment drifts of the Lower Continental Rise Hills, eastern U.S.A.. Damuth and Hayes (1977) reported a similar echo

characteristic from channelised regions on the upper continental rise of the Brazilian margin (their type IIIC) and inferred a turbidity current origin. On the NW Chatham Rise the echo type IB has a clear spatial relationship to the down-slope ends of current-eroded scours; the belt of type IB widens eastward and realigns itself with the toe of each oblique-to-slope scour channel (Fig. 3.2). It is also associated with surficial slump deposits (types ID and IF, Fig. 3.2), and with deep-seated (> 200 m) rotational slide surfaces seen on airgun profiles of parts of the slope. Hence the echo type is inferred to be the product of both along slope contour current and down-slope mass wasting processes. Core U661 recovered well consolidated homogeneous mud of Pliocene age from the seabed (Figs. 3.2 and 3.6).

Type IC: Very irregular, sharp strong echo with no subbottom reflectors (Fig. 3.3F) is a minor type occurring in isolated areas on the upper slope below Mernoo Bank in 400–800 m water depth (Fig. 3.2). Slope angles of up to 10° occur between peaks and adjacent troughs. On airgun seismic profiles the peaks have no internal reflectors and appear to be volcanic protrusions with surrounding moat depressions. They also coincide with known magnetic anomalies (Wood *et al.,* 1989). Moat depressions around exposed volcanics are typical in other regions with vigorous bottom current activity (e.g., Jenkins, 1984; Lewis *et al.,* 1986).

Type ID: Overlapping hyperbolae with varying vertex elevations and no subbottom reflectors (Fig. 3.3G) occur in several areas (up to 140 km^2) within and marginal to the Hikurangi Channel at the base of both the Chatham Slope and eastern South Island slopes (Fig. 3.2). The reflection type is inferred to indicate returns from small, strongly reflective point sources on the seabed. They coincide with the toes of large slumps on airgun profiles, suggesting that the hyperbola are reflections off rafted slide debris or compressed sediment hummocks (type IVB of Pratson and Laine, 1989). In other parts of the world this echo type is not unique to mass wasting processes because Damuth and Hayes (1977) observed the same return from erosional and depositional bedforms created by northward flowing Antarctic Bottom Water in the southeast Atlantic.

Type IE: Irregular, prolonged echo with few discontinuous, hummocky subbottom reflectors (Fig. 3.3H) dominates the upper continental slope of Mernoo Bank (Fig. 3.2). The seabed exhibits a network of erosional furrows, up to 10 m deep, seen in both slope-parallel and slope-normal profile orientations. Piston cores (U642, U647) contain abundant (up to 63%) disseminated glauconitic sand, sometimes with dispersed broken shell fragments. Core U647, from 411 m water depth (Fig. 3.2) is relatively coarse grained (37–63% sand) and faintly stratified, although fine-scale lamination is absent (Fig. 3.6). The core has a high carbonate content of 40–59% due to an abundance of shell fragments. These shells include the gastropods *Bathypoma*

parengonius, Cominella alertae, Scaphander otagoensis and *Uberella vitrea*, the bivalve *Sacella bellula,* the scaphopod *Dentalium zelandicum,* and fragments of echinoderm plates.

Type IF: Irregular, sharp seabed echo with either few discontinuous subbottom reflectors or acoustically transparent subbottom (Fig. 3.3I, J) occurs in two areas on the mid slope (Fig. 3.2). It is interpreted to be the product of surficial slides or debris flows (e.g., Damuth, 1979), and parallel reflectors of hemipelagic sediments occur beneath the deposits (Fig. 3.3J).

Type IG: Defined canyons and flat-floored channels comprise a significant part of the echo-character map (Fig. 3.2). They include Pukaki Canyon on the northwestern side of Mernoo Saddle (Fig. 3.3K), the Hikurangi Channel (Fig. 3.3L), and a shallow channel running along the toe of the north Chatham Rise slope in the east of the investigated area (Fig. 3.3M). Pukaki Canyon is one of several very high relief eroded conduits that link the north Canterbury shelf with the southern Hikurangi Channel, both of which are products of turbidity currents. Late Miocene sediment is exposed locally in the axis of the canyon (e.g., core S871, see Fig. 4.2). The floor of the Hikurangi Channel is characterised by a prolonged echo with few discontinuous subbottom reflectors and piston cores from it consist predominantly of terrigenous sandy turbidites (e.g., Lewis, 1985). Gravel layers, correlatives of gravel turbidites in Kaikoura Canyon (Carter *et al.,* 1982), have been recovered in several cores from the channel south of Cook Strait. The smaller channel at the base of the north Chatham Rise slope near 177°E (Fig. 3.2, 3.3M) also exhibits a prolonged echo typical of sandy substrates, although sharp echo traces with subbottom reflectors occur along its northern side where muddy overbank turbidites from the Hikurangi Channel have spilled into it.

3.3.2 SMOOTH ECHOES

Type IIA: A smooth, distinct or occasionally semi-prolonged echo with outcropping subbottom reflectors (Fig. 3.4A) is widespread, and together with type IA echoes it defines the linear northeast trending, oblique-to-slope erosive scours on the Chatham Rise midslope between Mernoo Saddle and 176°E (Fig. 3.2). Type IIA also occurs on the upper slope near 177°E, where its full extent has not been mapped. Cores from this echo type (U641, U643, U650, U654; Fig. 3.2) consist predominantly of homogeneous mud together with mottled silt and sandy mud of Pliocene to Late Pleistocene age (Fig. 3.6).

Type IIB: Smooth, sharp, dipping echo with continuous parallel subbottom reflectors (Fig. 3.4B) characterises much of the mid and upper slope from about 500–1000 m

water depth, particularly between 175°10'E and 177°E (Fig. 3.2). Cores from eroded seafloor further down slope (echo types IA and IIA), where the subbottom reflectors crop out (Cores U640, U641, U650; Fig. 3.2), indicate that echo type IIB represents predominantly bioturbated hemipelagic mud along with occasional thin (< 20 mm) and irregular layers of glauconitic sand. The sandy layers are inferred to have been resedimented from the upper slope, where extensive greensand deposits occur (e.g., Norris, 1964), and then reworked by burrowing organisms and weak bottom currents. In studies elsewhere (e.g., Damuth, 1975; Damuth and Hayes, 1977) a similar echo type has also been shown to consist of muds with low sand percentages, and few, usually thin sand/silt layers.

Type IIC: Variable sharp to prolonged, smooth, near horizontal echo with parallel subbottom reflectors (Fig. 3.4C, D) occurs on the expansive floor of the Hikurangi Trough in association with types IIIC and IG echoes (Fig. 3.2). Both seismic penetration and subbottom reflector continuity are variable and inter-related with echo distinction; areas with sharp echoes exhibit good seismic penetration and continuous subbottom reflectors (Fig. 3.4C), whereas areas with prolonged echoes have poor seismic penetration and discontinuous subbottom reflectors (Fig. 3.4D). The echo type is interpreted to represent channel overbank turbidite deposits with varying concentrations of sand and varying thicknesses of sandy layers being responsible for the range in echo characteristics (Damuth and Hayes, 1977). Type IIC echo is very prolonged on the terrace opposite Cook Strait Canyon where considerable quantities of sand are inferred to have overspilled the wide and shallow Hikurangi Channel (Fig. 3.4D).

3.3.3 WAVY ECHOES

Type IIIA: Sharp wavy echoes with migrating and diverging subbottom reflectors in broad sediment lenses (Figs 3.3A-B, C; 3.5A, B) dominate the north Chatham Rise slope, down-slope from and in between the elongate scours (types IA and IIA) between Pukaki Canyon and 176°E (Fig. 3.2). The lenses contain migrating, wavy, onlapping packets of weak and strong reflectors and are generally veneered by an acoustically transparent layer up to 6 m thick. Cores from this surficial layer (U645, U651, top of U653; Fig. 3.2) consist of very soft homogeneous olive grey mud with little internal structure and very low sand content (Fig. 3.6). The lenses resemble turbidite channel levees with internal sediment waves (Fig. 3.3B) (e.g., Damuth, 1979; Normark *et al.*, 1980) but they occur on the continental slope well above the un-leveed part of the Hikurangi Channel, generally on the down-slope sides of current-eroded scours. The scours are clearly not distributary channels of a turbidite system, because they cut obliquely down slope. The lenses are inferred to be sediment drifts associated with current erosion of the continental slope.

Type IIIB: Sharp, slightly wavy echo with subparallel, migrating or diverging subbottom reflectors (Fig. 3.5C) occurs in two areas on the mid slope east of 176°E, in association with types IB and IIB echoes (Fig. 3.2). It is distinguished from echo type IIIA by the less regular, less conformable nature of subbottom reflectors, and the overall non-lenticular geometry of the deposits. It lacks the large-scale divergence of subbottom reflectors away from current scour channels that is seen in type IIIA; there is no association with any down-slope canyons or channelised sedimentary conduits and it appears to be a largely depositional echo character with sediment waves resulting from along-slope current activity.

Type IIIC: Variable sharp to semi-prolonged, gently dipping, slightly wavy echo with parallel or migrating subbottom reflectors (Fig. 3.5D) characterises large parts of the floor of the Hikurangi Trough on channel levees and in overbank regions (Fig. 3.2). The echo type represents classic abyssal deep-sea sediment waves resulting from channel overspill by turbidity currents (e.g., Damuth, 1979; Normark *et al.,* 1980; Carter *et al.,* 1990). As in echo type IIC the variation in distinction of the echo is inferred to be related to varying concentrations of sand/silt layers in the upper few metres of sediment (e.g., Damuth and Hayes, 1977). The sediment waves typically have wavelengths of 1–4 km, and amplitudes of up to 35 m occur. They commonly diminish in both amplitude and wavelength down the levee backslope, away from the channel. The waves migrate up slopes which are generally $< 0.5°$. Thus, the migration is usually towards the channel on the highest, northern levee, and away from the channel towards the toe of the north Chatham Rise slope on the lower, south side of the channel.

3.4 REGIONAL SEDIMENTATION PATTERNS DERIVED FROM ECHO-CHARACTER MAPPING

A regional perspective of the importance of different sedimentary processes can be derived from the distributions of the various echo types. The map in Figure 3.9 has been derived by grouping genetically-related echo types into five associations.

3.4.1 CANYON-CHANNEL-LEVEE AND OVERBANK TURBIDITE ASSOCIATION

A submarine canyon/deep-sea channel-levee-overbank turbidite association (types ID, IG, IIC, IIIC) includes Pukaki Canyon, the narrow part of the Hikurangi Trough between the Chatham Rise and South Island continental slopes, and the northward-widening flat floor of the Hikurangi Trough. Several features of the channel-levee system are also clearly expressed in the bathymetry (Fig. 3.1). The higher northern

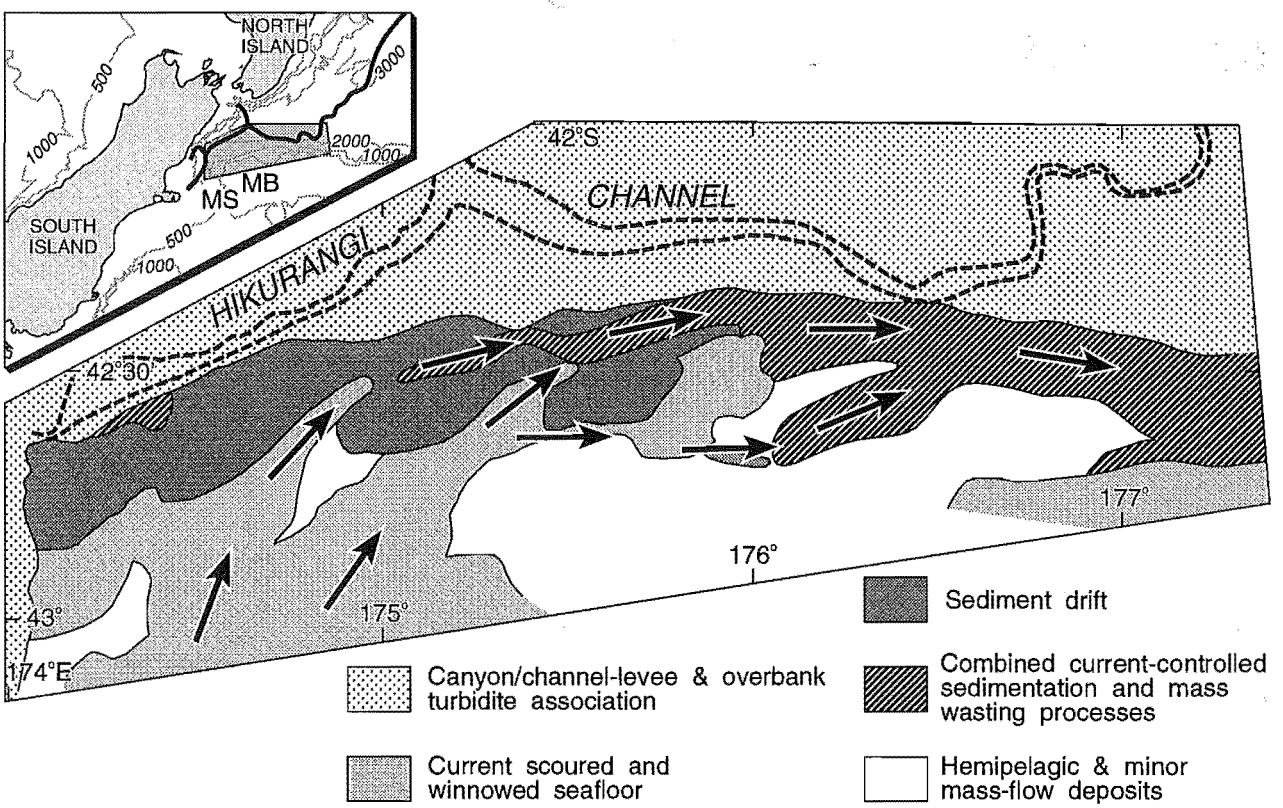

Fig. 3.9. Summary map of five associations of echo types depicting the relative importance of various sedimentary processes. Arrows indicate schematic late Quaternary bottom current directions. MS, Mernoo Saddle; MB, Mernoo Bank.

levee results from preferential development, presumably in response to southern hemisphere coriolis deflection to the left facing down channel (e.g., Carter and Carter, 1988). From its widest point near the mouth of Cook Strait Canyon, the channel runs east-southeast to the toe of the north Chatham Rise slope, where it is partially blocked by debris from a large slump (Fig. 3.2). The channel then begins to meander at 176°40'E, where it diverges from the toe of the slope, narrows to 1–3 km wide, and deepens below its levee crests.

South of the Hikurangi Channel the NW Chatham Rise slope encompasses four associations of echo types which indicate that current-controlled sedimentation processes prevail over most of the slope (Fig. 3.9).

3.4.2 CURRENT SCOURED AND WINNOWED SEAFLOOR

Current eroded seafloor (types IA and IIA) dominates the mid-slope between Mernoo Saddle and 176°E and between 700 m and 2000 m water depths. In a general sense, the eroded area forms an irregular belt about 30 km wide, that largely follows the bathymetric contours (Fig. 3.1) along slope for 160 km. Within this belt, however, the late Quaternary erosion is clearly concentrated in three oblique-to-slope, *en echelon* depressions which are 5–20 km wide, up to 105 km long and trend N 50°E. At the up-slope, southwestern end of the zone, where the scours merge, the seafloor is smoothly eroded (type IIA) whereas it becomes irregular down slope, in the northeastern end of each scour (type IA) where it narrows to form a well-defined channel separated by drift deposits (Figs 3.3A-C; 3.5A, B; 3.9). Along-slope profiles reveal up to 100 m relief between channel axes and adjacent drift crests (Figs 3.3A, 3.5B). The pattern of erosion is inferred to be a late Quaternary feature; eroded sediments of Late Pliocene-Late Pleistocene age have been exposed at the seabed (Fig. 3.6; see also Fig. 4.2).

In contrast to the late Quaternary pattern there are additional areas of the mid-slope that were previously eroded and which are now buried beneath late Quaternary depositional echo types (e.g., Fig. 3.5B; see also Figs. 4.1 and 4.8). These older erosion surfaces indicate that there are different patterns of earlier mid-slope erosion that appear to result from fluctuations in the position or erosive capacity of the currents (see Chapter 4). Up slope from the areas of deepest erosion there is an associated area that includes the network of small erosive channels on the sandy seabed (type IE) and the moat depressions around exposed volcanic cones (type IC). These bedforms suggest bottom current winnowing on the upper slope above the prominent current scours.

The eroded area on the mid-slope exhibits good seismic penetration, and parallel, almost horizontal, subbottom seismic reflections. Piston cores from this area contain various combinations of homogeneous, laminated and mottled sediment textures (Figs 3.6–3.8) together with reworked and cold-water-corroded nannofloras (section 4.3), reworked volcanic tephra (Appendix 3), and rare cemented horizons that correlate with seismically-defined unconformities (e.g., Fig. 3.7F, Chapter 4). These sedimentary features, together with intensive bioturbation, mixed terrigenous and biogenic compositions, fine grainsize, and inferred slow sedimentation, are consistent with hemipelagic sedimentation during periods of diminished and localised current activity (e.g., Doyle *et al.*, 1979; Gonthier *et al.*, 1984). Common worm-bored glauconitic aggregates (up 40 mm long) from the scour channel at site U652 and a hard 70 mm thick, pale green, fine-grained crust in core U653 represent *in situ* cementation and hard-ground formation of erosion surfaces in scour channel axes (Figs. 3.2, 3.6, 3.7B, 3.7F).

In cores from the mid-slope, the glauconitic sand in the mottled silts and muddy sand lithologies are inferred to have been redeposited in mass flows from the upper slopes of Mernoo Bank where carbonate and authigenic aprons exist (McDougall 1982), although textures of these deposits are not typical of turbidites (Walker and Mutti 1973) (Fig. 3.6). From the axis of one scour channel at 1700 m water depth, the top of core U646 and an accompanying grab sample at the same site recovered ferruginous nodules up to 60 mm long, and a small (< 25 mm) well rounded clast of weathered greywacke sandstone which are inferred to have been reworked from gravel lags on the upper flanks of Mernoo Bank (Fig. 3.2) (Fleming and Reed, 1951).

At several sampling sites in the most severely eroded lower-slope parts of current scours (U652, U646, U654, U640; Fig. 3.2), a very thin (< 100 mm) muddy veneer covers the erosion surface and the scattered surficial clasts. At site U653, soft mud 1.88 m thick covers the cemented erosion surface (Figs 3.3C and 3.6). The soft mud represents the thin, up-slope part of the seismically transparent veneer that caps the sediment drifts. In contrast, no muddy veneer occurs in cores or grab samples from current scoured or winnowed seafloor further up slope (cores U650, U641, U642, U647, U643; Fig. 3.2). This suggests a modern reduced phase of current activity with no present erosion in the deep, lower parts of scours channels.

3.4.3 SEDIMENT DRIFTS

The lower slope in between and below the scours is characterised by complex, lenticular sediment drifts that occur throughout a region 25 km wide and 165 km long (Fig. 3.9). The drifts are up to 120 m thick (assuming a seismic velocity of

1700 m/s). Several lines of evidence indicate sediment drifts. Firstly, seismic profiles orientated down slope (Figs 3.3B, 3.5A; see also Figs 4.3 and 4.5) and along slope (Figs 3.3A, 3.3C, 3.5A) show that the drifts have lenticular geometry with internal reflections converging towards the scour axes, indicating thinning of the deposits towards areas of strong current flow and increased deposition in areas of weaker flow. These lenses coalesce below the scour channels and extend to the toe of the slope, at the outer fringe of the Hikurangi channel system (Fig. 3.9). Secondly, the drift deposits show up-slope thinning and onlapping packets of weak and strong reflections that locally show subdued, migrating waves (e.g., Figs 3.3B, 3.5A, 3.5B). The sediment waves are developed on the down-slope side of each current scour and are capped by muddy sequences which wedge out up slope at the edge of the scour zone. Thus, the sediments were eroded by currents from the mid-upper slope and redeposited on the lower slope. The same sequence of wavy sediment packets can be correlated across and traced continuously around the ends of the oblique-to-slope scour channels from one lenticular part of the sediment drift complex to the next (see Section 4.2.3), thus indicating both that the scours were active simultaneously, and the current that formed them was braided into distinct cores. Thirdly, the sedimentary textures of the cores from the slope above the drifts are consistent with current-influenced, slow sedimentation between periods of strong and erosive current activity.

Piston cores of the acoustically transparent muddy veneer that caps the sediment drifts (U645, U651, U653; Figs 3.2 and 3.6) reveal a homogeneous, finely bioturbated texture but an absence of sandy winnowed lags typical of contourite deposits (Stow and Holbrook, 1984). These homogeneous cores may be comparable to the muddy contourite facies described from Northern Hemisphere deep-water sediment drifts (e.g., Stow and Holbrook, 1984; Gonthier *et al.*, 1984). Beneath the homogeneous muddy veneer are packets of strong wavy reflectors, which are inferred to be higher flow regime deposits containing layers or laminae of reworked silt and/or sand (see seismic units 6–2 on Figs. 4.2, 4.5 and 4.6).

3.4.4 COMBINED CURRENT-CONTROLLED SEDIMENTATION AND MASS WASTING PROCESSES

On the lower Chatham slope east of 175°E the drifts and scour channels merge into the elongate belt of channelised seafloor with sediment-draped quasi-hyperbolic highs (type IB) and areas of wavy sediment (type IIIB) that have been mapped to the edge of the investigated area. These echo types represent the combined effects of along-slope current-controlled processes and down-slope mass wasting. The strip of echo type IB is up to 20 km wide east of 176°E but narrows westward to only a few kilometres where it merges with the snout of the westernmost scour channel.

Furthermore this pattern of seabed morphology realigns itself at the snout of each scour channel (Fig. 3.2) and is clearly related to the bottom current activity.

There appears to be no significant interaction between the along-slope current-controlled sedimentary processes on the slope and the channel-levee turbidite system on the floor of the Hikurangi Trough, except perhaps for the isolated shallow channel running along the toe of the slope east of 177°E (Figs 3.2; 3.3M). This apparently sandy channel may represent current winnowing of the southern edge of the turbidite sediment wave field.

3.4.5 HEMIPELAGIC AND MINOR MASS-FLOW DEPOSITS

An association of echo types that represents a more passive sedimentary regime, is widespread above the deeply eroded zones (Fig. 3.9). It is inferred to represent mainly hemipelagic sedimentation together with intermittent mass flows redistributing glauconitic sand from the upper flanks of Mernoo Bank (type IIB) and with muddy debris flows (type IF).

3.5 WHAT SORT OF MID-BATHYAL CURRENTS?

The late Quaternary sedimentary evolution of the NW Chatham Rise clearly has been heavily influenced by strong bottom currents and large sediment drifts that have simultaneously accumulated on the lower slope. Meanwhile beyond the toe of the slope the narrow, canyon-channel system in the southern Hikurangi Trough acted as a conduit which bypassed mud and sand from the north Canterbury shelf to rapidly aggrading parts of the channel-levee system further northeast (Lewis and Pettinga, in press). The shape of the current scours and their relationship to the sediment drifts suggest that erosion involved a northward flowing current passing through the 580 m deep Mernoo Saddle, then cascading to over 2000 m on the northwest corner of the Chatham Rise (Fig. 3.9). The current braided on the mid-slope into several discrete cores that eroded the oblique-to-slope scours before merging again into a single contour current on the lower slope, in the area where combined current- controlled sedimentation and mass wasting processes occur.

Short-term current meter studies indicate only a very slow (< 0.08 m/s) overall net northward drift through Mernoo Saddle, but strong (> 0.4 m/s) peak tidal flows towards the north (Heath, 1976). More recently a current meter array moored in 500 m water in central Mernoo Saddle for five months, with two current meters deployed at 100 m and 300 m off the seabed respectively, recorded an overall average

net northward flow of 0.03 m/s to the north along with peak northward flows of 0.44 m/s, but periods of up to five weeks with no net flow and peak tidal flows of up to 0.67 m/s to the south (Greig and Gilmour, 1992). The high current speeds recorded are consistent with the evidence for erosion on the north side of the passage, but a mechanism is required to periodically produce a braided current with erosive capacity, descending to over 2000 m on the NW Chatham Rise slope. South of Mernoo Saddle intermediate depth water deeper than 580 m is forced upwards and periodically northwards through the western side of the saddle; only water deeper than about 800 m does not pass through and flows eastwards along the Chatham Rise (Heath, 1985). This upwelling and northwards flow includes a significant component of Antarctic Intermediate Water which is characterised by a salinity minimum at a depth of about 700 m south of the Chatham Rise. Heath (1972a ,b) considered that as this low temperature, low salinity (c. 5–6°C, 34.4 psu) Antarctic Intermediate Water flows northwards through the saddle, its salinity increases as it mixes with deep higher salinity subtropical water, causing it to sink, but only very slowly, to around 1000 m depth over the southern Hikurangi Channel. More recently, water sampled 100 m off the bottom of the saddle was found to have temperature characteristics (7.5–8.9°C) typical of mixed 300–600 m deep Southland Front water (Greig and Gilmour, 1992).

The recently reduced phase of current erosion in the lower slope parts of scour channels, suggested by the presence of soft mud < 100 mm thick covering the erosion surface at sites U652, U646, U654, and U640 (Fig. 3.2), may reflect reduced flow through the saddle in modern (post glacial) conditions relative to those during glaciations. Thus, the present day oceanography may not be representative of conditions at times of severe erosion of the slope. Vella (1963, 1973) considered that northward flow of subantarctic water through the Mernoo Saddle area was responsible for cooling shallow seas off southern North Island during glacial periods, allowing cool water and its associated fauna, such as the subantarctic scallop *Chlamys delicatula,* to invade the region that now forms much of onshore southeastern North Island. During periods of glacio-eustatic lowering of sea-level the northward flow of water through the passage was probably intensified due to several different causes. At these times Mernoo Bank and the Canterbury continental shelf were exposed (Fleming and Reed, 1951; Herzer, 1981), Mernoo Saddle was about 120 m shallower than present resulting in a greater constriction to the flow and therefore higher current speeds. This coincided with a more vigorous, higher energy regional bottom circulation system involving increased northward flow of cool subantarctic bottom water into the southwest Pacific (e.g., Kennett, 1982). Finally, the northward shift in the circum-polar wind system in glacial times produced more intense westerly winds (Stewart and Neall, 1984) which presumably enhanced both upwelling of cold, dense subantarctic water and its atmospheric forcing through the saddle.

There are several examples in other parts of the world where flow conditions are modified and bottom currents intensified by flow through constricting passages although none are closely comparable with this situation. For example, in the Tasman Sea basin, the Circum-Antarctic Current entering the southwest corner of the basin has exposed basement in the axis of the 2800 m deep Duyfken Passage, and formed an extensive sediment drift further east (Jenkins, 1984). A northward flowing Deep Western Boundary Current (DWBC) cascades to greater depths as it exits the Samoan Passage in the western Pacific Ocean (Reid and Lonsdale, 1974). In contrast to the bottom currents at the western end of the Chatham Rise this DWBC, turns to the left due to the coriolis force, not to the right, as it cascades to deeper water. Braided and channelised bottom currents separated by elongate basement ridges and associated sediment drifts occur in the Amirante Passage, western Indian Ocean, where thermohaline flow of another DWBC is intensified between the Mascarene and Somali Basins (Johnson and Damuth, 1979). Similarly, Dingle and Camden-Smith (1979) described braided currents and associated sediment drifts in the Agulhas Passage, southeastern Africa. They proposed a system of discrete current cells with intervening sediment drifts in areas of diminishing current activity. These current controlled channels, however, are essentially contour flowing and not oblique-to-slope and *en echelon* like the features described in this study.

Heezen and Johnson (1969) mapped an area of exceptional scour in the Strait of Gibraltar, where the powerful (locally > 1 m/s) Mediterranean Undercurrent carries salty Mediterranean water into the Atlantic Ocean. They mapped current-swept rock and gravel substrates in and just beyond the straits, merging down current into extensive sediment wave fields. Armi and Farmer (1985) discussed the internal hydraulics of the Strait of Gibraltar, where they recognised internal control of the flow conditions at three locations coinciding with bathymetric sills and narrows. Such hydraulic control occurs where the composite Froude number of the flow equals unity and the flow is considered to be critical. These hydraulic adjustments separate flows that are subcritical from those that are supercritical, and their locations are a function of several variables including the breadth and depth of the saddle, the thickness and relative density difference between different layers, the degree of coupling between the layers, and various upstream conditions (Armi, 1986). Additional oceanographic data and modelling are required to establish the flow conditions responsible for erosion of the NW Chatham Rise slope. It is likely that at least during glacial conditions a hydraulic control on the flow conditions occurs in the Mernoo Saddle region, producing supercritical flows within or immediately north of the saddle. Perhaps the braided flows responsible for the scours and coalescing drifts are produced by an internal hydraulic jump where north bound, cold water descends to deep water north of the saddle.

3.6 CONCLUSIONS

(1) The Hikurangi Channel is a major conduit for turbidity currents flowing into the Hikurangi Trough from the south. It is 4–5 km wide near its southwestern end, up to 10 km wide near the mouth of Cook Strait Canyon, and narrows to 1–3 km wide in the east of the study area where it begins to meander. East of Cook Strait the channel has a left-bank dominated levee characterised by extensive sediment wave fields.

(2) An adjacent, elongate region of mid-slope current erosion, 160 km long and up to 30 km wide, occurs between depths of 700 m and 2300 m on the northwest corner of the Chatham Rise. Several northeast trending oblique-to-slope *en echelon* current scour channels, 5–20 km wide and up to 105 km long, occur in this zone. The late Quaternary scours appear to have been formed by a northeastward-flowing current which crossed the Mernoo Saddle, then braiding as it cascaded down and across the mid-slope before merging again into an eastward flowing contour current on the lower NW Chatham Rise slope. The lower slope in between and below the current scours has been built up by complex of coalescing sediment drifts.

(3) The bathymetry reflects aspects of current-controlled sedimentation and down-slope mass wasting processes on the NW Chatham Rise continental slope, and turbidity current deposition in the Hikurangi Trough.

(4) The presently reduced phase of current erosion on the NW Chatham Rise slope reflects the post-glacial physical oceanography in the region. Severe phases of erosion are inferred to have occurred during glacial periods when flow through the Mernoo Saddle was intensified, and internal hydraulic adjustments in flow conditions occurred.

CHAPTER 4

LATE CENOZOIC SEISMIC-STRATIGRAPHY: NORTHWESTERN CHATHAM RISE

4.1 INTRODUCTION

The well established technique of high-frequency (3.5 kHz) echo-character mapping has been used successfully in Chapter 3 of this thesis to analyse the late Quaternary sedimentary processes on the NW Chatham Rise slope and in the southern part of the Hikurangi Trough. In general, complementary paleoceanographic information such as the meandering of a bottom current, or changes in the position of an oceanic convergence zone during paleoclimatic fluctuations, may be provided by high-resolution isotopic, sedimentological and micropaleontological studies of sediment cores (e.g., Prell *et al.,* 1979; Johnson *et al.,* 1988; Winter and Martin, 1990). Such high-resolution sedimentological analyses of DSDP cores have demonstrated orbital forcing on current-controlled sedimentation in mid-Pleistocene deep-sea sediment drifts in the north Atlantic (Wang and McCave, 1990; Robinson and McCave, in press). A longer-term record of current-controlled sedimentation patterns may be derived from seismic-stratigraphic analysis (Dingle and Camden-Smith, 1979; Markl and Bryan 1983; Reed *et al.,* 1987; Kennard *et al.,* 1990) or from studies of sedimentation hiatuses in cores of Cenozoic age (e.g., Watkins and Kennett, 1971; Osborn *et al.,* 1983; Burkle and Abrams, 1987). For example, seismic-stratigraphic analysis may reveal the timing of initiation of current erosion or of sediment-drift accumulation, the regional distribution of a sediment drift, and perhaps its evolutionary history (e.g., Fulthorpe and Carter, 1991).

This chapter presents the results of a high-resolution seismic-stratigraphic analysis of the sedimentary succession on the NW Chatham Rise continental slope. Although the slope is adjacent to the southern part of the Hikurangi Trough channel-levee system, it is away from the main depocenter for turbidite deposition. The slope has been sculptured by a mid-bathyal current which appears to have passed over the Mernoo Saddle. An outline of the evolution of the seismic units, within the time-framework provided by biostratigraphy of piston cores, is presented. The following seismic-stratigraphic analysis shows that the sedimentation patterns discussed in Chapter 3 (Fig. 4.1 — top) represent only the latest Quaternary (c. 0.25 Ma to present) sedimentation history and that current-influenced sedimentation patterns, now preserved in the subsurface sedimentary succession, have evolved since the mid Pliocene. Although there are many published examples where bottom currents are intensified by flow through constricting passages, there are fewer examples in which

Fig. 4.1. Lower map shows regional surface sediment distribution (modified from McDougall, 1982) and various late Cenozoic sedimentary aspects of the eastern South Island margin. Surface sediment types are shaded: **1,** planktic carbonate mud and sand (Bounty and Hikurangi Troughs), and authigenic sand (crestal Chatham Rise); **2,** terrigenous mud and sand; **3,** benthic carbonate gravel and coarse sand. Late Miocene-Early Pliocene sediment drifts on the South Island shelf are from Fulthorpe and Carter (1991). Large solid arrows are hypothetical current directions responsible for the Late Miocene drift deposits. Early Pliocene shelf edge and the region of exposed pre-Neogene strata are from Wood *et al.* (1989). Bold dashed lines are the axes of deep-sea turbidite channels. Regional bathymetric contours in metres. Top map shows enlargement of the late Quaternary sedimentation patterns on the NW Chatham Rise slope and southern Hikurangi Trough, derived by 3.5 kHz echo-character mapping (see Figs 3.2 and 3.9). Arrows indicate inferred late Quaternary current flows. Labelled lines show locations of seismic profiles in Figs 4.3 to 4.6.

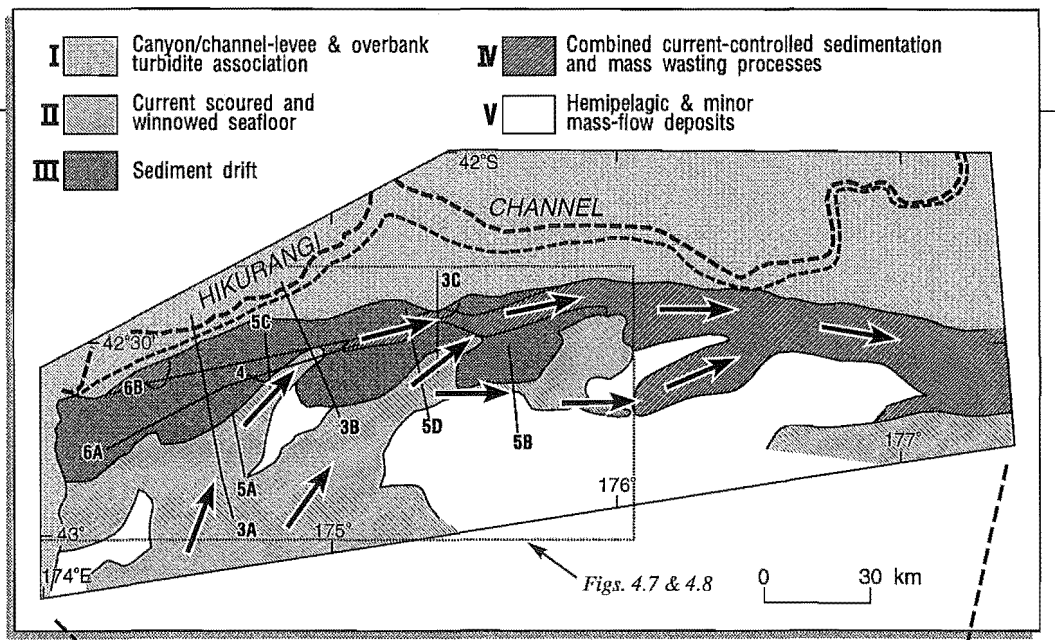
I Canyon/channel-levee & overbank turbidite association
II Current scoured and winnowed seafloor
III Sediment drift
IV Combined current-controlled sedimentation and mass wasting processes
V Hemipelagic & minor mass-flow deposits
42°S
CHANNEL
HIKURANGI
42°30'
43°
174°E
175°
176°
177°
3C
5C
4
6B
6A
3B
5D
5B
5A
3A
Figs. 4.7 & 4.8
0
30 km

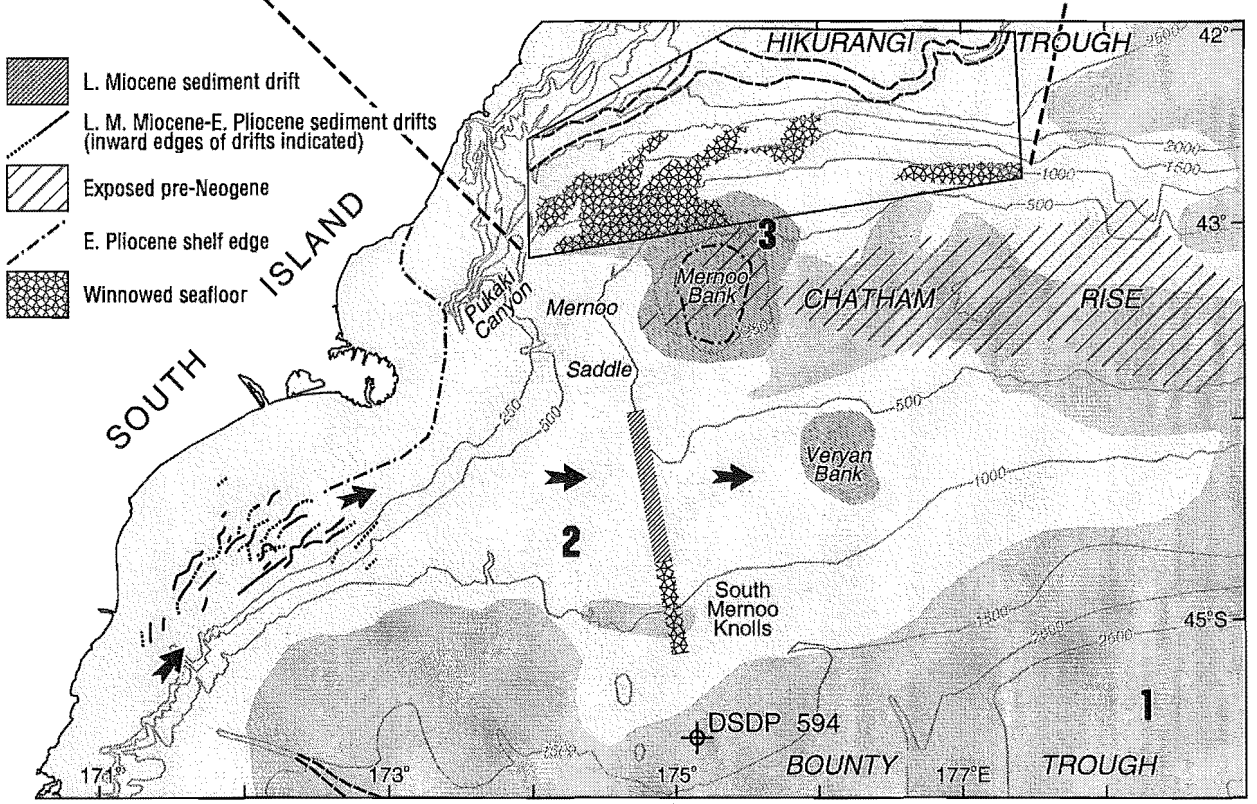
L. Miocene sediment drift
L. M. Miocene-E. Pliocene sediment drifts (inward edges of drifts indicated)
Exposed pre-Neogene
E. Pliocene shelf edge
Winnowed seafloor
HIKURANGI TROUGH
42°
43°
45°S
SOUTH ISLAND
Pukaki Canyon
Mernoo Saddle
Mernoo Bank
CHATHAM RISE
Veryan Bank
South Mernoo Knolls
DSDP 594
BOUNTY TROUGH
1
2
3
171°
173°
175°
177°E
250
500
1000
1500
2000
2500
2600

3.5 kHz echo-character mapping has been integrated with high-frequency seismic-stratigraphic analysis to examine Plio-Pleistocene erosional-depositional interactions that result from climatically-influenced fluctuations in the flow of mid-bathyal currents.

4.2 HIGH-RESOLUTION PLIOCENE-PLEISTOCENE SEISMIC STRATIGRAPHY: EVOLUTION OF SCOURS AND DRIFT DEPOSITS

4.2.1 METHOD OF APPROACH

A very strong reflection (labelled O, see Fig. 4.3) can be traced in seismic profiles within the faulted, down-slope thickening, Cenozoic sedimentary succession beneath the NW Chatham Rise slope to an Oligocene sequence in exploration wells on the South Island continental shelf (Wood *et al.*, 1989). Above this reflection, the base of a high-amplitude sequence (labelled reflection LM, see Fig. 4.3) was cored in Pukaki Canyon at the western end of the Chatham Rise (Fig. 4.1) and biostratigraphically dated to be Late Miocene (9.2–10.5 Ma; early Tongaporutuan; core S871, Fig. 4.2). Within the Pliocene-Pleistocene part of this stratigraphic succession, a very prominent onlap surface (labelled L), that is truncated by erosion on the rise crest, can be traced widely beneath the slope (Fig. 4.3). A mid-Pliocene age for this surface is suggested by three late Early Pliocene cores (U652, U653, U654; see Figs 3.2 and 4.7) from near the top of the underlying seismic unit (labelled 13, Fig. 4.2), and an Early Pleistocene core (U640) from three seismic units up section (unit 10, Fig. 4.2). Above surface L, 12 seismic units have been recognised, mainly in 3.5 kHz profiles. The units are referred to by numbers 1 to 12, and their bounding surfaces by letters A to L. Because these sedimentary units record the initiation and history of current erosion and deposition on the slope, the seismic stratigraphy of the older Cenozoic sequences below surface L are not discussed further in this chapter.

All 12 of the Pliocene-Pleistocene seismic units above surface L thin up slope and most wedge out beneath the upper slope, in water depths deeper than 700 m, although some extend as shallow as 500 m. All units exhibit onlap, and at least five truncate underlying reflections between 900 m and 2300 m water depth (Figs 4.3 to 4.6). A geological map of the area of prominent seafloor erosion between Pukaki Canyon and 176°E (Fig. 4.7) was produced by carefully correlating the units and their outcrop positions over the grid of seismic profiles (Fig. 1.3). The outcrop pattern is a function of the regional distribution of the current scours, the geometry of the units and, less significantly, the magnitude of displacements on late Cenozoic normal faults. East of 176°E, the microtopography on much of the slope is complex, and shallow subbottom seismic units cannot be mapped with confidence.

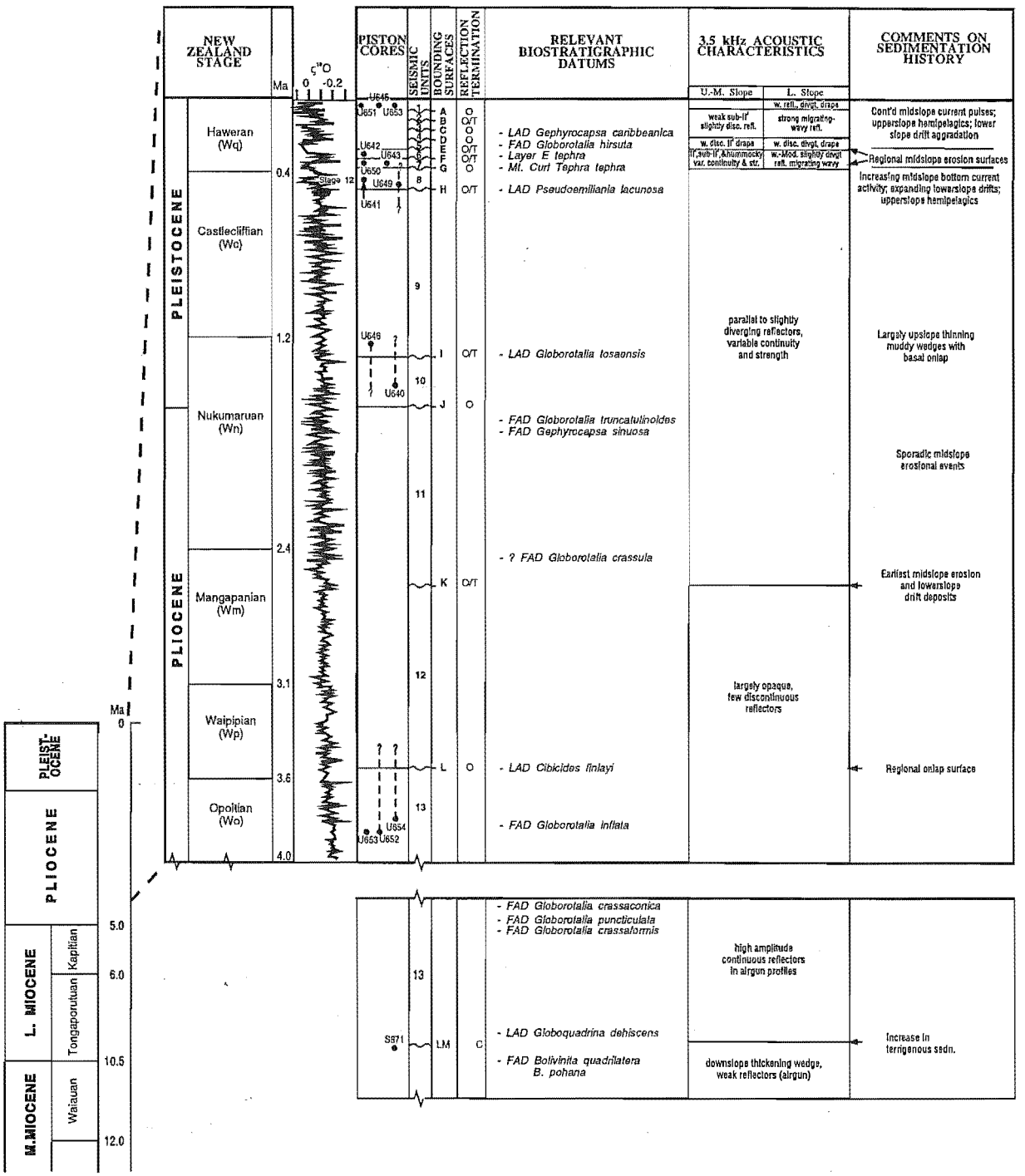

Fig. 4.2. Summary of late Cenozoic stratigraphy, NW Chatham Rise slope, including the general characteristics of the seismic units and their bounding unconformities (O, onlapping reflectors; T, truncation followed by onlap). For piston-core stratigraphic positions, dashed vertical lines and question marks indicate uncertainty in the unit sampled. Core locations shown on Figs 3.2 and 4.7. Note that cores sample only small parts of units so the ages of the unit boundaries are not well constrained. New Zealand geological time scale from Edwards *et al.* (1988). Oxygen isotope curve from Joyce *et al.* (1990).

Fig. 4.3. Single-channel airgun profiles 3A, 3B, and 3C of the NW Chatham Rise slope illustrating late Cenozoic seismic stratigraphy and the positions of late Quaternary sediment drifts and current erosion. Note that the trends of both the late Quaternary drift crests and the scour channels are obliquely in and out of the plane of the profiles (see map patterns and profile positions on Figs 4.1 — top, 4.7 and 4.8). Numbers indicate Plio-Pleistsocene seismic units, and letters denote prominent unconformities described in the text. See Fig. 4.2 for summary of seismic stratigraphy. Approximate water depths can be obtained from Fig. 4.1. LM, Late Miocene, O, Oligocene. **A.** Old (post-unconformity K) drift deposits, along with probable interfingering Hikurangi Channel turbidites, onlap beneath the large lobe on lower slope whereas younger (units 8–1) drifts extend further upslope, burying an old erosion surface (see also Fig. 4.6B). **B.** Prominent post-unconformity H drift deposits developed in a large, upslope-migrating sediment wave. **C.** Prominent post-unconformity G sediment forming an upslope-migrating drift. Note the occurrence of normal faults.

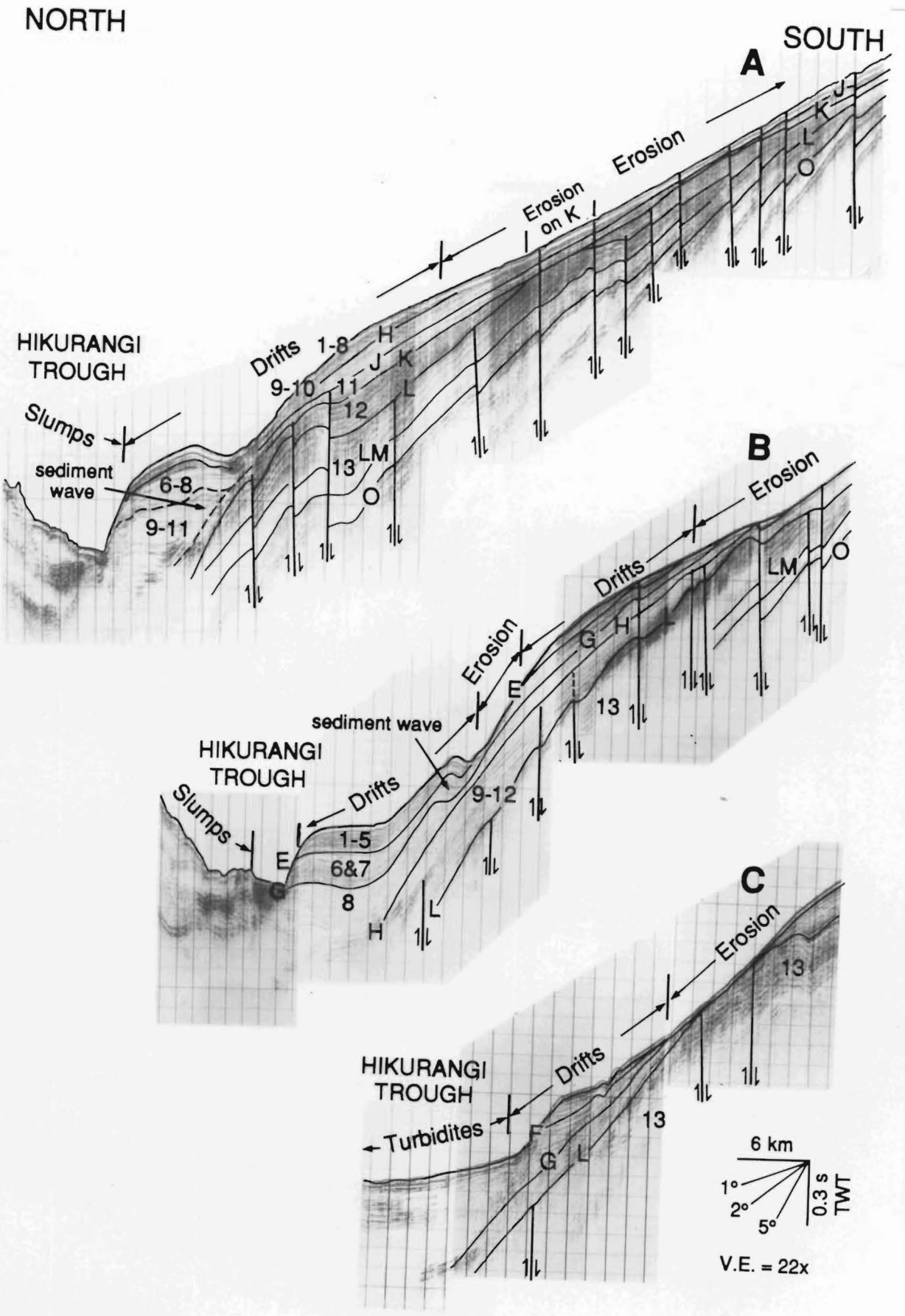
NORTH
SOUTH
A
Erosion
Erosion on K
J
K
L
O
HIKURANGI TROUGH
Drifts 1-8
H
9-10
11
12
13
LM
Slumps
sediment wave
6-8
9-11
B
Erosion
Drifts
LM
O
G
H
E
sediment wave
HIKURANGI TROUGH
Slumps
Drifts
1-5
6&7
8
9-12
C
Erosion
13
HIKURANGI TROUGH
Drifts
Turbidites
F
G
L
6 km
1°
2°
5°
0.3 s TWT
V.E. = 22x

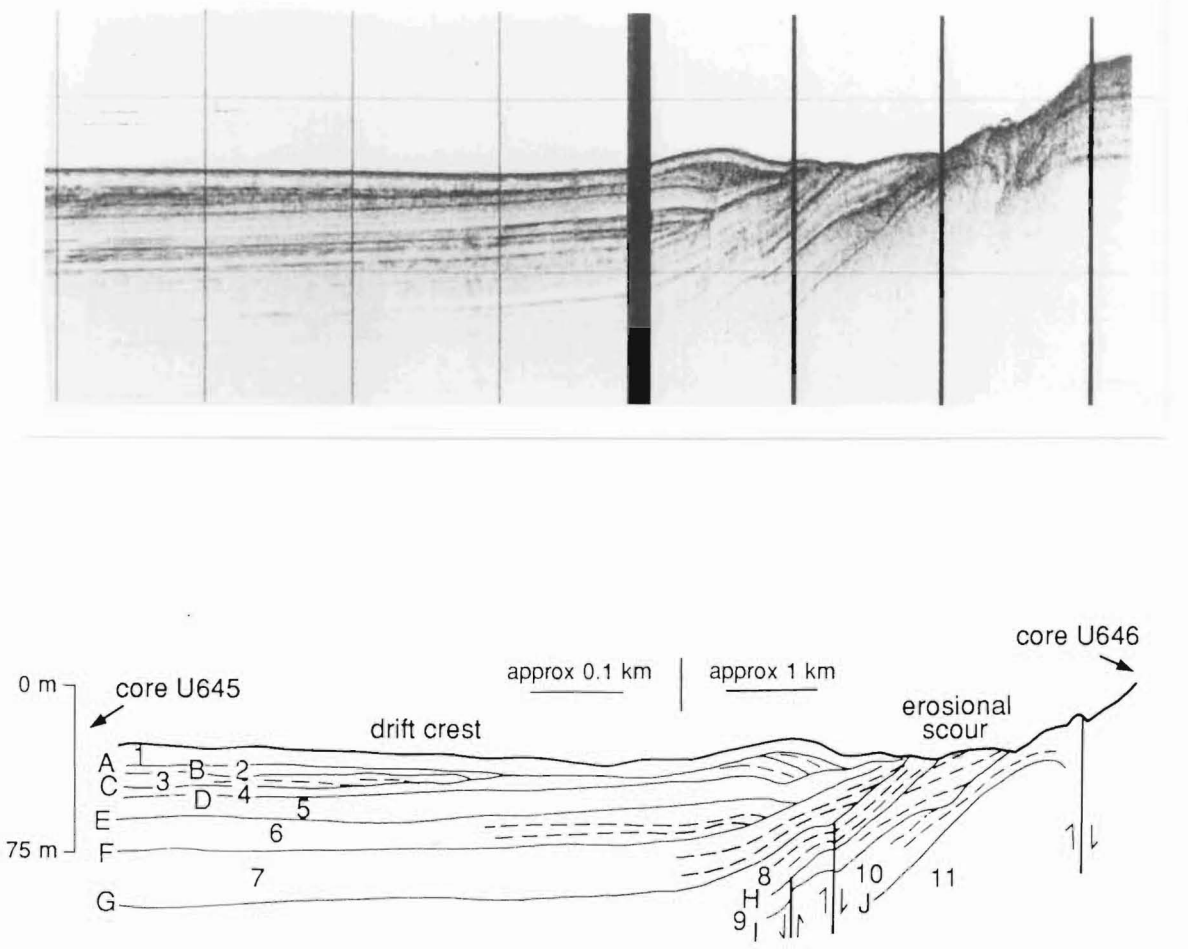

Fig. 4.4. 3.5 kHz seismic profile 4 recorded between core sites U645 and U646 (location on Fig. 4.1 — top and Fig. 4.7). Interpretation shows the mid-slope stratigraphic relationships between various units (numbered) and their bounding unconformities (lettered). The horizontal bottom trace left of the vertical black band (acoustic interference) was recorded while the ship was drifting slowly off station at core site U645. The section to the right of the vertical black band was recorded at normal underway speed (cf. with Fig. 4.5C). See Fig. 4.2 for seismic stratigraphy. Approximate water depths can be obtained from Fig. 4.1.

Fig. 4.5. Examples of 3.5 kHz seismic-reflection profiles 5A to 5D showing various stratigraphic relationships between Plio-Pleistocene units (numbered) and their bounding unconformities (lettered), continued on following page. Late Quaternary drift accumulations and erosional scours are shown on interpretations. Profile locations on Figs 4.1, 4.7 and 4.8. Note the positions of normal faults. **A.** Down-slope thickening units onlapping beneath the mid-upper slope. **B.** Lower slope lenticular sediment drift, reduced area of mid-slope erosion, and upper slope hemipelagic deposits. **C.** and **D.** Mid-slope current scour and lower slope sediment drifts with subdued, migrating sediment waves. Arrows above the seafloor indicate intersecting profiles. Approximate water depths can be obtained from Fig. 4.1

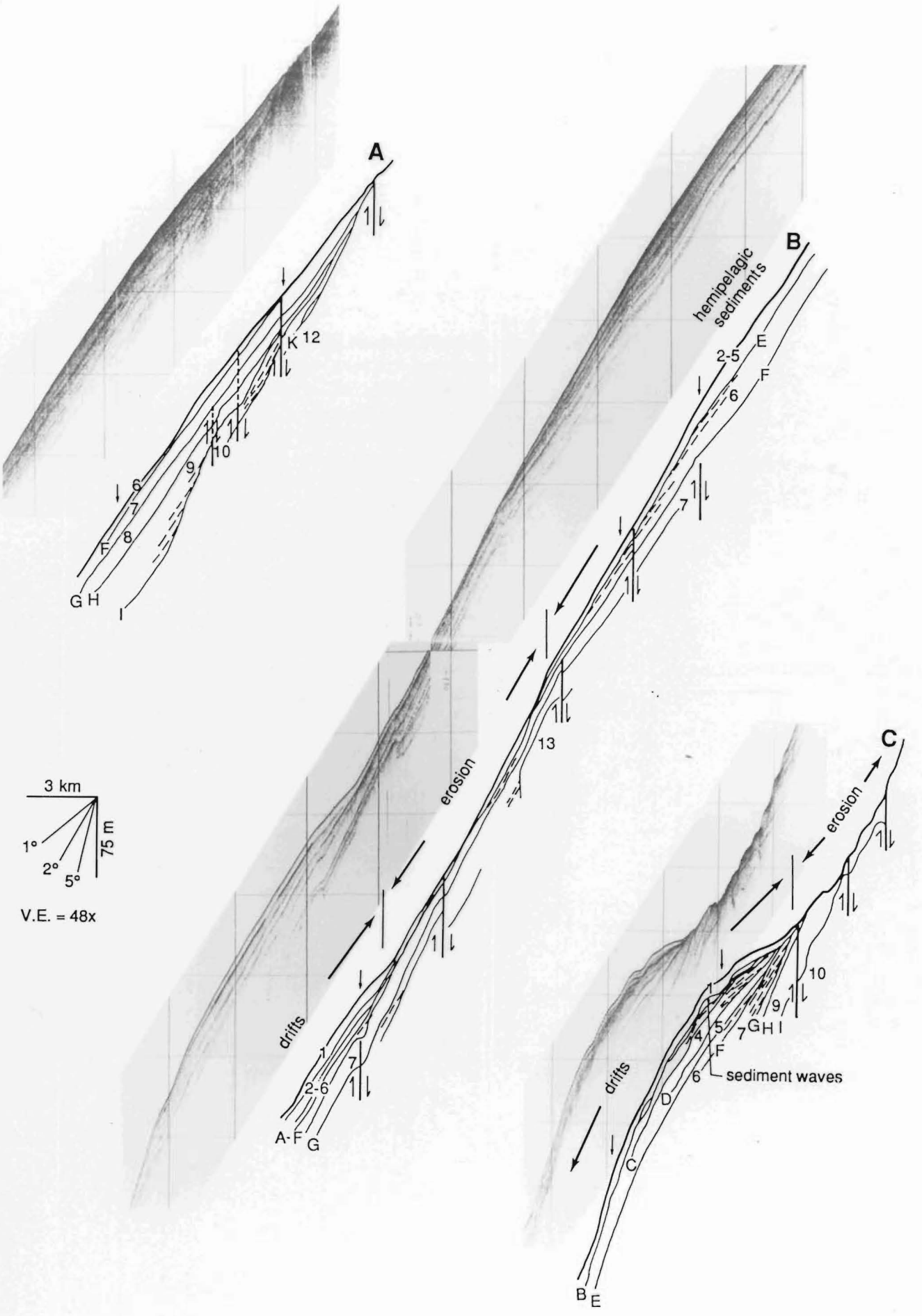
A
B
C
hemipelagic sediments
erosion
drifts
sediment waves
3 km
1°
2°
5°
75 m
V.E. = 48x

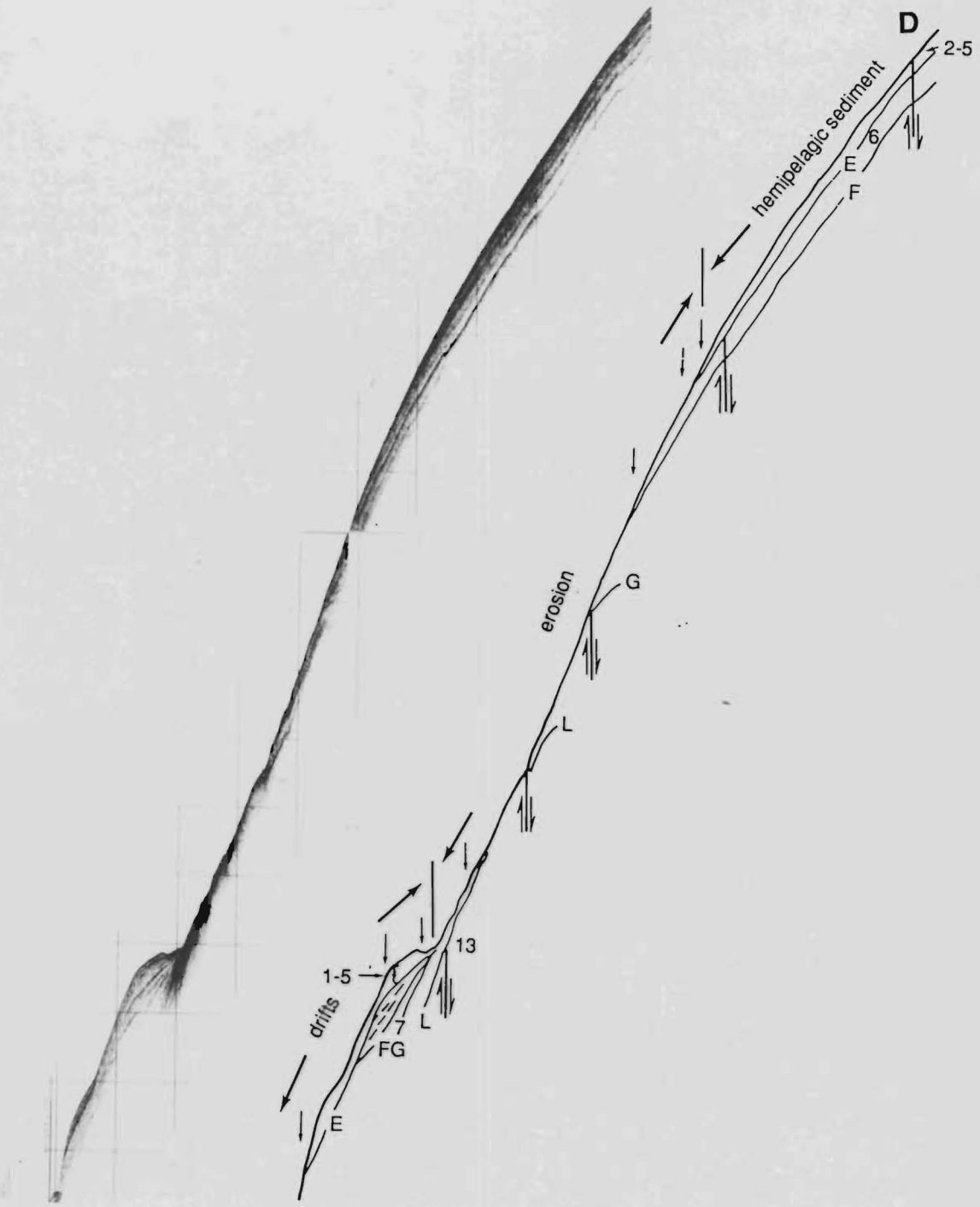
D
2-5
hemipelagic sediment
6
E
F
erosion
G
L
13
1-5
drifts
7
L
FG
E

Fig. 4.6. 3.5 kHz seismic profiles 6A and 6B parallel-to-slope showing the relationships between various Plio-Pleistocene units, and the positions of late Quaternary current scours and sediment drifts (continued on following page). Line drawings show interpretations. Profile locations on Figs 4.1, 4.7, and 4.8. Arrows above the seafloor indicate intersecting profiles. Approximate water depths can be obtained from Fig. 4.1.

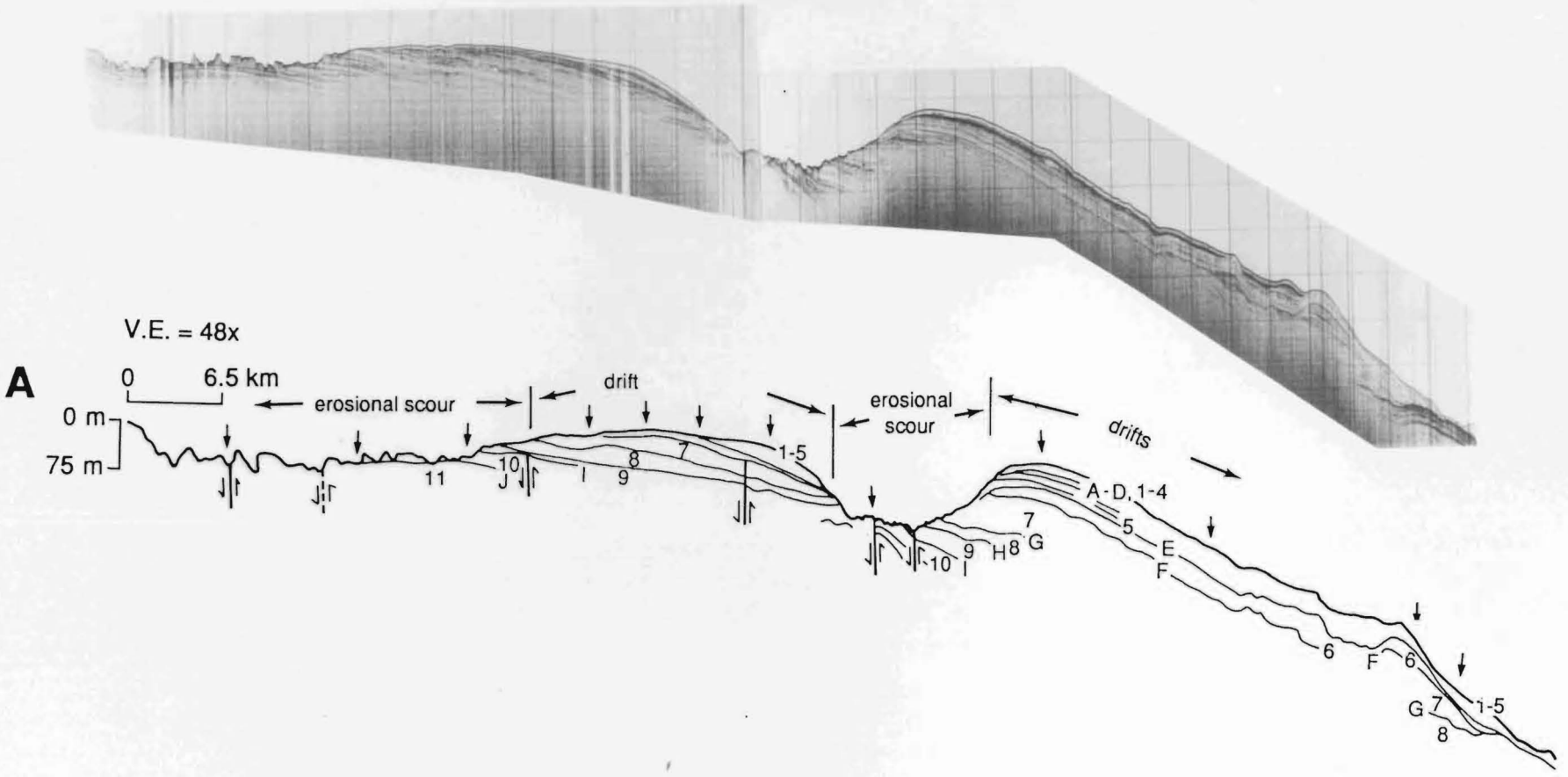
V.E. = 48x
A
0
6.5 km
0 m
75 m
erosional scour
drift
erosional scour
drifts
11
10
J
I
9
8
7
1-5
A-D, 1-4
5
E
F
6
F
6
G
7
8
1-5
10
I
9
H
8
G
7

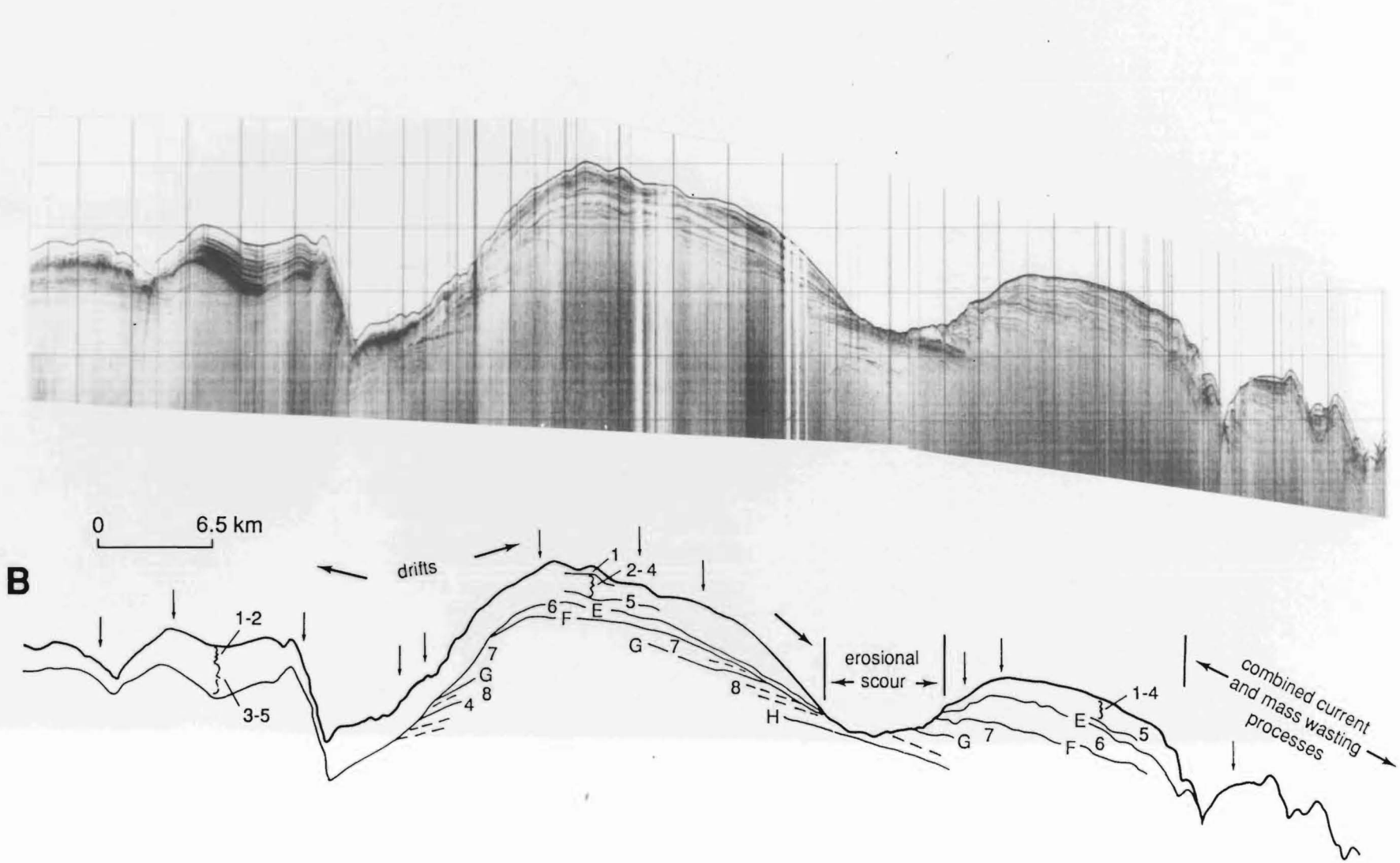
0
6.5 km
B
drifts
1
2-4
1-2
6
E
5
F
7
G
G
7
8
4
8
H
3-5
erosional
scour
1-4
E
5
G
7
F
6
combined current
and mass wasting
processes

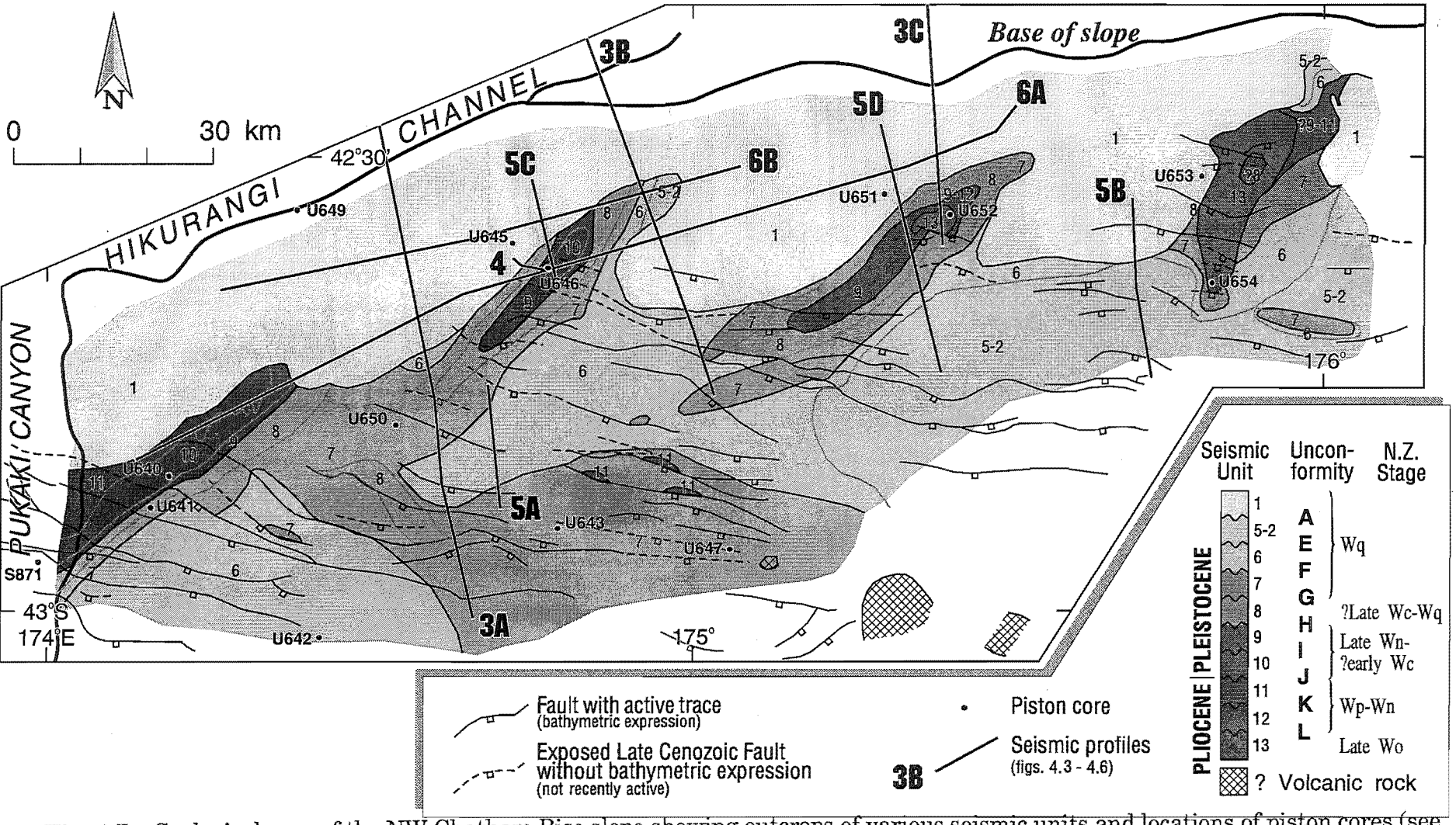

Fig. 4.7. Geological map of the NW Chatham Rise slope showing outcrops of various seismic units and locations of piston cores (see Fig. 4.1 for map location). Seismic profiles are shown in Figs 4.3 to 4.6. Tectonic structure is simplifed from Fig. 6.5. New Zealand stage symbols : Wo = Opoitian; Wp = Waipipian; Wn = Nukumaruan; Wc = Castlecliffian; Wq = Haweran.

A biostratigraphic framework for the seismic-stratigraphic analysis has been provided by nannofossil and foraminiferal studies of fourteen selected cores from seven different sedimentary units (Figs 4.2 and 4.7). The details of the biostratigraphy are presented in section 4.3. The ages of the sediments are tied to New Zealand Stage designations, which have been correlated elsewhere to the international time scale by Edwards *et al.* (1988) using widespread bioevents along with radiometric, magnetostratigraphic and oxygen isotope data. Two of the Late Pleistocene tuffaceous horizons in the cores have been correlated tentatively with tephra in several other southwest Pacific deep-sea cores and in sequences on land in New Zealand (Fig. 4.2) (Appendix 3).

4.2.2 SEISMIC UNITS 12–7 (c. 3.6 to 0.3 Ma)

The mid-Pliocene to Early Pleistocene seismic units 12 to 9 were deposited throughout most of the region as relatively simple down-slope thickening wedges whose internal reflections onlap the basal unconformities of each seismic unit (Figs 4.3 to 4.5). Locally, the units thicken on the downthrown sides of normal faults that were active during deposition (Fig. 4.3). Units 12–9 are up to 255 m total stratigraphic thickness (assuming a seismic velocity of 1700 m/s), and they generally crop out in areas of most intense Late Pleistocene current erosion; notably in the axes of oblique-to-slope scour channels (Fig. 4.7). The earliest mid-bathyal erosion recorded occurs on the mid-Pliocene unconformity K (Fig. 4.3A). Two younger erosional events are recorded as unconformities I (Late Pliocene) and H (mid-Pleistocene) (Figs 4.2 and 4.4). The erosional portions of surfaces K, I and H appear to be restricted to the mid-slope area directly north of Mernoo Saddle, between Pukaki Canyon and 175°E (Fig. 4.8A). The detailed distribution patterns of the eroded portions of unconformities K, I and H are not well constrained because of limitations in their correlation in 3.5 kHz profiles and limited resolution and local masking of reflections by bubble pulse reverberation in airgun profiles. The currents that caused the erosion may have formed an oblique-to-slope scour in the area coinciding with one of the prominent, Late Pleistocene scour channels (compare Figs 4.1 — top and 4.8A).

Some of the sediment eroded during this Late Pliocene-Early Pleistocene period is inferred to have been redeposited further north at the base of the slope in onlapping packets that form the oldest part of the now regionally extensive sediment drifts (Fig. 4.8A). Figure 4.3A shows these packets in units 11–9 onlapping the lower slope, and thickening rapidly beneath the southern margin of the Hikurangi Trough. Within the sediment packets subdued sediment wave migrate up-slope towards the erosional scours. The sediment waves appear to have formed by sediment 'spill-over' from the mid slope erosional scours. These older drift deposits of limited areal extent

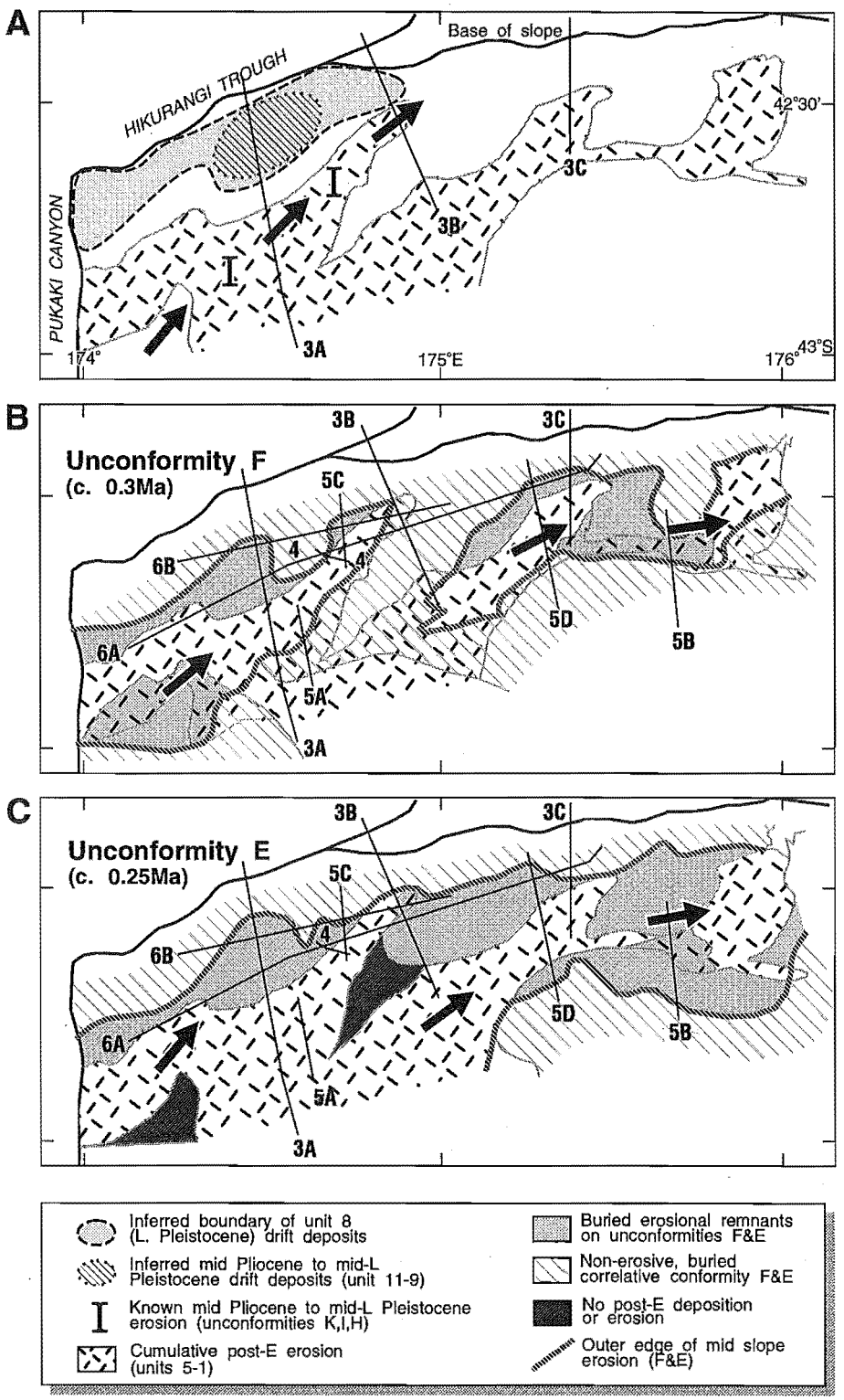

Fig. 4.8. Maps of the scour and drift region on the NW Chatham slope showing the areal distributions of some of the older (pre-unconformity E; > 0.25 Ma) drift deposits and erosional surfaces (see Fig. 4.1 — top for map location). For reference, in each map the late Quaternary (post-unconformity E) pattern of mid-slope scour is also shown. See Figs 4.3 to 4.6 for seismic profiles. **A.** Inferred distributions of units 11–9 (mid Pliocene to mid-Late Pleistocene) and unit 8 (Late Pleistocene) sediment drifts, together with known areas of erosion on mid Pliocene to mid-Late Pleistocene unconformities K, H and I. Arrows indicate the inferred direction of the associated bottom currents. **B.** Extent of erosion on unconformity F. **C.** Extent of erosion on unconformity E.

probably contain interfingering sandy turbidites of Hikurangi Channel axial dispersal, although most turbiditic material originating on the eastern South Island margin bypassed this southern part of the Hikurangi Trough, to be deposited north of the Chatham Rise (Fig. 3.2) (Lewis and Pettinga, in press). Up slope of the drifts, units 11–9 are thinner and hence, sedimentation rates were lower. The up-slope parts of units 9 and 10 were cored (U646 and U640, Figs 4.2 and 4.7) and consist predominantly of moderately to well compacted, hemipelagic, olive-grey, nannofossil-rich silty clays with minor amounts of glauconitic sand and rhyolitic ash (Figs 3.6 to 3.8).

The younger, Late Pleistocene seismic units 8 and 7 (Fig. 4.2) onlap their underlying boundaries (Figs 4.3 to 4.6) and also thicken dramatically down slope beneath the lower slope sediment drifts. Thickening occurs west of 175°E in unit 8 (Figs 4.3A, B; 4.8A) and west of 175°30'E in unit 7 (e.g., Figs 4.3B, C; 4.8A). Figure 4.3B shows that in part of the sediment drift complex this rapid lower-slope thickening of units 8 and 7 was accomplished by development of a single, large, up-slope-migrating sediment wave, which has subsequently evolved into a prominent bathymetric feature following further late Quaternary drift aggradation (see seismic units 6–1, section 4.2.3). About 30 km up slope and southwest of this sediment wave, the base of unit 8 (unconformity H) locally erodes the underlying strata (Figs 4.4 and 4.8A). Outcrops of unit 8 are restricted mainly to the axes of scour channels, whereas unit 7 crops out throughout a much larger area of eroded slope (Fig. 4.7). Cores from these units (U641, U649, U650, U643; Fig. 4.7), mainly from locations up-slope of the sediment drifts where the units are thinner, consist of olive-grey, hemipelagic, silty clays (Figs 3.6 to 3.8). In contrast, the toes of the drift deposits probably contain interfingering turbidites that overspilled the southern Hikurangi Trough axial channel.

In summary, units 12 to 7 were, apparently, deposited during a period of intermittent, but overall increasing, bottom-current activity. A sediment drift on the lower slope was initiated in the area between 174°35'E and 174°50'E during the time interval spanning deposition of units 11 to 9. The drift then aggraded and expanded along slope to extend from Pukaki Canyon to 175°E during the Late Pleistocene development of unconformity H and the deposition of unit 8 (Fig. 4.8A). This drift then expanded further eastwards to at least 175°30'E during the accumulation of unit 7 (e.g., Fig. 4.3C). By analogy with the seismic expression of the latest Quaternary drift deposits (units 6–1, section 4.2.3) and their relationship to the eroded areas of seafloor, which are well constrained (Fig. 4.1 — top), the bottom currents are inferred to have been active locally during the deposition of units 8 and 7 as well as during formation of their bounding unconformities.

4.2.3 SEISMIC UNITS 6–1 (c. 0.30 Ma to Present)

The stratigraphic relationships of the youngest six seismic units are well constrained by the 3.5 kHz data base. The Late Pleistocene unconformity F represents a period of dramatically increased current erosion (Fig. 4.2). A map of the erosional extent of this unconformity (Fig. 4.8B) indicates an area of expanded seafloor scour relative to the older erosion surfaces and to the most recent (post unconformity E, units 5–1, c. 0.25 Ma to present) erosional phase mapped in Chapter 3 using 3.5 kHz echo-character (compare Figs 4.1 — top and 4.8B). A broad, 30 km-wide, ENE-trending zone of erosion between Pukaki Canyon and 176°E occurred during the development of unconformity F. Within this zone of erosion there are oblique-to-slope *en echelon* scours, but these are wider and less well defined than the younger, late Quaternary (post unconformity E) scours mapped by 3.5 kHz echo-character mapping (Fig. 4.8B).

Following this period of extensive current erosion, the erosional surface of unconformity F on the lower slope was covered by drift deposits, which thin up-slope towards the contemporary scour axes and which formed during deposition of seismic unit 6 (Figs 4.3C; 4.4; 4.5B, C; and 4.8B). Beneath the upper slope in the west of the mapped area the erosional remnants of unconformity F were buried by parallel-bedded, hemipelagic deposits. In contrast, large mid-slope parts of the unconformity surface have since been removed from areas of deepest scour by younger erosional events (Fig. 4.8B), exposing older units beneath the unconformity (Fig. 4.7). Thus, unit 6 accumulated on the underlying erosion surface during continuing, but significantly reduced, bottom-current activity throughout a less extensive area of the mid-slope. On the mid-lower slope sediment accumulated in a down-slope thickening wedge, which forms part of the sediment drift deposits; while predominantly hemi-pelagic sediment buried the unconformity up slope from the current-swept seafloor.

The upper boundary of seismic unit 6 is a Late Pleistocene (c. 0.25 Ma) unconformity (labelled E in Fig. 4.2) whose erosional extent is the most widespread recorded beneath the slope (Fig. 4.8C). The upper and lower slope limits of this erosion occur at 700–900 m and 2000–2300 m water depths respectively, and outline an irregular, 30 km-wide, ENE-trending erosional zone on the mid-slope between Pukaki Canyon and 176°E. Although this zone represents a period of extensive erosion, the pattern of oblique-to-slope *en echelon* scour channels associated with younger, late Quaternary erosional phases (Fig. 4.1 — top) was not developed during this time. Nevertheless, on both erosion surfaces E and F there is evidence of the current separating into higher velocity cores. One high-velocity core produced deep erosion in an oblique-to-slope scour channel extending northeast from the eastern wall of Pukaki Canyon (Fig. 4.8B, C). The deeper part of this channel was later buried by sediment drift units 5 to 1 (Fig. 4.6B). The relationship of this relict scour

with Pukaki Canyon is unclear. The current either cut across the top of the existing Pukaki Canyon and eroded the scour channel above its eastern wall, or Pukaki Canyon formed after this phase of erosion, and truncated the previously formed scour channel.

Following these Late Pleistocene periods of widespread, intensive erosion, a significant reduction in current strength and erosive capacity of the bottom currents occurred, and seismic units 5 to 1 accumulated on part of the previously eroded slope (e.g., Fig. 4.6B; compare Figs 4.1 — top, 4.7 and 4.8C). It was during this latest, post-unconformity E (c. 0.25 Ma to present) phase of sedimentation history that the Late Pleistocene pattern of erosion and deposition mapped in Chapter 3 using 3.5 kHz echo-character methods became established. This latest Quaternary phase of sedimentation history involved a current that separated as it flowed obliquely down slope before apparently merging again further east into a single contour current on the lower slope above the Hikurangi Channel (Fig. 4.1 — top, "combined current-controlled and mass-wasting zone"). Three prominent southwest-northeast trending, oblique-to-slope, *en echelon* scour channels developed, apparently emanating from Mernoo Saddle. The current velocity fluctuated during this period between 0.25 Ma and present, when seismic units 5–1 were deposited. The boundaries of the units are predominantly onlap surfaces (A–D, e.g., Fig. 4.4); although they are very locally erosional and are inferred to represent pulses in localised sedimentation in between hiatuses. On the drift deposits down slope from the current-swept scours, subdued sediment waves are developed locally within units 5 to 1 (Figs 4.5 and 4.6B). These units can be correlated across and around the ends of the scour channels from one part of the sediment drift complex to the next. This indicates that the three oblique-to-slope scours were active simultaneously and the current that formed them had separated into distinct high-velocity cores. Profiles orientated down slope (e.g., Fig. 4.5) and along slope (Fig. 4.6) show the drifts are clearly lenticular, with units 5–1 thinning and wedging out towards the scours. This geometry becomes more pronounced where the subdued sediment waves are developed, adjacent to the deepest scours. In contrast, up-slope of the erosional zone east of 175°10'E, units 5 to 2 accumulated as parallel-bedded hemipelagic, sediments burying erosional parts of unconformity E (e.g., Figs 4.5B and 4.8).

Seismic unit 1 is the acoustically transparent veneer that thickens away from the edge of the eroded scours and extends to the toe of the slope between Mernoo Saddle and 176°E (cores U645, U651, U653; Figs 4.4 to 4.7). The veneer also occurs on parts of the irregular, lower slope further east (Fig. 4.6B). This youngest unit of homogeneous mud is acoustically similar to unit 5, whereas units 2 to 4 have higher amplitude, migrating wavy reflectors which are inferred to be higher flow regime deposits containing layers or laminae of reworked silt and/or sand (e.g., Fig. 4.5C).

4.3 BIOSTRATIGRAPHY OF SEDIMENTS

The biostratigraphic ages of cores are compatible with the younging demonstrated by seismic stratigraphy (Fig. 4.2). Seismic units are discussed below in order of decreasing age.

Reflector LM (S871)

Core S871 from the axis of Pukaki Canyon (Figs 1.5, 3.2, 4.1 and 4.7) was positioned very close to reflector LM, the base of the strongly reflective seismic unit 13 on airgun profiles (Fig. 4.3). The sample contains *Bolivinita quadrilatera* and *Bolivinita pohana* (first occurrence (FO) at the base of, and in, the early Tongaporutuan Stage, respectively; Edwards, 1987; Hornibrook *et al.,* 1989). The sample also contains *Globoquadrina dehiscens* (last occurrence (LO) at 9.2 Ma; Wright *et al.,* 1985) and *Globorotalia miotumida* (sinistral), which also indicate an early Tongaporutuan (Late Miocene) age of 10.5–9.2 Ma.

Seismic unit 13 (U653, U652, U654)

Three cores recovered samples from stratigraphic positions close to the top of unit 13. Each core contains *Globorotalia puncticulata* s.s., *Globorotalia crassaformis,* and *Globorotalia crassaconica,* taxa which first appear in the early Opoitian Stage (Early Pliocene, 5.0–3.6 Ma; Hornibrook, 1982; Edwards, 1987; Edwards *et al.,* 1988), together with Early Pliocene, Opoitian-Waipipian Stage *Globorotalia subconomiozea* (Scott *et al.,* 1990). Core U654 also contains more advanced *Globorotalia inflata* morphotypes and *Globorotalia puncticuloides*?, and may be a slightly younger sample than U653 and U652. However, it also contains *Cibicides finlayi* so it is not younger than Opoitian (Hornibrook *et al.,* 1989). Thus, unit 13 is inferred to extend from early Tongaporutuan (10.5–9.2 Ma) up to the late Opoitian-early Waipipian (c. 4.0–3.5 Ma, Late Miocene-late Early Pliocene) (Fig. 4.2).

Although the seismic stratigraphy of the easternmost core site (U661) is not established, the sample contains *G. crassaconica, G. subconomiozea,* sinistral forms of *G. crassaformis* and advanced *G. puncticulata*, along with *G. inflata*. It is inferred to be late Opoitian-Waipipian age.

Seismic units 12-11

No cores were recovered from units 12 and 11, so the precise ages of the units and their boundaries K and J are uncertain. The units fall within the period between early Waipipian and late Nukumaruan (c. 3.6–1.4 Ma).

Seismic unit 10 (U640)

Core U640 is inferred to be mid-late Nukumaruan (Late Pliocene-Early Pleistocene,

2.4–1.2 Ma) age (Fig. 4.2). The core contains well-developed specimens of *Globorotalia crassacarina* and *G. puncticuloides,* atypical specimens of *Globorotalia crassula,* and specimens of the nannofossils *Gephyrocapsa sinuosa* (FO in mid Nukumaruan; Edwards, 1987) and *Gephyrocapsa oceanica* group. *Globorotalia crassaformis* (thought to terminate in the Nukumaruan; Scott *et al.,* 1990) does not occur in the sample. Reworked Late Eocene-Miocene nannofossils are present in small numbers.

Seismic unit 9 (U646)

Core U646, positioned to sample unit 9, contains *G. crassula, G. puncticuloides, G. crassacarina,* and *Globorotalia truncatulinoides tosaensis* (well developed in the mid-late Nukumaruan; Scott *et al.,* 1990), along with specimens of *G. oceanica* group, *G. sinuosa,* and *Pseudoemiliania lacunosa.* The age of the core is inferred to be mid-late Nukumaruan Stage. Small numbers of reworked Late Eocene-Miocene nannofossils occur in the sample.

Seismic unit 8 (U641, ?U649)

Specimens of both *G. truncatulinoides* and *G. crassacarina* occur in U641, which was positioned to sample unit 8, indicating a late Castlecliffian age for the unit. Approximately 90% of *G. truncatulinoides* in core U649 have a keel developed on the last chamber, which suggests that the sample lies close to the transition to *G. truncatulinoides,* thought to occur in the Castlecliffian Stage (1.2–0.4 Ma) in the New Zealand region (Scott *et al.,* 1990). The samples do not contain *P. lacunosa* (LO at 0.46 Ma, late Castlecliffian; Edwards, 1987) or *Gephyrocapsa caribbeanica,* although the absence of the latter may be due to post-depositional dissolution of the species rather than deposition occurring after its extinction at 0.2 Ma (Edwards, 1987). Thus, unit 8 is inferred to be late Castlecliffian or earliest Haweran (mid-late Pleistocene) age (Fig. 4.2). Very minor reworking of Miocene nannofossils is recorded within the unit.

Seismic unit 7 (U650, U643)

Over 80% of specimens of *G. truncatulinoides* are keeled in core U650, and *P. lacunosa* is absent. These indicators, together with the seismic-stratigraphic position of the unit and the possible presence of Mt Curl Tephra in core U650 (Appendix 3), suggest a Haweran (Late Pleistocene, < 0.4 Ma) age for unit 7 (Fig. 4.2). It is inferred that the overlying unconformity F is close to c. 0.3 Ma. If so, *G. caribbeanica* is unexpectedly absent from U650 but this is inferred to be due to the substantial degree of corrosion resulting in reduced nannofossil content and low diversity in the sample. Minor amounts of reworked, mainly Oligocene nannofossils occur in the unit.

Seismic unit 6 (U642)

The presence of *G. truncatulinoides* (nearly all keeled), and the absence of *P. lacunosa,*

G. crassacarina, and the late Quaternary entrant *Globorotalia hirsuta,* together with the seismic-stratigraphic position of the unit and tentative correlation with a 0.27 Ma deep-sea tephra, layer E (Appendix 3), suggests an early-mid Haweran age for core U642. The absence of *G. caribbeanica* may not be reliable due to sample corrosion.

Seismic units 5-2

No cores were recovered from units 5–2, however, they are constrained by enveloping seismic units to a late Haweran (Late Pleistocene) age.

Seismic unit 1 (U651, U645, U653)

One of three cores from unit 1 was examined for microfossil content. A clear late Quaternary age for core U651 is indicated by the presence of *Emiliania huxleyi* and *G. hirsuta* (FO at 0.27 Ma and 0.23 Ma respectively; Edwards, 1987), and the absence of *P. lacunosa* and *G. caribbeanica.* This unit is inferred to be largely post last-glacial in age, based on an interpretation that it represents a recent phase of reduced current activity. Reworked Oligocene nannofossils include excellently preserved specimens of *Chiasmolithus altus,* suggesting a nearby source.

4.4 DISCUSSION

The mid-Pliocene to Recent (post-unconformity L) succession (seismic units 12–1) thickens down slope from the eroded crest of Mernoo Bank to > 400 m thick (> 0.5 s TWT) on the lower slope. The geometry of this succession clearly is not a simple wedge. Sedimentation on the slope has been heavily influenced by strong bottom currents since at least the middle Pliocene, and large lenticular drift deposits have built up the lower slope below areas of seafloor erosion. Beyond the toe of the slope, the narrow, southern Hikurangi Trough between the Chatham Rise and northeast South Island is a conduit for vast quantities of mud and sand to the rapidly aggrading channel-levee system east of Cook Strait, supplied from the northeastern South Island shelf (Chapter 3; Lewis and Pettinga, in press).

The seismic-stratigraphic relationships observed indicate that Pliocene-Recent sedimentation on the NW Chatham Rise slope has been episodic. The unconformities that bound Pliocene-Pleistocene units 12–1 represent intermittent periods of erosion and/or non-deposition. The age of the regional unconformity L, which is an onlap surface rather than an erosional surface over most of the slope, is constrained biostratigraphically to be late Early Pliocene-middle Pliocene (Fig. 4.2). Although better chronostratigraphy is required, the age of unconformity L may possibly be coincident or slightly older than the global 3.2 Ma climatic cooling event (Joyce *et al.,* 1990) characterised by a net increase in average global ice volume, bottom water

cooling, and possible increased glaciation in Antarctica (e.g., Kennett and von der Borch, 1986). Unconformity L formed well after the Late Miocene initiation of rapid uplift and erosion of the Southern Alps, with its consequent increased offshore terrigenous sedimentation (Lewis *et al.*, 1986; Wood *et al.*, 1989) and the surface probably pre-dates the first major glaciation, the Ross Glaciation, recorded onshore in New Zealand at 2.4–2.6 Ma (e.g., Nelson *et al.*, 1986; Edwards, 1987; Suggate, 1990). The Ross Glaciation is marked at DSDP site 594, which is 300 km to the south of the present study area, by the first major influx of hemipelagic detritus (Nelson, 1986). Further south, the levees of the Bounty Fan began aggrading at about 3.0 Ma (Carter *et al.*, 1990), probably within the interval spanned by units 12 and 11.

The mid-Late Pleistocene unconformity H marks the beginning of a significant change to a more vigorous, but episodic bottom-circulation system in the Mernoo Saddle region. Widespread mid-bathyal bottom-current erosion has continued since this time, however current strength has fluctuated dramatically. The intensity of erosion varied and two major phases of Late Pleistocene erosion are recorded by unconformities F and E (Fig. 4.8). During periods of diminished bottom-current activity between erosion of surfaces F and E, the sediment drifts on the lower slope continued to develop below mid slope scour channels, while hemipelagic sediment accumulated up slope of the current swept seafloor and temporarily blanketed parts of the scour depressions. Following erosion of unconformity E, the overall current intensity waned, but continued to fluctuate. The northeast-flowing current separated to form three prominent oblique-to-slope scour channels and deposit the associated units 5–1 on the drifts.

These observations show that (1) there was a significant increase in sedimentation in the late Early Pliocene resulting in regional onlap (surface L; c. 3.4–3.2 Ma); (2) erosion associated with limited bottom-current activity through Mernoo Saddle commenced in the mid-Pliocene (unconformity K, c. 2.5 Ma); (3) regional-scale mid-slope erosion and non-deposition did not commence until the mid-Pleistocene (unconformity H, c. 0.5–0.6 Ma); and (4) the younger pattern of prominent current scours and associated sediment drifts revealed by 3.5 kHz echo-character (Chapter 3 and Fig. 4.1 — top) commenced in the Late Pleistocene following erosion of unconformity E (c. 0.25 Ma, Fig. 4.2).

The maximum long-term sedimentation rates from lower slope areas of sediment drift accumulation are c. 80–125 mm/ka (270–430 m since c. 3.4 Ma). Considering (1) the late Quaternary rates of hemipelagic deposition on the eastern North Island lower continental slope (c. 100 mm/ka; Lewis, 1980), (2) the Pliocene-Pleistocene rates at DSDP site 594, 300 km south of the investigated area (25–150 mm/ka; Kennett *et al.*, 1986), and (3) the Pleistocene rates of abyssal pelagic sedimentation

up to 1000 km east of North Island (< 2 mm/ka; Watkins and Huang, 1977); then hemipelagic sediments accumulating up slope of sediment drifts on the NW Chatham Rise slope were probably deposited at short-term rates in the order of c. 50–150 mm/ka. This rate implies that individual cores (1.1–3.2 m long) represent between c. 7 and 64 ka of continuous sedimentation.

4.4.1 LIMITATIONS IN STRATIGRAPHIC RESOLUTION

The following limitations in stratigraphic resolution are noted: (1) six of the 13 Pliocene to Recent seismic units were not sampled (Fig. 4.2); (2) there is limited chronostratigraphic control provided by the biostratigraphy, partly because of high corrosion of the calcareous coccoliths in the samples, the limited number of planktic foraminifera datums in this part of the geological record and the uncertain paleoenvironmental control on some bioevents (e.g., Edwards, 1987); (3) there is uncertainty for some cores as to the exact seismic unit penetrated (Fig. 4.2) because of correlation difficulties resulting from faulting near the core site; and (4) the short (1–3 m) cores represent only small sections of the c. 10–40 m thick seismic units.

Apart from the two tentative Late Pleistocene tephra correlations, the ages of the cores have been assigned exclusively on the basis of their calcareous nannofossil and foraminiferan biostratigraphy. Thus, they are tied to the New Zealand late Cenozoic microfossil zonations which have been developed largely from onshore sequences and from the Tasman Sea DSDP core 284 (Beu *et al.*, 1987; Edwards, 1987). There is a possibility however, which cannot be discounted, that local anomalies in first and last appearances of significant taxa might occur due to unfavourable paleoenvironmental conditions in the region of subtropical convergence. At the western end of the Chatham Rise, the modern surface water circulation patterns and interactions between cool subtropical and subantarctic water are complex and variable, and the Subtropical Convergence Zone is not well defined (Heath, 1976, 1985). For example, south of the Subtropical Convergence Zone at DSDP site 594, the planktic foraminifer *G. inflata* appears at the Gauss/Matuyama boundary in the adopted magnetostratigraphy, c. 1 Ma earlier than it does at DSDP site 593 (N. Hornibrook, pers. comm., January 1992). Also, *G. crassula* makes its first appearance at that site in the late Nukumaruan, whereas, elsewhere in the New Zealand region, it is recognised as a datum close to the base of the Nukumaruan Stage (2.40–2.15 Ma; Edwards, 1987). The effect of bottom currents, even in areas of 'modified' hemipelagic sedimentation up slope of major seafloor scour and sediment drift accumulation, has been to produce low-diversity, corroded nannofloras with loss of solution-prone species. Bottom currents are also inferred to be responsible for reworking the small quantities of Oligocene and Miocene nannoflora into the Pliocene-Pleistocene sediments from

nearby sources, probably on the upper flanks of Mernoo Bank (Herzer and Wood, 1988).

4.4.2 PERIODICITY OF UNCONFORMITIES: A GLACIO-EUSTATIC CONTROL ON THE FLUCTUATION OF THE MID-BATHYAL CURRENTS

The cores have been used to place the seismic units into a broad chronostratigraphic framework; however they do not constrain the absolute lengths of time represented by individual units and their intervening unconformities. Although core U641 from unit 8 (Fig. 4.7) lacks *Pseudoemiliania lacunosa* (LAD 0.46 Ma, Fig. 4.2), the base of the unit could be older, perhaps 0.5–0.6 Ma. This suggests an average periodicity of the units in the range of 57–75 ka. In contrast, units 12 to 9 inclusive, deposited during a maximum interval of 3.0 Ma between unconformities L and H, represent a maximum unit periodicity of about 750 ka.

The < 100 mm thick bed of mud in the lower slope parts of the late Quaternary scour channels (representing an up-slope correlative of unit 1, which is not resolved on seismic profiles) has been interpreted as post-glacial material deposited during a Recent phase of reduced current flow (Chapter 3). It is inferred that during periods of Late Pleistocene glacio-eustatic lowering of sea-level, the northward flow of intermediate-depth water over Mernoo Saddle was intensified. This apparent climatic control on the Late Pleistocene paleoceanography at the western end of the Chatham Rise is reflected also in the evolution of the Plio-Pleistocene sedimentary units. Considering the limitations in stratigraphic resolution outlined in section 4.4.1, the averaged frequency of current-controlled unconformities observed within the Late Pleistocene interval is similar to the major (40 and 100 ka) variations in oxygen isotope characteristics of foraminifera in deep-sea cores (Fig. 4.2) (e.g., Nelson *et al.*, 1986b; Joyce *et al.*, 1990) and to the fifth or sixth order, orbital forced, sea-level cyclicity of Carter *et al.* (1991). The increase in bottom-current activity recorded on the slope by unconformity H coincides approximately with the mid-Pleistocene (c. 700 ka) transition, from the spectra of orbital forcing being dominated by a 40 ka period before 700 ka to a 100 ka period since that time (e.g., Shackleton and Opdyke, 1973; Prell, *et al.*, 1979; Joyce *et al.*, 1990) (Fig. 4.2). The increase in current intensity also coincides approximately with an increase in the magnitudes of sea-level change inferred from onshore sequence stratigraphy in New Zealand (e.g., Beu *et al.*, 1987; Edwards, 1987; Carter *et al.*, 1991). However, the seismic units and the intervening unconformities observed here do not result from sea-level lowering in the same way that sequences do in the Vail/Exxon conceptual sea-level model of sequence stratigraphy (e.g., Vail, 1987; Van Wagoner *et al.*, 1988; Vail *et al.*, 1990). Instead,

the seismic units result from fluctuations in the strength of mid-bathyal currents which are related to the associated climatic oscillations. In the conceptual model of sequence stratigraphy, a sequence is interpreted to be the depositional response to one cycle of eustatic sea-level change. The resolution of the available data presented here is not sufficient to tie individual couples of seismic units and unconformities to specific sea-level cycles.

If the above hypothesis of climatic control on the erosion and deposition is correct, there are some similarities and differences between this region and the climatic controls on deep currents in the North Atlantic. During glacial periods, bottom currents flowing across the Hatton and Gardar Drifts intensified and winnowed the silty fraction of the sediments (Wang and McCave, 1990). On the Feni Drift, where current velocities have been relatively lower, orbitally-forced fluctuations in current strength have produced coherent fluctuations in mass accumulation of the silt component of the sediment (Robinson and McCave, in press). The apparently higher velocities on the NW Chatham Rise slope during glaciations led to widespread erosion, producing unconformities detectable in high-resolution seismic profiles.

4.4.3 INTERACTIONS BETWEEN PALEOCEANOGRAPHIC FLUCTUATIONS AND THE LATE CENOZOIC SUBSIDENCE OF MERNOO SADDLE

In contrast to the NW Chatham Rise slope, current-controlled sedimentation processes were active, at least locally, south of Mernoo Saddle as early as late middle Miocene (Fulthorpe and Carter, 1991). Fulthorpe and Carter mapped a complex of sediment drifts beneath the present eastern South Island shelf, and showed how these late Middle Miocene to Early Pliocene deposits were progressively accreted to the paleoshelf foreslope (Fig. 4.1 — bottom). Further east, airgun records shot aboard *Glomar Challenger* reveal a lenticular prograding deposit of Late Miocene age just southeast of Mernoo Saddle (Fig. 4.1 — bottom) (cf. Lewis *et al.*, 1986). These sediment drifts have been buried by Pliocene-Pleistocene slope sediments, although recent scour has occurred around volcanic rocks of the South Mernoo Knolls (Fig. 4.1 — bottom). The Miocene sediment drifts may have been produced by deposition from an ancestral, intermediate-depth flow that turned east at a location south of the present Mernoo Saddle.

Why were intermediate depth currents active south of Mernoo Saddle during the Miocene time, but not active to the north of the saddle until mid-Pliocene time? Regional seismic mapping suggests that Mernoo Saddle began subsiding in the Miocene, possibly concomitant with uplift of Mernoo Bank to the east (Wood *et al.*, 1989). For the South Island margin, south of Mernoo Saddle, Field *et al.* (1989)

calculated, from petroleum exploration well data, subsidence rates of 30–70 m/Ma during the Miocene time and 50–350 m/Ma during the Pliocene-Quaternary. This rapid subsidence led to accommodation space for the flood of clastic sediment shed from the rising Southern Alps. Assuming that (1) late Cenozoic subsidence rates for the western end of the Chatham Rise, at the present location of Mernoo Saddle, and the adjacent South Island margin was between 50 and 100 m/Ma; and that (2) prior to subsidence, the western end of the rise was continuous with the rise crest to the east of Mernoo Bank (c. 400 m water depth); and (3) considering that Mernoo Saddle is now 580 m deep; then the saddle was a maximum of only 80 m deep at about 10 Ma (relative to present sea-level), 80–330 m deep at 5 Ma, and 330–455 m deep at 2.5 Ma when the first episode of mid-bathyal erosion occurred on the NW Chatham Rise slope. We can speculate how such water depths and subsidence history might have influenced bottom circulation in this region. By analogy with the strong (> 0.6 m/s) present-day tidal flows in the deeper part of Mernoo Saddle (Greig and Gilmour, 1992), sub-tidal erosion could have been an important sedimentary process in the saddle during Late Miocene and Early Pliocene times when the saddle was shallower (c. 80–330 m deep) than present, but no erosion is observed on the deeper, continental slope to the north of the saddle at these times. During late Quaternary glaciations, when Mernoo Saddle had subsided to > 500 m deep, some sort of internal hydraulic control of the flow conditions possibly caused the upwelled and mixed, northward-bound, mid-bathyal water passing through the saddle to descend to > 1000 m and erode the continental slope to the north (section 3.5). Perhaps during the Late Miocene and Early Pliocene time, Mernoo Saddle may not have been deep enough to allow the northward passage of up-welled Antarctic Intermediate Water and the generation of the necessary internal flow conditions to produce erosion on the NW Chatham Rise continental slope. The first phase of erosion of the northern continental slope in the mid-Pliocene appears to have begun after a critical amount of subsidence of the saddle had occurred and when certain physical oceanographic flow conditions were generated. By Late Pleistocene times, erosion on the NW Chatham Rise slope was reflecting mainly high-amplitude fluctuations in the mid-bathyal currents, associated with major climatic oscillations. High-amplitude sea-level fluctuations, together with rapid Pleistocene progradation of the South Island margin (e.g., Wood *et al.,* 1989) and its consequent gradual narrowing of Mernoo Saddle and constriction of northward-bound flows, masked the overall effects of slower regional subsidence.

4.5 CONCLUSIONS

(1) Thirteen unconformity-bounded, deep-sea seismic units of Pliocene-Recent age occur in the down-slope thickening late Cenozoic succession on the NW Chatham Rise slope. The stratigraphic relationships of these units reflect an episodic history of current erosion and deposition. The phases of erosion and non-deposition occur near the Subtropical Convergence Zone and reflect fluctuations in the flow of bottom water through the 580-m deep Mernoo Saddle, between the Chatham Rise and the South Island of New Zealand. Current erosion began in the mid-Pliocene (c. 2.5 Ma), but was most widespread regionally in the Late Pleistocene (c. 0.6–0.25 Ma).

(2) A set of oblique-to-slope, *en echelon,* current scours on the middle slope, which are associated with lower-slope sediment drifts, mapped in Chapter 3, is related only to the five youngest (0.25 Ma to present) of these 13 seismic units.

(3) The eight youngest units (8–1), which are Late Pleistocene in age, have a cyclicity of about 57–75 ka. The similarity of this frequency range to that of high-order (40 and 100 ka) glacio-eustatic cycles, together with considerations of the physical paleoceanography and a recent phase of reduced erosion during the Holocene, suggest that the paleoceanographic fluctuations causing the seismic units are related to high-amplitude Plio-Pleistocene glacial-interglacial climatic oscillations. In contrast four older units (12–9), deposited between late Early Pliocene and Late Pleistocene, have a maximum frequency of about 750 ka. This frequency suggests that during this time, many glacial-interglacial oscillations were not sufficiently expressed in the mid-bathyal paleoceanography to produce unconformities detectable on seismic profiles. The mid-bathyal current-influenced units and their intervening unconformities differ in origin to sequences in the Vail/Exxon conceptual sea-level model of sequence stratigraphy.

(4) In contrast to the NW Chatham Rise slope, current-controlled sedimentation south of Mernoo Saddle occurred earlier in time, between the late Middle Miocene and Early Pliocene. Considering a possible late Cenozoic subsidence history of Mernoo Saddle, it is possible that prior to the mid-Pliocene, Mernoo Saddle may not have been deep enough to permit sufficient volumes of bottom water through to produce the internal flow conditions necessary to cause erosion on the continental slope north of the saddle. Apparently, the initiation of erosion did not occur until the saddle had subsided to a critical depth, which coincidently occurred at the onset of Pliocene-Pleistocene climatic oscillations. Phases of widespread Late Pleistocene erosion reflect mainly the high-amplitude glacio-eustatic oscillations and their effect on the bottom-water current flows in the region.

CHAPTER 5

THREE-PHASE EXTENSIONAL FAULTING, NORTHWEST CHATHAM RISE: INHERITED STRUCTURAL CONTROL ON LATE CENOZOIC DEFORMATION

5.1 INTRODUCTION

Many sedimentary basins, orogenic belts and cratonic massifs record a history of poly-phase tectonic deformation resulting from changes in plate boundary configurations. The deformational phases in different areas include various combinations of extension, shortening and wrench tectonics, and commonly involve reactivation of pre-existing basement structures either with a similar sense of displacement or an opposite sense resulting in structural inversion (Carter and Norris, 1976; Ratcliffe *et al.,* 1986; Allmendinger *et al.,* 1987; van Hoorn, 1987; Montenat *et al.,* 1988; Hayward and Graham, 1989; Korsch and Lindsay, 1989; Cabrera *et al.,* 1991; among others). In some regions multiple episodes of extensional tectonics have been identified (e.g., Chadwick, 1986; Bles *et al.,* 1989; Wood *et al.,* 1989; Fitzgerald *et al.,* 1990; Willcox and Stagg, 1990; Zhao and Windley, 1990). Continental extension may be produced in many different plate tectonic settings including continental rifts, foreland basins, wrench systems, fore-arc margins, over-thickened collision zones, back-arc rifts and complex subduction roll-back settings (e.g., Harding and Lowell, 1979; Bally *et al.,* 1981; Jackson and White, 1989). Whether or not new faults are created or whether pre-existing structures are reactivated during a superimposed deformation phase depends greatly upon the orientations and magnitudes of the principal stresses, the mechanical properties and isotropy of the upper crust, and the orientation and frictional properties of existing structural discontinuities (Stearns *et al.,* 1981; Sibson, 1985; Pinet and Colletta, 1990; Thatcher and Hill, 1991).

Many New Zealand sedimentary basins record multiple deformational phases which commonly begin with continental rifting associated with the late Mesozoic fragmentation of the Pacific sector of Gondwana (Laird, 1981; Carter, 1988; Bishop, 1992a) and evolve with the Australia-Pacific plate-boundary zone in the Cenozoic. Late Cenozoic oblique convergence at the plate boundary is expressed as distributed deformation across a zone up to several hundred kilometres wide (eg., Walcott, 1978, 1987; Norris *et al.*, 1990) and some regions exhibit structural inversion by transpressive overprinting of Mesozoic and/or early Cenozoic extensional structures (eg., Carter and Norris, 1976; King, 1990; Uruski, 1992).

The NW Chatham Rise (Fig. 1.1) is one such area characterised by poly-phase and active extensional tectonics. The primary aims of this chapter are: (1) to document with the new seismic reflection data the separate phases of continental extension of the NW Chatham Rise; (2) to understand the phases in the light of relevant reconstructions of the New Zealand region and data from other New Zealand sedimentary basins of similar ages; (3) to examine the evolving patterns of fault reactivation and renewed structural style; and (4) to discuss the control of structural heredity on the late Cenozoic deformational style of the NMFZ. This study could have implications for the interpretation of other areas of active extensional tectonics where deformational style and fault kinematics may be influenced by pre-existing structural trends. In this chapter the Late Miocene and Pliocene aspects of the late Cenozoic deformation are discussed. The Quaternary tectonics of the NMFZ is discussed in Chapter 6.

5.2 THREE PHASES OF EXTENSIONAL TECTONICS

5.2.1 STRATIGRAPHY AND METHOD OF APPROACH

The late Mesozoic to Recent seismic-reflection stratigraphy of the NW Chatham Rise is summarised in Figure 5.1. The Cretaceous and Paleogene stratigraphy is adopted from regional interpretations by Herzer and Wood (1988) and Wood *et al.* (1989), and is discussed briefly in sections 5.2.2 to 5.2.4 together with each phase of syn-sedimentary tectonic deformation. Stratigraphic control comes from biostratigraphic analysis of seafloor dredge and core samples from the crest of the rise and from regional seismic correlations to onshore exposures and oil industry wells on the margin of eastern South Island. The late Cenozoic stratigraphy in Figure 5.1 was established in Chapter 4 of this thesis and is summarised from Figure 4.2. Although the mid-Cretaceous to Recent sedimentary succession generally thickens down slope from the eroded crest of Mernoo Bank, where basement is exposed, to > 1.5 km thick beneath the lower slope, this pattern is interrupted on the upper slope where thick accumulations of Late Cretaceous sediments occur in faulted basins.

This analysis of poly-phase deformation relies on the recognition of contemporaneous sedimentation and tectonic faulting, expressed in seismic-reflection data as discrete phases of growth faulting and basin evolution (Herzer and Wood, 1988). There are corresponding changes in sedimentation style that also reflect periods of active tectonism. Isopach mapping of successive sedimentary units reveals those faults which were active during the accumulation of each sequence. Such mapping indicates three discrete phases of normal faulting separated by periods of inferred tectonic quiescence and condensed sedimentation or non-deposition. These faulting episodes are: (1) Late Cretaceous, (2) Late Eocene, and (3) Late Miocene-Recent. The

Fig. 5.1. Summary of seismic stratigraphy of the NW Chatham Rise region. a. Labelled reflections traced on Figs 5.2, 5.4, 5.6 and 6.1 to 6.4. b. Plio-Pleistocene seismic units from Fig. 4.2. c. Seismic units of Wood *et al.* (1989).

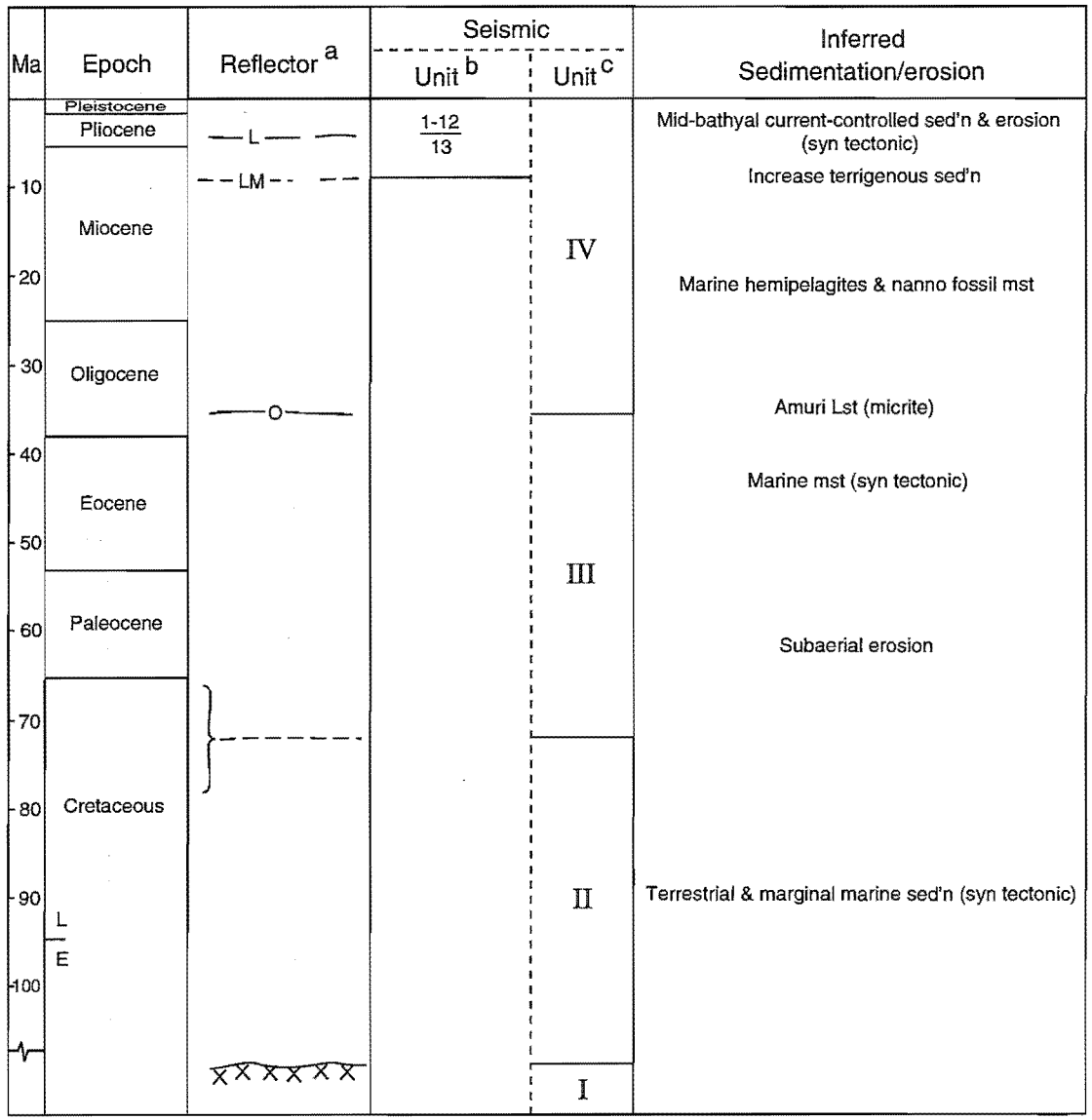
Ma
Epoch
Reflector a
Seismic
Unit b
Unit c
Inferred
Sedimentation/erosion
Pleistocene
Pliocene
Miocene
Oligocene
Eocene
Paleocene
Cretaceous
L
E
10
20
30
40
50
60
70
80
90
100
L
LM
O
1-12
13
IV
III
II
I
Mid-bathyal current-controlled sed'n & erosion
(syn tectonic)
Increase terrigenous sed'n
Marine hemipelagites & nanno fossil mst
Amuri Lst (micrite)
Marine mst (syn tectonic)
Subaerial erosion
Terrestrial & marginal marine sed'n (syn tectonic)

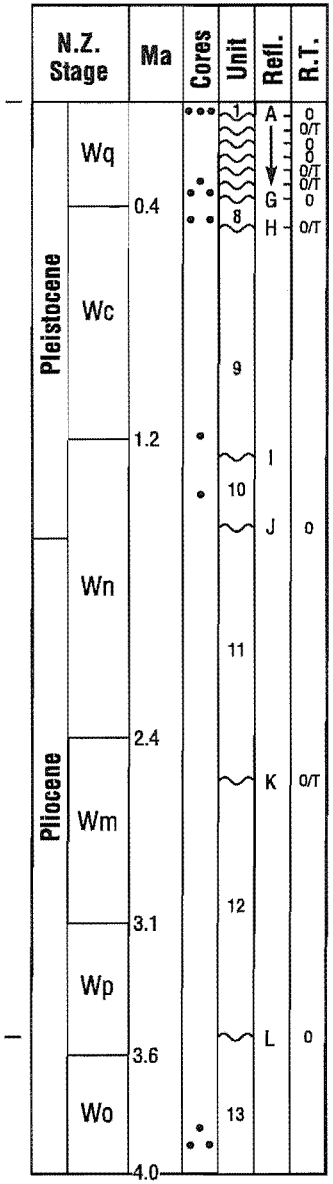
N.Z. Stage
Ma
Cores
Unit
Refl.
R.T.
Pleistocene
Pliocene
Wq
Wc
Wn
Wm
Wp
Wo
0.4
1.2
2.4
3.1
3.6
4.0
1
8
9
10
11
12
13
A
G
H
I
J
K
L
0
0/T

term NMFZ applies only to the Late Miocene-Recent phase of normal faulting, which is restricted to the NW Chatham Rise region.

The late Cenozoic high-resolution seismic stratigraphy of the NW Chatham Rise (Fig. 5.1) provides a useful temporal framework for interpretation of the late Cenozoic tectonic development of the NMFZ. Many of the normal faults have growth characteristics in the Plio-Pleistocene succession and the widespread sequences and their bounding unconformities provide useful markers for analysing the evolving pattern of fault activity. Fault correlations between seismic profiles were based on the following combination of parameters, which are discussed fully in Chapter 6: (1) style of faulting expressed in the upper sedimentary cover, including the presence or absence of extensional forced flexures and the general characteristics of reflection terminations against faults; (2) fault dip directions constrained by intersecting profiles; and (3) the magnitude of vertical displacement of both the seafloor and various subbottom reflections.

5.2.2 LATE CRETACEOUS FAULTING

A Late Cretaceous phase of normal faulting produced east-west trending half-graben basins on the NW Chatham Rise upper slope and rise crest, some of which were infilled with > 2 km of syn-tectonic sediment. Reflections within the basins diverge and fan into the bounding faults, indicating contemporaneous sedimentation, faulting, tilting, and subsidence (Fig. 5.2). The deeper basins contain a basal succession of high-amplitude continuous reflectors beneath a succession of weaker, more discontinuous reflections. The syn-tectonic basin-fill sediments have not been sampled in this region but, by analogy with correlative sequences in eastern South Island, beneath the Canterbury shelf and on Chatham Island, they are inferred to comprise terrestrial and shallow marine conglomerates, sands and silts of mainly Santonian-Campanian age (Fig. 5.2; unit II).

The Cretaceous faults beneath the NW Chatham Rise all dip and down throw to the south, up slope (Fig. 5.3). Two major faults (labelled faults A and B in Fig. 5.3) have been mapped to extend for at least 110 km along strike from the middle of Pegasus Canyon on the South Island margin (c. 1400 m water depth) up and across the slope to the shelf depths (c. 150 m) of northern Mernoo Bank. By analogy with active extensional fault systems that have been studied in detail elsewhere in the world, it is likely that the faults mapped here are segmented into < 25 km-long segments (Jackson and White, 1989). Faults A and B are subparallel and 4–10 km apart, and fault B is sinuous over its western 60 km (Fig. 5.3). To the north of fault B, down slope towards the Hikurangi Channel, the Cretaceous sequence is absent and

Fig. 5.2. Seismic reflection profiles 1–1', 2–2' and 3–3' showing the syntectonic mid-Late Cretaceous sequence (shaded). Profile positions and labelled faults are shown on Figs 5.3, 5.5 and 5.7. Profiles 1–1' and 2–2' are single-channel airgun profiles and profile 3–3' is a multichannel record shot by Mobil Exploration Co. Arrows above the seabed show the positions of intersecting seismic profiles. The upper scale applies to both profiles 1–1' and 2–2'. See Fig. 5.1 for stratigraphy.

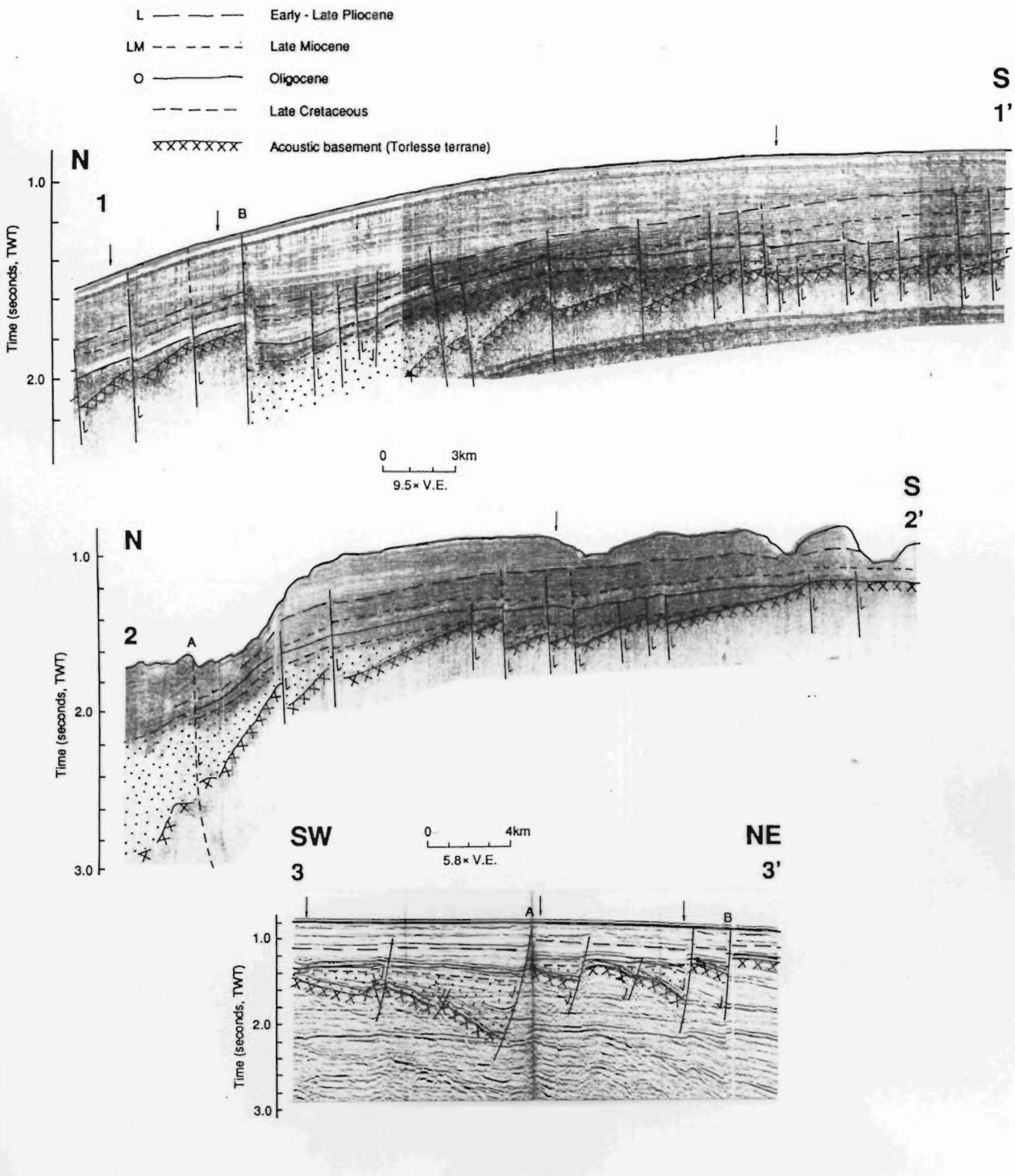
L
Early - Late Pliocene
LM
Late Miocene
O
Oligocene
Late Cretaceous
Acoustic basement (Torlesse terrane)
N
S
1
1'
B
Time (seconds, TWT)
1.0
2.0
0
3km
9.5× V.E.
N
S
2
2'
A
1.0
2.0
3.0
Time (seconds, TWT)
SW
NE
3
3'
0
4km
5.8× V.E.
A
B
1.0
2.0
3.0
Time (seconds, TWT)

Fig. 5.3. Isopach map of syntectonic mid-Late Cretaceous sequence on the NW Chatham Rise, based on an interval velocity of 3400 m/s. The sequence is shaded on Fig. 5.2 and has not been decompacted. Major faults and positions of sonobuoy refraction velocity analyses (solid circles) are indicated, together with positions of seismic profiles in Figs 5.2, 5.4 and 5.6. Labelled faults are referred to in the text. Contours in metres. ND = no data. Diagonally stripe-shaded areas are where the sequence is absent due to non-deposition and erosion. For reference, several late Quaternary features are shown: zone of prominent mid-slope current erosion from Fig. 3.9 is lightly shaded; shelf edge at c. 150 m water depth is the dash-dot-dash line; dashed line is the base of the North Chatham Slope; several submarine canyons at the head of the Hikurangi Channel are arrowed. KC, Kaikoura Canyon; PC, Pegasus Canyon; PKC, Pukaki Canyon. Late Cenozoic volcanic rocks are cross-hatch shaded. Inset map (bottom right) shows the regional distribution of mid-Late Cretaceous faults mapped by Wood *et al.* (1989). MB, Mernoo Bank.

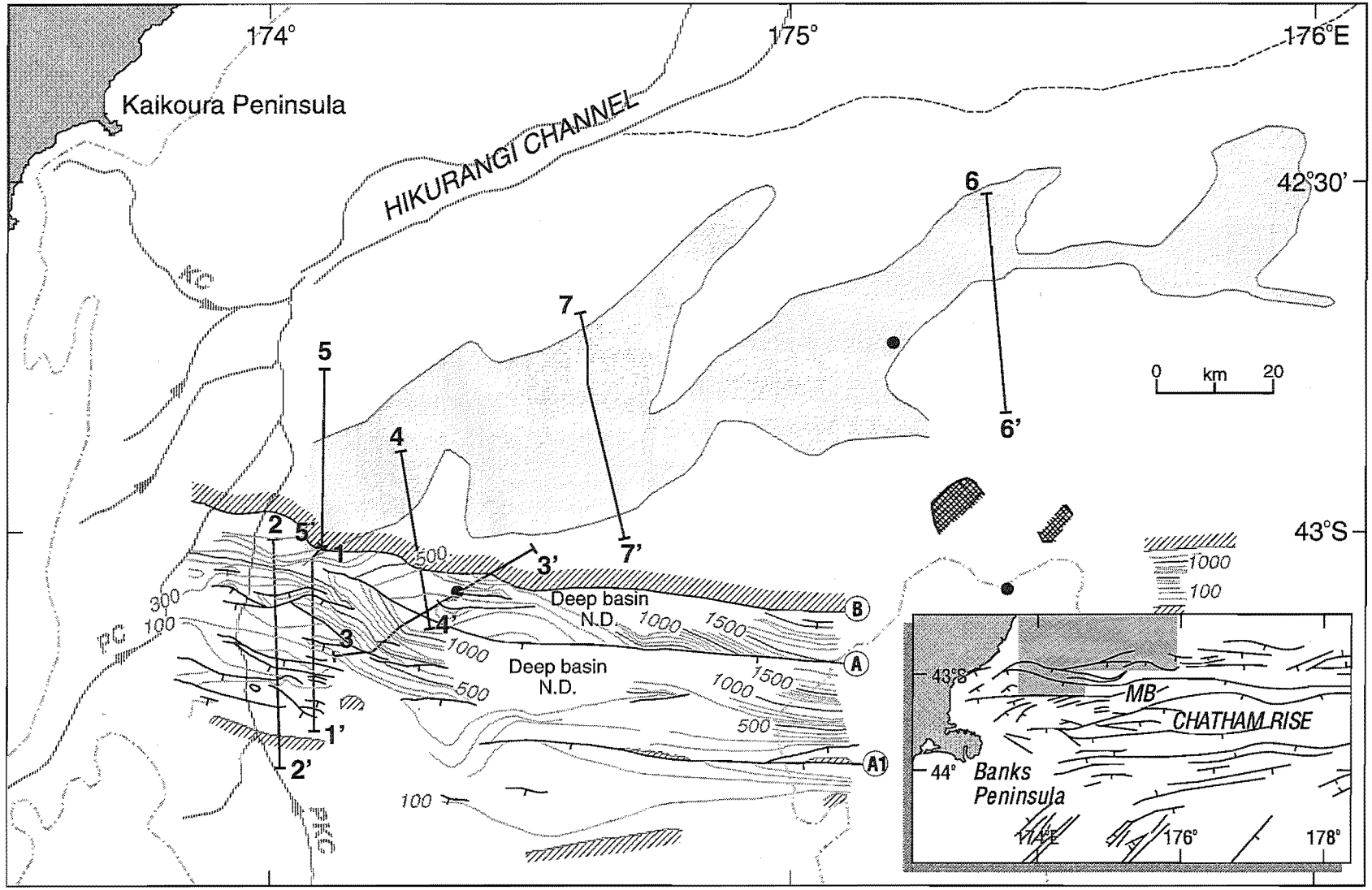
174°
175°
176°E
Kaikoura Peninsula
HIKURANGI CHANNEL
42°30'
43°S
0 km 20
1
1'
2
2'
3
3'
4
4'
5
5'
6
6'
7
7'
Deep basin
N.D.
Deep basin
N.D.
A
A1
B
300
100
500
1000
1500
PC
MB
CHATHAM RISE
Banks
Peninsula
43°S
44°
176°
178°

presumably was either eroded away or was never deposited outside of the faulted basins. Within the major half-graben up slope of fault A, there are numerous, minor synthetic structures which are discontinuous, typically < 30 km in length, and which have Cretaceous vertical displacements generally of < 300 m (Fig. 5.3). Although the overall basin trend is roughly east-west to WNW-ESE, some fault segments trend slightly northeast-southwest resulting in about 30° total range in strike. Isopachs of the Cretaceous basin-fill show clearly that along-strike ramps occur on the basement surfaces of the half-grabens (Fig. 5.3). Such ramps, which are well developed on the hangingwall block of fault B and between overlapping faults near the western tip of fault A, accommodated differences in vertical displacement and conserved extension. There is no clear evidence for highly transverse, oblique-slip faults within transfer zones between faults.

5.2.3 EOCENE FAULTING

Following an extensive period of emergence, or shallow marine erosion or non-deposition over much of the western Chatham Rise region during the Paleocene and possibly the Early-mid Eocene, regional subsidence and transgression led to widespread sedimentation in the Late Eocene and much of the Oligocene (Herzer and Wood, 1988; Wood *et al.*, 1989). Part of this transgression coincided with a second, Eocene phase of widespread normal faulting, and renewed syn-tectonic sedimentation (Fig. 5.4). The absence of Paleocene graben-fill deposits suggests that there was a lengthy period (c. 20–30 Ma) between the Late Cretaceous and Eocene phases of faulting when half-graben basins were not forming.

On the NW Chatham Rise slope, a very characteristic down-slope thickening wedge with moderate-amplitude reflections on the upper slope grading laterally down slope into a weakly reflective unit with few, discontinuous internal reflections is inferred to be Eocene age. The sequence is absent from parts of Mernoo Bank, but it thickens to around 600 m on the lower slope near the Hikurangi Channel (Fig. 5.5), where it lies above a thin Paleocene sequence onlapping the lower rise (Wood *et al.*, 1989). The unit may be represented by a mixed calcareous-terrigenous mudstone lithology (Fig. 5.1). Overlying this unit in seismic profiles is a widely traceable, thin packet of high-amplitude reflections (or, in some profiles, a single reflection) (Figs 5.2 and 5.4). The reflections represent a very thin sequence that appears to be conformable on the NW Chatham Rise slope and which can be traced in seismic profiles to Resolution-1 petroleum exploration well on the Canterbury shelf (Fig. 2.1). At Resolution-1 well the reflections coincide with a Late Oligocene-Early Miocene erosional unconformity on the Amuri Limestone Formation, a regionally extensive, condensed, pelagic limestone unit. On the Canterbury shelf and onshore in north Canterbury

Fig. 5.4. Single-channel seismic reflection profiles 4—4' and 5–5' showing the inferred Late Eocene syntectonic sequence (shaded) below strong reflectors of the Oligocene Amuri Limestone formation. Labelled faults and profile positions are shown on Figs 5.5 and 5.7. Arrows above the seabed show the positions of intersecting seismic profiles. Scale applies to both profiles.

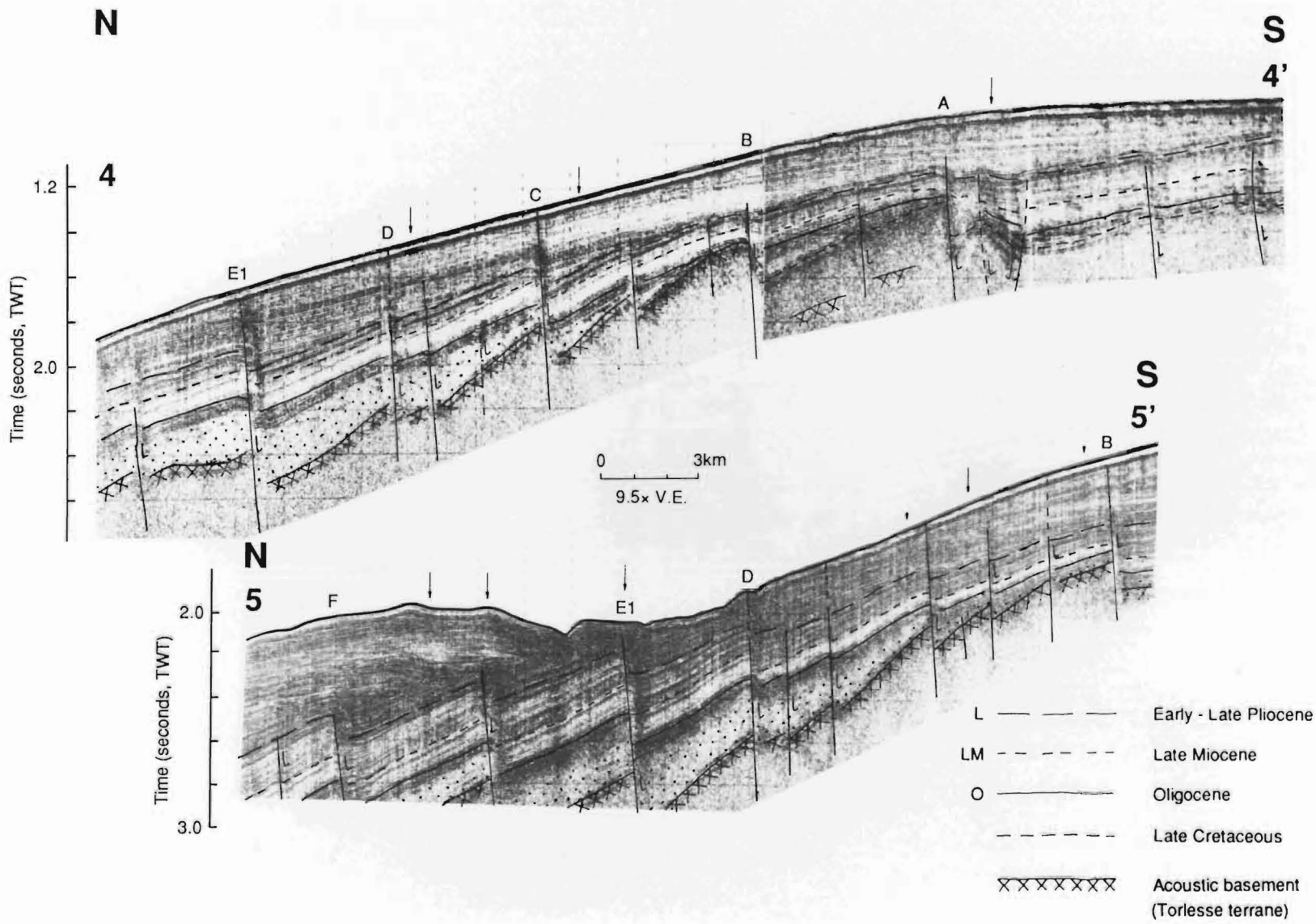
N
S
4'
4
A
B
C
D
E1
1.2
2.0
Time (seconds, TWT)
S
5'
B
0
3km
9.5× V.E.
N
5
F
E1
D
2.0
3.0
Time (seconds, TWT)
L
Early - Late Pliocene
LM
Late Miocene
O
Oligocene
Late Cretaceous
Acoustic basement
(Torlesse terrane)

Fig. 5.5. Isopach map of the combined Eocene and Oligocene sequences on the NW Chatham Rise, based on an interval velocity of 3000 m/s. The faults mapped are inferred to be of Late Eocene age. The growth of these faults is shown by the shaded sequence on Fig. 5.4. Labelled faults are referred to in the text. Contours in metres. Diagonally stripe-shaded areas are where the sequence is absent. For reference, several late Quaternary features are shown: prominent mid-slope current erosion from Fig. 3.9 is lightly shaded; shelf edge at c. 150 m water depth is the dash-dot-dash line; dashed line is the base of the NW Chatham Slope; several submarine canyons at the head of the Hikurangi Channel are arrowed. KC, Kaikoura Canyon; PC, Pegasus Canyon; PKC, Pukaki Canyon. Neogene volcanic rocks are cross-hatch shaded. Solid circles are sonobuoy refraction locations. Inset diagram (bottom right) shows the regional distribution of faults of the same age, from Wood *et al.* (1989). MB, Mernoo Bank.

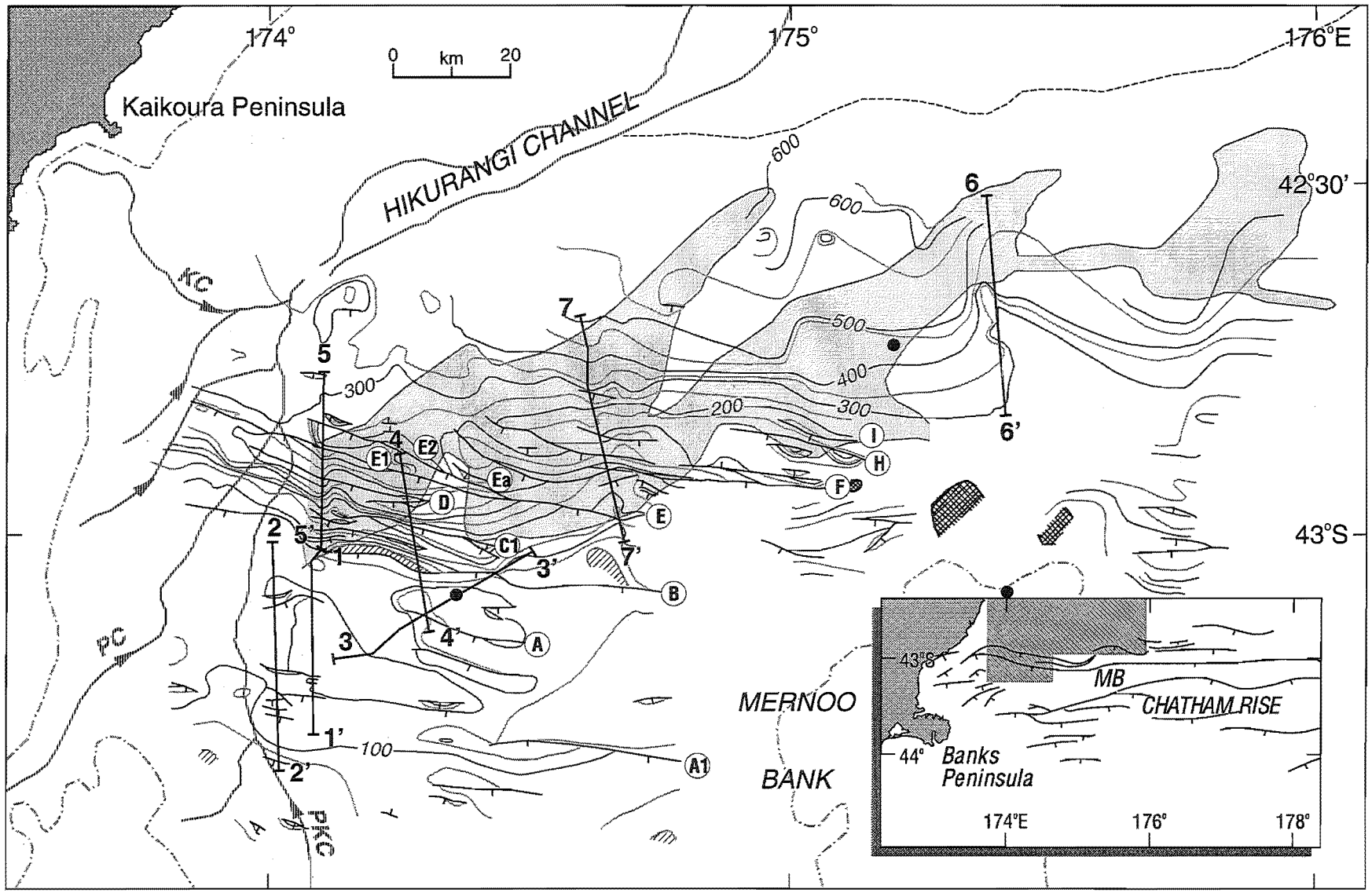
174°
175°
176°E
0 km 20
Kaikoura Peninsula
HIKURANGI CHANNEL
600
500
400
300
200
100
42°30'
43°S
KC
PC
PKC
1
1'
2
2'
3
3'
4
4'
5
5'
6
6'
7
7'
E1
E2
Ea
D
C1
E
F
H
I
B
A
A1
MERNOO
BANK
43°S
MB
CHATHAM RISE
44°
Banks
Peninsula
174°E
176°
178°

the Amuri Limestone is mostly Early-middle Oligocene in age (Fig. 5.1) (Field *et al.*, 1989; Wood *et al.*, 1989; Lewis, 1992), but it is older (Paleocene) in northeastern South Island (Suggate *et al.*, 1978). Over much of the Chatham Rise crest east of the NMFZ the reflections correlate with a Late Oligocene unconformity (Wood *et al.*, 1989).

Beneath the NW Chatham Rise slope the thickness of the Oligocene sequence is difficult to estimate because it is very thin and its base cannot be identified due to reflections from multiple wavelets of the outgoing seismic signal (Fig. 5.4). Nevertheless, there is no evidence for growth faulting during the deposition of this unit and an isopach map of the combined Eocene-Oligocene sediments essentially illustrates the distribution and displacement magnitudes of Late Eocene faults in the region (Fig. 5.5). During this phase of extension the Cretaceous-age fault B was reactivated, together with parts of faults A, A1 and a few other associated minor structures on the upper slope. However, most of the Eocene faults on the NW Chatham Rise slope developed immediately down slope of fault B (compare Figs 5.3 and 5.5). New faults (including those lettered C, D, E, F, H and I on Fig. 5.5) developed parallel to fault B within a 30 km-wide deformation zone that has been mapped for about 160 km along strike from Pegasus Canyon in the west, across the mid-slope north of Mernoo Bank. Overall the fault zone comprises an array of east-west and WNW-ESE trending, overlapping normal faults, which appear to be up to at least 80 km in length and which have maximum Eocene vertical displacements of 230 m. Most of the faults dip up slope, down-throwing to the south. At the lower slope, northern edge of the extensional zone the faults characteristically step to the left in a very weak *en echelon* pattern. As with the Cretaceous fault system, no highly-oblique transfer faults nor fault-block, trap-door structures (e.g., Harding and Lowell, 1979) of Eocene age are recognised.

5.2.4 LATE CENOZOIC FAULTING

Lewis *et al.* (1986) recognised widespread late Cenozoic normal faulting and associated active seismicity in the NMFZ as being distinct from the now-inactive Late Cretaceous and Eocene structures preserved on much of the Chatham Rise outside of the NMFZ. Since the end of the Late Eocene phase of tectonism the rest of the rise beyond of the NMFZ has essentially remained a tectonically stable, submerged plateau on the Pacific Plate, with a complex history of erosion and non-deposition (Cullen, 1980; Wood *et al.*, 1989). There is no evidence for active faulting in the NMFZ during the deposition of the weakly reflective, down slope thickening sequence between the Late Miocene and Oligocene reflections (LM and O; Figs 5.1, 5.4 and 5.6). This sequence is possibly a mid-bathyal muddy deposit that accumulated synchronously with an

Fig. 5.6. Single-channel seismic reflection profiles 6–6' and 7–7' showing renewed Late Miocene (8–6 Ma) to Recent normal faulting. Labelled faults and profile positons are shown on Figs 5.5 and 5.7. Arrows above the seabed show the positions of intersecting seismic profiles.

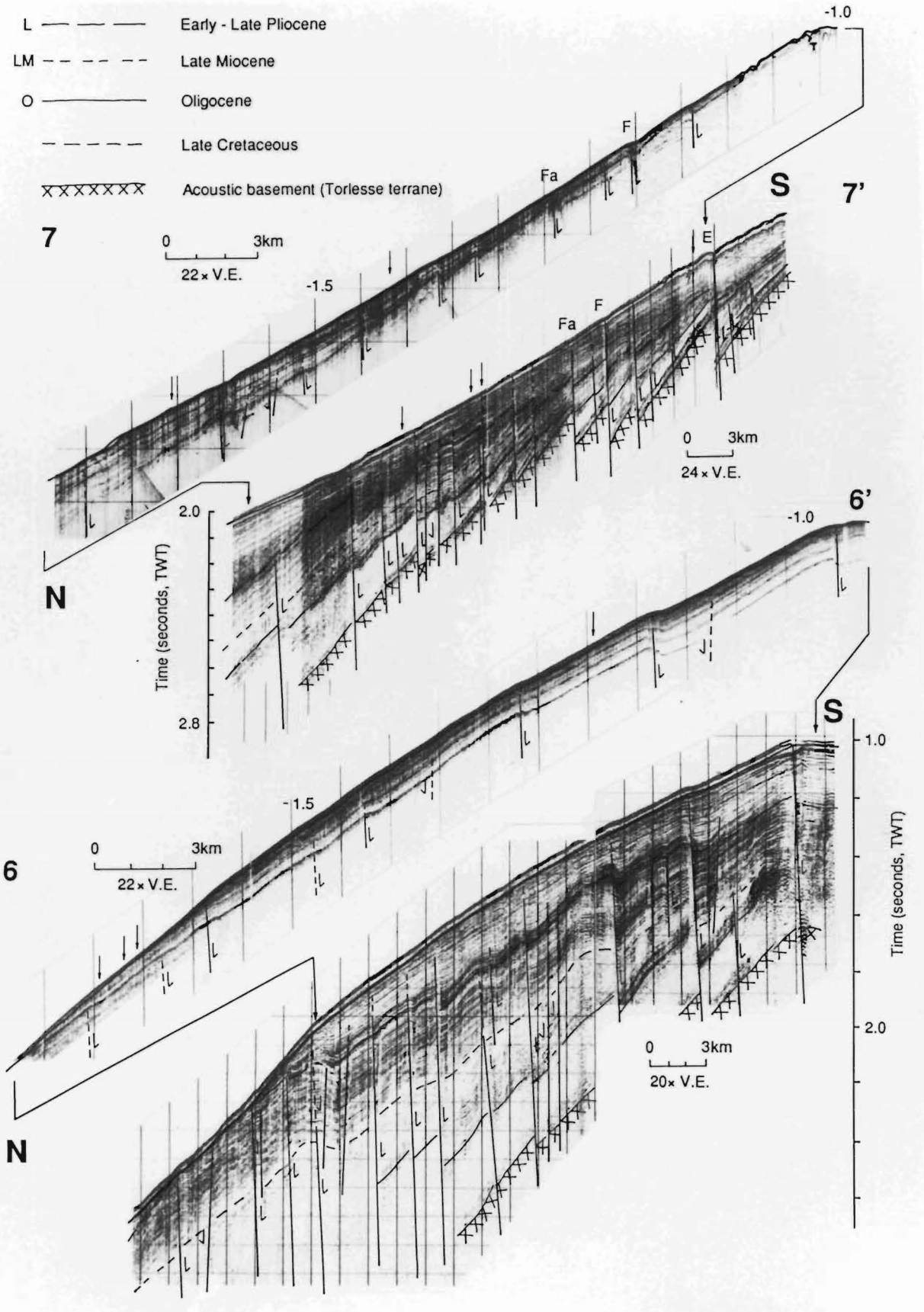
L Early - Late Pliocene
LM Late Miocene
O Oligocene
Late Cretaceous
Acoustic basement (Torlesse terrane)
7
0 3km
22× V.E.
-1.5
Fa
F
E
S
7'
-1.0
0 3km
24× V.E.
6'
N
2.0
Time (seconds, TWT)
2.8
6
0 3km
22× V.E.
-1.5
0 3km
20× V.E.
1.0
2.0
Time (seconds, TWT)

Early-Middle Miocene erosional unconformity on the eastern South Island continental shelf (Field *et al.*, 1989; Wood *et al.*, 1989).

The timing of renewed, late Cenozoic faulting and development of the NMFZ is recorded by the stratigraphic position of renewed syntectonic sedimentation and growth faulting. This latest, third phase of deformation began in the Late Miocene at about 8–6 Ma (assuming a constant sedimentation rate between the mid Pliocene, c. 3.4 Ma reflector L and Late Miocene, 10–9 Ma reflector LM) (Figs 5.1, 5.2, 5.4 and 5.6). The distribution of normal faulting at that time is not well constrained by the available data. However, faulting had become widely distributed by Early Pliocene time (c. 5–4 Ma) (Figs 5.6 and 5.7) and remained widespread throughout most of the Pliocene (c. 5–2 Ma) (the majority of structures in Figure 5.7 displaying growth faulting during this time interval).

A structural contour map of the mid Pliocene regional onlap surface, reflector L, illustrates the extent of post mid-Pliocene deformation (Fig. 5.7). In Chapter 6 it is shown that many of the faults south of fault A and west of Mernoo Bank, together with many of the northern faults on the lower slope in water presently > 1500 m deep have not been active since the Late Pliocene-Early Pleistocene. The zone of Quaternary and presently-active extensional faulting is concentrated on the upper and middle parts of the slope, with much of the strain being accommodated on reactivated Eocene faults (compare Figs 5.5 and 6.5). Thus the structural contour map (Fig. 5.7) essentially shows the distribution of mid-Late Pliocene faults.

Although the Cretaceous and Eocene phases of extension effected much of the New Zealand region outside of the NMFZ (see Section 5.4), on the northwest corner of the Chatham Rise Pliocene faulting was more pervasive than it was during the two older (Late Cretaceous and Eocene) phases of extension. Many of the Cretaceous faults and nearly all of the Eocene faults (including faults labelled A-I) were reactivated in a normal sense and lengthened during the late Cenozoic deformational phase, indicating a strong inheritance for the late Cenozoic deformation (compare Figs 5.3, 5.5 and 5.7). Furthermore, many new basement-involved structures developed sub-parallel to the older fault basins, particularly north of fault I.

The distribution of the mid-Late Pliocene faults defines a deformation zone extending down slope for up to 100 km from Mernoo Bank to near the base of the NW Chatham Rise slope, and along slope for at least 200 km. The style of the deformation is an array of east-west to WNW-ESE striking, commonly overlapping normal faults which nearly all dip and down-throw to the south. The faults are typically 2–5 km apart and some have been mapped as discrete structures up to 115 km in length (e.g., fault E, Fig. 5.7) although in detail these are likely to be segmented (e.g., Jackson,

Fig. 5.7. Structural contour map of an early Late Pliocene (c. 3.4 Ma) reflector L at the base of seismic unit 12. Contours are in metres below sea-level assuming velocities of 1500 m/s in water and 1700 m/s in sediment. Positions of profiles 1–1' to 7–7' in Figs 5.2, 5.4 and 5.6 are indicated. Diagonally-striped areas are where reflector L has been eroded out, exposing older units. Labelled faults are referred to in the text. For reference, several late Quaternary features are shown; prominent mid-slope current erosion from Fig. 3.9 is lightly shaded; shelf edge at c. 150 m water depth is the dash-dot-dash line; dashed line is the base of the North Chatham Slope; several submarine canyons at the head of the Hikurangi Channel are arrowed. KC, Kaikoura Canyon; PC, Pegasus Canyon; PKC, Pukaki Canyon. Neogene volcanic rocks are cross-hatch shaded. Inset map (bottom right) illustrates the displacement of reflector L by shading between four pairs of adjacent contours; the largest fault displacements of reflector L occur on the mid-slope, as expressed by the steps in the 1500–1600 contour shading.

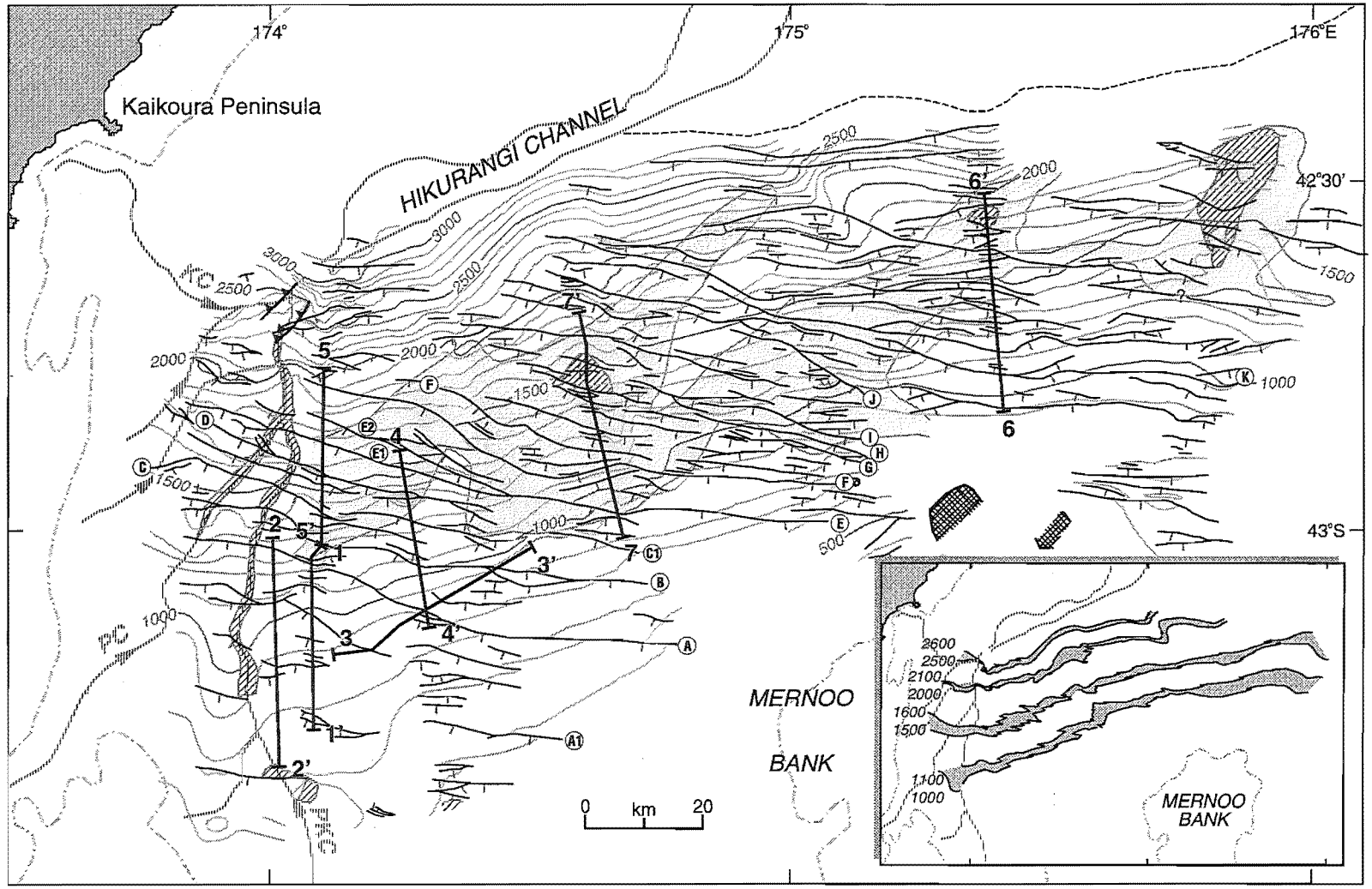
174°
175°
176°E
42°30'
43°S
Kaikoura Peninsula
HIKURANGI CHANNEL
MERNOO
BANK
0 km 20
2600
2500
2100
2000
1600
1500
1100
1000
MERNOO
BANK

1987). The maximum vertical displacement of the Pliocene reflector L is about 170 m and vertical displacements of 30–80 m are common. The largest throws are concentrated in the southwest.

5.3 FAULT SYSTEM GEOMETRY AND EXTENSION

Although the half-graben exhibit diverging reflections and thickening of sediments towards the major bounding faults, and thus imply rotation of the hangingwall, such rotation may be accommodated by either listric faults or by domino-style arrays of planar faults which rotate about horizontal axes during extension (Wernicke and Burchfiel, 1982; Jackson and McKenzie, 1983; Jackson *et al.,* 1988; McClay, 1990; Lister *et al.,* 1991). The available seismic reflection data are of insufficient quality and penetration to determine clearly whether the faults are listric or planar, but it is clear that the foot-wall blocks have rotated, so the system is an array of rotating faults. A moderately large earthquake at the western end of the NMFZ in 1965 has a focal mechanism consistent with planar geometry (see sections 6.2.4 and 6.3). It is not known whether mid or upper crustal detachment surfaces exist or whether the faults terminate within semi-ductile crust beneath the brittle seismogenic zone. There is no evidence in the seismic profiles for roll-over anticlines in hangingwall sequences which are commonly associated with listric faults (e.g., Crans *et al.*, 1980). Some seismic profiles (e.g., Fig. 5.2, profile 2–2') exhibit variable dips of the top of the basement reflection, which usually dips at $< 13°$, in different hangingwall blocks. This variation in hangingwall basement dip is inferred to result, not from variable rotation on listric faults, but from along-strike variations in half-graben development within an array of domino-style faults. For example, in any given profile some faults are imaged at positions of maximum throw, whereas others are imaged near the ends of fault segments or in parts of segments with diminished throw. Hence, they display less hangingwall rotation than adjacent blocks. Overall, the regularly spaced, subparallel pattern of faults which nearly all down throw to the south, is consistent with a domino-style array of planar faults. In this style of deformation, the footwall block of one fault is the hangingwall block of the adjacent structure; the upper crustal blocks are tilted between the faults and they rotate about horizontal axes as the faults rupture (e.g., Jackson *et al.,* 1988).

Assuming that the major faults are planar, as are the majority of normal faults in other areas of active continental extension (Jackson, 1987), and that their dips are 30–60° (e.g., Thatcher and Hill, 1991), then Late Cretaceous extension of the NW Chatham Rise slope was of the order of 4–10% (β = 1.04–1.10; where $\beta = \text{Sin}(\theta_0 + \psi)/\text{Sin}\,\theta_0$; with θ_0 = present fault dip and ψ = tilt of the fault in a given time period; Jackson and McKenzie, 1983; Jackson and White, 1989) in the far west and 7–23% (β = 1.07–1.23) 100 km further east, closer to Mernoo Bank. Extension values for indi-

vidual half-grabens range from 3–28% if the faults dip at 30°, to 1–9% if the faults dip at 60°. In contrast, the amount of Eocene extension of the NW Chatham Rise was only 2-7% (β = 1.02-1.07). In the Late Miocene-Recent phase of deformation the fault zone on the NW Chatham Rise widened to 100 km but the total amount of post mid-Pliocene extension (calculated on reflector L, Figs 4.2 and 5.1) is extremely small (< 2%).

5.4 CRETACEOUS AND EOCENE PLATE TECTONIC SETTINGS

5.4.1 CRETACEOUS: EXTENSION PRIOR TO BREAK-UP OF GONDWANA

The convergent plate tectonism that characterised the Pacific coast of Gondwana during the late Paleozoic and Mesozoic continued in the New Zealand region until about 100 Ma (late Albian) (Bradshaw, 1988). The youngest Mesozoic convergence is recognised in middle Cretaceous accretionary complex in eastern North Island and northeast South Island (Spörli, 1987; Korsch and Wellman, 1988; Spörli and Ballance, 1989; Barnes and Korsch, 1991). A strong basement reflector in seismic-reflection profiles, inferred to represent subducted paleo-Pacific oceanic crust, dips southward beneath the northern slope of the Chatham Rise (Davy, 1992). Thus, the northern margin of the rise is not a classical rifted margin but is probably an ancient forearc slope above a failed subduction zone and ancient accretionary wedge (Fig. 5.8).

Regional mapping by Herzer and Wood (1988) and Wood *et al.* (1989) shows that the major Late Cretaceous half-graben basins mapped in detail in this thesis continue eastward across Mernoo Bank for at least a further 100 km (Fig. 5.3 — bottom right) and that similar east-west trending half-grabens are widespread over the entire Chatham Rise. Whatever the cause of the end of subduction along the Pacific Gondwana margin at about 100 Ma, the Late Cretaceous normal faulting of the Chatham Rise represents extension of a recently quiescent accretionary wedge. The normal faults are inferred to have formed together with closely synchronous rifting in the Bounty Trough, Great South Basin and Campbell Plateau regions (Fig. 5.8) during a lengthy (c. 10–15 Ma) precursory period of continental extension along the edge of Gondwana. Final break-up and seafloor spreading in the Tasman Sea and southwest Pacific Basin began at 83 Ma (Cullen, 1969; Grindley and Davey, 1982; Kamp, 1986a; Carter, 1988; Korsch and Wellman, 1988; Wood *et al.*, 1989). The oldest dated Cretaceous extensional features in the New Zealand region which formed during this phase are about 100 Ma old and, thus, are almost contemporaneous with the final stages of convergence at the edge of Gondwana (Bradshaw, 1991). These extensional features include, among others, the roughly correlative basins containing the Keyburn and Tupuangi Formations, and the Hawks Crag Breccia, together with the Paparoa Metamorphic Core Complex (Suggate *et al.*, 1978;

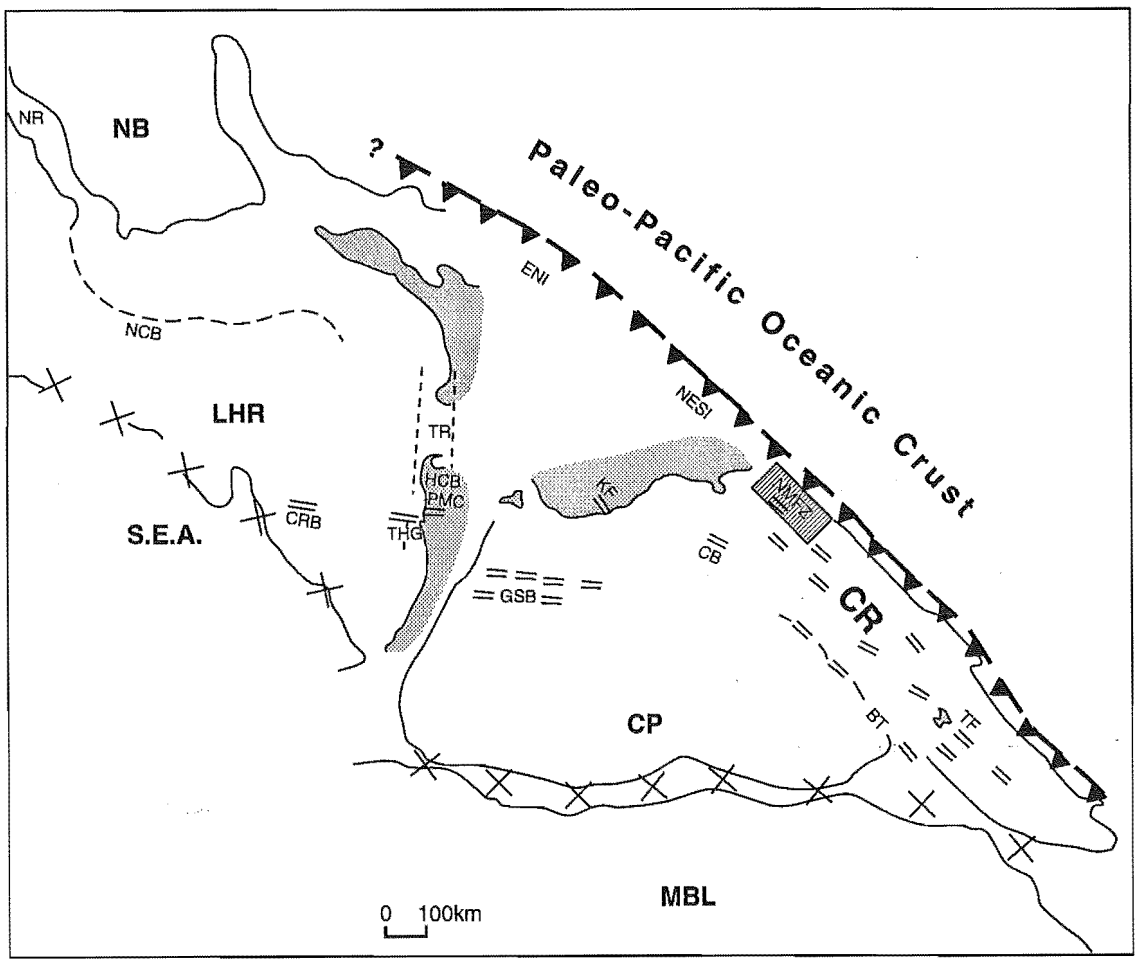

Fig. 5.8. Reconstruction of the Pacific sector of Gondwana at about the Albian-Cenomanian boundary (c. 97 Ma) (late-Early Cretaceous), modified from Grindley and Davey (1982), Bradshaw (1991) and Bishop (1992). Widespread normal faulting of the Bounty Trough/ Chatham Rise region had begun as precursory extension of Pacific Gondwana prior to final separation (at c. 82 Ma) along the line of large X's. Late Mesozoic subduction had just ceased (at c. 100 Ma) at the edge of the continental block (dashed barbed line). Extension in the Taranaki Rift system (TR; 80–60 Ma) mainly post-dates the beginning of ocean-floor spreading in the Tasman Sea. Part of present day New Zealand (stippled) and the present day 2000 m isobath are shown for reference. CR, Chatham Rise; MBL, Marie Byrd Land; CP, Challenger Plateau (narrowed by about 200 km to account for 100–80 Ma crustal thinning (Bradshaw, 1991); SEA, south eastern Australia (east of Tasmania); NR, Norfolk Ridge; NB, Norfolk Basin; LHR, Lord Howe Rise; ENI, eastern North Island; NESI, north eastern South Island. **RIFTS** (parallel dashed lines): BT, Bounty Trough prior to opening; TF, Tupuangi Formation, Chatham Island; CB, Clipper Basin; GSB, Great South Basin; HCB, Hawks Crag Breccia; PMC, Paparoa metamorphic core complex; CRB, Challenger Basin; THG, Tukutai half graben; KF, Keyburn Formation; NMFZ, present location of the North Mernoo Fault Zone.

Tulloch and Kimbrough, 1989), the offshore Tukutai half-graben (Bishop, 1992a) and perhaps the Challenger Basin (Wood, 1991) (Fig. 5.8).

The majority of rifting of the Chatham Rise-Bounty Trough regions occurred prior of final separation along the Campbell Plateau-Marie Byrd Land and Lord Howe Rise-southeast Australia margins in the Campanian (c. 83 Ma) (Fig. 5.8) but significant continental extension continued within the thinned New Zealand plateau throughout the Campanian-Danian (c. 80–60 Ma) period, long after seafloor spreading had begun. These regions included parts of the Chatham Rise (Wood *et al.*, 1989), Campbell Plateau (Bradshaw, 1991) onshore north Canterbury (Nicol, 1993) and western New Zealand (King, 1990; Thrasher, 1990; Bishop, 1992a).

5.4.2 LATE EOCENE: INTRA-PLATE EXTENSION PERIPHERAL TO THE NEWLY-FORMED AUSTRALIA-PACIFIC PLATE-BOUNDARY ZONE

Early studies of seafloor magnetic data suggested that there was no relative plate motion between the Pacific and Australian plates in the New Zealand region between the times of anomalies 31 and 25 (68–59 Ma), and that the Australia-Pacific plate boundary developed through New Zealand in about the Late Eocene (Molnar *et al.*, 1975; Weissel *et al.*, 1977; Stock and Molnar, 1982). In recently revised estimates, Stock and Molnar (1987) and Stock (1989) predicted that 230 ± 170 km of relative plate motion occurred at an orientation of 075° ± 50° during the interval between 59 and 42 Ma (Early-Middle Eocene), and that at least 900 km of relative plate motion has occurred since 42 Ma (Late Eocene). Walcott (1989) considered that the plate boundary developed at about 45 Ma (between anomalies 21 and 18) and that the early history of the boundary was represented by a subduction zone north of New Zealand and a small amount of complex transform motion through the New Zealand region.

There has not been agreement, however, as to the nature and exact location of the early plate boundary in the New Zealand region, to the timing of its inception, or to the amount of relative plate motion that must be accommodated. In contrast to the late Paleogene plate reconstructions and predictions of relative plate motions that have been derived from seafloor magnetic data (Stock and Molnar, 1982, 1987; Walcott, 1984b, 1987), the apparent finite displacement of Mesozoic terranes in the South Island by the Alpine Fault is no more than 500 km (not 900 km) and this displacement is inferred to have taken place since the Early Miocene (25 Ma) (Carter and Norris, 1976; Stock and Molnar, 1982, 1987; Walcott, 1984b, 1987; Kamp, 1986b; Cooper *et al.*, 1987; Korsch and Wellman, 1988; Rait *et al.*, 1991). Kamp and Fitzgerald (1987) looked elsewhere in the Australia-Antarctica-Pacific plate circuit to

account for the apparent 400 km disparity in relative plate motion in the New Zealand region and they suggested that 138 km of the difference can be accommodated by extension between east and west Antarctica. Alternatively, Regenauer-Lieb (1992) recently argued that all of the 400 km of the missing relative motion was accommodated by visco-elastic bending of the New Zealand region between 40 Ma and 25 Ma, prior to the inception of the Alpine Fault system.

Normal faulting has been recognised as an important component of the deformation within parts of the New Zealand region in the Late Eocene-Early Oligocene and several models have been proposed for the tectonic environment, invoking either deformation within the early phase of the present New Zealand plate boundary or deformation prior to the inception of the modern boundary. These models include, among others, a northward propagating plate- boundary zone dominated by oblique rifting linked to seafloor spreading in the south Tasman Sea (an aulacogen) (Carter and Norris, 1976; Norris and Carter, 1980), and regionally extensive continental rifting (Challenger Rift) linked to spreading centres both to the north and south of New Zealand (Kamp, 1986b).

The anomaly 18 (42 Ma, Late Eocene) plate reconstruction favoured here (Fig. 5.9) is based on the finite rotation data of Stock and Molnar (1987), which predicts 900 km of dextral motion on the New Zealand plate boundary since the Late Eocene. On the reconstruction are the main areas that are known to have been undergoing tectonic deformation at that time and the inferred orientation of the newly-formed Australia-Pacific plate boundary zone. At this time seafloor spreading was taking place in the Emerald Basin south of New Zealand, and extensional or strike-slip basins were developing in the head of the Solander Trough and Waiau Basin (Norris and Carter, 1980; Kamp, 1986b; Uruski and Turnbull, 1990; Uruski, 1992). To the west and northwest of the Solander Trough and Waiau Basin, the region that is now north Westland and onshore Taranaki (Fig. 5.9), syn-tectonic Eocene sediments also accumulated in north to NNE trending basins (Nathan *et al.*, 1986; Laird and Nathan, 1988; Bishop, 1991; Hoolihan and Yang, 1991, W.L. Leask, pers. comm., 1992). Strike-slip faulting of possible mid-Late Eocene age has been inferred in part of the Waikato region (Kirk, 1991). In contrast, the offshore Taranaki region, most of southeast South Island (offshore Canterbury and Great South Basins) and the area now represented by east coast North Island and northeastern South Island appear to have been tectonically stable and undergoing slow subsidence during the Eocene (Suggate *et al.*, 1978; Carter, 1988; Field *et al.*, 1989; King, 1990; King and Thrasher, 1992). To the north of New Zealand, there may have been oblique, northeast-facing subduction beneath the western side of the Norfolk Ridge and the northern part of Northland in the Middle-Late Eocene (Kroenke, 1984; Eade, 1984, 1988) (Fig. 5.9) but how this boundary linked to deformation in central New Zealand is uncertain

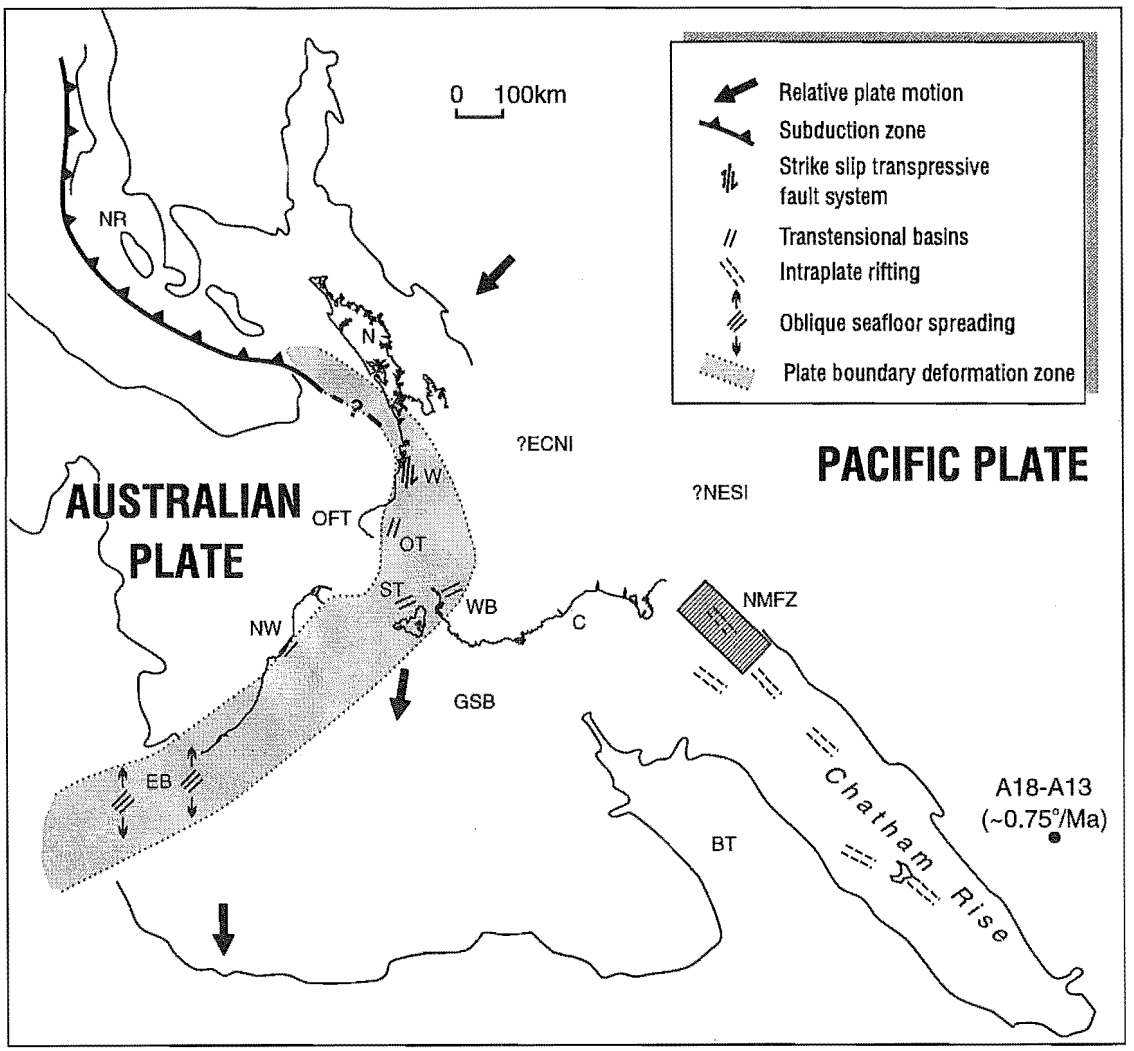

Fig. 5.9. Reconstruction of the Pacific-Australia plate boundary at the time of seafloor magnetic anomaly 18 (42 Ma, Late Eocene), based on rigid-plate rotation data of Stock and Molnar (1987). For reference, the 2000 m isobath outlines the submerged New Zealand continental plateau. Areas of major late Cenozoic deformation have been left off the reconstruction. Large dot shows the stage pole for rotation of the Pacific plate between the times of anomalies 18 and 13 (35 Ma), along with the rotation rate for the period. NR, Norfolk Ridge; W, Waikato; OFT, offshore Taranaki; ECNI, east coast North Island; NESI, north eastern South Island; NMFZ, present location of the North Mernoo Fault Zone; BT, Bounty Trough; GSB, Great South Basin; NW, north Westland; EB, Emerald Basin; ST, Solander Trough; WB, Waiau Basin; OT, onshore Taranaki; N, Northland.

because of the tectonic complexities in Northland resulting from a Paleogene re-organisation and flip in subduction direction and the subsequent emplacement of the Northland Allochthon in the latest Oligocene and Early Miocene (e.g., Spörli, 1989; Hayward *et al.*, 1989).

The deformed regions described above define a Late Eocene deformation zone that trended northeasterly in southern New Zealand, northerly in central New Zealand and northwesterly to the north of New Zealand. The directions of relative plate motion predicted by the A18–A13 (42–35 Ma) stage pole requires that the basins in the southern and central parts of the deformation zone were components of a disseminated and complex zone of transtension (Fig. 5.9) (Walcott, 1989). Conceivably, the strike-slip components have not been preserved or not yet recognised due to late Cenozoic inversion tectonics and further strike-slip faulting. The present interpretation of seafloor magnetic anomalies in the Emerald Basin is not well constrained (Weissel *et al.*, 1977), but the basin may have been linked to New Zealand by a series of transform faults and short, active spreading segments comparable to the present situation in the Gulf of California (e.g., Crowell, 1986). The plate boundary is inferred to have been largely transform or transpressive in central and northern North Island, and convergent in the far north of New Zealand.

King (1990) presented reconstructions which are consistent with the data compiled here and by Walcott (1989) and which account for changing styles of sedimentation in the Early Miocene and the disparity between the late Cenozoic displacement by the Alpine Fault and the total Late Eocene-Recent relative plate motion predicted by the seafloor magnetic data. A pre-Miocene strike-slip fault system is inferred to have extended in a roughly north-south orientation, parallel to the trend of basement terranes, from Waikato through present day onshore Taranaki and through north-western South Island, where it became more divergent, passing to the west of the late Paleozoic-Mesozoic basement terranes that now crop out in the Marlborough fault system east of the Wairau Fault (see Fig. 8.3). Changes in the motion of the Pacific Plate in the Early Miocene (Walcott, 1987) resulted in the inception of the modern transpressive Alpine Fault system which now displaces late Paleozoic basement terranes in the South Island about 480 km.

The Late Eocene faults beneath the NW Chatham Rise (Fig. 5.5) and similarly-aged faults elsewhere on the Chatham Rise mapped by Wood *et al.* (1989) are, therefore, inferred to have formed within the Pacific Plate, close to the pole of rotation and highly oblique to the orientation of the plate boundary (Fig. 5.9). This intra-plate extension occurred possibly between 500-1200 km east of the plate boundary and concentrated along weakened crust of the Chatham Rise which had already undergone subduction imbrication and rifting in the Cretaceous (Fig. 5.8).

5.5 DISCUSSION

One of the most striking features of the NMFZ is the broad similarity of structural style and fault orientations to that which developed during older extensional episodes, despite different tectonic settings and variations in the width of the fault zone and extensional locus (Fig. 5.10). Both the Eocene and the late Cenozoic deformations involved reactivation of some pre-existing structures and development of new, synthetic, basement-involved, normal faults. Both of these deformations exhibit strong structural heredity.

Although Mesozoic Torlesse terrane greywacke has been dredged from Mernoo Bank and can be traced as acoustic basement in seismic reflection profiles of the western Chatham Rise (e.g., Lewis *et al.*, 1986; Herzer and Wood, 1988) (Figs 5.2 and 5.4), its internal structure is unknown. Based on onshore structural studies of young (Early-mid Cretaceous), probably-correlative Torlesse basement in northeastern South Island and southeastern North Island (MacKinnon, 1983; Bradshaw, 1988; George, 1990; Barnes and Korsch, 1991), the Torlesse basement beneath the western Chatham Rise is inferred to be a weakly metamorphosed, imbricated accretionary complex consisting predominantly of multiply-folded, shear-fractured greywacke and argillite with common melange zones and minor faulted slivers of exotic ocean-floor assemblages. The regional structural grain of the late Mesozoic complex, displayed onshore by linear markers such as the Esk Head Melange, appears to trend offshore from northeastern South Island onto the western Chatham Rise (e.g., Bradshaw, 1988) suggesting that the overall structural fabric in the basement beneath the NW Chatham Rise slope may strike roughly east-west to WNW–ESE.

The east-west striking, mostly south-dipping, Late Cretaceous normal faults that developed on the Chatham Rise in response to crustal stretching and rifting of the Bounty Trough region (Fig. 5.3; Wood *et al.*, 1989) may have reactivated similarly-trending basement discontinuities such as thrust faults and steeply-dipping sheets of melange. Normal-sense reactivation of pre-existing thrust faults and fault parallelism with other basement fabrics such as metamorphic foliations is common in many other rift systems (Ratcliffe *et al.*, 1986; Montenat *et al.*, 1988; Greiling *et al.*, 1988; Root, 1989; Stein and Blundell, 1990; de Voogd *et al.*, 1990; Jolivet *et al.*, 1991; Matos, 1991). Sibson (1985) showed theoretically that such normal-sense reactivation of pre-existing thrust faults requires abnormally high fluid pressures and the effective least principal stress to be tensile.

Most of the Eocene extension of the NW Chathamn Rise was accommodated on newly-formed basement-involved normal faults, indicating that the deformation resulted from significant tectonic stresses rather than simple differential sediment

Fig. 5.10. Summary maps showing the distribution of extensional faults active during three separate phases in the tectonic evolution of the NW Chatham Rise. A. Mid-Late Cretaceous; B. Eocene; C. Late Miocene to Recent. A and B are summarised from sediment isopach maps (Figs 5.3 and 5.5) and C is derived from a structural contour on the Early Pliocene reflector L (Fig. 5.7). Transfer zones between faults are finely stipped. For reference, several late Quaternary features are shown: prominent mid-slope current erosion is shaded (Fig. 3.9); shelf edge (c. 150 m water depth) is dashed; toe of the north Chatham Rise slope is dotted; and several submarine canyons at the head of the Hikurangi Channel are arrowed. See labelled faults on seismic profiles 1–1' to 9–9' (Figs 5.2, 5.4 and 5.6).

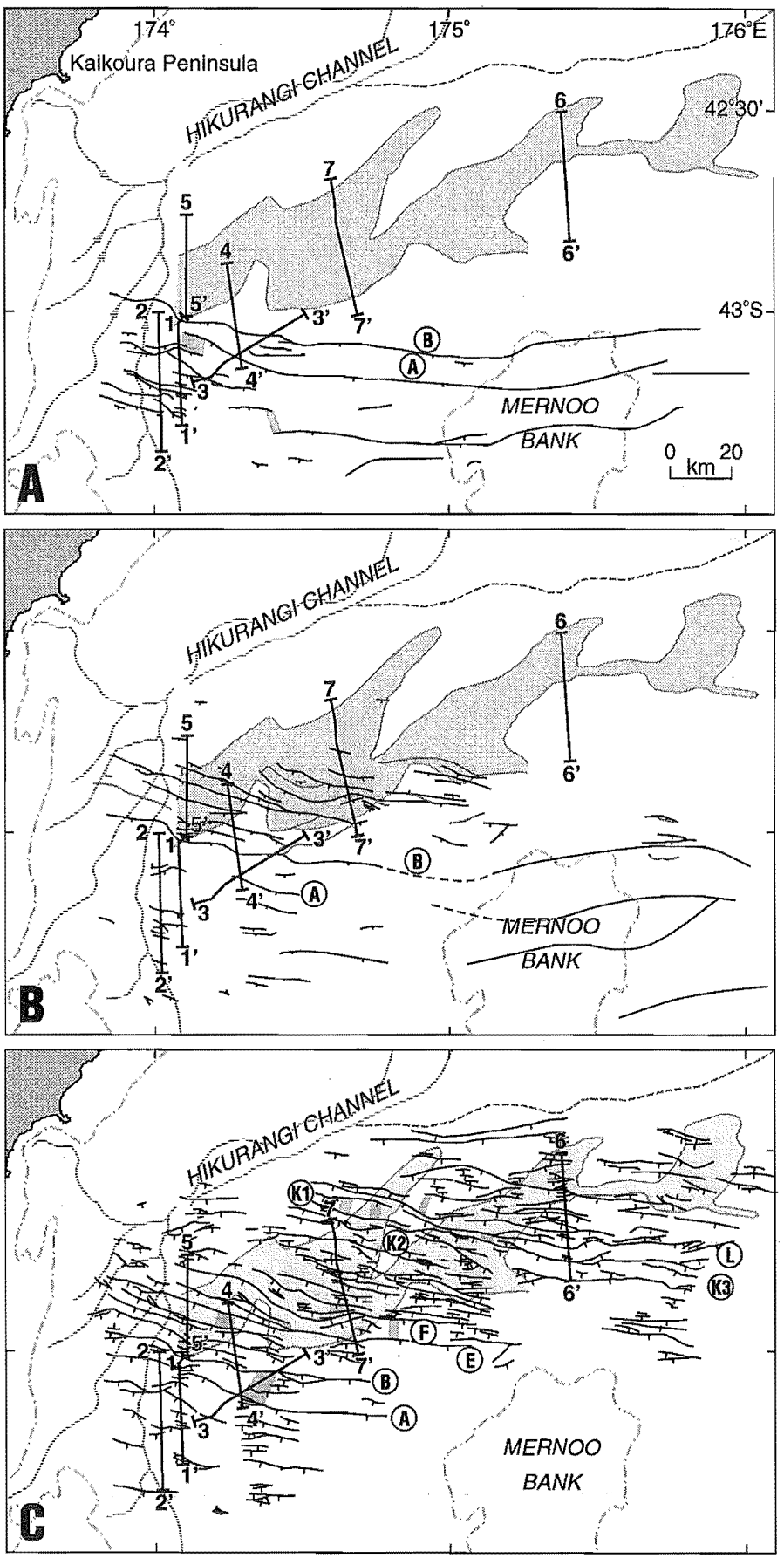
174°
175°
176°E
Kaikoura Peninsula
HIKURANGI CHANNEL
42°30'
43°S
MERNOO
BANK
0 km 20
A
B
C
1
2
3
4
5
6
7
1'
2'
3'
4'
5'
6'
7'
A
B
E
F
K1
K2
K3
L

compaction and subsidence on pre-existing structures. However, the origin of the intra-plate stresses responsible for these faults and structures of similar age elsewhere on the Chatham Rise is problematical. The latest Eocene was a time when there were major plate boundary re-organisations north of New Zealand involving obduction of New Caledenia ophiolites and relocation of subduction zones (Kroenke, 1984; Eade, 1984, 1988). Although highly speculative, one possibility is that tensional stresses on the Chatham Rise were generated by differential anti-clockwise rotation of different regions within the Pacific Plate caused by cessation of subduction beneath the Norfolk Ridge and relocation of the convergent plate boundary north of New Zealand, whilst continuous, northeasterly trending dextral transtensional was occurring in central and southern New Zealand (Fig. 5.9).

The fact that most of the Eocene extension of the NW Chatham Rise occurred on newly created faults indicates that although two-dimensional Mohr-Coulomb criteria for reactivation of the Cretaceous normal faults was achieved (e.g., Stearns *et al.*, 1981; Sibson, 1985; Thatcher and Hill, 1991), it was mechanically easier to generate new faults in crust to the north of the pre-existing structures. The Cretaceous faults had more resistance to failure than older, probably similarly orientated discontinuities in the basement, possibly because their coefficients of friction were higher than the internal friction of the adjacent crust, or because abnormally high pore pressures existed in other basement shear zones. In either case the similar style and parallelism of the Eocene faults compared to the Cretaceous faults and possible alignment of the new structures with basement fabrics suggests a strong structural heredity during the Eocene deformation.

The development of the NMFZ resulted from the initiation of renewed tensional stresses in the NW Chatham Rise in the Late Miocene. All of the major Eocene faults and some of the Cretaceous normal faults in this area were reactivated. Furthermore, many new basement-involved structures were generated during Late Miocene and Early Pliocene times, particularly north of the Eocene faults. By Early Pliocene time, the deformation was more widely distributed and pervasive in the NW Chatham Rise region than during either of the two preceding episodes of extension. However, the style and orientation of both the newly created faults and the propagating segments of reactivated structures follows the pattern that was created during the older, New Zealand-wide extensional events. This suggests that despite possible differences in the magnitudes and orientations of principal stresses, in fault-slip vectors and in overall extension directions during the different deformational episodes, the orientations of the pre-existing Torlesse basement fabrics together with the superposed Cretaceous and Eocene fault geometries, strongly influenced the style of late Cenozoic deformation in this region.

There are nevertheless, differences in probable respective fault kinematics, fault-basin evolution, and driving forces despite similarly small amounts of strain accumulation and a domino-style of faulting during each extensional phase. Firstly, both the Late Cretaceous and the Eocene faults in the NW Chatham Rise region are only parts of much larger fault systems covering much of the Chatham Rise (Wood *et al.*, 1989), whereas the Late Miocene-Recent normal faults are restricted to the NMFZ. Secondly, the Cretaceous faults developed in terrestrial and marginal marine settings and most of the extension of the NW Chatham Rise slope was accommodated on two or three major structures bounding half- grabens that filled with syn-tectonic sediments. In contrast, both the Eocene and late Cenozoic phases of extension of the NW Chatham Rise developed in a totally submarine setting and strain was more widely distributed across broader fault systems. Thirdly, the tectonic settings in which the three tensional stress fields developed are different. The Late Cretaceous faults were associated with rifting of a recently quiescent accretionary wedge during precursory extension near the edge of Gondwana prior to final continental rupture and seafloor spreading in the Tasman Sea and southwest Pacific Basin. The Eocene faults developed on the Pacific Plate in an intra-plate setting but in a position peripheral enough to be kinematically linked to the evolving Australia-Pacific plate boundary. The Late Miocene-Recent fault system, which is comparatively less extensive regionally, developed on the Pacific Plate at the complex southern end of the Hikurangi Subduction zone and reflects tensional stresses within the Australia-Pacific plate-boundary zone.

5.6 CONCLUSIONS

(1) The active NMFZ on the northwestern corner of the Chatham Rise developed in the Late Miocene but three discrete phases of syn-sedimentary continental extensional tectonics are recorded in the region. The first, Late Cretaceous phase involved east-west trending, mostly south dipping, normal faults and associated half-graben basins, which developed over most of the Chatham Rise during rifting of the Bounty Trough near the edge of the Gondwana supercontinent. During this phase of extension, two major fault-bounded half-grabens containing up to 2 km of syn-tectonic sediment, together with other smaller basins, developed in the present region of the NMFZ. The faults accommodated 4–23% extension. Throughout the Paleocene most of the western Chatham Rise was subaerial or very shallow marine and sediments of this age occur only on the lower flanks of the rise. Consequently, syn-tectonic Eocene sediments overlie basement and Late Cretaceous strata throughout most of the region.

(2) The second phase of normal faulting also developed over wide regions of the Chatham Rise beyond the NMFZ and is tentatively inferred to be of Late Eocene age. This faulting occurred within the Pacific Plate possibly at least 500 km from the main deformation zone of the newly-formed Australia-Pacific plate boundary. In the present region of the NMFZ, the faults inherited older basement and Cretaceous structures but mainly formed in new crust to the north of the Cretaceous faults as an array of overlapping, domino-style faults dipping south and up slope. The faulted basins contain up to 230 m of syn-tectonic sediment and resulted in 2–7% extension. It is speculated here that the Eocene extensional fault system on the Chatham Rise may have been generated by differential rotation of the Pacific Plate as the position of the convergent plate boundary north of New Zealand was being re-organised whilst transtension continued through the central New Zealand region linking with oblique rifting in the Emerald Basin to the south of New Zealand.

(3) The third phase of normal faulting began in the Late Miocene (c. 8–6 Ma) and is referred to as the NMFZ. The deformation is restricted to the southern end of the Hikurangi subduction margin. The east-west to WNW-ESE trending, southward dipping, domino-style faults were most widely distributed in the Early Pliocene (5–3 Ma) when the fault system covered the whole NW Chatham Rise slope, attaining a width of about 100 km. The maximum post mid-Pliocene (c. 3.4 Ma) vertical displacement is 170 m and total extension is extremely small (< 2%). Relay ramp structures characterise the transfer zones between major fault segments. Most of the Eocene faults and many of the Cretaceous structures in this region were reactivated and many new basement-involved faults were generated both within the area encompassed by the older normal faults and also on the lower slope further north.

(4) Despite different dynamic forces and probably dissimilar regional stress fields during different extensional episodes, the geometries and map patterns of both the reactivated faults and the newly formed basement-involved structures indicate a strong structural heredity for both the Eocene and the late Cenozoic deformations. Thus, the kinematics of active deformation in this part of the Australia-Pacific plate boundary is likely to be strongly influenced by structural discontinuities produced during previous deformational phases.

CHAPTER 6

STYLE AND KINEMATICS OF QUATERNARY NORMAL FAULTS, NORTH MERNOO FAULT ZONE, NORTHWESTERN CHATHAM RISE

6.1 INTRODUCTION

The present structure of the NMFZ evolved from three separate phases of basement-involved normal faulting, separated by long periods of tectonic quiescence (Fig. 5.10) (Herzer and Wood, 1988; Wood *et al.*, 1989). Chapter 5 presented detailed interpretations of each phase of normal faulting (mid-Late Cretaceous, Eocene and Late Miocene-Recent). The first two phases were part of widespread extensional fault systems that developed over the entire Chatham Rise region. The third phase has been confined to the NMFZ on the northwestern edge of the Chatham Rise and the Pacific edge of the present plate-boundary zone (Fig. 1.1). This chapter focuses on the c. 100 x 300 km region of seismically-active normal faults. Seismic reflection profiles have been utilised here to study the Quaternary evolution and neotectonics of the NMFZ, within the stratigraphic framework established in Chapter 4. The specific aim of this chapter is to discuss the style and possible kinematics of deformation.

In other parts of the world, normal fault systems occur in a variety of plate tectonic settings and they represent an important mechanism for extending continental crust (e.g., Harding and Lowell, 1979; Jackson, 1987). Extensional styles and settings have received considerable attention from researchers in the last 20 years or so, because many ancient normal fault systems are important petroleum provinces and because many active systems generate large magnitude earthquakes and thus, have implications for seismic hazard assessment and for studies of plate-boundary kinematics. Despite differing dynamic forces responsible for extension in different tectonic settings and the variety of possible map view patterns of extensional faults, together with variations in crustal thicknesses, heat flow characteristics and seismogenic depth, global compilations show that there are several features common to most continental, seismically active normal fault systems (Jackson, 1987; Jackson and White, 1989). The faults commonly occur in sets that bound tilted upper crustal blocks and they are rarely continuous along strike for more than 25 km, although the total surface rupture of several fault segments during large earthquakes may exceed 70 km (de Polo *et al.*, 1991). Faults commonly change strike and step over from one to the next in *en echelon* patterns, with segmentation lengths comparable to the thickness of the seismogenic layer. Large seismically active normal faults appear to be approximately planar and to rotate 'domino-style' arrays of blocks about horizontal

axes as they move. The majority of seismogenic faults dip in the range of 30–60° (Jackson, 1987); dips of < 30° or > 70° are rare, although they may occur (e.g., Abers, 1991; Thatcher and Hill, 1991). The NMFZ might be expected to exhibit some of these physical characteristics.

It was shown in Chapter 5 that during Pliocene times normal faults were widely distributed in the NMFZ, deforming the full width of the NW Chatham slope (Figs 5.7 and 5.10). Since that time the fault zone has continued to evolve to its present day geometry (Figs 6.1 to 6.5). Most of the normal faults beneath the lower NW Chatham slope, in water deeper than about 1500 m, together with many of the upper-slope faults south of fault A, have not been active since the Late Pliocene-Early Pleistocene (c. 2–1 Ma) (Fig. 6.1, profiles 1–1', 4–4'; compare Figs 5.7 and 6.5). Most of the structures beneath the lower slope have been buried by Pleistocene sediment drifts that show only local evidence of late Quaternary displacement. Furthermore, a small area in the northwestern corner of the NMFZ, at the head of the Hikurangi Trough, has been overprinted during the Quaternary by thrust faults and folds of the southern Hikurangi margin (Figs 5.7, 6.2 and 6.5). In contrast, beneath the mid-upper Chatham Rise slope, many normal faults have remained active since the Early Pleistocene and surface traces are widespread on the seafloor (see Fig. 6.5). The normal faults exhibit growth characteristics through the Quaternary period with vertical displacement decreasing with diminishing stratigraphic age (Figs 6.1, 6.3, 6.4 and 6.6).

6.2 ACTIVE NORMAL FAULTING

6.2.1 GENERAL DISTRIBUTION AND DEFINITIONS

Although the active normal faults in the NMFZ are widespread they are concentrated in an 80 km wide, east-west trending zone which cuts obliquely across the mid-upper slope between 42°25'S and 43°S (Figs 6.3 to 6.5). This zone, carefully mapped from its western end near Pegasus Canyon to 176°E, but extending further east to at least 177°30'E, coincides approximately with the area of complex late Quaternary current erosion and with some intervening areas of hemipelagic sedimentation (Fig. 3.9). Consequently, within the most active part of the fault zone, Holocene sediments are absent and several Plio-Pleistocene sequences are exposed at the seabed; their exposure pattern reflecting the shape of the current scours, the geometry of the sequences, and less significantly, the magnitudes of the displacements on the faults (Fig. 4.7).

The normal faults are referred to in this thesis as being 'active' if they have seafloor expression, irrespective of the age of the sedimentary sequence exposed at

Fig. 6.1. Single-channel airgun seismic reflection profiles 1–1' and 4–4' across the western end of the NMFZ showing normal faults beneath the lower and upper slope that have not been active since the Late Pliocene-Early Pleistocene. Some late Quaternary normal displacements occur on the mid slope. See Fig. 6.5 for profile positions. Circled letters above faults are fault traces labelled on Figs 5.3, 5.5, 5.7, 5.10 and 6.5

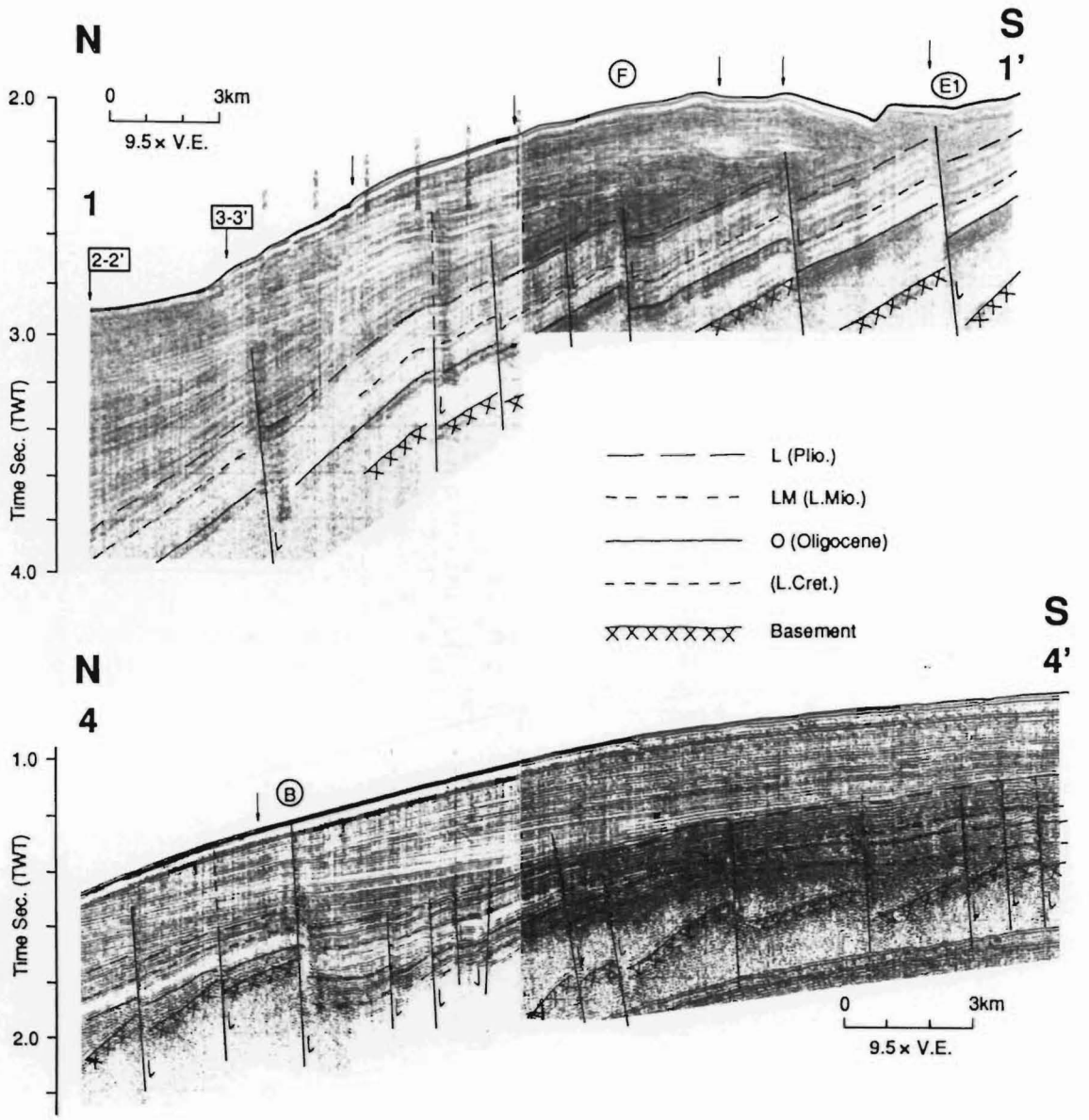
N
S
1'
1
0
3km
9.5× V.E.
2.0
3.0
4.0
Time Sec. (TWT)
3-3'
2-2'
F
E1
L (Plio.)
LM (L.Mio.)
O (Oligocene)
(L.Cret.)
Basement
S
4'
N
4
1.0
2.0
B
0
3km
9.5× V.E.

Fig. 6.2. Single-channel airgun seismic reflection profiles 2–2' and 3–3' across the extreme southern end of the imbricated frontal wedge of the Hikurangi margin. The profiles show the positions of Quaternary thrust faults and fault propagation folds that overprint, but do not reactivate, the normal faults at northwestern corner of the NMFZ (see also profile 1, Fig. 7.3). Numbers beneath profiles are TWT time in seconds. Arrows above profiles are the positions of intersecting profiles. See Fig. 6.5 for profile positions.

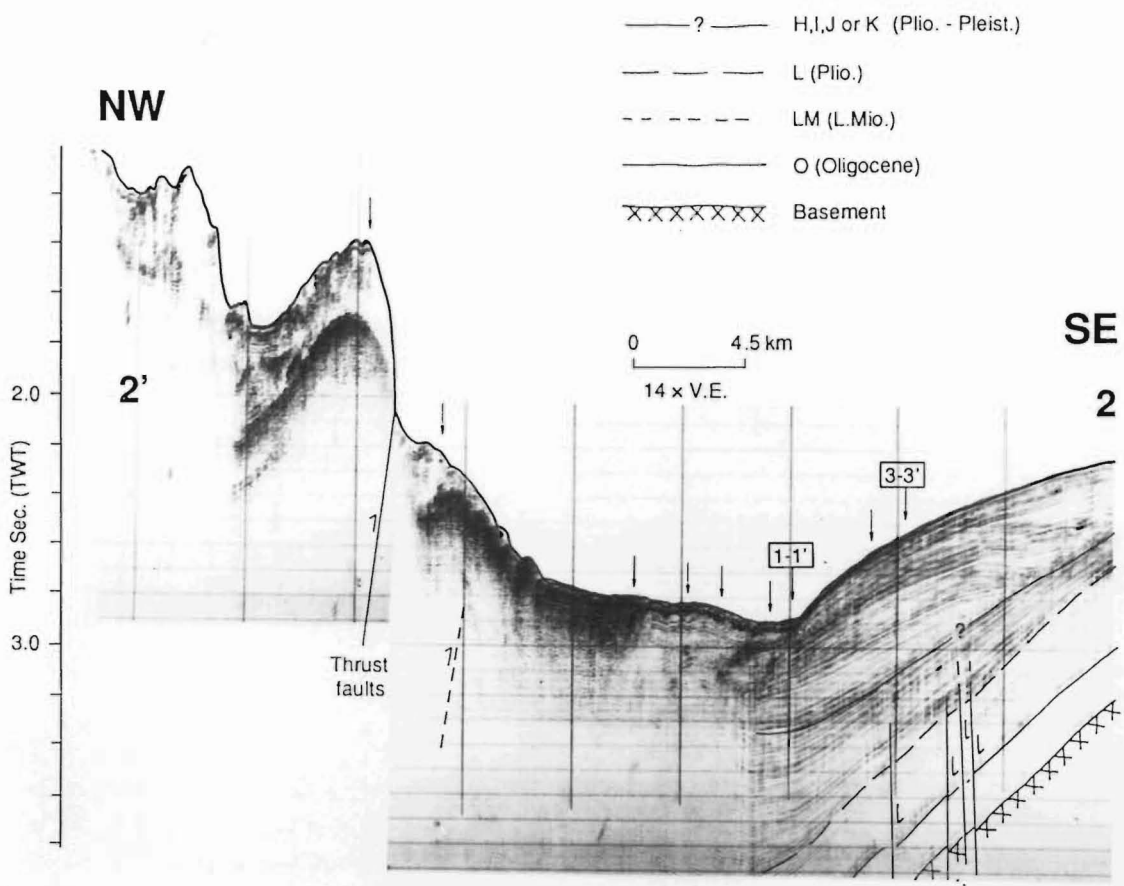
? H,I,J or K (Plio. - Pleist.)
L (Plio.)
LM (L.Mio.)
O (Oligocene)
Basement
NW
SE
2'
2
0 4.5 km
14 x V.E.
Time Sec. (TWT)
2.0
3.0
3-3'
1-1'
Thrust faults
L
?

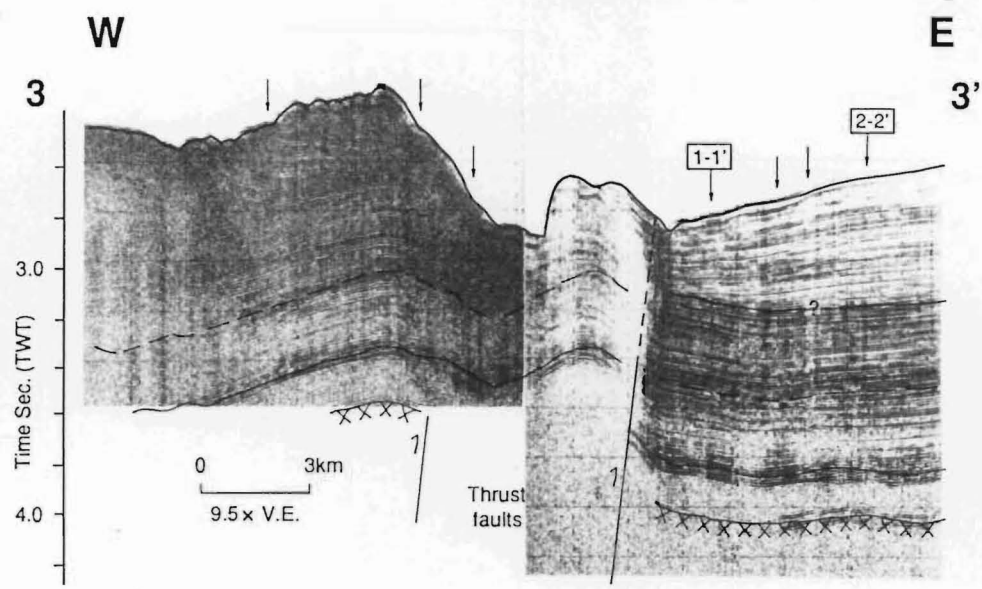
W
E
3
3'
2-2'
1-1'
Time Sec. (TWT)
3.0
4.0
0 3km
9.5 x V.E.
Thrust faults
?

Fig. 6.3. Single-channel airgun and 3.5 kHz seismic reflection profiles 5–5' to 7–7' across the NMFZ. Numbers beneath the 3.5 kHz profiles are TWT time in seconds. Arrows above profiles are the positions of intersecting profiles. V (profile 7–7'), volcanic rock. See Fig. 6.5 for profile positions. Circled letters above faults are traces labelled on Figs 5.3, 5.5, 5.7, 5.10 and 6.5.

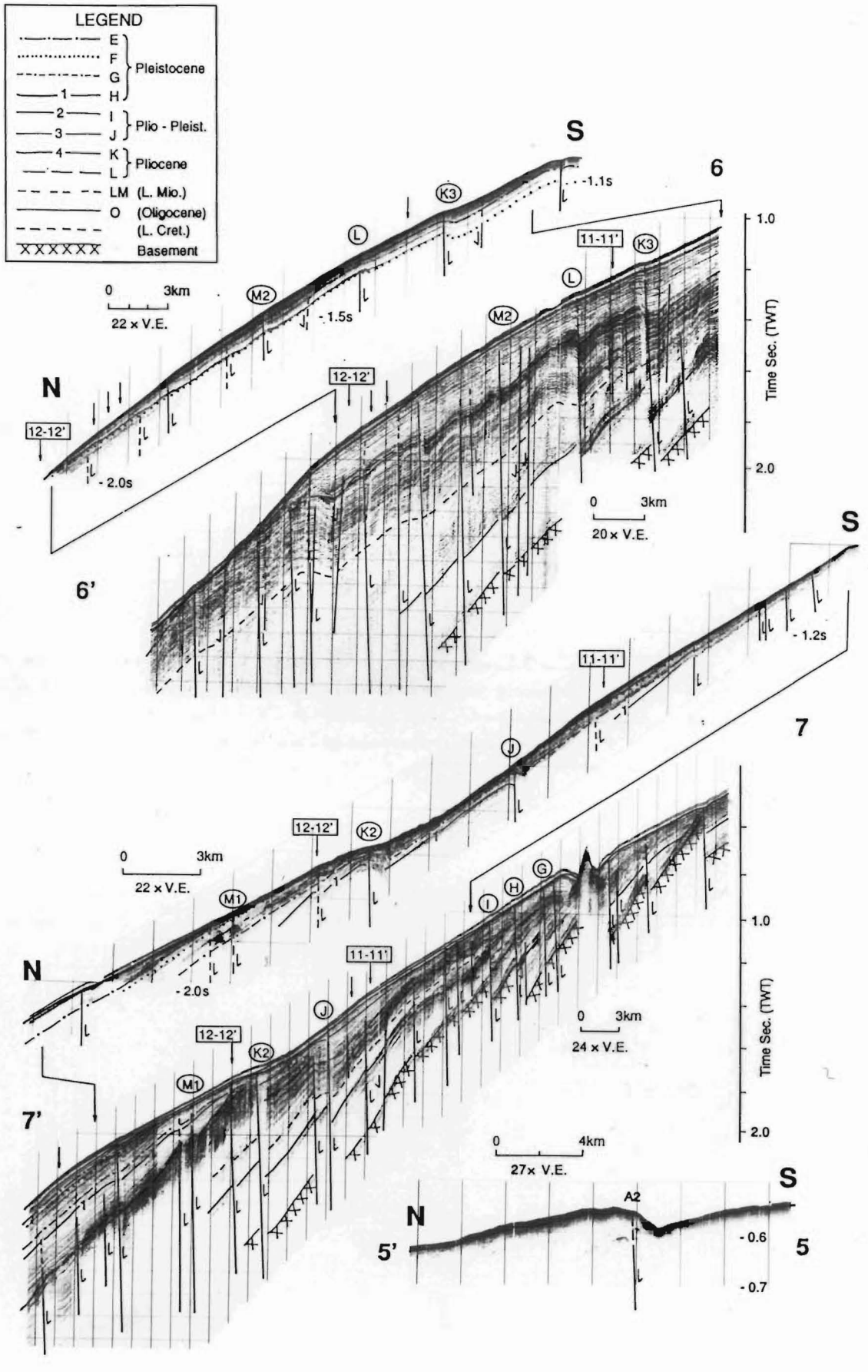
LEGEND
E
F
G
H
Pleistocene
1
2
I
J
Plio - Pleist.
3
4
K
L
Pliocene
LM (L. Mio.)
O (Oligocene)
(L. Cret.)
Basement
S
6
-1.1s
K3
L
11-11'
0 3km
22 x V.E.
M2
-1.5s
N
12-12'
-2.0s
6'
20 x V.E.
Time Sec. (TWT)
1.0
2.0
S
-1.2s
7
J
K2
M1
I
H
G
24 x V.E.
7'
0 4km
27x V.E.
S
A2
N
5'
-0.6
-0.7
5

Fig. 6.4. Single-channel airgun and 3.5 kHz seismic reflection profiles 8–8' to 10–10' (down slope) and profiles 11–11' and 12–12' (along slope) through the NMFZ (North Mernoo Fault Zone). See Fig. 6.5 for profile positions. Circled letters above faults are traces labelled on Figs 5.3, 5.5, 5.7, 5.10 and 6.5. See Fig. 6.3 for legend. Numbers beneath profiles are TWT time in seconds. Arrows above profiles are the positions of intersecting profiles.

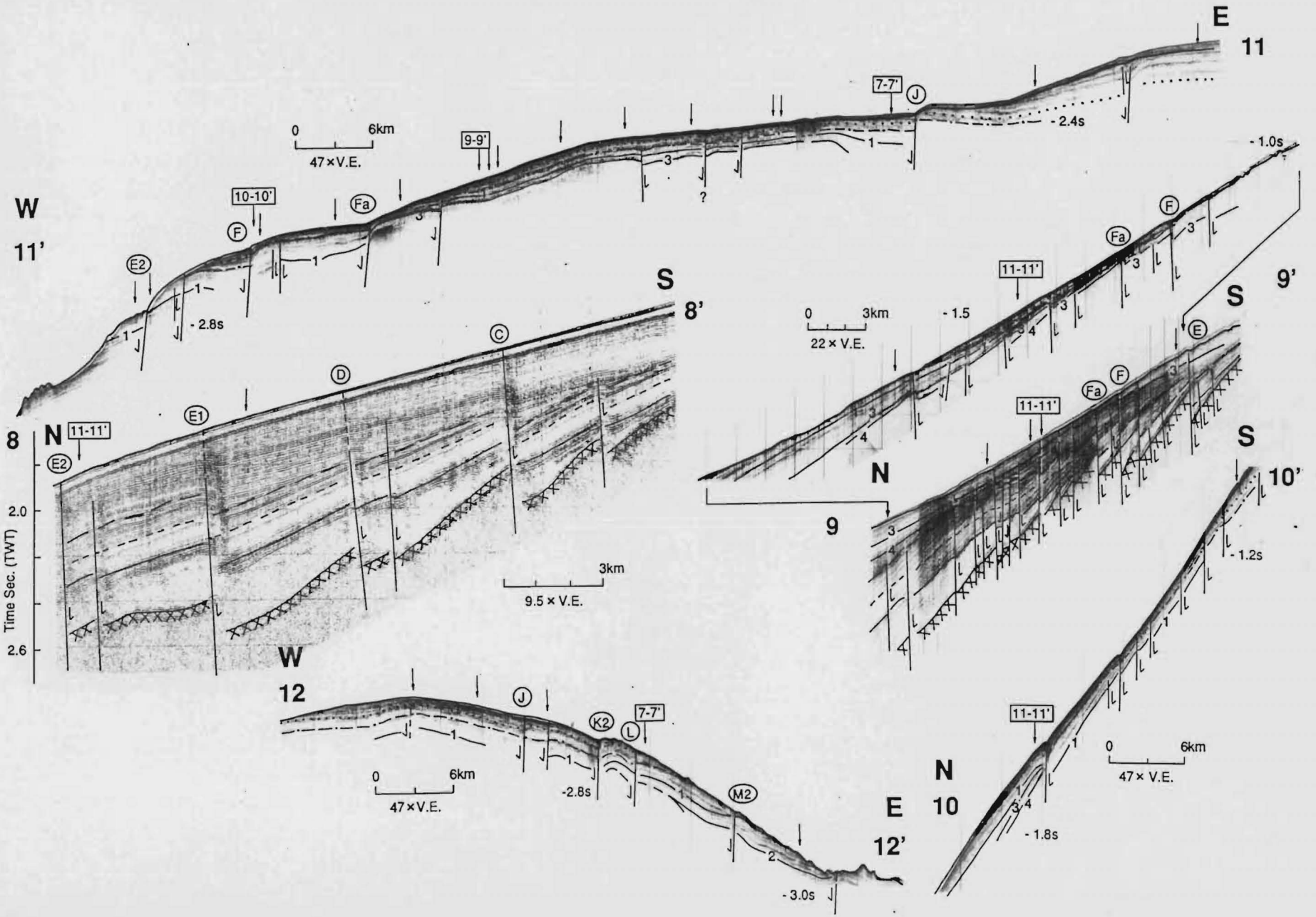
W
11'
E
11
7-7'
J
9-9'
10-10'
F
Fa
E2
E1
C
D
- 2.8s
- 2.4s
- 1.0s
0 6km
47×V.E.
S
8'
8
N
11-11'
2.0
2.6
Time Sec. (TWT)
3km
9.5 × V.E.
0 3km
22 × V.E.
- 1.5
S
9'
E
N
9
S
10'
- 1.2s
W
12
K2
L
M2
-2.8s
- 3.0s
N
E
10
12'
- 1.8s

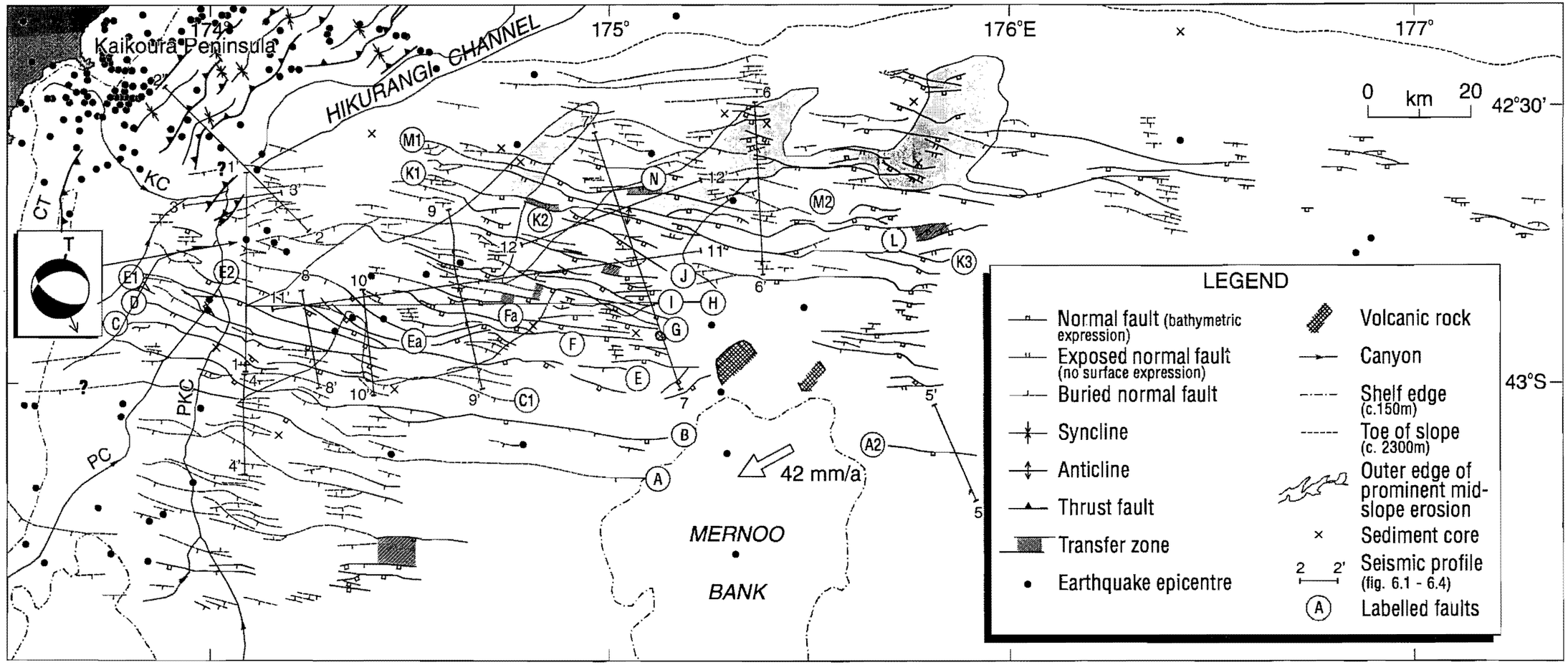

Fig. 6.5. Structure and historical (post 1964) seismicity of the North Mernoo Fault Zone and the adjacent, southern part of the imbricated frontal wedge of the Hikurangi margin. Large arrow at Mernoo Bank is the vector of motion of the Pacific Plate relative to the Australian Plate (De Mets *et al.*, 1990). The focal mechanism is for a 1965 $M_w = 6.1$ earthquake from the western end of the extensional province; the small arrow beneath the focal mechanism is the aximuth of the slip vector and T is the tension axis. The locations of only those sediment cores which constrain the late Cenozoic seismic stratigraphy are shown. See labelled faults A–N on seismic profiles, Figs 6.1 to 6.4. KP, Kaikoura Peninsula; CT, Conway Trough; KC, Kaikoura Canyon; PC, Pegasus Canyon; PKC, Pukaki Canyon.

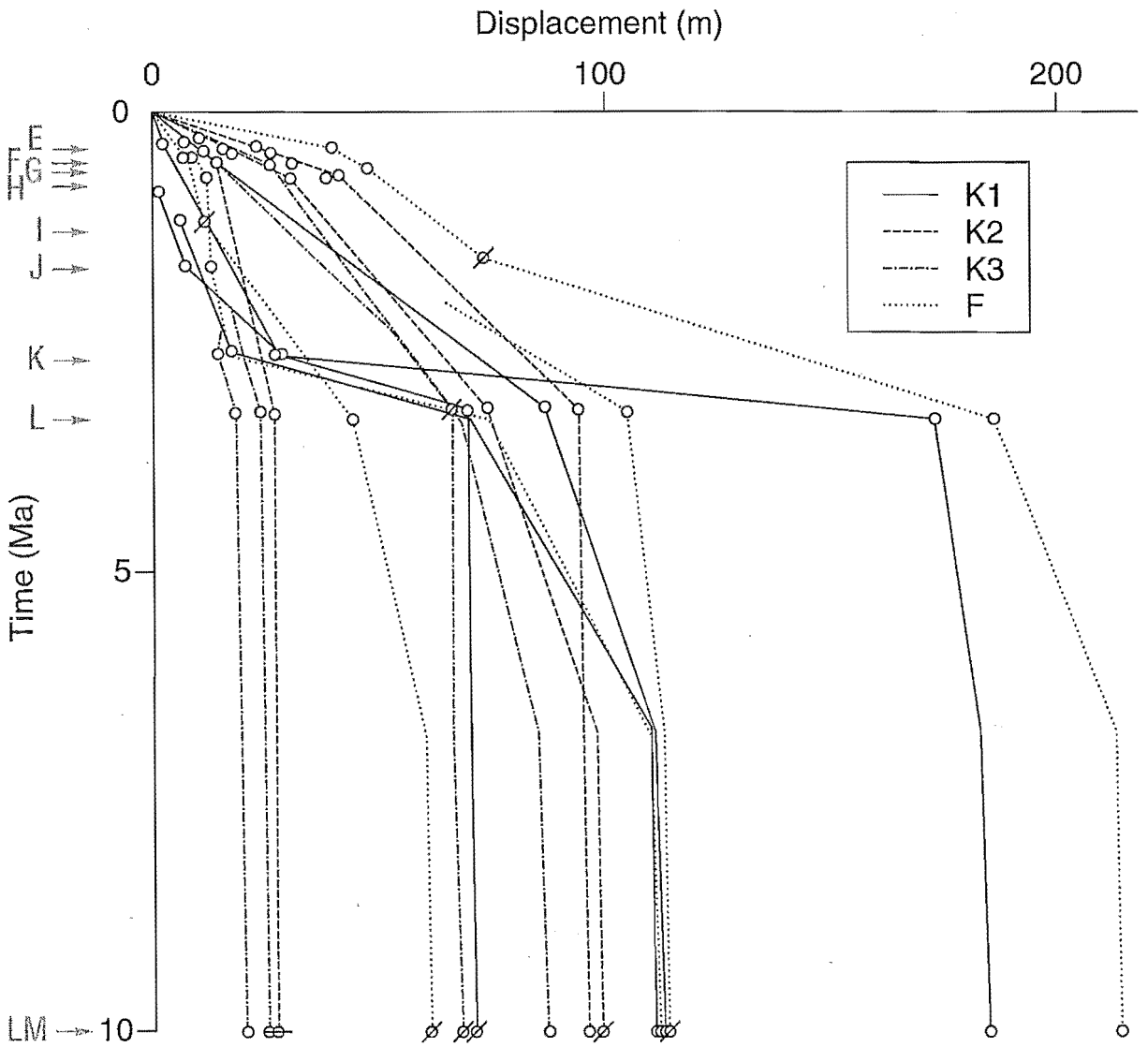

Fig. 6.6. Time-displacement curves for fault F and three geometric segments of fault K illustrating growth faulting since the Late Miocene. Each line represents the displacement history of the faults at positions where the faults are intersected by seismic reflection profiles. The displacements are calculated in metres assuming velocities of 1500 m/s in water and 1700 m/s in the sediment. Open circles are well constrained reflectors (c. ± 5% displacement); circles with lines through them are less well constrained reflectors (c. ± 15% displacement). See Fig. 4.2 for stratigraphy of reflectors G to L and LM. See Fig. 6.5 for position of faults. Note the large differences in the time-displacement curves for fault F which are consistent with the geometric fault segmentation.

the seabed (Figs 6.3 and 6.4). This is justified because much of the seafloor was sculptured during the last major phase of mid-slope current erosion which is inferred to have occurred during the peak of the last glaciation (c. 22–14 ka), although localised mid-slope erosion may have continued to present day (Chapters 3 and 4). Thus, many of the surface displacements are likely to represent fault rupture during the last few tens of thousands of years. Surface scarp preservation is highly variable. In areas of greatest erosion, some faults can be traced to the seabed in seismic profiles, clearly displacing the shallowest reflections, but the faults have no surface expression, making determination of their most recent activity difficult. They may represent exhumed Plio-Pleistocene faults that have not ruptured in late Quaternary time, or their late Quaternary displacements may have been removed by erosion (Figs 6.3 to 6.5). On the available, highly-exaggerated seismic profiles, it is commonly difficult to determine whether the surface expressions of active faults are localised rupture scarps or the compressed images of forced flexures (section 6.2.2). The surface expressions are referred to here as surface scarps.

6.2.2 DEFORMATIONAL STYLE

Comparison of Figures 5.10 and 6.5 suggests that the style of active faulting is strongly influenced by the tectonic fabric that had developed by the Early-mid Pliocene, which in turn was inherited from previous phases of extension and probably also from older basement fabrics (Chapter 5). Late Quaternary displacements occur on several of the Late Cretaceous faults, on most of the Late Eocene faults and on many other faults that developed in the late Cenozoic. The active extensional system consists of subparallel faults trending W–E to WNW–ESE, with typical strikes of 095° in the eastern part of the fault zone, changing slightly to 105° in the west (Fig. 6.5). Minor fault sinuosity or zig-zag produces local NE-SW trends resulting in about 30° total range in strike. No evidence has been found for transverse faults which, in some other fault systems, produce multi-directional patterns and footwall trapdoor blocks (Harding, 1984; Harding and Lowell, 1979), or which might represent oblique-slip transfer faults (e.g., Gibbs, 1984, 1990; Etheridge *et al.*, 1985) or cross-faults that sometimes develop to accommodate variable hangingwall extension above major breakaway faults (Sengor, 1987). Instead, the NMFZ exhibits a relatively simple pattern of overlapping faults, which are nearly all dipping southward (up slope) and are commonly 2–5 km apart (Figs 6.3 to 6.5). There is a left-stepping arrangement to the faults along the northern part of the fault zone (Figs. 5.7 and 6.5) and overall, a weak *en echelon* pattern, although this impression may be biased by the data coverage in the east. On a few seismic profiles from the upper slope north and northeast of Mernoo Bank, surface traces are common and possibly continue along slope into the upper slope area east of 176° E, which has not been mapped here (Fig. 6.5).

Several faults have been traced along strike for distances of 90–115 km (e.g., faults B, E, F, K and L; Fig. 5.7 and 6.5) and surface displacement is recorded on a few structures for up to 80 km in length (Fig. 6.5). These observations rely on correlations between profiles commonly several kilometres apart. However, based on other, well studied active normal fault systems elsewhere in the world, the faults are likely to be discontinuous, and overlapping or approaching segments are unlikely to exceed 25 km in length (Jackson, 1987, Jackson and White, 1989; de Polo *et al.*, 1991). Some evidence for segmentation of the long fault traces mapped here is seen in the variations in vertical displacements of both the seafloor and various subbottom reflections, along the strike of individual faults (Fig. 6.6). For example, considering that total vertical displacements of the Pliocene reflector L of 30–80 m are common and that 170 m is the maximum (Fig. 5.7), the displacements of this reflector by individual faults commonly vary along strike by a factor of 3 and may vary by a factor > 10. Further evidence for segmentation includes the presence of transfer zones (Morley *et al.*, 1990) which have been mapped in the fault system (Figs 5.10 and 6.5). Such transfer zones conserve extension along the strike of the faults (Morley *et al.*, 1990) and two types of synthetic transfer are inferred here (Fig. 6.7): (1) an overlapping transfer, where the ends of faults overlap and throw is transferred at fault tips from one fault to the other via a relay ramp (e.g., Larsen, 1988; Peacock and Sanderson, 1991); and (2) a collateral transfer, where throw is transferred to an adjacent, parallel structure, but within segments and not at the fault tip. Thus, it is inferred that the along-strike variations in vertical throw on the faults results from a combination of different displacement histories on individual fault segments whose boundaries have not been detected with the available data, together with along-strike ramping of surfaces within hangingwalls, between collateral transfer zones (Fig. 6.7).

Seismic reflectors within the sedimentary cover show no evidence of hangingwall rollover (reverse drag), which is a characteristic of thick sequences deformed by listric faults (Hamblin, 1965; Bruce, 1973; Crans *et al.*, 1980; White *et al.*, 1986). Nevertheless, the seismic expression of faulting in the sedimentary cover varies slightly, but not systematically, from one fault to the next. Reflectors from Paleogene and most of the Neogene sequences appear to terminate abruptly against the faults (Figs 6.1 to 6.4). Commonly, such reflection terminations are marked by up-sequence trails of acoustic diffractions on profiles (e.g., profiles 1–1', 4–4' and 8–8'; Figs 6.1 and 6.4). In contrast, reflections within Quaternary sequences are locally gently folded into monoclines above some faults, indicating a less brittle deformation of the younger sequences (e.g., fault K2, K3, Fig. 6.3) (Harding, 1984; Withjack *et al.*, 1990). The less compacted, unlithified cover sequences are deforming by subtle extensional forced folding and minor secondary faulting which develops above the leading edge of the master fault; as the faults propagate up-sequence contemporaneously with

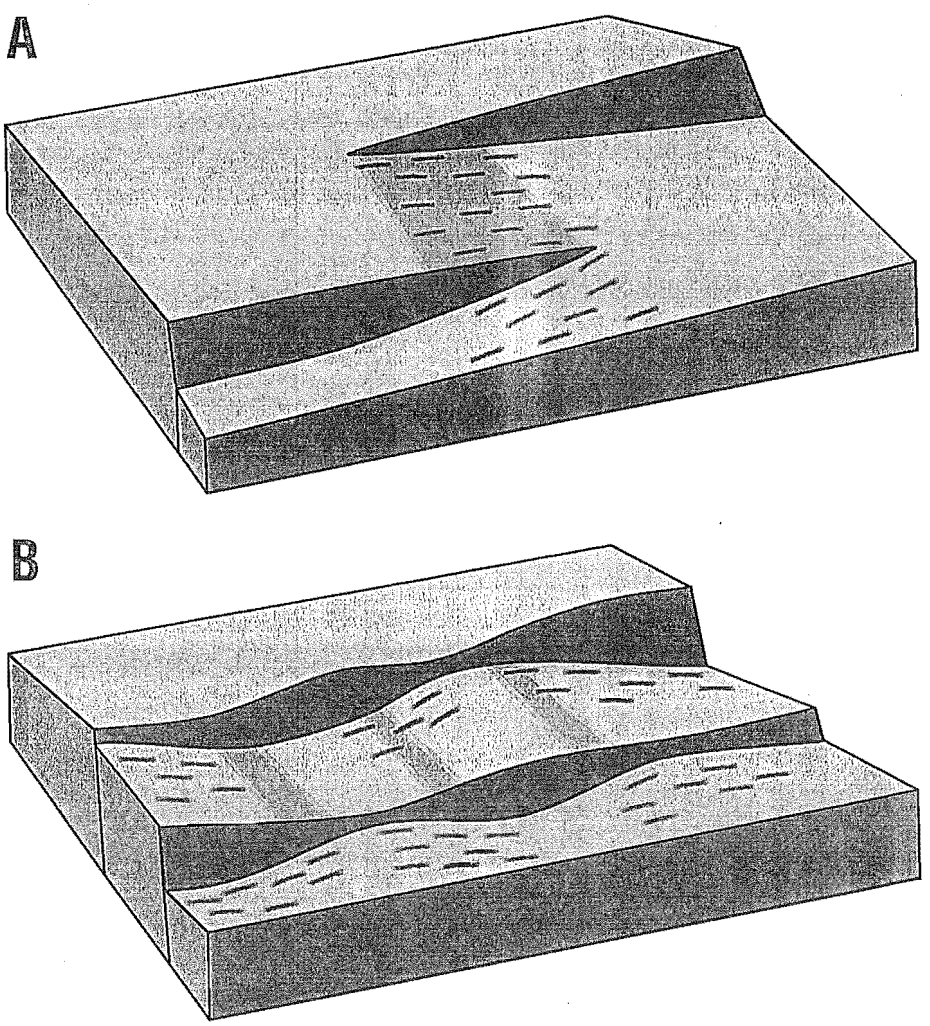

Fig. 6.7. Schematic block diagrams illustrating synthetic overlapping (A) and collateral (B) transfer zones (shaded areas trending normal to the faults) in the North Mernoo Fault Zone. Dashes indicate positions of relay ramps.

sedimentation, they develop growth characteristics and the forced flexures rupture and become accentuated by dip-slip drag.

The heights of surface scarps vary between different faults and along individual faults. Considering the lower limit of scarp height that can be measured on the 3.5 kHz profiles is about 1.5 m, vertical offsets most commonly are < 4 m and less commonly 4–7 m. There are segments of at least six different faults with scarps that locally exceed 9 m in height (faults H, J, N, K2, E2, A2; Figs 6.3 to 6.5) and one scarp is 35–40 m high (Fig. 6.3, fault A2). Although variations in surface scarp height can be related to displacement transfer along strike, in many areas of mid-slope current erosion, significant variations in fault scarp height reflect differences in scarp preservation, not late Quaternary displacement. In deeply eroded areas, faults with possible late Quaternary activity may have no surface scarp preserved (Fig. 6.5).

6.2.3 EXTENSION

The widespread distribution of late Quaternary faults with similar vertical displacements indicates that strain is disseminated, not concentrated on a few major structures. Ignoring the probable minor amounts of internal deformation that may occur within crustal blocks bounded by large normal faults (Kautz and Sclater, 1988), and assuming that the NMFZ is extending by movement on planar faults which dip at 30–60° (see section 6.3) and cut through the seismogenic crust, rotating as they move (Jackson, 1987; Jackson and White, 1989), the amount of horizontal extension (β) can be estimated (Jackson and McKenzie, 1983). Using reflector L (c. 3.4 Ma) as a reference surface (Fig. 5.7), the total amount of horizontal extension perpendicular to the fault system since the mid Pliocene is estimated at 0.4–1.2 km (0.4–1.3%) in the west and possibly only half this amount east of Mernoo Bank. The uncertainities in these estimates could be as much as 30% considering (i) that throw on the faults varies dramatically along strike, (ii) the ability to measure the throws on some faults in the profiles is probably ± 5–10%, and (iii) the seismic velocity interval of 1700 m/s from seabed to reflector L could be in error by as much as 20–30%. Nevertheless, the amounts of extension are extremely small, which may be a reason why the deformation is diffuse and why transverse, oblique-slip transfer faults have not developed (Morley *et al.*, 1990).

Although the largest vertical displacements observed on the Pliocene reflector L occur in the northwestern part of the fault zone, where throws of > 60 m are common, much of the extension in that area occurred before Late Pliocene-Early Pleistocene. The late Quaternary extension, judging from surface scarp heights, appears be concentrated further to the southeast on the upper northern slope of Mernoo Bank, but this pattern is biased by the variable scarp preservation which makes estimation of the late Quaternary extension difficult (compare Fig. 5.7 and 6.5).

6.2.4 HISTORICAL SEISMICITY

The level of historical (since 1964) shallow seismicity (mostly crustal events < 40 km deep) in this region is low compared to many other areas within the New Zealand plate-boundary zone, including the Marlborough fault system to the northwest (Fig. 6.5) (Reyners, 1989). Generally the historical events have been of small magnitude ($< M_L = 4.5$), with locations not accurately constrained because they lie outside of the New Zealand National Seismograph Network. They appear to represent a mixture of upper and lower crustal events with hypocentres commonly assigned to nominal (restricted) depths of 12 and 33 km using the New Zealand crustal model, which assumes a 12 km thick upper crust and a crust-mantle boundary at 33 km depth.

The largest historical earthquake in the western Chatham Rise region, and the only event for which a reliable focal mechanism has been derived, occurred in 1965 at the western end of the NMFZ (Fig. 6.5) (Anderson *et al.*, in press). This event ($M_W = 6.1$) has been modelled by Anderson *et al.* (in press), using long period body waveforms, as two subevents with seismic moments of 9.4×10^{17} and 5.6×10^{17} Nm respectively and with hypocentral depths of 16 -1/+9 km and 16 -6/+9 km respectively. Assuming that the south dipping nodal plane is the fault plane, then the dip of the fault at the centroid is 55 ± 5° towards the SSW and the slip vector is about 158°, implying a component of left-lateral slip. The epicentral location shown in Figure 6.5 could be inaccurate by as much as 20 km (H. Anderson, pers. comm., 1992).

6.3 FAULT KINEMATICS

As they have done since their development or reactivation in the Late Miocene-Early Pliocene (section 5.2.4), the normal faults of the NMFZ define an elongate extensional zone, that is highly oblique (60–70° clockwise) to the overall trend of the New Zealand plate-boundary zone including the subduction thrust front (Figs 1.1 and 6.5). The present trend of the normal faults is 20–30° clockwise from the present plate motion vector in this region (De Mets *et al.*, 1990). There are presently few data available to constrain the offshore kinematics of faulting. The historical seismological record shows little activity and although many of the seismic profiles are inferred to image basement, they are not of sufficient quality to constrain the geometry of the fault planes within basement.

The 1965 $M_W = 6.1$ oblique-slip normal earthquake at the western end of the NMFZ must be interpreted with caution because of the uncertainty in its depth and whether this single event is representative of the kinematics of upper crustal faulting. However, if it is assumed that this was a typical upper crust event related to the

surface normal faulting, then some implications for fault kinematics arise. A dip of 55 ± 5° of the fault plane at the focal depth would be consistent with the geometry expected in a domino array of planar faults that cut the entire upper seismogenic layer (Jackson and White, 1989). Considering the dip of the fault plane at the hypocentre and the inferred projection of the fault towards the surface, then if this earthquake produced surface rupture, either its surface trace has not been located with the available seismic reflection data or more likely its true epicentre must be c. 20 km south of that determined from modelling of its long period body waveforms (Fig. 6.5) (Anderson *et al.*, in press). An oblique-slip component of faulting is common in many other regions of active continental extension (Jackson and White, 1989), but there are no geological data available from the NMFZ (such as offset piercing points) to either refute or support a component of left-lateral slip on the faults. The slip vector orientation derived from the focal mechanism is almost perpendicular to the relative plate motion vector and to the slip vectors of strike-slip earthquakes in the Marlborough fault system (Fig. 6.5). This difference in slip vectors between the normal and strike-slip faults, together with the occurrence of fold and thrust fault systems between them (northeastern Canterbury and offshore Marlborough), indicates that they are not simply 'linked' in the sense of transfer faulting (Gibbs, 1984). Similar discrepancies occur between the normal fault slip vector and the slip vectors of thrust faults in north Canterbury; the latter having variable but overall northwesterly azimuths (Nicol, 1991).

Although the average trend of the normal faults is approximately east-west, the lengthening direction across the extensional zone as a whole is not known. The tension (T) axis of the 1965 fault plane solution is orientated NNE–SSW, which may or may not reflect NNE–SSW regional extension (e.g., Molnar and Chen, 1982). Mechanisms from many events might give a truer picture of the regional strain field (e.g., Robinson, 1986). In other extensional provinces, the direction of rifting is commonly oblique to the boundaries of the extending zone (e.g., Tron and Brun, 1991) and the overall direction of motion accommodated by the fault system may not be the same as the slip vectors on the faults (or the T axes) because the faults can rotate (e.g., McKenzie and Jackson, 1986). If the 1965 event was representative of the large scale deformation, the left-lateral oblique slip vector suggests that a component of simple shear may be distributed across the extensional fault system. A simple block model constructed by McKenzie and Jackson (1986) illustrates how left-lateral oblique-slip normal faulting combined with clockwise rotations of the fault-bounded crustal blocks can achieve overall extension with a small component of right-lateral shear (Fig. 6.8). Such oblique extension might be responsible for the weak *en echelon* pattern in the NMFZ (Figs 5.7 and 6.5); similar patterns have been produced in scale model experiments of oblique rifting (Tron and Brun, 1991).

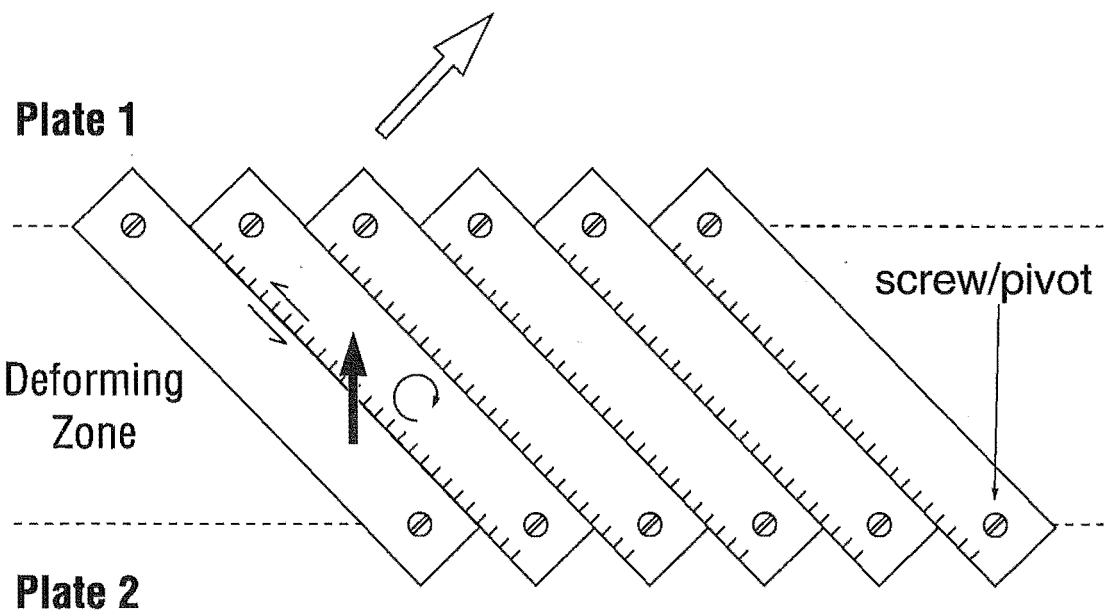

Fig. 6.8. A simple pinned block model, constructed by McKenzie and Jackson (1986) and represented by slats screwed to two rigid plates, illustrates how overall right-lateral oblique rifting (large white arrow) may be accomplished by left-lateral oblique-slip normal faults that rotate clockwise under extension. Dark arrow indicates the slip vector on the faults between adjacent blocks.

6.4 CONCLUSIONS

(1) The seismically active North Mernoo Fault Zone (NMFZ) represents a large (c. 100 x 300 km) region of continental crust on the edge of Pacific Plate that is undergoing a small amount of extension as it interacts with the obliquely convergent New Zealand plate-boundary zone. The fault system consists of a southward dipping domino-style array of overlapping normal faults, that trend at a high angle to the plate-boundary zone and which developed or were reactivated in the Late Miocene. Normal faults with late Quaternary displacement are widely distributed in the NMFZ, but, in many places surface scarps are poorly preserved due to widespread current erosion of the seafloor. In the Quaternary, the northwestern corner of the fault zone (not active since the Late Pliocene-Early Pleistocene) has been overprinted by thrust faults and folds of the southern Hikurangi margin frontal wedge.

(2) The pattern of normal faults, together with a possible component of oblique slip (indicated by the focal mechanism of an historical mid-crustal $M_W = 6.1$ earthquake within the NMFZ), are consistent with a model of rotating faults within an extensional system undergoing a small amount of dextral shear.

CHAPTER 7

LATE CENOZOIC SEDIMENTATION AND TECTONICS OF THE NORTH CANTERBURY CONTINENTAL SHELF

7.1 INTRODUCTION

The north Canterbury continental shelf lies to the west of the NMFZ and Mernoo Saddle, and WSW of the deeply-encised submarine canyons at the head of the Hikurangi Trough (Fig. 7.1). The shelf narrows from almost 80 km wide east of Banks Peninsula to < 1 km wide at the head of Kaikoura Canyon, a few kilometres south of Kaikoura Peninsula (Herzer and Carter, 1983). The shelf lies in < 150 m water depth and is encised by two very prominent bathymetric depressions. One depression is the head of Pegasus Canyon, 40 km northeast of Banks Peninsula where water depths increase rapidly to > 1000 m in the canyon axis. The other depression is the Conway Trough, an 8–10 km wide by 40 km long, north-south oriented, rectangular basin which merges into the head of Kaikoura Canyon (Fig. 7.1). The Conway Trough is very steep-sided and deepens from about 250 m deep at its southern end to > 1000 m deep at its northern end.

Prior to the present study, there existed only a limited amount of seismic-reflection data from the north Canterbury shelf. These data included some open-file oil industry profiles, which were obtained during reconnaissance surveys and interpreted in various ways (Fig. 7.2). There were also some previous 3.5 kHz data obtained by DSIR during several surveys on R.V. *Tangaroa*. Multichannel, oil company profiles show up to 2.0 km of Cretaceous-Recent cover sediments overlying acoustic basement (Torlesse terrane of Mesozoic age) (Field *et al.*, 1989; Wood *et al.*, 1989) and a zone of late Cenozoic faulting and folding beneath the inner, northwestern part of the shelf (Carter and Carter, 1982; Carter, R.M. and Carter, 1985a; Herzer and Bradshaw, 1985).

It was clear from early studies that the shelf straddles the southeastern edge of the plate-boundary deformation zone in northern South Island; but neither has there been agreement regarding the style of deformation and tectonics of the region (Fig. 7.2), nor has it been clear how the deformation on the shelf relates to faulting on the NW Chatham Rise. Carter and Carter (1982) and Carter, R.M. and Carter (1985) postulated the existence of the Motunau Fault, which they inferred to be an incipient major strike-slip structure extending along the north Canterbury range front and across the continental shelf to link up with the southern end of the Hikurangi subduction zone (Fig. 7.2A). They inferred that on the continental slope the surface

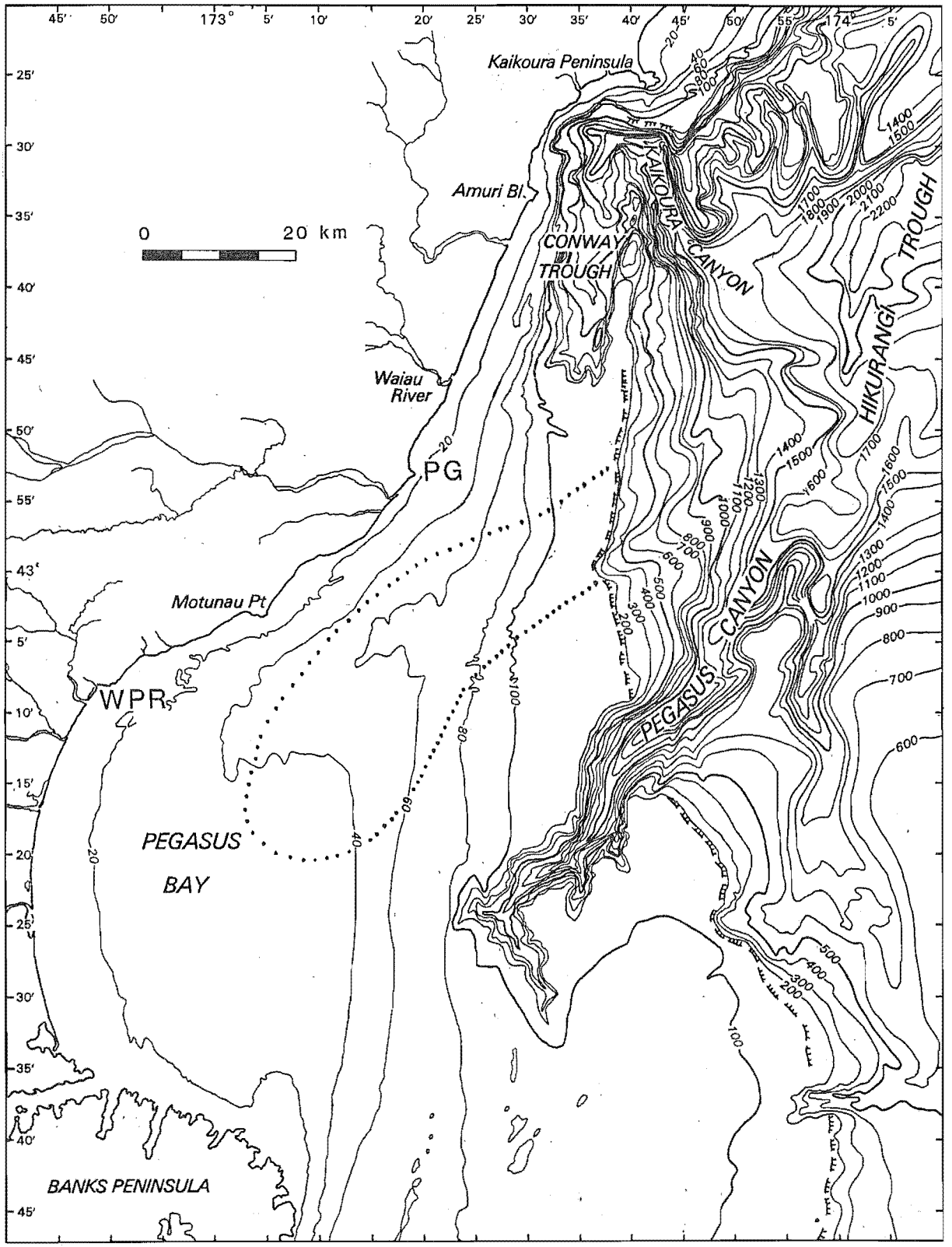

Fig. 7.1. Metric bathymetry of the north Canterbury continental margin, simplified from Herzer and Carter (1983). Line with ticks is the shelf edge. Bold dotted line is the approximate outline of an Early Pleistocene buried submarine canyon (see section 7.3.1) (after Herzer and Lewis, 1979). WPR, Waipara River; PG, Point Gibson.

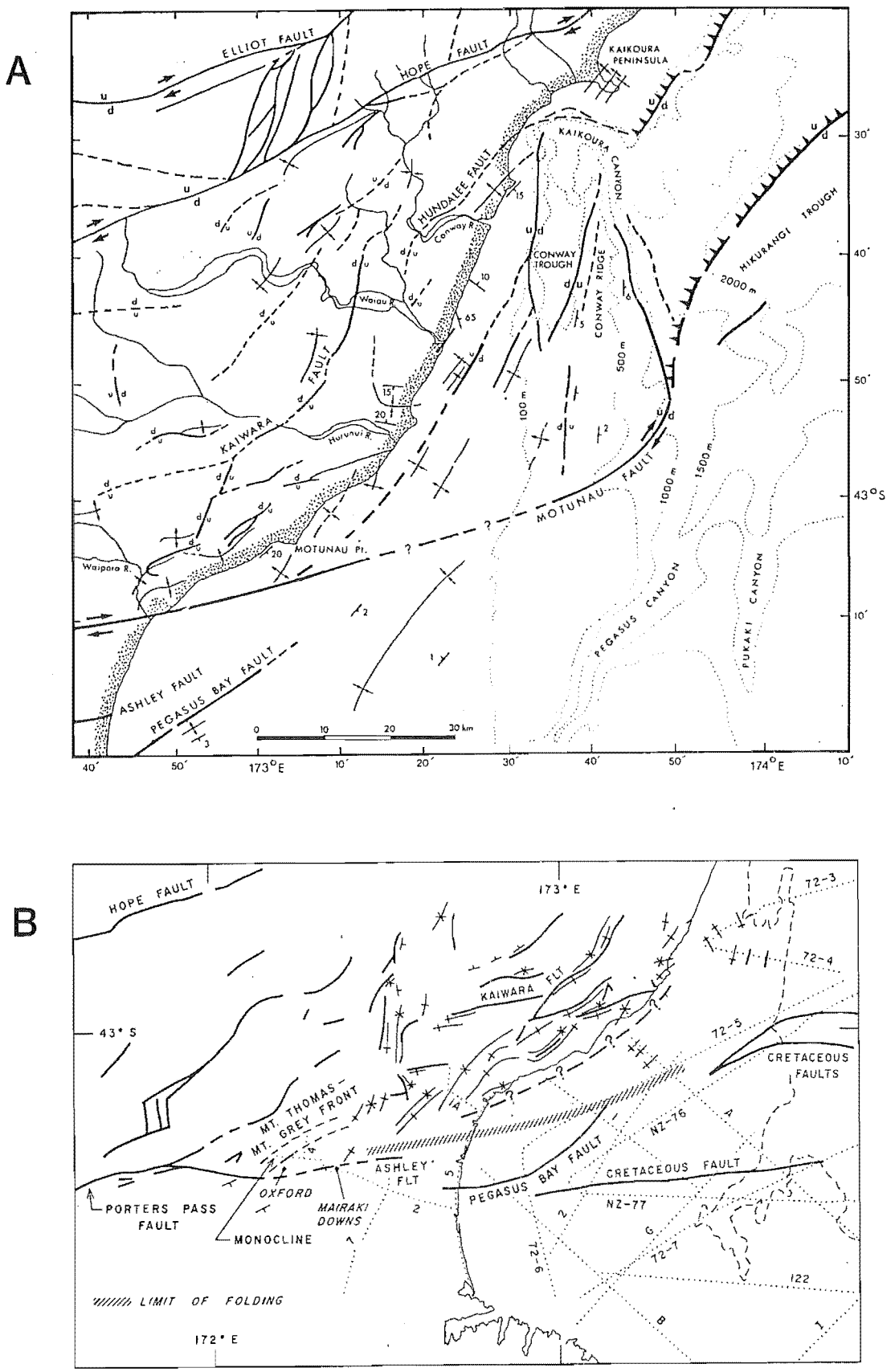

Fig. 7.2. Previous interpretations of the active tectonics of the offshore north Canterbury region. **A.** The strike-slip Motunau Fault and associated structures, after Carter and Carter (1982) and Carter, R.M. and Carter (1985). **B.** Interpretation by Herzer and Bradshaw (1985) in which the dashed line with question marks is the position of a possible deep-seated strike-slip fault in basement rocks beneath the coastal region. Dotted lines offshore are oil company seismic profiles.

expression of the Motunau Fault is marked by a minor submarine canyon and considered the southern extent of the deformation zone to be the Pegasus Bay Fault, lying 20 km north of Christchurch City. Carter *et al.* (1982) referred to the Conway Trough as a transform basin that is receiving late Quaternary mud derived from the south at a very rapid rate, possibly up to 1.7 m/ka.

Herzer and Bradshaw (1985) disputed the existence of the Motunau Fault but agreed that an incipient zone of dextral shear underlies the north Canterbury range front and the fold belt beneath the Waipara coastal hills (Fig. 7.2A). They considered this zone of dextral shear to be widespread and accommodated by displacement on many different faults and folds in the cover rocks, rather than as a discrete strike-slip structure expressed at the land surface and the seabed. On land, this model has been supported by Yousif (1987) and the recent work of Cowan (1992), which is discussed further in Chapter 8. Herzer and Bradshaw (1985) emphasised the importance of the reverse-slip Pegasus Bay Fault, believing this fault to be the only active structure offshore between Motunau Point and Banks Peninsula (Fig. 7.2B). The Pegasus Bay Fault is considered by Elder *et al.* (1991) to be one of the most important potentially seismogenic structures capable of generating severe ground shaking in Christchurch City. Several Cretaceous normal faults have been mapped beneath the shelf, some of which were reactivated in the mid Cenozoic (Late Oligocene-Early Miocene) but which do not displace the Middle Miocene to Recent sequence (Fig. 7.3, profile 2) (Herzer and Bradshaw, 1985; Field *et al.*, 1989; Wood *et al.*, 1989).

Various aspects of the late Quaternary sedimentation on the north Canterbury shelf and slope have been addressed by other workers (Herzer, 1977b, 1979, 1981; Herzer and Lewis, 1979; Carter and Herzer, 1979; Carter *et al.*, 1982; Gibb and Adams, 1982; Griggs *et al.*, 1983; Carter, L. and Carter, 1985). The present distribution of surface sediments on the shelf reflects the late Quaternary history of high-amplitude glacio-eustatic fluctuations (e.g., Herzer, 1981) and the modern hydraulic regime (Carter and Herzer, 1979, Carter, L. and Carter, 1985).

This chapter reports on new data obtained on R.V. *Rapuhia* research cruises 2034 (1990) and 2046 (1991), which have been interpreted together with existing data sets (Figs 1.4 and 1.5). The new data were acquired with the specific aims of: (1) mapping in detail the expression of active basement structures within the covering sedimentary succession; (2) establishing a high-resolution Plio-Pleistocene seismic-stratigraphy within the deformation zone beneath the inner shelf; and (3) constraining the nature of deformation at the southeastern edge of the plate-boundary zone in northern South Island. This chapter presents a preliminary interpretation of the Plio-Pleistocene seismic-stratigraphy (section 7.3) and a new interpretation of the late Cenozoic structure of the north Canterbury shelf (section 7.4). Detailed seismic-

Fig. 7.3. Oil company seismic-reflection profiles 1 and 2 illustrating the major elements of the sedimentary cover succession beneath the north Canterbury shelf and margin. Acoustic basement is the reflection with X's beneath it. The lower major unit is the Late Cretaceous and Paleogene succession that infills and blankets half-graben. Reflection O is the base of the Oligocene, Amuri Limestone Formation. The major unit overlying this is a Middle-Late Miocene to Recent succession consisting of an inferred limestone unit equivalent to the Middle Miocene, White Rock limestone (reflection WR) and progradational subunits 1 and 2. Basement faults imaged beneath the shelf are normal and are predominantly Late Cretaceous in age. Two faults beneath the shelf (labelled R in each profile) show normal reactivation in the Middle Miocene but no displacement since that time. Profile 1 shows numerous southward-dipping normal faults (including faults A, B, C, D, E1 and F, see Figs 5.3, 5.5, 5.7, 6.5 and 7.11) beneath the continental slope and Pegasus Canyon, that were reactivated with normal sense or initiated in the late Cenozoic. The position of basement in the hanging-wall of the major structure labelled fault B is masked by multiple reflections. Fault B was previously interpreted by Carter and Carter (1982) as a NE–SW-trending strike-slip fault and was not considered to be a tectonic structure at all by Herzer and Bradshaw (1985). The three unlabelled faults on the right are seaward-verging thrusts, imaged very obliquely here where the profile runs towards the Malborough continental slope after changing course. The positions of the profiles are shown on Fig. 7.11, but note that profile 1 extends off the map. Small arrows above the seabed indicate the positions of intersecting profiles.

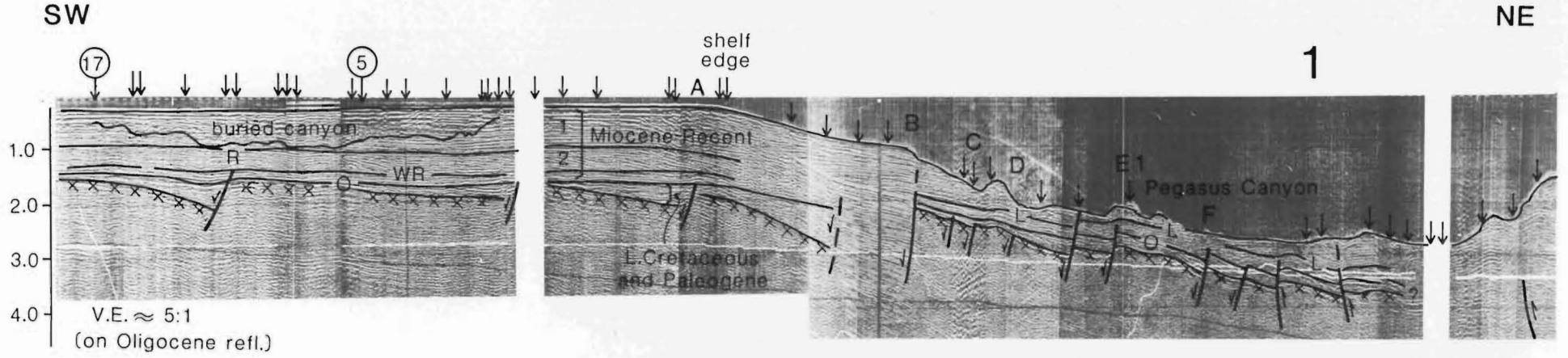
SW
NE
1
17
5
shelf
edge
A
B
C
D
E1
F
buried canyon
R
WR
Q
1
2
Miocene-Recent
L.Cretaceous
and Paleogene
Pegasus Canyon
L
Q
1.0
2.0
3.0
4.0
V.E. ≈ 5:1
(on Oligocene refl.)

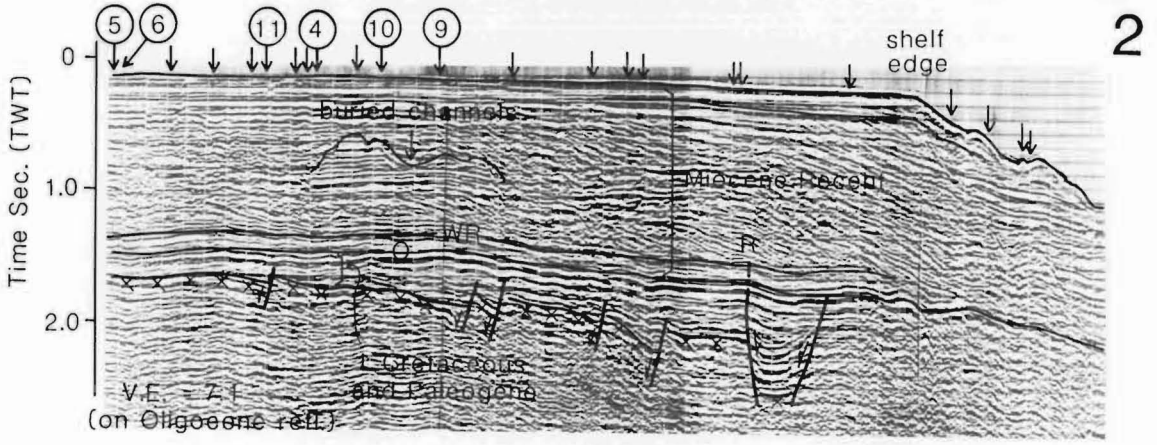
2
5
6
11
4
10
9
shelf
edge
buried channels
Miocene-Recent
WR
Q
L.Cretaceous
and Paleogene
Time Sec. (TWT)
0
1.0
2.0
V.E. ≈ 1:1
(on Oligocene refl.)

stratigraphic analysis of the data set is in progress as part of on-going research at the New Zealand Oceanographic Institute, at the time of writing this thesis. It is anticipated that detailed analysis of the data will have implications to the assessment of seismic hazard in Christchurch City and the north Canterbury region, but such an analysis lies beyond the scope of this thesis. The results presented in this chapter reveal styles of sedimentation and tectonics that contrast with the abutting active NMFZ. The north Canterbury shelf is being shortened by thrust faults and folds, and the stratigraphy reflects changes in shoreline position and accommodation space, that result directly from glacio-eustatic sea-level cycles. The implications of the results to regional tectonic and sedimentary models are discussed in Chapter 8.

7.2 SEISMIC-STRATIGRAPHIC OVERVIEW OF THE CRETACEOUS TO RECENT COVER SUCCESSION

The north Canterbury continental shelf and upper slope is underlain by a sedimentary succession up to 2 km thick and resting on Torlesse terrane basement. The succession can be divided broadly into two major units; a Late Cretaceous and Paleogene unit and a Miocene-Recent unit (Fig. 7.3). The lower unit is of Late Cretaceous to Oligocene age and correlates broadly with the Eyre Group exposed in Canterbury (Field *et al.*, 1989; Wood *et al.*, 1989). The unit is a largely regressive succession deposited during thermal subsidence of the New Zealand region, as it drifted from Antarctica and Australia, following Late Cretaceous-age seafloor spreading in the Tasman Sea and South Pacific Ocean (e.g., Fulthorpe and Carter, 1989). The upper unit of Miocene to Recent age correlates with the Motunau Group in Canterbury. This unit is a progradational succession (Fig. 7.3, profile 2) that developed in response to uplift and erosion of the Southern Alps due to late Cenozoic convergence between the Pacific and Australian plates (Carter, 1988; Fulthorpe and Carter, 1989; Field *et al.*, 1989).

Late Cretaceous half-graben beneath the shelf (Fig. 7.3) are tectono-stratigraphically related to the Late Cretaceous basins on the NW Chatham Rise (Fig. 5.3) and are infilled with syntectonic sediments that are locally > 250 m thick (Wood *et al.*, 1989). The Late Cretaceous sediments are blanketed by Paleogene sediments, which are typically 100–200 m thick, and by the condensed Amuri Limestone Formation of Oligocene age. The base of the Amuri Limestone is recorded in seismic-reflection profiles by a strong reflector (labelled O in Figs 5.1 and 7.3) at about 1.5 s (TWT; c. 1500 m). Reflector O has been traced to the Amuri Limestone in oil company wells south of Banks Peninsula (Wood *et al.*, 1989) and beneath the north Canterbury submarine canyons to the NW Chatham Rise slope. The Amuri Limestone forms the top of the regressive, lower seismic unit. At Resolution-1 well, south of

Banks Peninsula (Fig. 2.1), the limestone is 22 m thick and is disconformably overlain by the 20 m-thick White Rock Limestone of late Early Miocene (Altonian) age (Wood *et al.*, 1989).

The White Rock limestone unit, or a stratigraphic correlative, can be traced beneath the north Canterbury shelf where it is recorded by a strong seismic reflection (labelled WR on Fig. 7.3). This thin limestone forms the basal part of the upper seismic unit (Motunau Group). Above the limestone reflector is an 800-1500 m-thick prograding succession predominantly of siltstones (Fig. 7.3). This Middle Miocene to Recent succession downlaps onto the White Rock Limestone and is chrono-stratigraphically equivalent to the Tokama Siltstone, Greta Formation, Kowai Formation and the overlying late Quaternary gravels of the Canterbury plains (Field *et al.*, 1989). It was not until late in the development of this upper prograding sedimentary succession that the present style of tectonic deformation of the shelf began (see sections 7.3 and 7.4).

7.3 PLIO-PLEISTOCENE SEISMIC STRATIGRAPHY

7.3.1 BURIED EARLY PLEISTOCENE SUBMARINE CANYON

The Middle Miocene to Recent progradational unit is divided into two major progradational sub-units (labelled 1 and 2 on profile 1, Fig. 7.3) separated by a continuous horizontal reflection. The lower sub-unit (mainly Pliocene and Pleistocene age) exhibits prograding clinoforms beneath the mid to outer shelf and shelf edge and smooth, near-horizontal reflections beneath the middle shelf. Beneath the northern part of Pegasus Bay there is a buried channel complex that is cut into the otherwise similar, upper sub-unit (Fig. 7.3) (Herzer and Lewis, 1979). The extent of the channel complex is constrained only by three oil company multichannel seismic profiles and one along-shelf single-channel airgun profile obtained on *Rapuhia.* Herzer and Lewis named the channel complex the Motunau Canyon and inferred it to be at least 20 km wide, 65 km long, and trending subparallel to the coastline about 10–20 km offshore (Fig. 7.1). The edges of the channel complex are distinct, steeply dipping, erosion surfaces which truncate the near-horizontal regional reflections. The channel axis lies up to 800 m beneath the present seabed. Herzer and Lewis interpreted the infilled channel complex as a buried submarine canyon system that was active during the Early Pleistocene, prior to the development of Pegasus Canyon (Fig. 7.1). They inferred that the canyon system was fed apically by northward moving sand and gravel on the shelf and transversely by debris flows from inner-shelf feeder channels. The feeder channels were encised into mudstone of Late Pliocene to Early Pleistocene age, known locally as the Greta Formation, and the

infilled channels are now partially exposed in the uplifted coastal cliffs near Motunau Point (Fig. 7.1) (Lewis, 1976).

The Early Pleistocene submarine canyon beneath northern Pegasus Bay was infilled with sediment of middle to Late Pleistocene age, that is recorded by prograding, discontinuous, irregular and hyperbolic seismic reflections (e.g., Fig. 7.3), and was blanketed by Late Pleistocene and Holocene muddy sediments (Figs 7.4 to 7.6). Herzer and Lewis (1979) inferred that the canyon became inactive during a mid Pleistocene glaciation, when Pegasus Canyon developed by retrogressive slumping and captured a critical supply of longshore-transported sand and gravel derived from the south. Once the main supply of coarse-grained sediment was prevented from reaching the canyon in northern Pegasus Bay, the canyon became buried by mud carried in suspension. The Motunau Canyon infilled rapidly; post glacial rates of mud deposition in Pegasus Bay are up to 3 m/ka (Herzer, 1981) (Fig. 7.4, profile 5). The northward movement of modern sand and gravel is largely restricted to the sublittoral zone, so that Pegasus Canyon also is now abandoned (Carter and Herzer, 1979; Herzer, 1981; Carter *et al.*, 1982). A similar sedimentary regime probably existed for the Motunau Canyon during each interglacial (Herzer and Lewis, 1979).

7.3.2 MIDDLE PLEISTOCENE TO RECENT STRATIGRAPHY: INNER TO MIDDLE SHELF

The newly acquired, single-channel airgun and 3.5 kHz seismic profiles (Fig. 1.4), together with carefully positioned sediment cores (Fig. 1.5), provide considerable stratigraphic detail of the middle Pleistocene to Recent succession within a deforming region beneath the inner shelf. A preliminary interpretation of the seismic-stratigraphy is illustrated in Figure 7.4 and summarised in Figure 7.5. Twelve seismic-stratigraphic units are clearly expressed in 3.5 kHz profiles of the inner shelf between the Waipara River mouth and Point Gibson (Figs 7.1 and 7.6 to 7.11). In this area there are numerous growing folds in the sedimentary succession (Fig. 7.11) and coastal uplift nearby at a rate of c. 1–2 m/ka (Carr, 1970; Yousif, 1987; Barrell, 1989; Cowan, 1992). All of the units are regionally extensive, bounded by erosional unconformities, and they thin towards the shore and on the flanks of folds that have been growing contemporaneously with their deposition (Figs 7.4, 7.6 and 7.7; profiles 3, 4 and 6 to 13). Reflections within the units onlap and less commonly downlap onto the basal unconformities. In order of increasing age, the units are referred to by numbers 1c to 12c and the intervening unconformities by letters Ac to Kc (Fig. 7.5). The nomenclature follows that used in Chapter 4 for the description of the Plio-Pleistocene seismic units beneath the NW Chatham Rise slope, except a lower case 'c' (for Canterbury) has been added to the number and letter codes in this chapter to distinguish the units and unconformities in the two regions.

Fig. 7.4. 3.5 kHz profiles 3 to 6 and single-channel airgun profile 6 illustrating the Plio-Pleistocene seismic stratigraphy of the inner to middle shelf. The positions of the profiles are shown on Fig. 7.11. The stratigraphy of unconformities Ac to Kc is shown on Fig. 7.5. Anticlinal folds D^c, F^c, G^c and H^c are labelled above the seabed and the positions of the tips of inferred thrust faults deeper in the sedimentary succession are indicated schematically beneath the folds. Small arrows above the seabed indicate the positions of intersecting profiles. On airgun profile 6, C = channel.

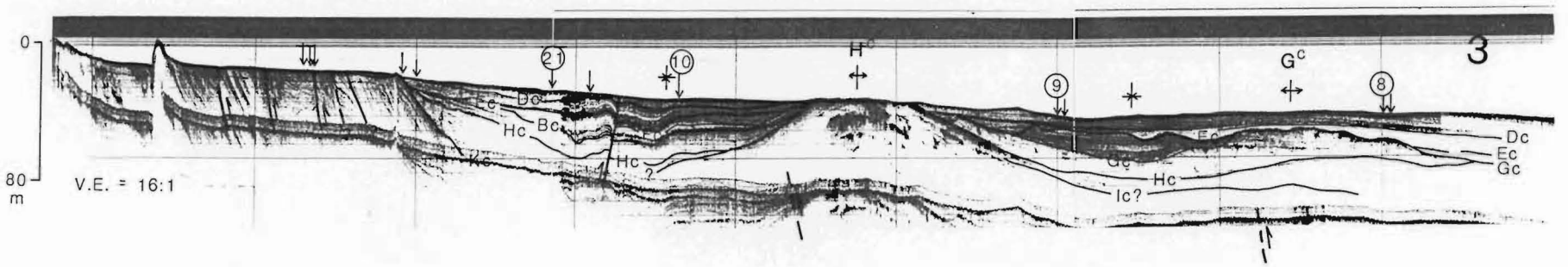
0
80
m
V.E. = 16:1
21
10
H^c
9
G^c
8
3
Dc
Ec
Gc
Hc
Ic?
Bc
Cc
Kc
Jc
Ic
Fc
2

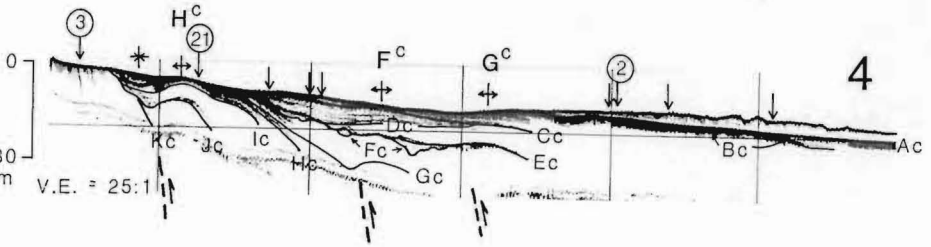
3
H^c
21
F^c
G^c
2
4
0
30
m
V.E. = 25:1
Kc
Jc
Ic
Hc
Fc
Gc
Dc
Cc
Ec
Bc
Ac

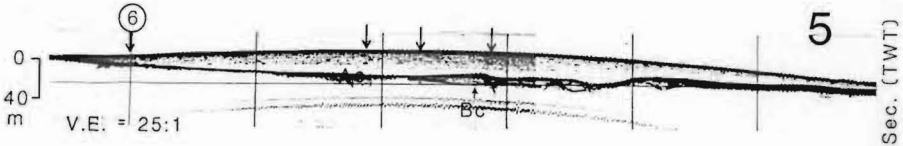
6
5
0
40
m
V.E. = 25:1
Ac
Bc

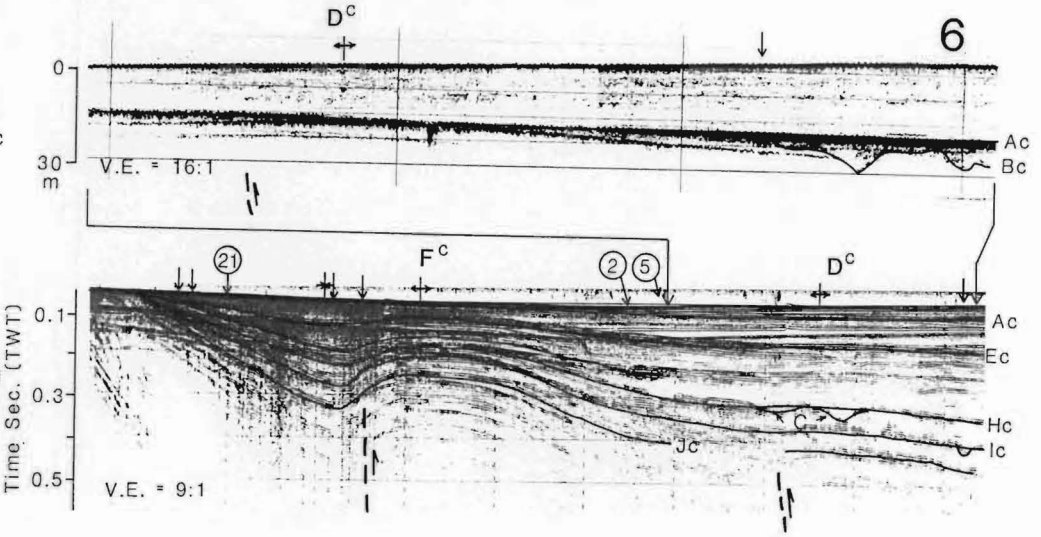
D^c
6
0
30
m
V.E. = 16:1
Ac
Bc
21
F^c
2
5
D^c
Time Sec. (TWT)
0.1
0.3
0.5
V.E. = 9:1
Ac
Ec
Hc
Ic
Jc
Cc

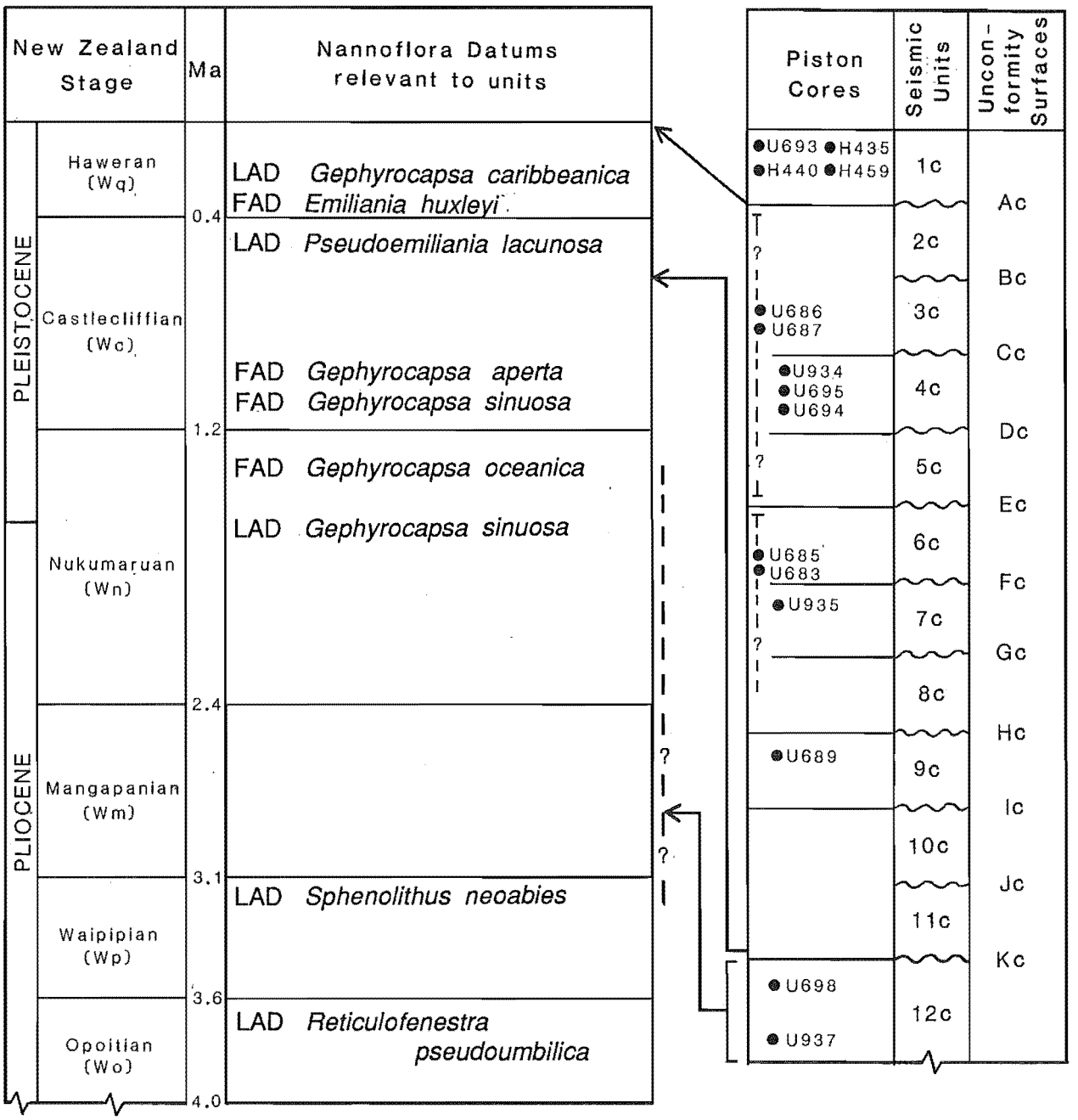

Fig. 7.5. Stratigraphy of the Plio-Pleistocene succession beneath the inner to middle shelf. Seismic units 1c to 11c are middle-Late Pleistocene in age and unit 12c is Late Pliocene to Early Pleistocene. Locations of cores are shown on Fig. 7.11. Vertical dashed lines from cores indicate the uncertainty in the seismic unit sampled by the core. FAD and LAD are first and last appearance datums respectively.

Fig. 7.6. 3.5 kHz and single-channel airgun profiles 7 to 9 of the Motunau to Point Gibson coastal zone, approximately normal to the major structures and arranged in order from NE (profile 7) to SW (profile 9). The positions of the profiles are shown on Fig. 7.11. The stratigraphy of unconformities Ac to Kc is shown on Fig. 7.5. The positions of folds are indicated above the seabed with conventional map symbols and anticlines G^c and H^c are labelled. The positions of the tips of inferred thrust faults deeper in the sedimentary succession are indicated schematically beneath the folds. Small arrows above the seabed indicate the positions of intersecting profiles.

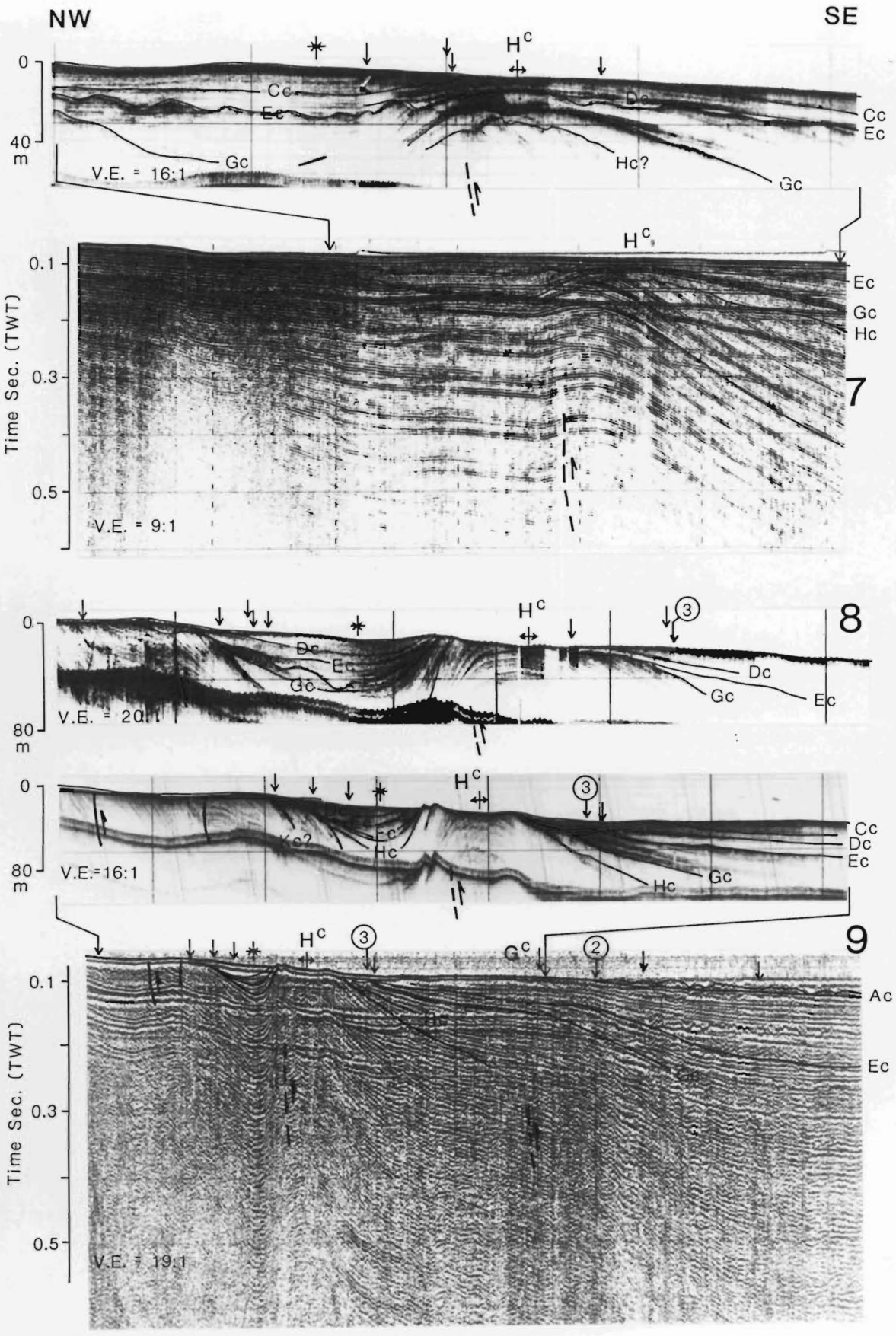
NW
SE
0
40
m
Cc
Ec
Gc
Dc
Hc?
Hc
V.E. = 16:1
0.1
0.3
0.5
Time Sec. (TWT)
V.E. = 9:1
7
8
80
V.E. = 20:1
V.E.=16:1
9
Ac

Fig. 7.7. 3.5 kHz profiles 10 to 13 and single-channel airgun profile 13 of the Motunau to Point Gibson coastal zone, approximately normal to the major structures and arranged in order from NE (profile 10) to SW (profile 13). The positions of the profiles are shown on Fig. 7.11. The stratigraphy of unconformities Ac to Kc is shown on Fig. 7.5. The positions of folds are indicated above the seabed with conventional map symbols and anticlines $\mathbf{B^c}$, $\mathbf{C^c}$, $\mathbf{F^c}$, $\mathbf{G^c}$ and $\mathbf{H^c}$ are labelled. The positions of the tips of inferred thrust faults deeper in the sedimentary succession are indicated schematically beneath the folds. Small arrows above the seabed indicate the positions of intersecting profiles.

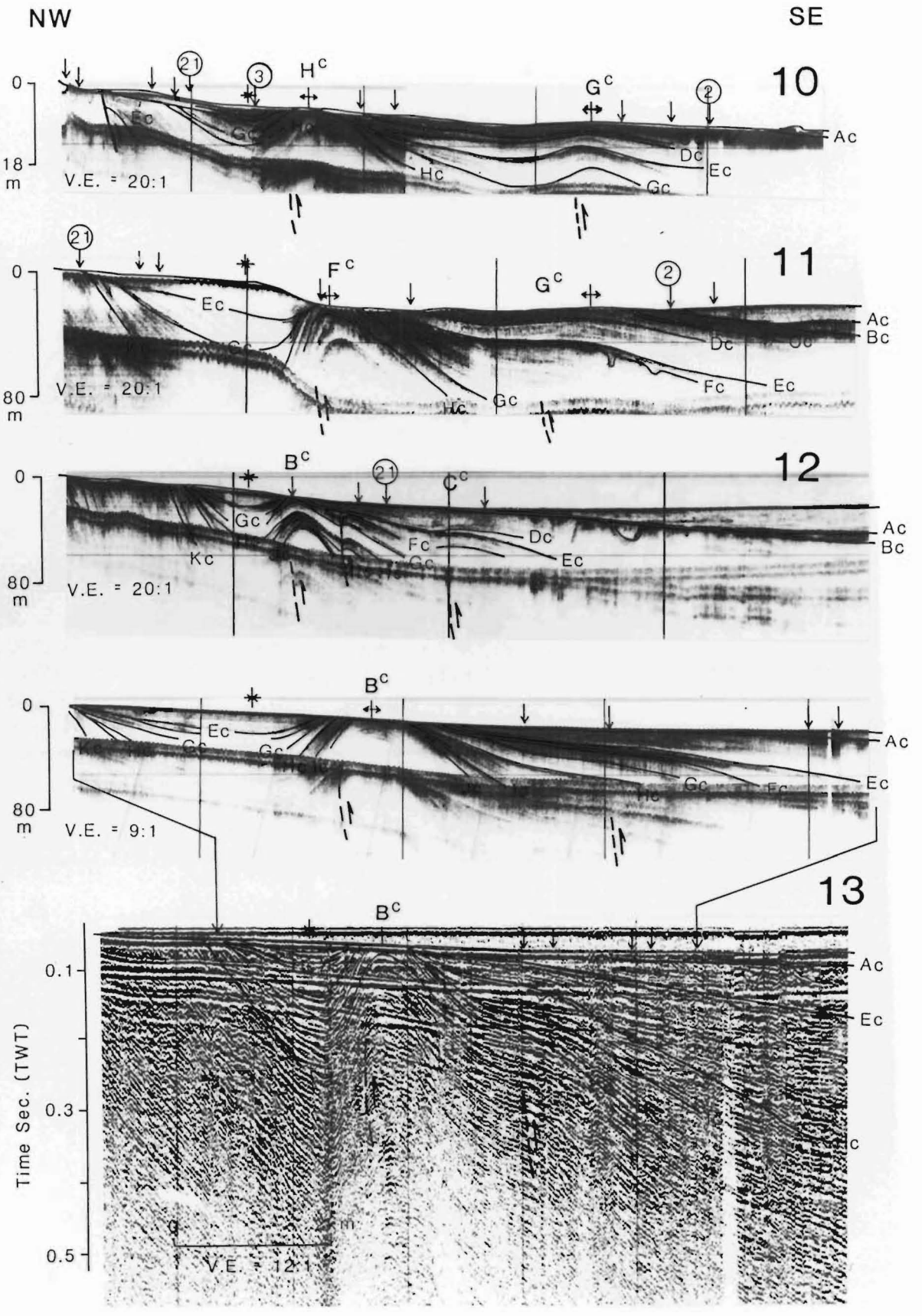
NW
SE
10
11
12
13
0
18
m
80
m
V.E. = 20:1
V.E. = 9:1
V.E. = 12:1
Ac
Bc
Cc
Dc
Ec
Fc
Gc
Hc
Kc
Time Sec. (TWT)
0.1
0.3
0.5

Fig. 7.8. 3.5 kHz and airgun profiles 14 to 17 of the Pegasus Bay Fault and Fold A^c in Pegasus Bay (continued on following page). Profile 14 is an oil company multichannel profile. The other airgun lines are single channel. The positions of the profiles are shown on Fig. 7.11. The stratigraphy of the labelled unconformities is shown on Fig. 7.5. The positions of folds are indicated above the seabed with conventional map symbols and anticline A^c is labelled. The position of the tips of inferred thrust faults deeper in the sedimentary succession are indicated schematically beneath the folds on the single-channel profiles. The Pegasus Bay Fault is imaged displacing the base of the sedimentary succession on profile 14, which intersects the structure obliquely. Small arrows above the seabed indicate the positions of intersecting profiles. On profile 17, C = channel.

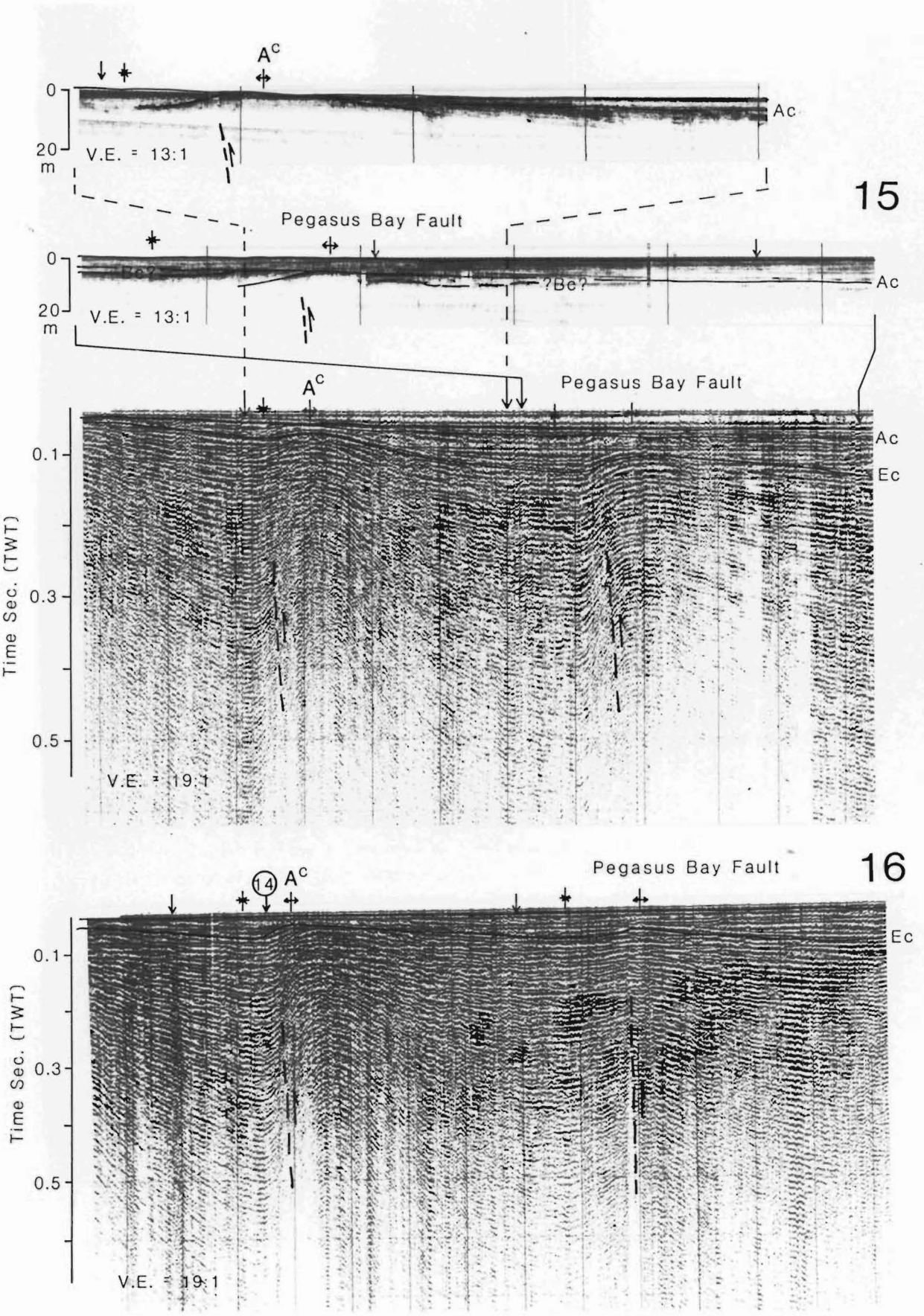
A^c
0
20
m
V.E. = 13:1
Ac
15
Pegasus Bay Fault
?Bc?
Ac
Pegasus Bay Fault
Ac
Ec
0.1
0.3
0.5
Time Sec. (TWT)
V.E. = 19:1
16
14
Pegasus Bay Fault
Ec

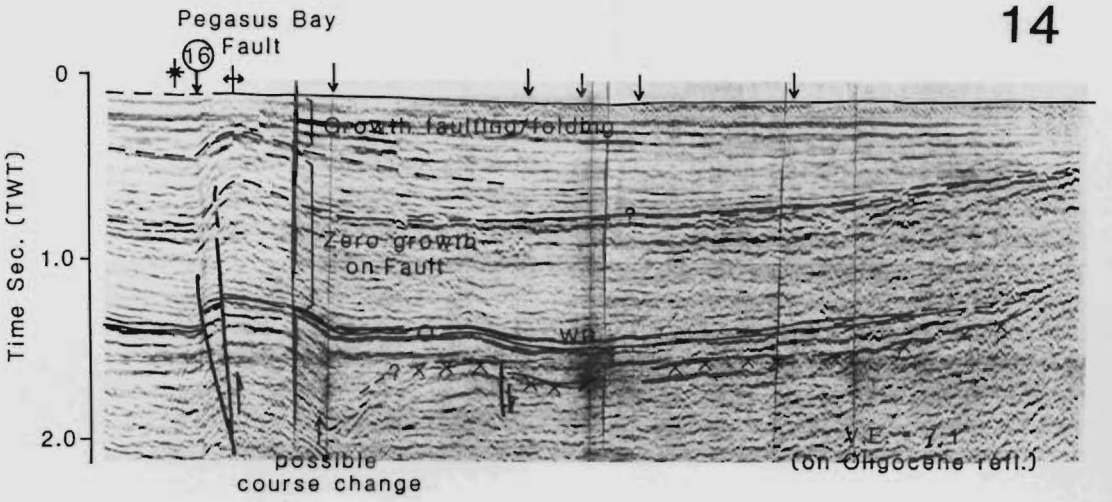
14
Pegasus Bay
Fault
16
0
1.0
2.0
Time Sec. (TWT)
Growth faulting/folding
Zero growth
on Fault
WB
possible
course change
V.E. = 1.1
(on Oligocene refl.)

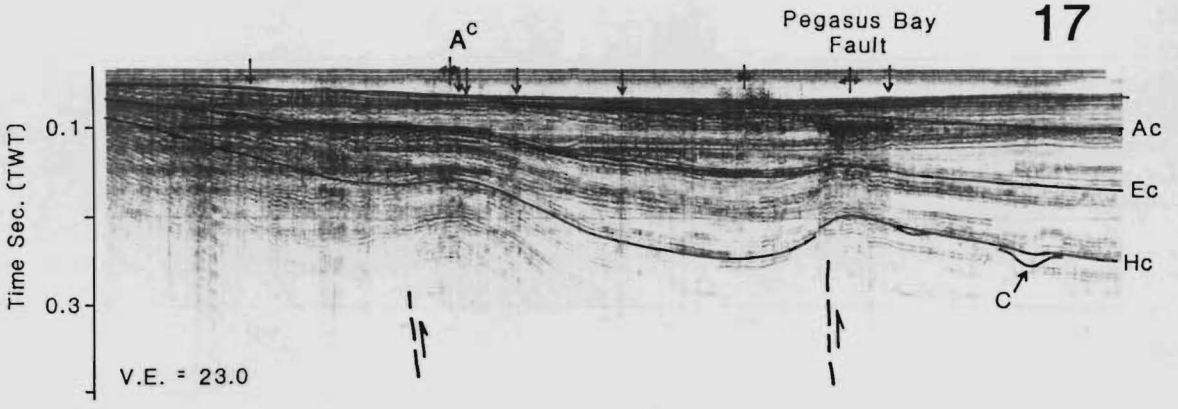
17
Pegasus Bay
Fault
A^c
0.1
0.3
Time Sec. (TWT)
Ac
Ec
Hc
C
V.E. = 23.0

Fig. 7.9. 3.5 kHz profiles 18 to 20 illustrating small-scale faults and folds in the Late Pliocene to Early Pleistocene seismic unit 12c. Single-channel airgun profile 20 intersects a small, steeply dipping fault, labelled T on Fig. 7.11, of uncertain trend and kinematic significance. The shore-parallel, single-channel airgun profile 21 illustrates a very oblique intersection of two major structures, E^c and H^c. Fold positions are indicated above the seabed with conventional map symbols. The positions of the tips of inferred thrust faults deeper in the sedimentary succession are indicated schematically beneath the folds on profile 21. The positions of the profiles are shown on Fig. 7.11. The stratigraphy of the labelled unconformities is shown on Fig. 7.5. Small arrows above the seabed indicate the positions of intersecting profiles.

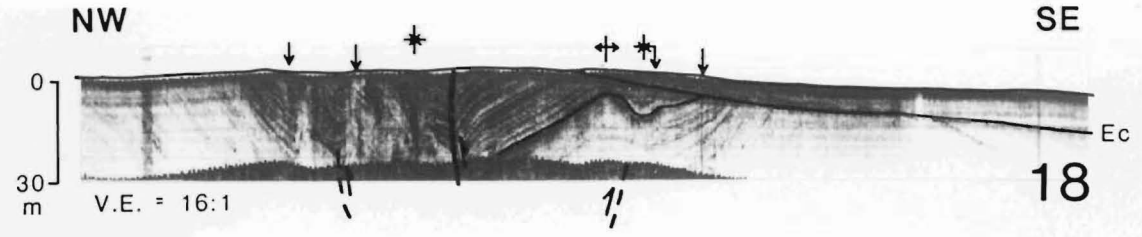
NW
SE
0
30
m
V.E. = 16:1
Ec
18

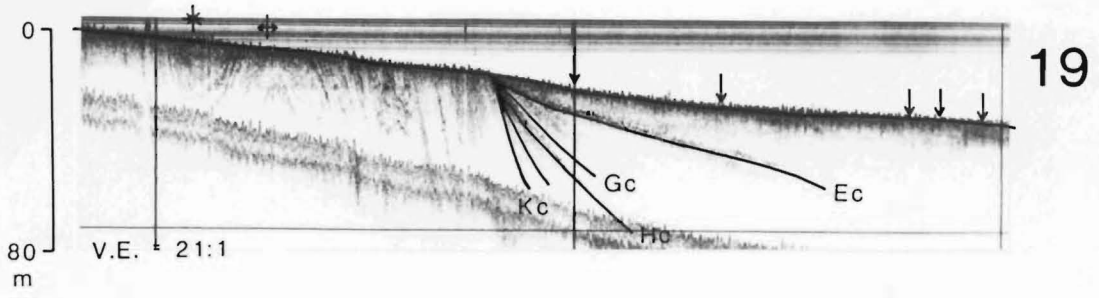
0
80
m
V.E. = 21:1
Kc
Gc
Ec
Hc
19

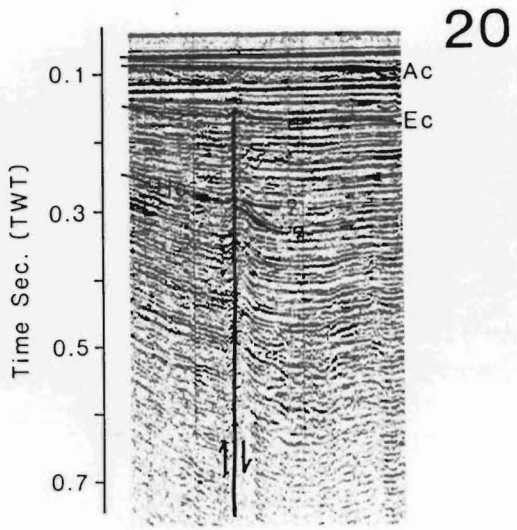
20
0.1
0.3
0.5
0.7
Time Sec. (TWT)
Ac
Ec
Hc

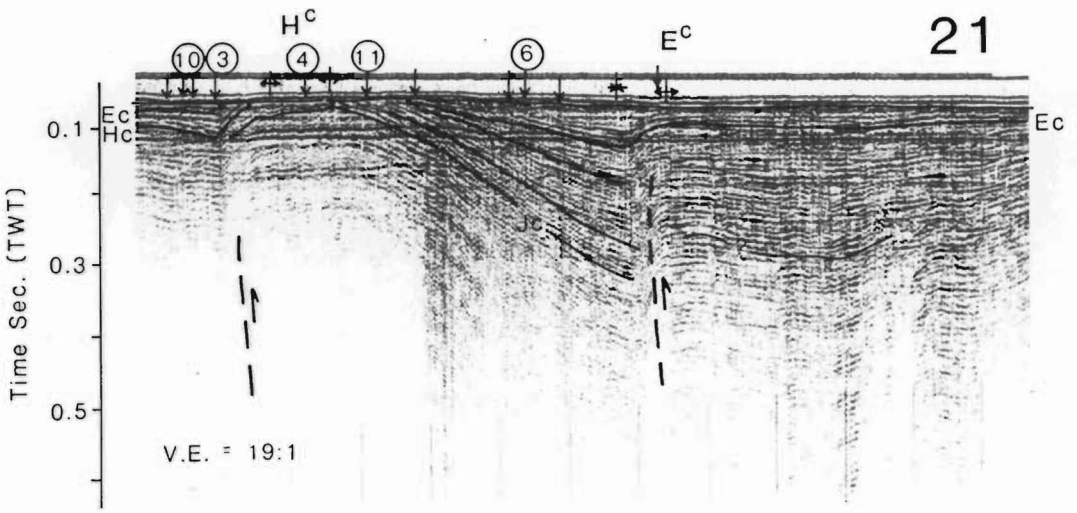
21
H^c
E^c
10
3
4
11
6
Ec
Hc
0.1
0.3
0.5
Time Sec. (TWT)
Jc
Ec
V.E. = 19:1

Fig. 7.10. 3.5 kHz profiles from the northern part of the Canterbury shelf. Profile 22 crosses the southern end of the Conway Ridge and Conway Trough, and profiles 23 to 27 are from just south of the trough. Positions of the profiles are shown on Fig. 7.11. The positions of folds are indicated above the seabed with conventional map symbols and anticlines $\mathbf{H}^c$, $\mathbf{I}^c$ and $\mathbf{J}^c$ are labelled. The positions of the tips of inferred thrust faults deeper in the sedimentary succession are indicated schematically beneath the folds. Small arrows above the seabed indicate the positions of intersecting profiles.

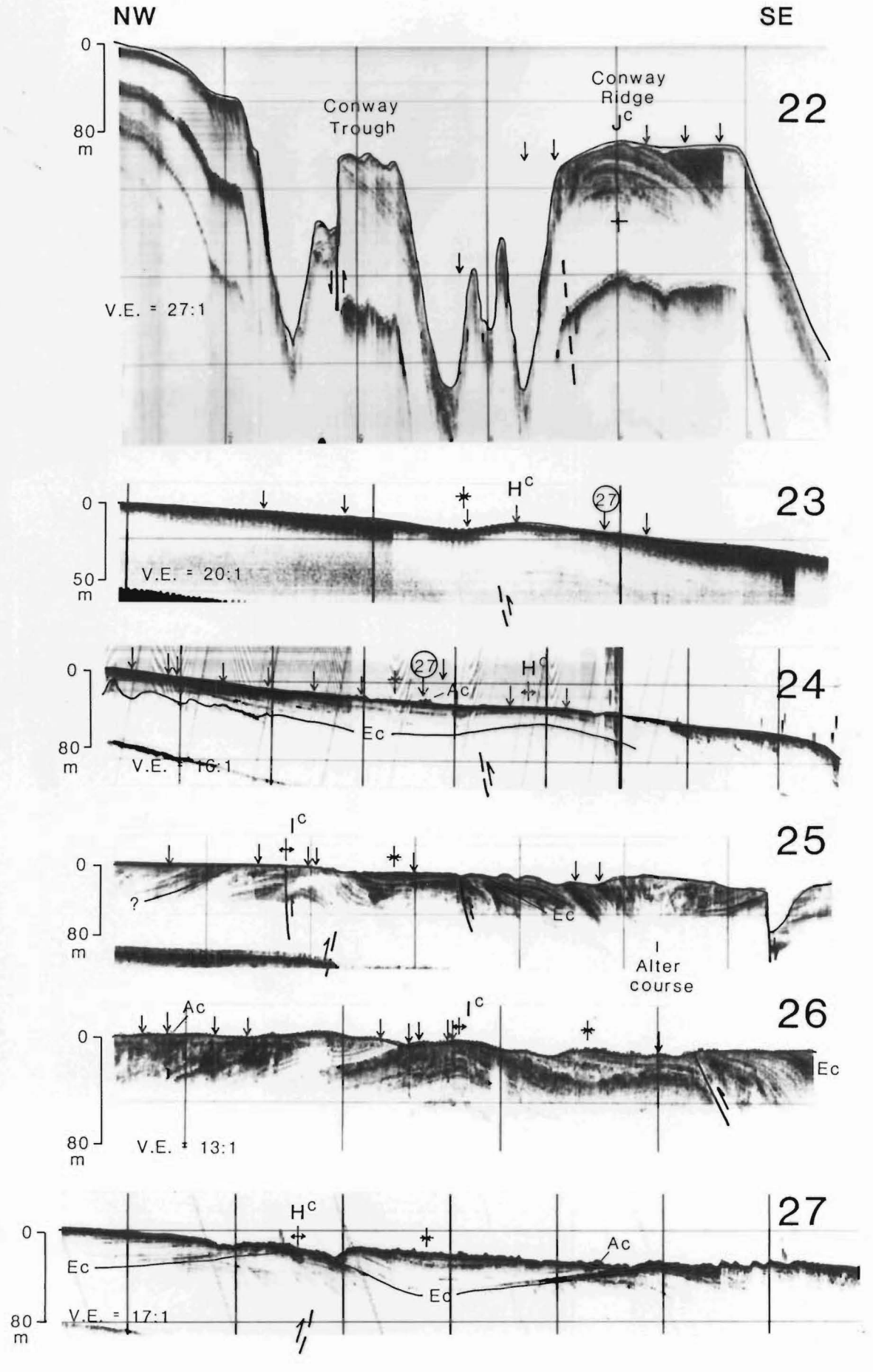
NW
SE
0
80
m
Conway
Trough
Conway
Ridge
J^c
22
V.E. = 27:1
0
50
m
H^c
27
23
V.E. = 20:1
0
80
m
27
H^c
Ac
24
Ec
V.E. = 16:1
I^c
25
0
80
m
?
Ec
Alter
course
Ac
I^c
26
0
80
m
Ec
V.E. = 13:1
H^c
27
0
80
m
Ec
Ac
Ec
V.E. = 17:1

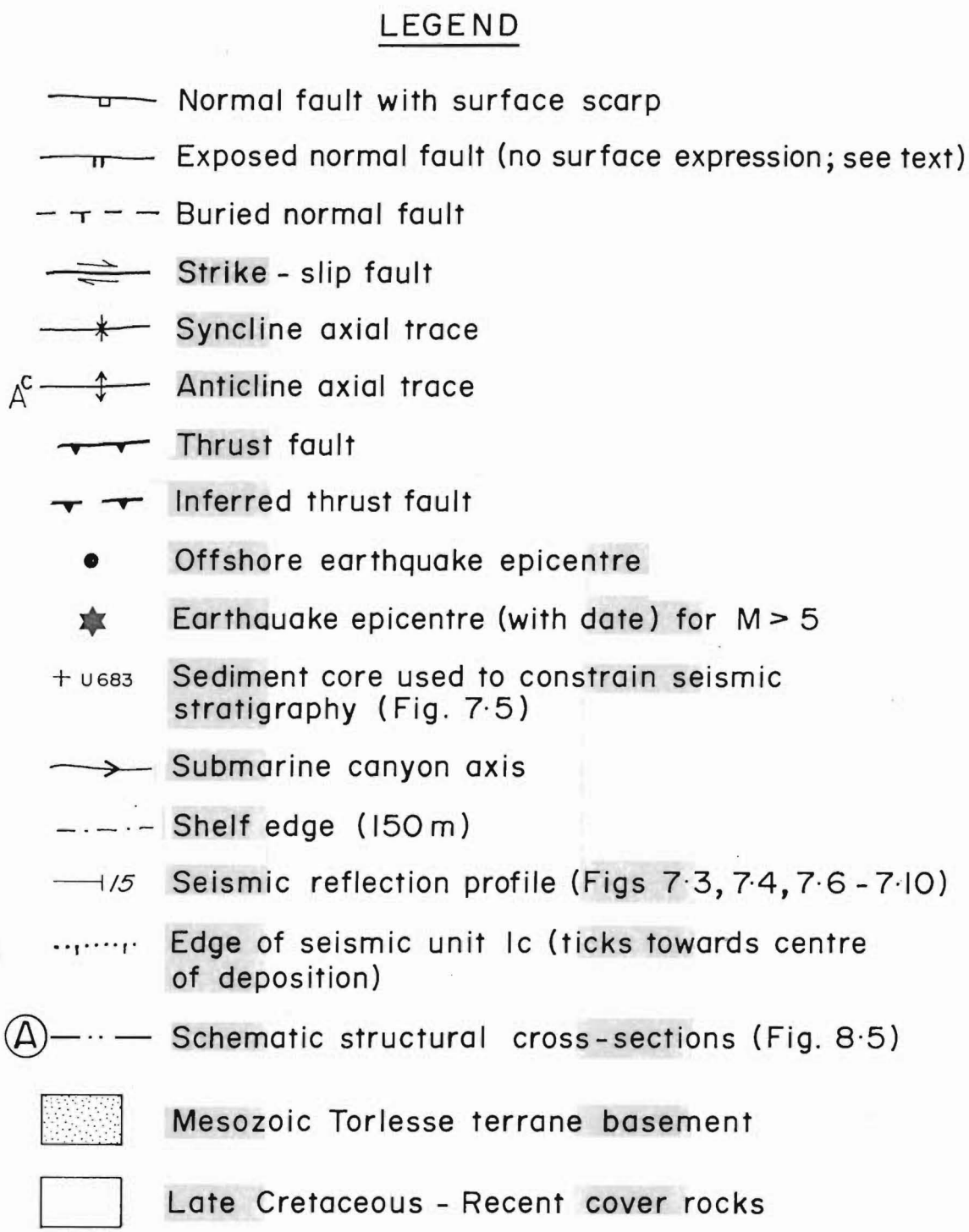

Fig. 7.11. Regional tectonics of north Canterbury and positions of seismic-reflection lines illustrated in Figs 7.3 to 7.4 and Figs 7.6 to 7.10. The onshore compilation is modifed from Gregg (1964), Yousif (1987), Nicol (1991), Cowan (1992) and Pettinga (pers. comm., August 1993). The instrumentally located, historical earthquake epicentres for the onshore region have been omitted for clarity (refer to Reyners (1989) and Cowan (1992)). Seismic coverage for the offshore region is shown in Fig. 1.4. GF, Glentui Fault; WMR, Waimakariri River mouth; AR, Ashley River mouth; KR, Kowai River mouth; WPR, Waipara River mouth; HR, Hurunui River mouth; WR, Waiau River mouth; CR, Conway River mouth. PKC, Pukaki Canyon; HC, Hurunui Canyon; KC, Kaikoura Canyon; CR, Conway Ridge. Inset diagram, upper left, summarises the tectonics of northern South Island and shows the locations of the regional tectonic maps in this thesis. PPAFZ, Porter's Pass-Amberley Fault Zone; NMFZ, North Mernoo Fault Zone; H, Hanmer Basin. The vector is for the present motion of the Pacific Plate relative to the Australian Plate (De Mets *et al.*, 1990).

p. 125

Fig. 7.11

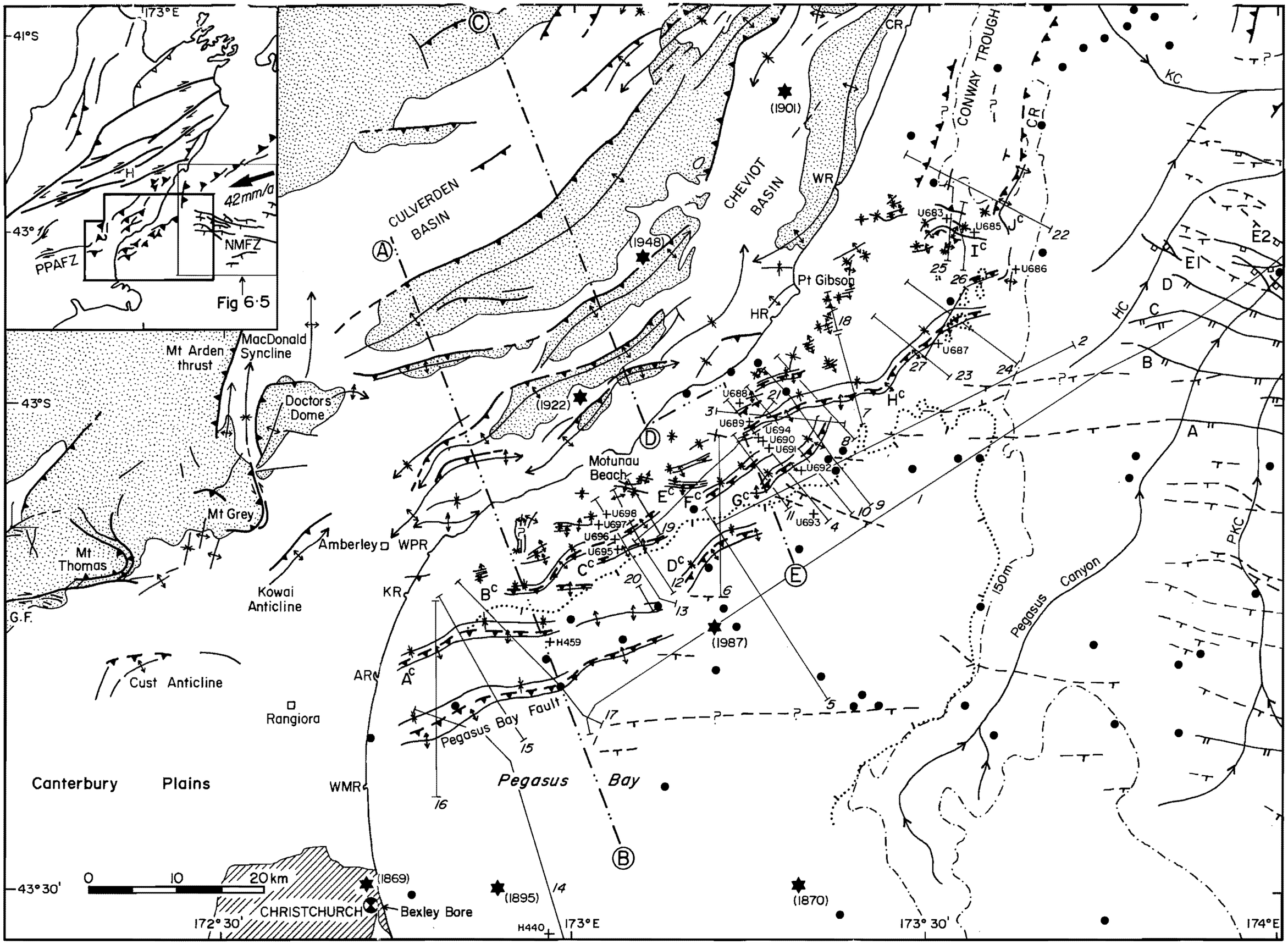
173°E
41°S
H
42mm/a
43°
NMFZ
PPAFZ
Fig 6·5
MacDonald Syncline
Mt Arden thrust
43°S
Doctors Dome
Mt Grey
Mt Thomas
Amberley
WPR
Kowai Anticline
G.F.
Cust Anticline
Rangiora
Canterbury Plains
WMR
KR
AR
CULVERDEN BASIN
CHEVIOT BASIN
WR
CR
CONWAY TROUGH
KC
(1901)
(1948)
(1922)
(1987)
(1869)
(1895)
(1870)
Pt Gibson
HR
Motunau Beach
Pegasus Bay Fault
Pegasus Bay
Pegasus Canyon
150m
HC
PKC
U683
U685
U686
U687
U688
U689
U694
U690
U691
U692
U693
U698
U697
U696
U695
H459
H440
CHRISTCHURCH
Bexley Bore
0 10 20 km
43°30'
172°30'
173°30'
174°E
A
B
C
D
E
E1
E2
A'
A^C
B^C
C^C
D^C
E^C
F^C
G^C
H^C
I^C
J^C

Unit 12c

This unit, which underlies reflector Kc, is exposed in a coastal bathymetric platform which is about 3–8 km wide and extends for over 60 km from off the Waipara River mouth to at least Point Gibson (Figs 7.1, 7.4, 7.5 and 7.6). The unit is folded and faulted and has internal reflections dipping mainly offshore at up to 11°. Horizons that are more resistant to erosion protrude up to 12 m above the platform surface, appearing as isolated pinnacles in the highly exaggerated 3.5 kHz profiles (Fig. 7.4, profiles 3 and 4). Cores and side-scan sonographs show that the platform is covered by modern sand and a thin (0–30 cm) veneer of reworked pebble-shell gravel that is inferred to have been deposited during the early Holocene shoreline transgression. Two cores from the unit (U698 and U937) sampled well compacted and locally cemented, marine sandy mudstone from beneath a 0.1–0.2 m-thick veneer of unconsolidated gravel. Core U937, from 4.5 km offshore and 13 km northeast of Motunau Point (Fig. 7.11), contains the nannoflora *Coccolithus pelagicus* (Opoitian to present), and reworked specimens of *Reticulofenestra pseudoumbilica* (late Otaian to Opoitian) and *Sphenolithus neoabies* (late Tongaporutuan to Waipipian). Specimens of *Gephyrocapsa* (first appearing in the Opoitian but not normally found in Waipipian to lower Nukumaruan strata) are absent (Edwards, 1987). Thus, this sample is Late Pliocene in age, but its age cannot be constrained better than late Waipipian to early Nukumaruan stage (Fig. 7.5). Core U698, from near the top of unit 12c about 7 km south of Motunau Point (Fig. 7.11), contains specimens of *Gephyrocapsa sinuosa* (middle Nukumaruan to early Castlecliffian), *Helicosphaera sellii* (early Kapitean to late Nukumaruan) and *Pseudoemiliania lacunosa* (Opoitian to late Castlecliffian). The sample is, therefore, middle to late Nukumaruan age (Early Pleistocene). Thus, unit 12c is Late Pliocene to Early Pleistocene age and is interpreted to be part of the upper Greta Formation which is exposed in nearby coastal cliffs (Gregg, 1964; Lewis, 1976).

In 3.5 kHz profiles, the surface of unit 12c at its exposed outer edge dips offshore at about 10° beneath the mid Pleistocene to Recent succession in northern Pegasus Bay. Unit 12c cannot be traced further offshore in the available single-channel airgun profiles, which only reveal details of the upper 0.5 s (TWT; c. 400 m) subbottom. The unit is not identified at the surface north of Point Gibson, where Mesozoic Torlesse basement crops out in coastal cliffs (Gregg, 1964).

Units 11c to 9c

These units, bounded by reflections Kc and Hc, thin and pinch out shorewards onto the outer edge of the exposed part of unit 12c (Figs 7.4, 7.6 and 7.7). The units crop out locally in the cores of anticlines **Bc** and **Hc**, about 8–10 km off the coast south of Motunau and midway between Motunau and Point Gibson (Fig. 7.11). At these locations near the inner edge of the units, the thickness of each unit ranges from zero

to about 20 m. The units thin over the crests of anticlines indicating that fold growth was active during their deposition. Further offshore, the units dip away beneath younger units. The upper surface of unit 9c (reflector Hc, Fig. 7.5), which can be traced widely in the high-resolution airgun profiles, descends to 280 ms (TWT) subbottom depth (c. 225 m) beneath the mid shelf in northern Pegasus Bay, 20 km southeast of Motunau Point (Fig. 7.4, profile 6). At this location, unit 9c is about 50 m thick. Further south, in central Pegasus Bay, the top of unit 9c descends to subbottom depths of 140 m and 160 m to the southeast and northwest of the Pegasus Bay Fault respectively (e.g., Fig. 7.8, profile 16; Fig. 7.11).

Unit 9c was sampled at location U689 (Figs 7.5 and 7.11) from beneath a 0.1 m-thick veneer of muddy gravel. The sample consists of consolidated, olive grey, marine sandy silt with a thin horizon of dispersed broken shell fragments. The presence of abundant specimens of the nannoflora *Gephyrocapsa aperta* and the absence of *Pseudoemiliania lacunosa* (last appearing at the top of oxygen isotope stage 12, c. 0.46 Ma) indicates a late Castlecliffian or Haweran age (middle-late Pleistocene) (Beu *et al.*, 1987; Edwards, 1987). An attempt was made to sample unit 10c at location U696 (Fig. 7.11), but the corer recovered only the ubiquitous, unconsolidated gravel veneer on the surface. Based on their stratigraphic positions (Fig. 7.5) and a very preliminary interpretation of the erosion surfaces in terms of sequence stratigraphy (section 7.3.3), units 10c and 11c are inferred to be of middle Pleistocene age (c. 700–500 ka).

Units 8c to 6c

These units also thin and pinch out shorewards against the outer edge of the unit 12c erosion platform (Figs 7.4, 7.6 and 7.7). The bounding surfaces Gc (top of unit 8c) and Ec (top of unit 6c) (Fig. 7.5) are very prominent erosion surfaces which can be traced widely on many 3.5 kHz profiles and single-channel airgun profiles throughout the deformation zone beneath the inner shelf. Surface Ec commonly truncates older erosion surfaces. The erosion surfaces commonly have relief of 5–10 m over several hundred metres, but the depressions and ridges cannot be mapped with the available data set (e.g. Fig. 7.4, profile 3). The surface Fc, between units 6c and 7c, is recognised less widely but is clearly an irregular, channelised erosion surface of regional extent (Figs 7.4, 7.6 and 7.7). Where reflector Fc is missing it is inferred that unit 7c has been removed by erosion. Each unit ranges in thickness from zero to 30–50 m and each thins over the crests of anticlines, indicating continuing syn-sedimentary tectonic folding throughout this period of sedimentation history. Beneath the mid shelf east of Motunau, units 8c to 6c together represent up to 130 m stratigraphic thickness (e.g., Fig. 7.4, profile 6) and erosion surface Ec descends to > 160 m subbottom depth (see Fig. 7.12).

A sediment core was obtained from unit 7c where it crops out at site U935 (Figs 7.5 and 7.11). The core contains about 0.3 m of consolidated, homogeneous marine muddy silt which overlies c. 0.1 m of gravelly mud with common greywacke pebbles. Overlying the silt is the ubiquitous, unconsolidated muddy-gravel veneer which is 0.1 m thick at this site and is shown in section 7.3.3 to be the post-glacial age, transgressive sediment lag. The upper 0.1–0.2 m of unit 7c (the silt horizon) is an unusual, well oxidised rusty olive brown colour with well cemented aggregates. The silt beneath is olive grey colour, typical of most Pleistocene cores from the region. It is possible that this oxidised upper part of the silt layer is a soil horizon that developed from the unit 7c mudstone when it was subaerially exposed during lowered sea-level of the last glaciation (section 7.3.3). If so, the soil horizon survived the passage of shoreline transgression during post-glacial sea-level rise.

The unit 7c marine silt lithology in core U935 contains common specimens of the nannoflora *Gephyrocapsa aperta* which suggests a Castlecliffian or Haweran age (Fig. 7.5) (Edwards, 1987). The absence of *Pseudoemiliania lacunosa* from this sample may not be diagnostic of age because small numbers of the specimen may be easily corroded. The biostratigraphy and stratigraphic position of the unit are consistent with a middle to Late Pleistocene age. Two other cores (U685 and U683) from the north Canterbury shelf south of the Conway Trough, where the structure appears to be complex and the Pleistocene stratigraphy is not well established, recovered sediment from beneath reflector Ec, probably from unit 6c (Figs 7.5 and 7.11). The sediment is consolidated, marine, medium to dark grey sandy silt (U683) and clayey silt (U685) overlain by 0.3 m and 0.5 m of unconsolidated gravel respectively. Sample U683 contains low numbers of the nannoflora *Emiliania huxleyi* (first appearing in the early Haweran, base of oxygen isotope stage 8, at c. 0.3 Ma, but only abundant above stage 5), but no specimens of *Pseudoemiliania lacunosa* (Fig. 7.5). Also absent, but possibly due to post-depositional corrosion, are specimens of *Gephyrocapsa caribbeanica* (last appearing possibly in the top of oxygen isotope stage 7, Edwards, 1987). Unit 6c is, therefore, Haweran age (< 0.3 Ma) (Late Pleistocene).

Units 5c to 3c

The relationships between these units are most easily recognised in the region where anticlines $\mathbf{F}^c$ and $\mathbf{G}^c$ occur, about 20 km east of Motunau and about 10–15 km offshore (Fig. 7.11). In this region the units together represent between zero and 40 m stratigraphic thickness (Fig. 7.4, profiles 3 and 4; Figs 7.6 and 7.7). This thickness increases further offshore to almost 70 m beneath the mid shelf in northern Pegasus Bay (e.g., Fig. 7.4, profile 6). The top of unit 5c (reflector Dc, Fig. 7.5) is the only unit boundary that is not clearly a regionally extensive erosion surface. However, in all 3.5 kHz profiles the reflector coincides with a prominent change in acoustic impedance and with multiple reflections in unit 4c that downlap onto unit 5c (e.g., Fig. 7.4,

profile 4), so it must represent a significant hiatus in time. The inner edge of unit 5c is almost acoustically-transparent with only a few, weak and discontinuous reflections present. The upper boundary of unit 4c (reflector Cc) is an erosion surface that clearly truncates strata in units 4c and 5c (Fig. 7.4, profile 4) beneath the inner shelf, but cannot be traced in airgun profiles to the middle shelf. Unit 3c, which can be widely traced on profiles in Pegasus Bay, has internal reflections that onlap reflector Cc beneath the inner shelf and are themselves truncated by numerous, shallow channels that form the base of the overlying unit 2c (Fig. 7.5). Unit 3c was mapped by Herzer (1977b, 1981) as the lower member of the Canterbury Bight Formation and was interpreted as an interglacial, progradational highstand deposit.

No cores were obtained from the Late Pleistocene unit 5c, but three samples (U694, U695, U934; Fig. 7.11) were obtained from exposures of unit 4c. The samples consist of semi-consolidated, greyish olive, marine silt and sandy silt. At each site the unit is overlain by about 0.1 m of unconsolidated pebble-gravel and at site U695, this is capped by 0.1 m of modern mud (unit 1c). Based on the stratigraphic position of Unit 4c, the unit is clearly of Late Pleistocene age, but the nannoflora assemblages in the cores cannot constrain their ages to be better than early Castlecliffian to mid Haweran. For example, core U695 contains the nannoflora *Gephyrocapsa aperta* (Castlecliffian to present) and *G. oceanica* (late Nukumaruan to present) but lacks any specimens of *Pseudoemiliania lacunosa*. The corroded nature of the nannoflora in the cores suggests that the absence of *Emiliania huxleyi* may be due to post-depositional dissolution.

Units 2c and 1c

Unit 2c is identified in seismic-reflection profiles beneath unit 1c in central Pegasus Bay and on the mid shelf east of Motunau. The unit infills and blankets shallow channels that are encised into unit 3c and is up to 15 m thick (Fig. 7.4., profiles 4 to 6; Fig. 7.7, profiles 11 and 12). Beneath the inner shelf the unit thins shoreward and pinches out onto the underlying Pleistocene sequences. The irregular erosional base of the unit (reflector Bc) is difficult to correlate between profiles because: (1) the sediments in the unit are commonly recorded by prolonged echoes on the 3.5 kHz profiles, which suggests that they are predominantly sandy (e.g., Damuth, 1980); and (2) the channels are discontinuous and locally nested (e.g., Fig. 7.4, profile 5). Unit 2c was mapped by Herzer (1977b, 1981) as the upper member of the Canterbury Bight Formation. In Pegasus Bay, Herzer considered the buried channels to be coastal-plain river channels and the fill to be fluvial sedimentary facies that developed during the last glacial age when the shelf was exposed to subaerial erosion. Cores H777 and H810 (Fig. 1.5) from this unit are last glacial age (Herzer, 1981). The top of unit 2c is marked by a strong reflector (Ac, Fig. 7.5) that is slightly uneven and rises gently towards the shore. This reflection records the reworked and eroded surface of

unit 2c and correlates with the surface gravel veneer, which is ubiquitous (but not detected in seismic profiles) beneath the inner and northern shelf inshore of unit 1c (Fig. 7.11). In many profiles there are two prominent rises (steps) in surface Ac at about 75 m and 55 m beneath present day. These steps formed at still-stands in the post-glacial shoreline transgression at about 15 ka and 12 ka (e.g., Carter, L. and Carter, 1985; Carter *et al.*, 1985).

Unit 1c is well developed in Pegasus Bay (Fig. 7.11), is post-glacial in age and was mapped by Herzer (1977b, 1981) as the Pegasus Bay Formation. Cores U693, H440, H435 and H459 (Figs 1.5 and 7.11) show that the unit consists predominantly of silty mud. The unit is broadly lenticular in geometry, attains a thickness of 32–34 m in central Pegasus Bay and thins both towards the coastline and offshore towards the shelf edge (Fig. 7.4, profiles 4 to 6; Fig. 7.7, profiles 11 to 13). Unit 1c thins northwards also and largely pinches out on the mid to outer shelf about 20 km south of Point Gibson (Fig. 7.11). Ten to 15 km further north, east of Point Gibson, there are a few isolated, thin (< 5 m) additional patches of the unit. The geometry and depocentre of the unit are reflected by the 20–60 m bathymetric contours (Fig. 7.1). The post-glacial age and thickness of the unit imply sedimentation rates of up to 3 m/ka. In Pegasus Bay, weak reflections within the unit onlap the shoaling inner shelf and downlap the outer shelf. Shallow gas is common in the thickest part of the unit in central Pegasus Bay (Herzer, 1981). On the mid to outer shelf east of Motunau the unit includes a 255 km^2 zone of ridges and gullies (with up to 10 m of relief) that has been interpreted by previous workers as a low-angle slump modified by storm-generated bottom currents (Herzer and Lewis, 1979; Carter, L. and Carter, 1985).

7.3.3 EUSTATIC AND TECTONIC CONTROLS ON PLEISTOCENE SEQUENCE STRATIGRAPHY

It is well known that the stratal patterns of sediments deposited at continental margins record the sedimentation response to cycles of relative change of sea-level. Such changes of sea-level result largely from the interactions between glacio-eustacy, tectonic uplift or subsidence, and sediment supply (e.g., Vella, 1963; Lewis, 1973; Mitchum *et al.*, 1977; Vail *et al.*, 1977, 1990; Vail, 1987; Carter *et al.*, 1991; Mitchum and Van Wagoner, 1991; Christie-Blick, 1991; among others). Analyses of petroleum exploration cores indicates that during the Pliocene to Recent period, the offshore Canterbury basin south of Banks Peninsula subsided at rates up to 350 m/Ma (0.35 m/ka) (Field *et al.*, 1989). This subsidence helped to create accommodation space for the voluminous clastic sediment eroded from the rising Southern Alps and prograded over Canterbury shelf. Fulthorpe and Carter (1989) described a cyclicity

to Canterbury margin sedimentation, possibly controlled by relative sea-level changes, in the Middle-Late Miocene succession south of Banks Peninsula. High-frequency, high-amplitude sea-level cycles resulting from major glacio-eustatic fluctuations have been shown to be the dominant control on the depositional facies and stratal geometry of late Quaternary sediments, including seismic units 1c to 3c (Fig. 7.5), on the Canterbury shelf (Herzer, 1977b, 1981; Griggs *et al.*, 1983).

The sequence-stratigraphic model, developed by researchers at Exxon Production Research Company in the 1980s (e.g., Van Wagoner *et al.*, 1988; Vail *et al.*, 1990), is now a widely excepted stratigraphic framework in which to interpret unconformity-bounded sedimentary sequences resulting from sea-level cyclicity. Although the sequence-stratigraphic model was first developed to account for sea-level cycles of 0.5–5.0 Ma duration (third-order cycles), it has been shown recently to be a very powerful tool for interpretation of high-frequency, cyclothemic sequences controlled by glacio-eustatic sea-level cycles corresponding approximately to the 40 ka and 100 ka Milankovitch frequencies (Carter *et al.*, 1991; Abbott and Carter, in press), which have been dominant during the Plio-Pleistocene (Shackleton and Opdyke, 1973; Ruddiman *et al.*, 1989; Joyce *et al.*, 1990). The basic element of sequence stratigraphy is the unconformity-bounded sequence, which represents sedimentation within a complete sea-level cycle (Vail, 1987; Vail *et al.*, 1990). Ideally, the sequence consists of lowstand, transgressive and highstand systems tracts, which are genetically-related depositional units formed during different phases of the sea-level cycle. During the lowstand phase of high-amplitude sea-level cycles, such as occurred during the Pleistocene, much of the continental shelf is subaerially exposed and the lowstand systems tract is deposited mainly on the continental slope and in the deep ocean basin. The transgressive systems tract forms diachronously on the continental shelf during a relative rise of sea-level. During a relative highstand phase of a sea-level cycle following shoreline transgression, the highstand systems tract progrades and downlaps onto the flooded and locally sediment-starved shelf (see Fig. 8.1).

It is not the intention of this thesis to make a detailed interpretation of the Pleistocene seismic units beneath the north Canterbury shelf in terms of the sequence-stratigraphic model. Such interpretation must await further seismic-stratigraphic analysis of the erosional unconformities and the geometric relationships between the different units, and may then be followed by tentative correlations to the marine oxygen isotope scale. Nevertheless, the mid-Late Pleistocene to Recent seismic units 11c to 1c (Fig. 7.5) are interpreted to be the result of interactions between major glacio-eustatic fluctuations in sea-level (c. 120–140 m, Abbott and Carter; in press), superimposed on a shelf that is undergoing tectonic tilting and active folding and faulting (see section 7.4). Therefore, some pertinent comments relating the seismic units to the sequence-stratigraphic model are made here. High-resolution seismic

stratal patterns and dated sediment cores indicate that sequences 1c and 3c are progradational highstand systems tracts and that unit 2c represents fluvial sediment deposited on the coastal plain during lowstand conditions (Herzer, 1981). The geometry of unit 1c (Fig. 7.4) and the present day hydraulic conditions on the shelf indicate that the modern mud is derived mostly from rivers south of Banks Peninsula and transported northwards by coast-parallel currents (Carter and Herzer, 1979; Carter *et al.*, 1982). Unit 1c is prograding northwards, offshore and onshore from the northeastern tip of Banks Peninsula (Fig. 7.11). The unit onlaps the shoaling inner shelf, downlaps the outer shelf and partially covers the very thin (< 30 cm) shelf-wide pebble-gravel lag, which represents the youngest (post last-glacial) transgressive systems tract of the sedimentary succession. This transgressive gravel layer is too thin to be detected seismically and appears as a strong, single reflector marking the underlying ravinement surface (reflector Ac). The gravel veneer was deposited diachronously during the post last-glacial shoreline transgression between c. 18 ka and 6.5 ka (Herzer, 1981; Carter *et al.*, 1982; Gibb, 1986). At core site U935, the transgressive systems tract overlies a possible soil horizon that developed in the top of the sequence 7c during subaerial exposure, but was not eroded sufficiently by shoreface ravinement to be removed. In terms of the Exxon sequence stratigraphic model, reflector Bc is the subaerial lower boundary of the youngest 'sequence' (sea-level cycle) and reflector Ac is the shoreface ravinement surface and also the mid-cycle downlap surface **within** the sequence (see Fig. 8.1A). By analogy, the Pleistocene erosion surfaces Kc to Cc (Fig. 7.5) are inferred to be transgressive shoreface ravinement surfaces or subaerial erosion surfaces. The inner to mid shelf seismic units are inferred to be predominantly highstand systems tracts, although minor fluvial deposits may be locally preserved in incised channels beneath the transgressive surfaces (e.g., Fig. 7.4, profile 6; Fig. 7.8, profile 17). Cores from several seismic units (Fig. 7.5) all contain a remarkably similar, massive muddy silt lithology that is consistent with deposition on the inner shelf beyond the sandy, shoreface sediment wedge. Reflections within these highstand silts onlap the shoaling inner shelf, analogously to the reflections within seismic unit 1c.

The wave-planed surface of the exposed, Late Pliocene to Early Pleistocene coastal unit 12c extends up to 8 km offshore. This unit has been progressively uplifted, together with the coastal hills of north Canterbury, and repeatedly eroded during successive shoreline transgressions in the Pleistocene. In contrast, there appears to have been progressive subsidence of the mid to outer shelf, which created the accommodation space for the deposition of mid-Late Pleistocene to Recent sediments. The mid-Late Pleistocene erosion surface Hc (c. 500 ka), which is inferred to be a transgressive ravinement surface from a previous rise of sea-level, descends up to 225 m beneath the mid shelf in northern Pegasus Bay. If the strata immediately above and beneath reflector Hc were deposited at water depths close to their present

day mid-shelf analogues, then the position of reflector Hc implies regional subsidence of the mid shelf at a rate of about 0.4 m/ka. The abandoned Early Pleistocene submarine canyon beneath the shelf (section 7.3.1; Herzer and Lewis, 1979) provided additional accommodation space for the mid Pleistocene highstand deposits. Units 11c to 1c all thin and wedge out against the outer edge of the exposed unit 12c. Therefore, this location must be close to the axis of regional tilt, separating the rising coastal zone from the subsiding mid-outer shelf (the zero isobase of Lewis, 1971) (see Fig. 8.1A). It is shown in section 7.4 that within the western, shoreward edge of the subsiding part of the shelf, seaward of this conceptual axis of tilt, thrust faults and fault-propagation folds have been progressively deforming the inner edge of units 11c to 1c (Fig. 7.11). The folds have been active throughout the deposition of the units and they locally modify the stratal patterns. However, considering the probable rates of post-glacial sea-level rise (c. 8-30 m/ka; Carter *et al.*, 1991), and the extremely slow, inferred rates of fold growth (see section 7.4.2), the localised uplift and subsidence produced by the folds is unlikely to have contributed significantly to the origin of the sequences.

7.4 TECTONIC DEFORMATION

The seismic-reflection profiles that existed prior to this study, including the oil company, multichannel profiles, were not obtained with the specific aim of mapping and analysing the late Cenozoic deformation beneath the shelf. Consequently, many of those profiles lie outside the deformation zone or have the wrong orientation to image the structures. The extent of the deformation zone is well constrained by the distribution of the new, closely spaced, high-resolution seismic profiles (Fig. 1.4), which have been used to map the zone in detail (Fig. 7.11). Individual structures are intersected by up to 20 profiles, which are spaced closely enough to enable confident correlations of the major structures and stratigraphic reflections. The single-channel seismic profiles, however, image only the upper few hundred metres of the sedimentary cover succession, so they reveal only the shallow-seismic characteristics of the structures. Growth folds are widespread in the Pleistocene succession (Figs 7.4 and 7.6 to 7.10). It is assumed that the folds reflect the strain imposed on the cover sequence by basement faulting. Sections 7.4.1 to 7.4.4 discuss the style and timing of deformation of the cover sequence and the historical record of seismicity in the region. The implications for regional tectonic interpretations are discussed in Chapter 8.

7.4.1 DEFORMATION OF THE COVER SEQUENCE

Late Cenozoic deformation in north Canterbury extends 20 km offshore from central Pegasus Bay to Kaikoura, and almost to the western end of the North Mernoo Fault

Zone (Fig. 7.11). The main structural grain within the zone is northeast-southwest, broadly similar to the coastal region onshore, but 30–90° different from the average trend of structures in the western end of the NMFZ. The southernmost late Cenozoic structural element on the shelf is the Pegasus Bay Fault, which was first recognised in oil company seismic profiles (Carter and Carter, 1982; Carter, R.M. and Carter 1985; Herzer and Bradshaw, 1985) and has been re-mapped here (Fig. 7.11). North of the Pegasus Bay Fault, ten major folds are developed in the upper few hundred metres of the sedimentary cover sequence and for convenience, they have been labelled **A**^{c} to **J**^{c} (the superscript 'c', for Canterbury, is to distinguish these structures from labelled normal faults in the NMFZ; see Fig. 7.11). It is argued in the following section that folds **A**^{c} to **J**^{c} are developing above thrust faults similar to the Pegasus Bay Fault. In addition, numerous other smaller-scale structures beneath the shelf are mapped, but not labelled.

7.4.1.1 Major Structures

There are two major structures in Pegasus Bay (the Pegasus Bay Fault and fold **A**^{c}), seven major structures between the Waipara River mouth and Point Gibson (folds **B**^{c} to **H**^{c}) and a major structure (**J**^{c}) that underlies the Conway Ridge (Fig. 7.11). The average trend of the axial traces of the folds changes broadly from 070° in northern Pegasus Bay, south of Motunau Point, to 060° between Motunau Point and Point Gibson. Still further north, the structures that bound the Conway Trough trend at 015°. This northward anticlockwise swing in average trend of the structures mirrors the broad change in structural trend onshore between the north Canterbury range front and the Hope Fault (Fig. 7.11). In detail, however, there is considerable variation in the trend of structures beneath the shelf. The axial traces of the major folds are slightly sinuous; they vary along strike typically by 20–30° and locally by 50° (fold **B**^{c}, Fig. 7.11). Notably, parts of some structural elements (e.g., folds **B**^{c}, **I**^{c} and **E**^{c}) are oriented at 100–105°, which is roughly parallel to the average trend of normal faults in the western end of the NMFZ and Late Cretaceous faults onshore (e.g., Nicol, 1993). Overall, when the deformation zone is viewed longitudinally, there is a weak *en echelon* pattern with structures overlapping in a left stepping arrangement.

The major folds range in length from about 10 km (folds **C**^{c}, **D**^{c}, **F**^{c}, **G**^{c}) to 35 km (fold **H**^{c}; Fig. 7.11) and overlapping structures range from about 2 km to 10 km apart. The seismic-reflection profiles show clearly that all of the major anticlines in the Pleistocene succession are asymmetric and verge towards the coast (northwestward). The anticlines are paired with asymmetrical synclines; the parallel structures sharing the steep limbs of the folds (Figs 7.6 to 7.8). The unconformity-bounded Pleistocene seismic units thin towards the crests of the anticlines and the dips of the strata progressively steepen with stratigraphic depth, indicating that the folds have been

growing during the deposition and episodic erosion of the sediments. In the available seismic profiles the folds look much tighter than they really are because of the large vertical exaggerations (typically 9–25:1) of the profiles. The steepest strata, in the Late Pliocene to Early Pleistocene unit 12c, dip at only 11° (e.g., Fig. 7.4, profiles 3 and 4; Fig. 7.6, profile 9; Fig. 7.7, profiles 10-13). The middle Pleistocene unconformities Jc and Ic dip up 10° (typically 5–8°) on the steep, northwest limbs of the folds and generally 2–7° less on the gentle, southeast limbs. The dips of Late Pleistocene strata generally do not exceed a few degrees.

The axes of the major folds plunge predominantly northeastward. This is well expressed in a structural contour of the Late Pleistocene (< 0.3 Ma) erosion surface Ec (e.g., folds **A**^{c}, **H**^{c} and Pegasus Bay Fault; Fig. 7.12), which also illustrates the areas of greatest uplift. In the best developed parts of folds, deeper stratigraphic horizons are exposed at the surface as a result of uplift and erosion, and these horizons dip away with the plunge of the folds. This can be illustrated by comparing stratigraphic horizons in profiles 12 and 13 where they intersect fold **B**^{c} (Figs 7.7, 7.11). The northern end of the same fold projects beneath the southeast end of profile 19 but this part of the fold is recorded only in deeper-penetrating airgun profiles, not by the 3.5 kHz profile 19, which images only the upper 50 m subbottom (Fig. 7.9). Fold **A**^{c} is well developed about 5–10 km off the Ashley River mouth (Fig. 7.11) and opens towards central Pegasus Bay (compare profiles 15, 16 and 17; Fig. 7.8). In contrast, the fold developed above the tip of the Pegasus Bay Fault is well developed in central Pegasus Bay (Fig. 7.8, profiles 15 and 17) and opens towards the coastline a few kilometres north of the Waimakariri River mouth (Fig. 7.8, profiles 14 and 16). Multiple-interference in profiles 15 and 16 makes interpretation of the subbottom reflections difficult.

Not all tectonic folds must be directly related to faulting. However, good quality, multichannel seismic-reflection data, drill cores and field mapping in other parts of New Zealand (e.g., Pettinga, 1982; Davey *et al.*, 1986; Cape *et al.*, 1990; Melhuish, 1990, Beanland and Berryman, 1991; Nicol, 1991; Lewis and Pettinga, in press) and in other parts of the world (e.g., Suppe, 1985; Jamison, 1987; Carver, 1987; Hull, 1987; Yeats, 1987; Mitra, 1990) show that large-scale asymmetric folds commonly are directly related to thrusts or reverse faults in the upper crust. Such folds may represent fault-propagation folds, which develop at the upward termination of thrust faults, or they may represent fault-bend folds which develop as the hangingwall of a thrust is transported through a ramp region (Suppe, 1985; Jamison, 1987; Mitra, 1990). The oil company multichannel seismic-reflection profile 14 (Fig. 7.8) indicates that the Pegasus Bay Fault is a thrust or reverse fault with a fault-propagation fold developing in the hangingwall above the fault tip (Fig. 7.8). The fault displaces and folds the Oligocene seismic reflector (labelled O), but an asymmetric

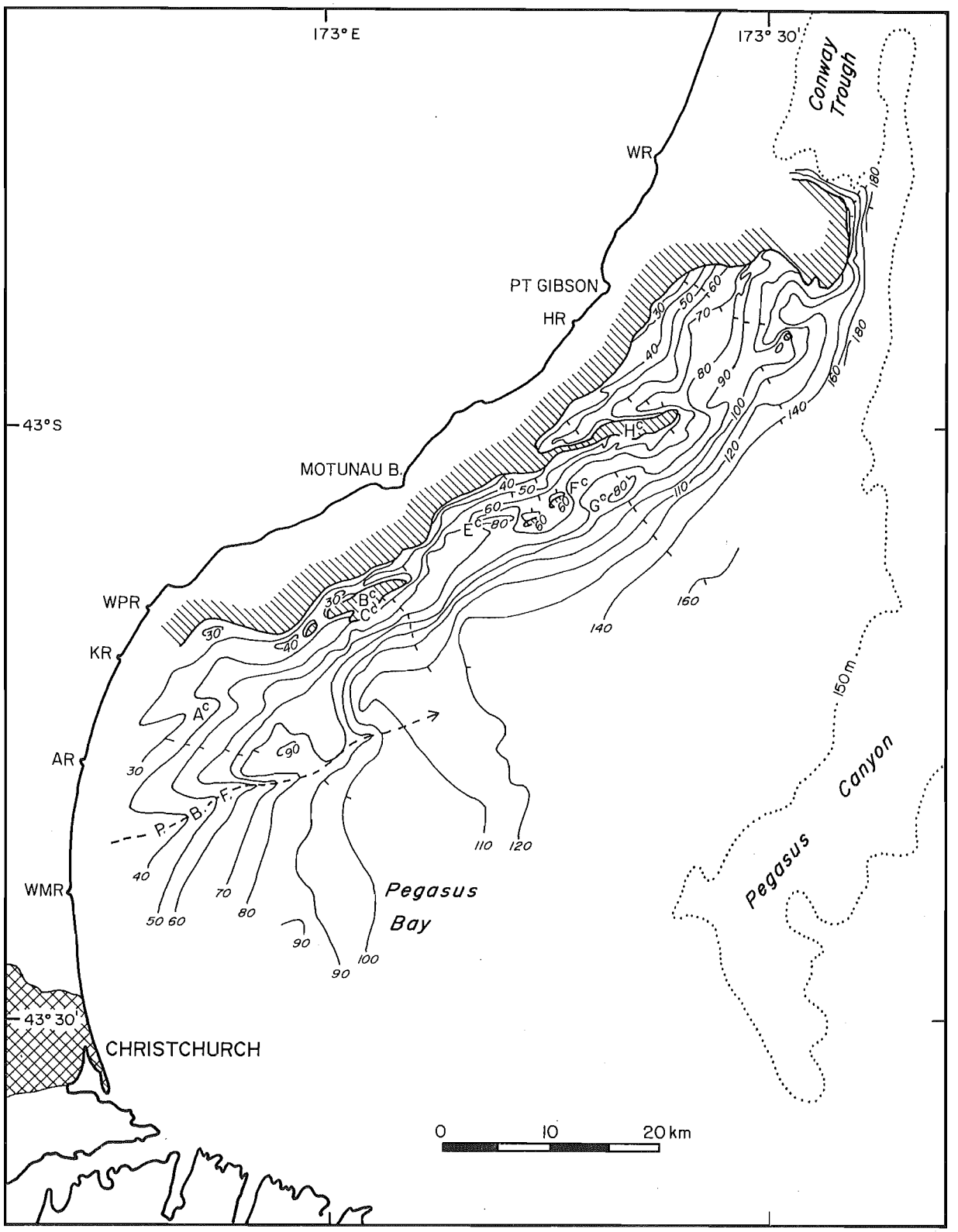

Fig. 7.12. Structural contour of the Late Pleistocene unconformity Ec. Contours are in metres below sea-level assuming a velocity of 1500 m/s for the water and 1600 m/s for the sediment. Hatch-shaded region is where the surface has been uplifted and eroded away. The positions of the major folds $\mathbf{A}^c$ to $\mathbf{C}^c$ and $\mathbf{E}^c$ to $\mathbf{H}^c$ are indicated, together with the Pegasus Bay Fault, PBF (axial traces of these structures are shown on Fig. 7.11 and, for clarity, are shown here only for the Pegasus Bay Fault). The dash-dot-dash line is approximately the shelf edge at 150 m water depth. WMR, Waimakariri River mouth; AR, Ashley River mouth; KR, Kowai River mouth; WPR, Waipara River mouth; HR, Hurunui River mouth; WR, Waiau River mouth.

growth fold dominates the Pleistocene part of the succession (e.g., Fig. 7.8, profiles 14 to 17). By analogy, the other asymmetric anticlines beneath the north Canterbury shelf are interpreted to be developing above the propagating tips of southeastward-dipping reverse faults which displace the basement rocks and the lower part of the sedimentary cover sequence (Fig. 7.11). Therefore, the Pegasus Bay Fault is considered here to be no different from, and no more significant tectonically than, the other major structures labelled **A**^{c} to **J**^{c}. The actual fault planes cannot be unequivocally identified in the newly-acquired single-channel, airgun seismic-reflection profiles which show that the Pleistocene succession is shortening mainly by folding (Figs. 7.4 and 7.6 to 7.8). Thus, the folds appear to be reflecting the strain that must be accommodated at the termination of the faults (e.g., Suppe, 1985; Jamison, 1987; Mitra, 1990). Onshore in north Canterbury, thrust faults have commonly transported the asymmetric folds on the hangingwall of the faults by propagating through the steep, foreland limb (Fig. 7.11) (Yousif, 1987; Nicol, 1991; Mould, 1992). This has resulted in Mesozoic basement rocks being uplifted and exposed in the cores of anticlines. The reverse faults beneath north Canterbury and the continental shelf may flatten into thrusts at deeper levels in the upper crust (see Fig. 8.5).

Despite wave-planing of the shelf during the last-glacial shoreline transgression, some folds south of Conway Trough have up to several metres of bathymetric expression, which may reflect fold growth, and hence, fault rupture, during the last 6500 years (fold **G**^{c}, Figs 7.4 and 7.7, profiles 3 and 10; fold **H**^{c}, Fig. 7.10, profiles 23 and 24; fold **J**^{c}, Fig. 7.10, profile 22). On the other hand, several metres surface expression of some structures, or segments of them, may reflect only the differences in erosional resistance of different stratigraphic horizons exposed at the seabed (e.g. fold **H**^{c}; Figs 7.4, 7.6 and 7.10, profiles 3, 8, 9 and 27; and fold **I**^{c}, Fig. 7.10, profile 26). The crests of some structures have been smoothly wave-planed by the post last-glacial transgressive shoreline and show no evidence of deformation of surface Ac and the Holocene seismic unit 1c (e.g., Pegasus Bay Fault and fold **A**^{c}, Fig. 7.8 profiles 14 to 17; fold **B**^{c}, Fig. 7.7, profiles 12 and 13).

In contrast to the structures on the shelf south of Conway Trough, the structurally-controlled Conway Ridge has considerable bathymetric expression, lying up to 500 m above the floor of Conway Trough (Figs 7.1 and 7.11). The asymmetrical, west-verging anticline **J**^{c} underlies the southern end of the ridge which suggests that the ridge has been uplifted an active thrust fault (Fig. 7.10, profile 22). The considerable bathymetric relief is likely to be the result of both thrusting beneath the ridge and erosion of the trough by sand and gravel sediment enroute to the Hikurangi Trough (e.g., Carter *et al.*, 1982; Lewis, under review). Despite erosion probably playing a part in the origin of Conway Trough, the bathymetric relief of Conway Ridge possibly indicates that the fault beneath fold **J**^{c} has been more active than faults beneath the

shelf further south (see section 7.4.2). Similar, but opposite-verging (eastward) thrust faults underlie many prominent bathymetric ridges within a few tens of kilometres of Conway Trough, on the Marlborough slope (e.g., Figs 6.2, 6.5 and 7.11) (Lewis and Pettinga, in press). No structure beneath the western flank of the Conway Trough can be resolved in the available profiles, but by analogy with the comparable Cheviot and Culverden basins onshore, the western flank of the Conway Trough may be underlain by a westward-dipping (offshore verging) thrust fault (Nicol, 1991; Mould 1992) (Fig. 7.11). The structure beneath the shelf immediately south of Conway Trough appears to be complex and dominated by an abrupt change in the orientation of structures, to an east-west strike.

Carter and Carter (1982) and Carter, R.M. and Carter (1985) differed from Herzer and Bradshaw (1985) in their interpretation of an apparent offset in reflections and prominent change in acoustic impedance which occurs in profile 1 (across fault B, right-hand side of Fig. 7.3) where the profile crosses the upper continental slope east of Point Gibson (Fig. 7.11). Carter and Carter interpreted the impedance change to result from basement rock faulted against Cenozoic sediments by a strike-slip fault they named the Motunau Fault (Fig. 7.2). In contrast, Herzer and Lewis disputed the existence of such a strike-slip fault beneath the shelf and slope, and interpreted the apparent reflection offset as a velocity pull-up caused by a bathymetric scarp. The new structural interpretation presented in Figures 5.3, 5.5, 5.7, 6.5 and 7.11 shows that profile 1 crosses the western end of the extensional NMFZ. Several normal faults are evident in profile 1, which turns off the shelf to run approximately down the axis of Pegasus Canyon (Fig. 7.11) and then turns northwest to cross the southern end of the imbricate-thrust faulted lower Marlborough slope. The prominent acoustic change in profile 1 occurs where the profile intersects fault B, which is a normal fault that bounds a major half graben containing over 1 km of Late Cretaceous sediments (Fig. 5.3). Thus, it is considered here that Carter and Carter (1982) were correct in their interpretation of a major fault in profile 1 at this position, but the fault has a normal sense of throw, trends east-west and is part of the NMFZ, not part of a NE–SW trending, strike-slip fault system crossing the shelf. There is no conclusive evidence of a strike-slip fault trace anywhere on the north Canterbury shelf.

7.4.1.2 **Small-scale Structures**

Relatively small-scale faults and folds, possibly hundreds of metres to a few kilometres in length, are common in, but are not restricted to the Late Pliocene to Early Pleistocene seismic unit 12c (Fig. 7.11). The small structures may vary significantly in trend from east-west to north-south, although they are more difficult to correlate between profiles than are the major structures because of their lengths. They include complex groups of folds and minor reverse faults that occur locally within the hinge

region of larger folds (e.g., Fig. 7.9, profile 18). Simple pairs or groups of symmetrical anticlines and synclines, which may not be directly fault controlled, are common (e.g., Fig. 7.9, northwestern end of profile 19). Some small asymmetric folds with no evidence of fault displacement in the uppermost strata appear to be small-scale fault-propagation folds (Fig. 7.6, profile 8; Fig. 7.9, profile 18). There are also common, minor thrust faults which clearly displace the uppermost strata and may have small drag folds associated with them (e.g., Fig. 7.4, profile 3; Fig. 7.6, profile 9; Fig. 7.7, profile 10). These faults generally verge in a similar direction (NW) to the major fault-propagation folds **A**^{c} to **J**^{c} and at least one fault appears to be an upward-splay (branching imbricate) off the major thrust fault beneath fold **B**^{c} (Fig. 7.7, profile 11). At least one small, E–W trending thrust fault, between the Conway Trough and fold **I**^{c}, verges south (Fig. 7.10, profiles 25 and 26). In addition two small back-thrusts are recognised. One displaces Late Pleistocene strata in the hinge of the syncline associated with fold **H**^{c} (Fig. 7.4, profile 3) and another back-thrust displaces the crest of anticline **I**^{c} (Fig. 7.10, profile 25).

7.4.2 TIMING AND RATES OF DEFORMATION

Although many of the newly acquired, single channel, high-resolution seismic profiles show progressive deformation of the inner shelf since the middle to Late Pleistocene, none of these profiles image deep enough into the Plio-Pleistocene succession to constrain the time of initiation of the late Cenozoic deformation. The multichannel profile 14 (Fig. 7.3, obtained by Mobil International Oil Company in 1972), shows that the western part of the Pegasus Bay Fault exhibits growth only for the upper 0.3–0.4 s (TWT, c. 250–350 m). Based on preliminary correlations with (1) nearby high-resolution airgun profiles in Pegasus Bay; and (2) the stratigraphy of the 433 m-deep Bexley Bore, at the coast in New Brighton, Christchurch (Canterbury Regional Council, M35w/6038) (Fig. 7.11); the upper 250–350 m of sediment is equivalent to the middle Pleistocene to Recent succession, represented approximately by seismic units 11c to 1c (Fig. 7.5). Thus, the Pegasus Bay Fault is inferred to have ruptured for the first time in the middle Pleistocene (c. 0.5–0.7 Ma).

In Marlborough and the northern part of north Canterbury, deformation in the Miocene was widespread and much of the pre-Miocene cover sequence was stripped off by erosion following uplift above sea-level (e.g., Wilson, 1963; Prebble, 1980; Field *et al.*, 1989; Rait *et al.*, 1991). In contrast, in the southern part of north Canterbury, significant deformation and uplift did not commence until the Pleistocene (Nicol, 1991; Cowan, 1992). Cowan (1992) used inferred stratigraphic ages of terraces and gravels in the Porter's Pass-Amberley Fault Zone (Fig. 7.11 — upper left) and coastal terraces near Motunau to constrain both the rates and timing of

tectonic uplift in those areas. He concluded that deformation and uplift of the north Canterbury range front and Waipara coastal hills commenced within the last 1 Ma and possibly within the last 0.5 Ma. These ages are consistent with the inferred development of the Pegasus Bay Fault and indicate a southward migration of the deformation front associated with the plate-boundry zone in northern South Island. The timing of development of the Conway Trough and the inception of deformation beneath the northern part of the shelf, immediately south of the trough, is not constrained by the available data, but might also be Pleistocene.

The quality of the available seismic-reflection profiles is not sufficient to determine the slip rates of the faults, because the geometry of the faults and the quantitative relationship between fault displacement and fold growth are not known. Whether or not the anticlines represent fault-propagation folds or fault-bend folds, the difference in vertical elevation between anticlinal crests and synclinal troughs cannot be greater than the total slip on the underlying fault. Models of such folds (Suppe, 1985; Mitra, 1990), in fact, suggest that relative uplift of the anticlines is usually considerably less than the total slip on the faults, because most thrust faults flatten with depth. The total structural elevation (combined vertical displacement and folding) of the Oligocene reflector (labelled O) by the Pegasus Bay Fault, where the fault is intersected by profile 14, is 0.17 s (TWT), which is equivalent to 170 m, assuming a seismic velocity of 2.0 km/s for the middle Miocene to Recent succession (Wood *et al.*, 1989). This value represents a minimum rate of dip-slip displacement of 0.24–0.34 mm/yr for the shallow structural expression of the fault, assuming that displacement commenced at 0.5–0.7 Ma. Anticlinal crests of major folds in the Pleistocene succession between Pegasus Bay and Point Gibson have been uplifted, relative to synclinal troughs, at vertical rates ranging from 0.02 to 0.14 mm/yr (typically 0.05–0.09) mm/yr. These estimates are based on the folding of surfaces Ec (c. 250–300 ka), Gc and Hc (c. 450 ka) (Figs 7.4 and 7.6 to 7.8). Fold J^c may be more active, but the rate of uplift of the Conway Ridge cannot be measured because the stratigraphy in this region is not constrained. Furthermore, it is not known what role erosion of Conway Trough has played in generating the 500 m of bathymetric relief across the eastern flank of the trough. If all of the elevation of Conway Ridge is the result of thrust faulting on a major structure, which also developed in the middle to Late Pleistocene (c. 500–700 ka), then the ridge might have grown at a rate of 0.7–1.0 mm/yr (0.3 mm/yr if the ridge started developing in the Early Pleistocene; e.g., Nicol, 1991, Mould, 1992).

7.4.3 RELATIONSHIP BETWEEN QUATERNARY AND CRETACEOUS STRUCTURES

Late Cretaceous normal faults that bound half-graben beneath the shelf (e.g., Fig. 7.3) are tectonostratigraphically related to the Cretaceous normal faults beneath the

western Chatham Rise (Figs 5.3 and 7.11) and to Cretaceous normal faults in north Canterbury (e.g., Nicol, 1991, 1993). Because of the very limited number of seismic profiles that image basement beneath the shelf, correlations of Cretaceous faults are tentative. Those on Figure 7.11 differ slightly from those of Wood *et al.* (1989) and Field *et al.* (1989) (Fig. 5.3 — bottom right). The faults trend approximately east-west and dip predominantly to the south. During the late Cenozoic, some Cretaceous faults have been reactivated as normal faults in the North Mernoo Fault Zone (Chapter 5) and as oblique-slip reverse and oblique-slip normal tear faults in north Canterbury (Nicol, 1991). There is no conclusive evidence in the available seismic-reflection profiles of the north Canterbury shelf to indicate reactivation of the Cretaceous normal faults during the Pleistocene. It is possible, however, that oblique-slip tear faults are present locally in the basement rocks and that east-west trending components of the fold and thrust belt (e.g., **E**^{c} and **I**^{c}) are reactivating and inverting basement faults that first developed during the Cretaceous. Some of the newly acquired seismic-reflection profiles were positioned carefully between the ends of the major folds, in search of transfer structures such as tear faults. It is anticipated that tear faults might be reflected in the vertically-exaggerated profiles as near-vertical structures with reflection termination characteristics and geometry that are distinctly different from the major fault-propagation folds. Only one such structure, labelled T on profile 20 (Fig. 7.9) occurs, but the fault is minor, cannot be traced to any other profile, so its orientation is not constrained, and it has no clear relationship to the major folds **A**^{c} and **D**^{c} nearby (Fig. 7.11). The profiles indicate that the folds in the Pleistocene succession simply die out at their ends and are not linked by shallow tear faults; displacement along the fold system is conserved by overlap of the folds.

7.4.4 HISTORICAL SEISMICITY

The distribution of shallow seismicity (mostly crustal events < 40 km deep and magnitude M > 3) beneath the north Canterbury continental margin since 1964 is shown on Figure 7.11. The level of seismic activity is low compared to the Marlborough region (onshore and offshore) and parts of onshore Canterbury (not shown on Fig. 7.11 for clarity) (Reyners, 1989; Cowan, 1992). Offshore, seismic activity increases dramatically northwards, from just south of Kaikoura (Fig. 6.5). This increase probably reflects activity within the subducting oceanic slab beneath Marlborough (e.g., Robinson, 1986, 1991) and an increase in seismic activity in the overlying crust (Arabasz and Robinson, 1976). Most of the historical crustal earthquakes beneath the north Canterbury shelf, which have been recorded instrumentally since 1964, have been of small magnitude (M < 5). At the time of writing, these include about 40 events with magnitude M > 3 between the Conway Trough and Banks Peninsula (Fig. 7.11). Epicentres are scattered throughout the southeastern edge of the fold and

and thrust belt and several occur further southeast. Hypocentral positions are not well constrained, having commonly been assigned to nominal depths of 12 km and 33 km using the standard New Zealand crustal model.

Seven earthquakes of magnitude M > 5 have occurred in the north Canterbury region during historical times. These are annotated with dates on Figure 7.11. Six of the events (four onshore and two offshore) have approximate epicentral locations assigned on the basis of historical reports of Modified Mercalli felt intensity (Elder *et al.,* 1991). The two largest historical, shallow (< 12 km) events in the region were the 1901 'Cheviot' earthquake with surface wave magnitude estimate of M_s = 6.9 and the 1922 'Motunau' earthquake of M_s = 6.4 (Dowrick, 1991). Although Elder *et al.* (1991) inferred the epicentral locations of these two events to be on land (Fig. 7.11), the uncertainties in their locations are such that one or both epicentres may have been offshore (Dowrick, pers. comm., July 1993). The 1948 earthquake in the Waikari Valley was of magnitude M = 6.2 and the three events south of the Pegasus Bay Fault (Fig. 7.11), including the damaging 'New Brighton' earthquake in 1869, have inferred magnitudes of M = 5-6 (Elder *et al.* 1991). The other M > 5 event occurred beneath the northern end of the Pegasus Bay Fault in 1987 (Fig. 7.11) and was a deep crustal event with a focal depth that has been restrained to 30 km. None of these moderate to large events have been associated with observed surface ruptures.

Cowan (1992) and Reyners and Cowan (in press) utilised the velocity results of three man-made explosions and an 11-week, regional microearthquake study in 1990 to make inferences about the crustal structure beneath the northern Canterbury plains and the Porter's Pass-Amberley Fault Zone (Fig. 7.11 — upper left). They interpreted the continental crust beneath this region and Pegasus Bay to be 27 km thick, the upper 12 km and lower 10 km of which are seismically active. Earthquake hypocentres indicate the middle crust is relatively aseismic. Cowan (1992) showed that west of Amberley (Fig. 7.11), earthquake hypocentres in the upper seismic horizon are concentrated between 7 and 10 km and focal mechanisms are predominantly strike-slip. In contrast, focal mechanisms in the lower seismic horizon are a mixture, including many oblique-slip normal solutions, two of which occurred beneath Pegasus Bay. During the 1990 microearthquake survey, no shallow crustal events were recorded beneath the coastal hills of north Canterbury and the continental shelf. Such data are required to constrain better the kinematics of deformation and in particular, to resolve the lateral component of displacement on the basement faults.

7.5 CONCLUSIONS

(1) The north Canterbury shelf is underlain by up to 2 km of sedimentary cover resting on Torlesse basement. Two major units are present. The lower unit is up to 500 m thick and includes Late Cretaceous sediments that infill normal-faulted half graben, together with a thin blanket of Paleogene sediments which are capped by the Amuri Limestone Formation of Oligocene age. The upper unit consists of a thin (c. 20 m) limestone unit of late Early Miocene age, overlain by a succession of Middle Miocene to Recent progradational siltstones up to 1500 m thick. The upper part of the progradational unit contains an Early Pleistocene canyon complex beneath the mid to outer shelf, that was infilled and covered during the middle-Late Pleistocene.

(2) Twelve unconformity-bounded seismic units beneath the inner to middle shelf are identified here using high-resolution seismic-reflection profiles. Nannoflora biostratigraphy of cores from at least six units constrain the ages of the sediments. The oldest unit (12c) is Late Pliocene to Early Pleistocene in age, dips regionally offshore at about 11° and is exposed at the seabed in an uplifted coastal erosion platform 3–8 km wide. Units 11c to 1c are middle-Late Pleistocene to Recent in age and represent about 250–300 m of sediment beneath the inner to middle shelf. Most of the units are inferred to be predominantly silty mud deposited on the inner to middle shelf during highstand phases of eustatic sea-level. The units dip regionally offshore at angles typically < 5° and all thin shoreward and wedge out against the outer edge of unit 12c. This location, near the outer edge of unit 12c, is approximately the axis of regional tilting. Seaward of this axis, mid shelf subsidence of about 0.4 m/ka is inferred to have occurred to create the accommodation space for these sediments. Growth folds have progressively modified the stratal patterns beneath the inner shelf, but the folds did not control the origin of the units.

(3) Between central Pegasus Bay and Kaikoura, contractional deformation extends offshore for 20 km. The trend of the major structures is roughly parallel to the coastline, swinging from NE–SW in Pegasus Bay to more northerly close to Kaikoura. Eleven major structures have been identified and carefully mapped. The most prominent bathymetric and structural feature on the shelf is the Conway Trough, a 10 x 40 km, north-south-trending rectangular basin in the northern part of the shelf. Uplift of Conway Ridge by an E-dipping thrust fault (labelled **J**^{c}) together with probable erosion of Conway Trough mainly during glaciations, combine to produce up to 500 m relief across the eastern flank of the trough. South of Conway Trough, ten other major structures include the Pegasus Bay Fault, which has been re-mapped here, and similar structures

labelled $\mathbf{A}^c$ to $\mathbf{I}^c$. All of these structures are expressed in the middle to Late Pleistocene cover succession as pairs of asymmetrical anticlines and synclines. The major folds are 2–10 km apart, overlap, range from about 10 to 35 km in length, nearly all verge to the northwest (landward) and several plunge to the northeast. They are interpreted to be fault-propagation folds which have developed above the propagating tips of basement-involved thrust faults. There is no evidence within the Pleistocene cover sequence for major strike-slip deformation but reactivation and inversion of Late Cretaceous normal faults is possible. The available data suggests that the thrust faults developed in the middle to Late Pleistocene and show growth since that time. On the limbs of the major folds, the middle-Late Pleistocene strata dip at up 10° on the steep limbs and generally 2–7° less on gentle limbs. South of Conway Trough, rates of vertical fold growth range typically from 0.02 to 0.14 mm/yr. The Conway Ridge could have developed at up 0.3–1.0 mm/yr. Some folds have deformed the modern seabed indicating rupture of the underlying thrust during the Holocene, but the nearest structures to Christchurch City, the Pegasus Bay Fault and fold $\mathbf{A}^c$, show no evidence of growth during the last 6500 years. There are a variety of smaller-scale faults and folds, including a few antithetic back-thrusts, which are concentrated in, but not restricted to, the Late Pliocene to Early Pleistocene coastal unit 12c.

(4) The Canterbury shelf has experienced a moderately low level of crustal seismicity since 1964. Although there have been seven earthquakes of magnitude M>5 in north Canterbury during historical times, including three offshore, the focal positions of the events are not well constrained and no focal mechanism data exists to constrain the kinematics of deformation.

CHAPTER 8

SYNTHESIS AND CONCLUSIONS

8.1 CONTRASTING STYLES OF LATE CENOZOIC SEDIMENTATION: NORTHWESTERN CHATHAM RISE AND NORTH CANTERBURY CONTINENTAL MARGIN

The late Cenozoic uplift of the Southern Alps has had a profound effect on the style of sedimentation on the continental margins around New Zealand. The initiation of significant uplift of the alps in the Late Miocene is recorded by fission track analyses of uplifted minerals (Kamp *et al.*, 1989) and by an increase in terrigenous sedimentation and changes in sequence architecture in offshore sedimentary basins (e.g., Nelson, 1986; Lewis *et al.*, 1986; Fulthorpe and Carter, 1989; Field *et al.*, 1989; Carter and McCave, under review). In the offshore Canterbury basin, the increased erosion of the alps is marked by the start of major terrigenous input and shelf progradation (Field *et al.*, 1989; Wood *et al.*, 1989; Fulthorpe and Carter, 1989). At DSDP site 594 on the southwestern Chatham Rise (Fig. 4.1), it is reflected by a gradual change from carbonate to hemipelagic sedimentation (Kennett *et al.*, 1986) and on the NW Chatham Rise it is marked by reflector LM (c. 9–10 Ma; Fig. 4.2), which marks a significant seismic-stratigraphic change in acoustic impedance. In response to an increased rate of uplift and erosion of the Southern Alps during the Plio-Pleistocene (Lamb, 1988; Kamp *et al.*, 1989), sedimentation rates increased in the Canterbury Basin (Field *et al.*, 1989), the Bounty Trough (Carter *et al.*, 1990), the western platform of Taranaki (Beggs, 1990) and the Hikurangi Trough (Lewis and Pettinga, in press; Carter and McCave, under review). Although the Quaternary rate of tectonic uplift of the alps locally reaches 10 mm/yr (Wellman, 1979), uplift and erosion are inferred to be in a state of balance (Adams, 1980).

Chapters 3, 4 and 7 of this thesis discuss the styles and major controls on Pliocene-Recent marine sedimentation in the NW Chatham Rise and north Canterbury regions, both of which are proximal to sediment sources in the Southern Alps. Analysis of a large amount of single channel, high-resolution seismic reflection profiles from both of these areas have been used here to establish a high-resolution seismic stratigraphy. The seismic-stratigraphic resolution in both regions is similar. Thirteen unconformity-bounded seismic units (labelled 1–13) of Plio-Pleistocene age are recognised beneath the NW Chatham Rise continental slope (Fig. 4.2) and 12 unconformity-bounded seismic units (labelled 1c–12c) are recognised beneath the north Canterbury shelf (Fig. 7.5). Specific stratigraphic units in each area cannot be tied across the deep, steep-sided submarine canyons that separate the two regions. The fortuitous exposure of seismic units at the seabed in both areas enabled stratigraphic

sampling, using conventional piston coring equipment. Chronostratigraphic resolution of these units is constrained mainly by the numbers of units sampled, the short cores which sample only small fractions of the units, and by the resolution of the foraminifera and nannoflora biostratigraphy of the cores, which have been tied to the international time scale by independent dating methods in other areas (Edwards *et al.*, 1988). Despite these uncertainties a broad Plio-Pleistocene time framework has been successfully established in both regions and used to constrain their sedimentation history and the tectonic evolution.

Although there are similarities in seismic-stratigraphic resolution and in the Plio-Pleistocene fluctuations in deposition and erosion in both the NW Chatham Rise slope and the north Canterbury shelf regions, there are several very significant differences. The differences in the geometry and origin of the sedimentary units and their intervening unconformities are illustrated conceptually in Figure 8.1. The most obvious differences are the water depths and distance of sedimentation site from land. Most of the north Canterbury shelf lies in water less than 100 m deep and the inner to middle shelf is presently < 60 m deep. By analogy with the youngest three seismic units on the shelf, and by considering the core lithologies from older units, each of the Late Pliocene to Recent seismic units 1c to 12c and their intervening erosional unconformities Ac to Kc (Fig. 7.5) are inferred to have developed on the shelf in water depths of < 60 m (Fig. 8.1 A, C and D). In contrast, the NW Chatham Rise slope lies seaward of major submarine canyons linking the Canterbury shelf with the deep-sea Hikurangi Channel, and extends from the shelf depths of Mernoo Bank (< 150 m) to the edge of the > 2000 m deep Hikurangi Trough. The seismic units 1 to 13 and their intervening unconformities A to L (Fig. 4.2) developed in water c. 500–2000 m deep and 70–240 km off the South Island. The different sedimentation sites and proximity to sediment sources are reflected in the inferred rates of Quaternary sedimentation. Whereas silty mud accumulated on the north Canterbury shelf at up to 3 m/ka (Herzer, 1981), contemporary hemipelagic mud on the NW Chatham Rise slope accumulated at rates that probably never exceeded a few decimetres per thousand years (Chapter 4, this study).

It is well known that high-amplitude glacio-eustatic changes in sea-level have been a major control on continental margin sedimentation throughout the Plio-Pleistocene period (e.g. Curray, 1961; Vella, 1963; Lewis, 1973; Chappell, 1974; Herzer, 1977b; Chappell and Veeh, 1978; Kennett, 1982; Pillans, 1990; Mitchum and Van Wagoner, 1991; Abbott and Carter, in press; among others). During the middle-Late Pleistocene (c. 700 ka to present), glacio-eustatic sea-level fluctuations of > 100 m occurred with a cyclicity of about 100 ka (e.g., Prell *et al.*, 1979; Joyce *et al.*, 1990). The inner to middle north Canterbury continental shelf has been periodically exposed and eroded during regression and transgression of the shoreline and during

Fig. 8.1. Synthesis of late Cenozoic sedimentation styles and controls in the NW Chatham Rise and north Canterbury regions. **A.** Conceptual sequence-stratigraphic model showing the relationships between coastal uplift and tectonic shortening, outer shelf subsidence and glacio-eustatic sea-level changes on the north Canterbury shelf (SB = sequence boundary in the Vail/Exxon model). **B.** Conceptual model of sediment drift aggradation, localised current scours and extensional tectonics on the NW Chatham Rise slope. **C.** Bathymetric cross-section X–X" between the north Cantebury coast and the northern, upper slope of Mernoo Bank. **D.** Regional bathymetry and locations of sections X—X" and Y–Y". Area of late Quaternary current erosion is shaded. Solid arrows are modern sediment transport directions; Broken arrows are inferred late Quaternary mid-bathyal current directions. Dashed lines are canyons and the Hikurangi Channel. PC, Pegasus Canyon; KC, Kaikoura Canyon. **E.** Conceptual sequence-stratigraphic model of Vail (1987). TST, transgressive systems tract; HST, highstand systems tract; MFS, maximum flooding surface; LST, lowstand systems tract; lsw, lowstand wedge; sf, slope fan; bf, basin fan.

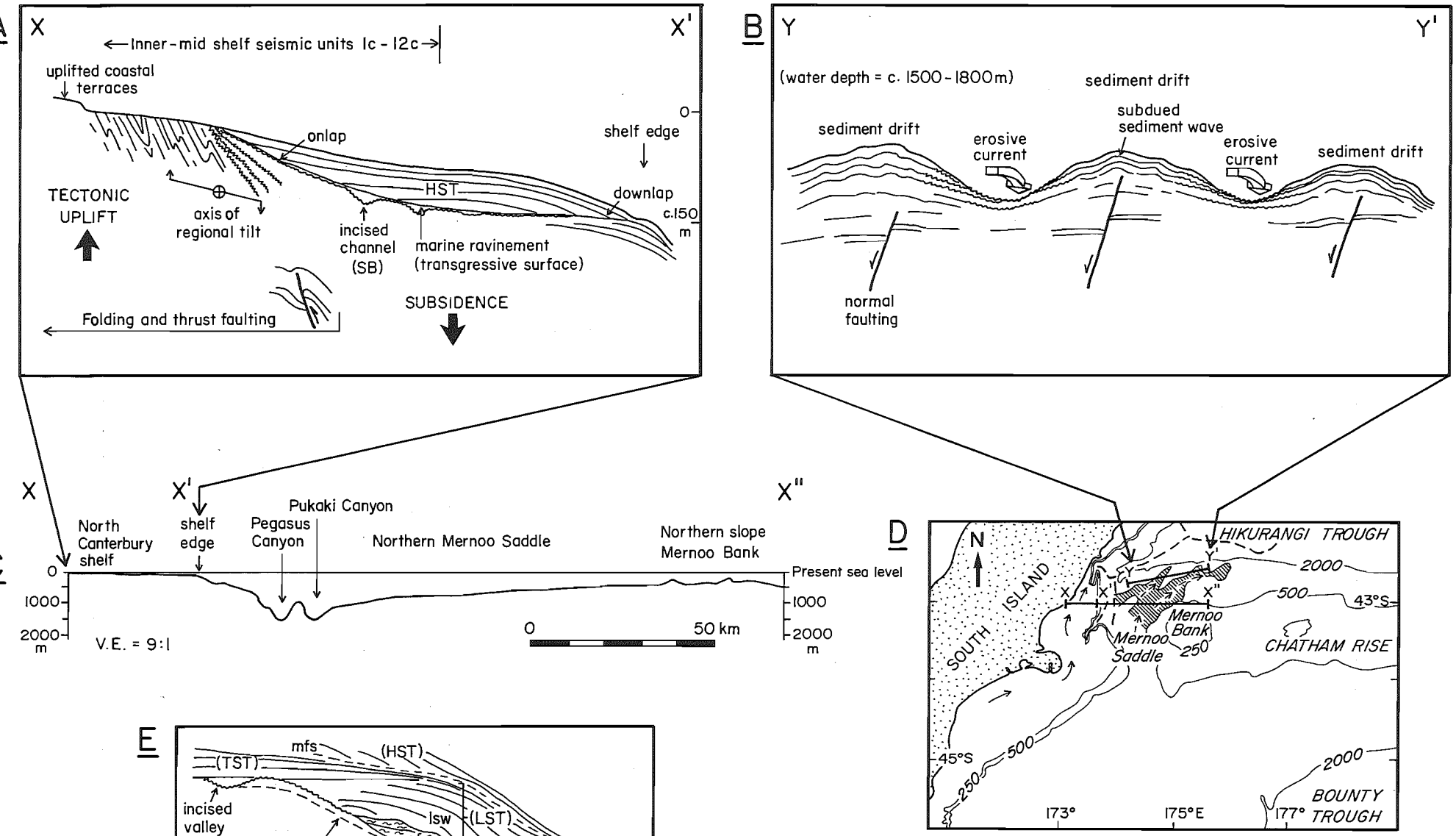
A
X
X'
←Inner-mid shelf seismic units Ic - I2c→
uplifted coastal terraces
onlap
0
shelf edge
TECTONIC UPLIFT
axis of regional tilt
HST
downlap
c.150 m
incised channel (SB)
marine ravinement (transgressive surface)
SUBSIDENCE
Folding and thrust faulting
B
Y
Y'
(water depth = c. 1500 - 1800m)
sediment drift
subdued sediment wave
sediment drift
erosive current
erosive current
sediment drift
normal faulting
X
X'
X''
North Canterbury shelf
shelf edge
Pukaki Canyon
Pegasus Canyon
Northern Mernoo Saddle
Northern slope Mernoo Bank
Present sea level
0
1000
2000 m
V.E. = 9:1
0
50 km
1000
2000 m
D
N
HIKURANGI TROUGH
SOUTH ISLAND
2000
500
43°S
Mernoo Bank
Mernoo Saddle
250
CHATHAM RISE
45°S
500
250
2000
BOUNTY TROUGH
173°
175°E
177°
E
mfs
(HST)
(TST)
incised valley
lsw
(LST)
canyon
sf
bf

relative lowstands of sea level. Based on a preliminary interpretation, most of the 12 seismic units recognised here are interpreted to be interglacial silty-mud deposits that prograded northeastwards, up the shelf, as well as seaward and landward, during relative highstands of sea-level (highstands systems tracts of Vail, 1987) (Fig. 8.1A and D). Landward progradation led to stratal onlap against the tectonically uplifting coastal platform, whereas seaward progradation produced stratal downlap on the outer shelf. The muds were transported and deposited under the influence of waves and storm generated currents (Carter and Herzer, 1979). Between the interglacial deposits there are inferred to be thin gravel horizons (transgressive systems tracts) deposited on successive shoreline ravinement surfaces, together with isolated pockets of probable glacial-age, fluvial sediment preserved in incised channels. In terms of the Vail/Exxon model of sequence stratigraphy (e.g., Vail, 1987; Van Wagoner *et al.*, 1988), the incised channels may represent the preserved remnants of type 1 sequence boundaries (major subaerial exposure of the shelf and coastal onlap stepping seaward of the shelf edge).

The water depths on the NW Chatham Rise continental slope eliminate subaerial exposure and shoreline ravinement as a mechanism for producing the many extensive erosion surfaces within the Plio-Pleistocene succession. Instead, echo-character mapping of the Quaternary sedimentation patterns (Chapter 3) and subsurface seismic-stratigraphic mapping of the sedimentary units and their intervening erosion surfaces (Chapter 4) indicate periodic seabed erosion by mid-bathyal currents. Erosional scours emanating from the 580 m-deep Mernoo Saddle indicate that the currents flowed northward through the saddle and obliquely across and down the NW Chatham Rise slope (Fig. 8.1D). Lenticular sediment drifts accumulated on the lower slope between areas of higher velocity current flow (Fig. 8.1B) and there has been minimal interaction between the currents and the Hikurangi Channel turbidite system in the axis of the Hikurangi Trough. In Chapters 3 and 4 it was argued that during periods of erosion of the slope, some type of internal hydraulic control on the flow conditions in Mernoo Saddle most probably generated the necessary currents on the slope further north (e.g., Armi and Farmer, 1985; Armi, 1986). Considering: (1) the periodicity of the middle-Late Pleistocene seismic units (c. 57–75 ka); (2) the apparent post-glacial reduction in current erosion on the lower slope; and (3) the modern physical oceanographic conditions in the Mernoo Saddle region; the periods of increased current velocities and major erosion of the slope are interpreted to have occurred during glaciations. Thus, whilst the seismic units and intervening unconformities beneath the slope do not result from wave-dominated processes during high-frequency sea-level cyclicity in the same way that seismic units do on the north Canterbury shelf, and sequences do in the Vail/Exxon sequence stratigraphic model (Vail, 1987), there is an indirect link with glacio-eustacy through the paleoceanographic changes induced by global climate cycles. Different sedimentation

styles beneath the north Canterbury shelf and the NW Chatham slope reflect differences in physical oceanography and response of the depositional sites to global climate cycles.

Furthermore, differences in stratal geometry result from the contrasting interactions between sedimentation and tectonic style in each area. Beneath the inner to middle north Canterbury shelf, the middle-Late Pleistocene to Recent seismic units thin shoreward against the outer edge of the exposed Late Pliocene-Early Pleistocene unit 12c and over the crests of large-scale, fault-propagation anticlines. This reflects the progressive tectonic uplift and shortening of the coastal region and inner shelf throughout this part of the sedimentary succession (Fig. 8.1A). In contrast, beneath the NW Chatham Rise slope, Plio-Pleistocene sediments typically thicken on the hangingwall towards the normal faults, reflecting the progressive extension throughout this part of the sedimentary succession (Fig. 8.1B).

In the Vail/Exxon sequence stratigraphic model, relative lowstands of sea-level during high-amplitude sea-level fluctuations coincide with the development of lowstand systems tracts on the continental slope and the deep ocean basin (Fig. 8.1E). These systems tracts include basin-floor fans, slope fans and lowstand wedges that prograde the continental margin. Herzer (1981) dated piston cores by the radiocarbon method and showed that prograding clinoforms beneath the present north Canterbury shelf edge and upper continental slope are lowstand deposits. In the present analysis, lowstand clinoforms observed beneath the upper slope have not been tied stratigraphically to specific episodes of subaerial exposure of the shelf. Herzer (1981) demonstrated also that the Pegasus and Pukaki canyons act as efficient conduits of coarse-grained terrigenous detritus to the Hikurangi Trough only during relative lowstands of sea-level, when the shoreline and longshore littoral sediment transport system supply such sediment directly into the heads of the canyons. In contrast, the Kaikoura Canyon, which extends inshore to <1 km from the coast, has funnelled sand and gravel to the Hikurangi Trough even during the Holocene (Carter *et al.*, 1982). This suggests that the Hikurangi Channel turbidite system (the basin floor systems tract of Vail, 1987) actively develops during relative lowstands of sea-level and also, to a lesser extent, during relative highstands (Lewis, under review).

In summary, typical middle-Late Pleistocene age, high-amplitude glacio-eustatic sea-level cycles coincide with the following effects off northeastern South Island during relative lowstands of sea-level (Fig. 8.1): (1) subaerial exposure and erosion of the Canterbury shelf and Mernoo Bank (e.g., Fleming and Reed, 1951; Herzer, 1981); (2) restriction of the flow of water through the Mernoo Saddle and the probable set-up of hydraulic controls on bottom-flow conditions in the saddle; (3) increased current velocities resulting in widespread erosion and sediment drift development on the NW

Chatham Rise continental slope; (4) out-building of the north Canterbury continental margin by lowstand clinoform progradation (Herzer, 1981; Field *et al.*, 1989; Wood *et al.*, 1989); and (5) active erosion of submarine canyons and mass transfer of gravel, sand and mud to the channel-levee turbidite system in the axis of the Hikurangi Trough (Herzer and Lewis, 1979; Carter *et al.*, 1982) . In contrast, during glacio-eustatic highstands of sea-level: (1) the north Canterbury shelf and Mernoo Bank are flooded; (2) Mernoo Saddle is up to c. 120 m deeper, the northward flow of water through the region (e.g., Heath, 1976, Greig and Gilmour, 1992) is less constricted and bottom current velocities and erosion on the NW Chatham Rise slope are reduced; (3) most of the north Canterbury submarine canyons (except the Kaikoura Canyon) are separated from the longshore movement of sand and gravel that is concentrated in the nearshore sublittoral zone (Herzer and Lewis, 1979; Carter *et al.*, 1982; Lewis, under review); and (4) the north Canterbury shelf, including the Conway Trough becomes the major depocentre for mud carried northward in suspension, and mud accumulates on the shelf at rates of up to 3 m/ka (Herzer, 1981; Gibb and Adams, 1982; Carter *et al.*, 1982). In contrast, the NW Chatham Rise slope together with the abandoned Pegasus and Pukaki canyons receive hemipelagic mud at significantly lower rates than on the shelf.

8.2 EVOLUTION OF THE PLATE-BOUNDARY IN NORTHERN SOUTH ISLAND: AN OVERVIEW

The southern end of the Hikurangi subduction zone is inferred to have extended as far south as Marlborough since the Early Miocene, when major tectonic shortening commenced on land (Prebble, 1980; Walcott, 1987; Waters 1988; Rait *et al.*, 1991). Since then, the orientation and configuration of the plate-boundary zone in central New Zealand has changed through time (e.g., Lamb, 1988; Lamb and Bibby, 1989). Reconstructions of the major elements of the plate boundary at 10 Ma and 4 Ma (Fig. 8.2) can be compared to the present day configuration shown in Figure 8.3. Ten million years ago (Fig. 8.2A) the northernmost faults in the Marlborough fault system (Wairau and Awatere Faults, see Fig. 8.3) are inferred to have been accommodating most of the relative plate motion between the Hikurangi subduction zone and the Alpine Fault system. At this time the imbricate thrust deformation front associated with the Hikurangi subduction zone is inferred to have had a more northerly orientation than present, and there was considerably less convergence across the Alpine Fault system compared to the last 5 Ma (Walcott, 1987).

As southwestward subduction of the Pacific Plate beneath northern South Island continued during the late Cenozoic, the subduction front at the trench rotated progressively clockwise and migrated southeastward towards its present position

Fig. 8.2. Reconstructions of the New Zealand region showing the inferred Australia-Pacific plate boundary configuration at 10 Ma (A) and 4 Ma (B), modified from Walcott (1987) and Lamb (1988) respectively. The submerged New Zealand continental plateau (stippled) is outlined by the 2000 m isobath and in A, the area of major late Cenozoic (post 10 Ma) deformation has been left blank. **A.** At 10 Ma the Alpine Fault system is inferred to have been linked to the Hikurangi subduction system by the northernmost Marlborough strike-slip faults. The subduction thrust front was oriented more northerly than present and the position of the present southern extent of oceanic subduction (heavy dotted line) was beneath present-day southern North Island. There was no extension at this time in the NMFZ. **B.** By 4 Ma the subduction thrust front had rotated clockwise to a northeast-southwest orientation, rapid oblique shortening was taking place on the Alpine Fault system, and extensional faulting was widespread in the NMFZ (see Fig. 5.7) as a result of the western end of the Chatham Rise interacting with the evolving transpressional plate boundary. Conventional symbols are used on faults. Bold arrows indicate the inferred direction of relative plate motion.

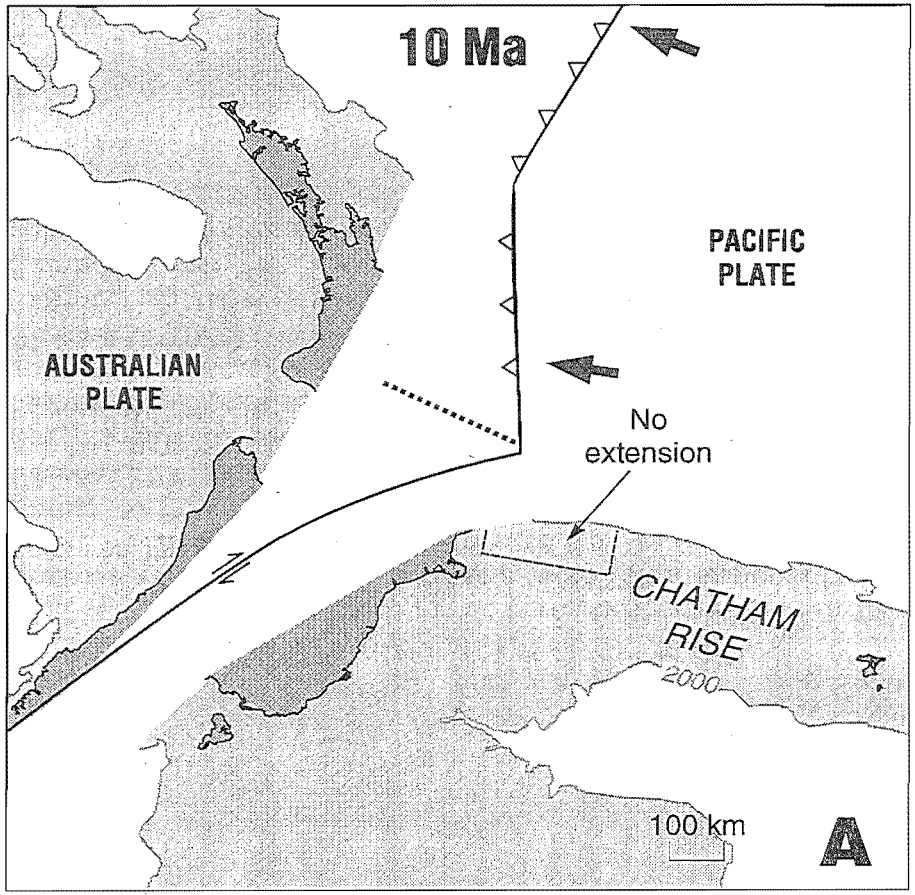
10 Ma
PACIFIC
PLATE
AUSTRALIAN
PLATE
No
extension
CHATHAM
RISE
2000
100 km
A

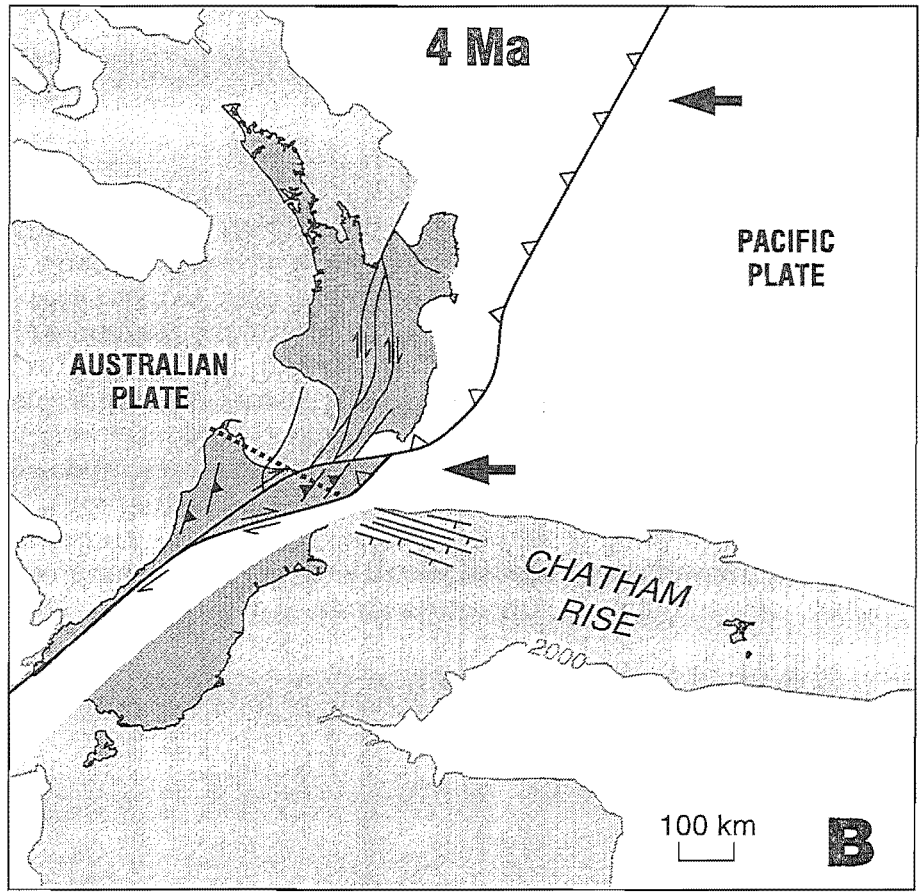
4 Ma
PACIFIC
PLATE
AUSTRALIAN
PLATE
CHATHAM
RISE
2000
100 km
B

Fig. 8.3. Regional tectonics in the transition zone between the obliquely convergent Hikurangi subduction system and the transpressive, Alpine Fault collision zone. NMFZ, extensional North Mernoo Fault Zone; MFS, strike-slipe Marlborough fault system; HMIFW, Hikurangi Margin imbricated frontal wedge; NC, North Canterbury region; AF, oblique-slip Alpine Fault; WF, Wairau Fault; AF, Awatere Fault; CF, Clarence Fault; HF, Hope Fault; PPAFZ, Porter's Pass-Amberley Fault Zone; W, Westport; C, Cheviot; BP, Banks Peninsula; KP, Kaikoura Peninsula; CS, Cook Strait; WN, Wellington; PC, Pegasus Canyon; MS, Mernoo Saddle; MB, Mernoo Bank. Major fault traces labelled with conventional symbols. Large arrow is the vector of relative motion between the Pacific and Australian plates (De Mets *et al.*, 1990). Water depths are metres. Heavy dotted line, southern extent of the subducted oceanic slab, as defined by data from the National Seismograph Network; fine dotted lines, tears in the subducted slab (Robinson, 1991). Offshore thrusts beneath the Marlborough slope are mapped from author's unpublished data. Inset diagram (bottom right) shows the major components of the plate boundary zone, with relative plate motion vectors. PT, Puysegur Trench; SA, Southern Alps; HT, Hikurangi Trough; KT, Kermadec Trench; CR, Chatham Rise; CI, Chatham Islands. Stippled area is the submerged New Zealand continental plateau outlined with the 2000 m isobath. Bold line is the average azimuth of principal horizontal compression in northern South Island.

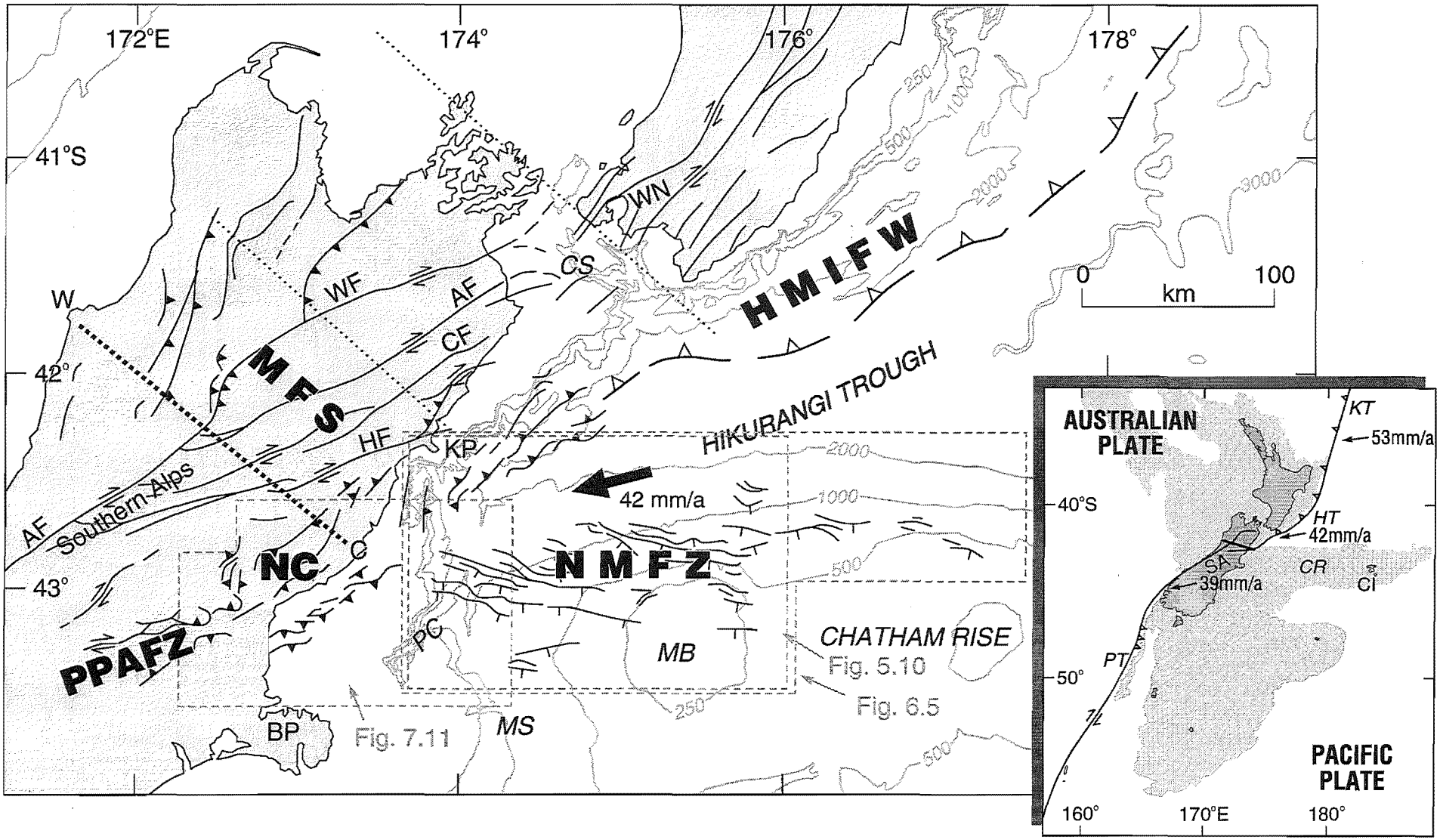
172°E
174°
176°
178°
41°S
42°
43°
W
WN
CS
WF
AF
CF
HF
MFS
HMIFW
HIKURANGI TROUGH
KP
42 mm/a
Southern Alps
AF
NC
C
NMFZ
PPAFZ
PC
MB
CHATHAM RISE
Fig. 5.10
Fig. 6.5
BP
Fig. 7.11
MS
2000
1000
500
250
0
km
100
AUSTRALIAN PLATE
PACIFIC PLATE
KT
53mm/a
HT
42mm/a
SA
39mm/a
CR
CI
PT
40°S
50°
160°
170°E
180°

(Figs. 8.2B and 8.3) (Walcott, 1987). This rotation occurred in response to a change in the relative plate motion between the Pacific and Australian plates and back-arc spreading in northern New Zealand. Lamb (1988) estimated from a 4 Ma plate reconstruction (Fig. 8.2B) that the thrust- faulted deformation front above the Hikurangi subduction zone has rotated c. 20° clockwise relative to the Pacific Plate since 4 Ma (compare Figs 8.2B and 8.3). The rotation of the subduction front during the late Cenozoic was accompanied by southeastward propagation of transpressive deformation in northern South Island (e.g., Scholz *et al.*, 1973; Campbell, 1991). This coincided with an increasing dip-slip component on the Alpine Fault, resulting in about 70 km of shortening normal to the fault and rapid uplift of the Southern Alps (Walcott, 1978; Kamp *et al.*, 1989; Norris *et al.*, 1990). The thrust faulting and tectonic uplift that dominated the structural style in central and coastal Marlborough during the Early Miocene (Prebble, 1980; Waters, 1988; Rait *et al.*, 1991) was overprinted by strike-slip displacement on the Clarence Fault, commencing in the Late Miocene (since 5–8 Ma; Browne, 1992). The Hope Fault is now the most active strike-slip structure and most Cenozoic deformation in north Canterbury, both onshore and offshore, is Pleistocene in age (Nicol, 1991; Campbell, 1991; Cowan, 1992; Chapter 7, this study). Considering that (1) the total strike-slip displacement on the Hope Fault is c. 19 km (Freund, 1971), and (2) typical late Quaternary rates of right-lateral slip on the fault are c. 15–30 mm/yr (Cowan, 1990; Van Dissen, 1991; Van Dissen and Yeats, 1991; Kneupfer, 1992); and allowing for slower rates of slip near the time of inception of the fault, the Hope Fault is unlikely to have been accommodating right-lateral displacement for more than 2 Ma (and probably < 1 Ma). About 60 km further south, strike-slip deformation in the Porter's Pass-Amberley Fault Zone and thrust faulting in Pegasus Bay began < 1 million years ago and possibly < 0.5 Ma (Cowan, 1992; Chapter 7, this study).

Renewed normal faulting commenced in the NMFZ at about 8–6 Ma, when most of the strike-slip displacement in northern South Island was being accommodated on the Wairau, Awatere and Clarence faults (see Fig. 8.3). The renewed normal faulting and widespread development of the NMFZ during Late Miocene-Late Pliocene times appears to be related to the encroachment of the incoming Chatham Rise against the evolving, transpressive plate-boundary zone. If the present day location of the southern limit of deep seismic activity (oceanic subduction) beneath northern South Island (the bold dotted line between Westport and Cheviot on Fig. 8.3) is translated obliquely back up the subducted slab interface at the present rate of relative plate motion (De Mets *et al.*, 1990), then at 8–6 Ma the position of this part of the slab was approximately beneath the present location of southern North Island (Fig. 8.2A). The same part of the subducted slab had moved to a position beneath the present northern coast of the South Island at about 4 Ma (Fig. 8.2B). By analogy, the crustal rocks overlying the slab, which now form central and coastal Marlborough, reached

their present location by southwestward translation and rotation on the right-lateral, strike-slip faults (Lamb, 1988; Lamb and Bibby, 1989).

The NMFZ continued to evolve during the Quaternary, contemporaneously with the rest of the plate-boundary zone. Shortening within the imbricate frontal wedge of the southern Hikurangi margin, beneath the Marlborough continental slope, has migrated southward and is now starting to impinge on the northwestern corner of the NMFZ. This is expressed as seaward-verging thrust faults and folds that overprint Pliocene-age normal faults at the southern end of the Hikurangi Trough (Fig. 6.2, profiles 2–2' and 3–3'; Fig. 6.5; Fig. 7.3, profile 1). The thrust faults do not reactivate the normal faults because of their unfavourable, NW-dipping geometry; the two fault systems differ in strike by 60–70° (Figs 6.5 and 8.3). In response to Quaternary overprinting and structural inversion of the northwestern corner of the NMFZ, the zone of active normal faulting at the western end of the NMFZ now crosses the submarine canyons about 15–20 km south of the subduction front. During the same time interval, thrust faulting and folding commenced beneath the north Canterbury shelf. Sections 8.3 to 8.5 discuss possible kinematic models for the extensional deformation in the NMFZ and the thrust faulting beneath the north Canterbury shelf.

8.3 LATE CENOZOIC TECTONIC EXTENSION OF THE NORTHWESTERN CHATHAM RISE

The general pattern of late Cenozoic deformation in the NMFZ, of disseminated, overlapping, sub-parallel normal faults typically 2–5 km apart and mostly dipping in one direction is consistent with observations from many active continental normal fault systems (e.g., Jackson and White, 1989) and with extensional deformation styles produced in scaled model experiments (McClay, 1990). As discussed in Section 8.2, there appears to be a genetic relationship between the evolution of the plate-boundary zone in northern South Island and the NMFZ since renewed normal faulting began in the NW Chatham Rise in the Late Miocene. The uncertainty in present fault kinematics makes it difficult to identify the cause (dynamics) of the extension of the NW Chatham Rise. The small amount of Late Pliocene-Recent extension (< 2%) and the position of the NMFZ on the Pacific edge of the plate-boundary zone (Fig. 8.3) suggest that it does not play a major role in directly transferring relative plate motion from the Hikurangi subduction zone to the Alpine Fault system. Herzer and Wood (1988) considered that the normal faulting may be related to doming and uplift of Mernoo Bank arising from the impact of the Chatham Rise against the plate boundary. Alternatively, Lewis *et al.* (1986) suggested the faulting might reflect the extensional component of regional strain resulting from a right-

lateral simple-shear couple across the plate boundary in northern South Island (Fig. 1.2). However, the model they presented is somewhat oversimplified, considering the relative positions of the NMFZ and the subduction zone, and it relies on the strain field predicted by clay models of strike-slip fault zones. Two other mechanisms for producing the extension are considered below: (1) lateral buckling of the crust at the southeastern edge of the Marlborough transpressional zone; and (2) flexure of continental crust at the outer edge of the subduction zone (Fig. 8.4).

8.3.1 LATERAL BUCKLING MODEL

Anderson *et al.* (in press) have proposed that a small amount of lateral-buckling of northern Canterbury and southern Marlborough may be responsible for the extension on the NW Chatham Rise. Their tentative model (Fig. 8.4A and B) is based on an adaptation of the McKenzie and Jackson (1986) model of normal faulting in other deforming zones (Fig. 6.8) and on a simplified model for extension of central Greece and the western Aegean Sea (Taymaz *et al.*, 1991). There is a change in the average trend of the strike-slip faults in Marlborough from c. 070° in the southwest to c. 055° in the northeast (Fig. 8.3). Because of the their orientation, with respect to the direction of relative plate motion (075°), in the northeast the strike-slip faults are undergoing oblique convergence, whereas the displacement in southwest is closer pure strike-slip (e.g., Lamb, 1988; Cowan, 1990; Van Dissen and Yeats, 1991; Anderson *et al.*, in press). Anderson *et al.* propose that a small amount of buckling of the upper crust is occurring where the Marlborough faults change strike. The buckling, resulting from movement of the Chatham Rise (Pacific Plate) past Marlborough and towards the Australian Plate, would result in left-lateral oblique-slip normal faulting and accompanying clockwise rotation of the fault-bounded blocks within the NMFZ (Fig. 8.4B). This tentative model is corroborated by the focal mechanism of the 1965 earthquake at the western end of the zone, which presumably is representative of the upper crustal normal faulting, since the earthquake is of moderately large magnitude and the faults are parallel to one of the nodal planes (Fig. 6.5). The model, therefore, provides a mechanism for producing left-lateral slip on the normal faults in the NMFZ and implies that N–S to NNE–SSW overall extension of the zone will result in slivers of crust being peeled off and rotated clockwise as the Chatham Rise plateau slides past southern Marlborough towards the Southern Alps collision zone (compare Figs 6.8 and 8.4B). Furthermore, the model predicts that extension in the NMFZ should be greatest at the western end of the zone, which it appears to have been over the last few million years, albeit the amount of extension and differences in extension throughout the zone are extremely small.

Fig. 8.4. Two possible models for the causes of extensional faulting in the NMFZ. (**A**) and (**B**) represent lateral-buckling of the upper crust in northern Canterbury-southern Marlborough and NW Chatham Rise (modified from Anderson *et al.*, in press). As the rise slides past the transpressional, Marlborough fault system towards the southern Alps, fault-bounded slivers of the northwestern corner of the Chatham Rise are peeled off and rotated clockwise (see text for explanation). The pinned slats in B are not intended to represent linked faults in a true scaled model. Instead, the simple model illustrates how left-lateral oblique-slip normal faulting and clockwise rotation of the fault bounded blocks may be accommodating NNE–SSW extension in the NMFZ, with extension increasing to the west of the zone, closest to the plate boundary. SWM, southwest Marlborough. **C.** Block diagram of the Hikurangi subduction-to-Alpine Fault transition viewed obliquely down the direction of relative plate motion (large black arrow). In this model, the extension in the NMFZ (large white arrows) is inferred to be left-lateral (NW–SE), parallel to the direction of down-dip tension (T) in the subducted oceanic slab. The NMFZ represents the upper crustal expression of flexural extension of the continental Pacific Plate where the NW Chatham Rise is bent downward into the southern end of the subduction zone. The geometry of the subducted oceanic slab and tension axes are from the micro-earthquake data of Robinson (1986, 1991); the southern extent of oceanic subduction (dotted) lines up closely with the onshore projection of the northern edge of the Chatham Rise.

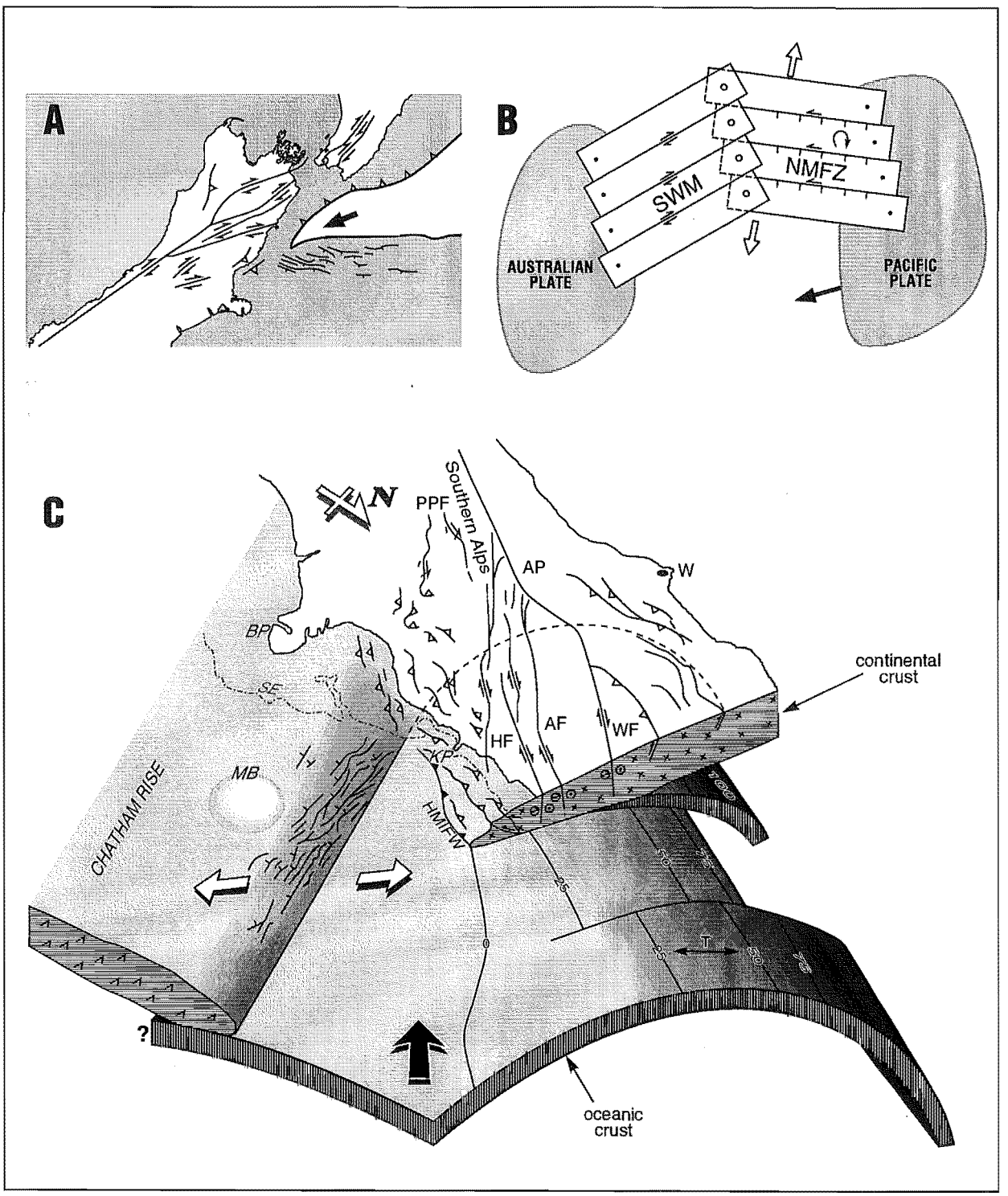
A
B
NMFZ
SWM
AUSTRALIAN PLATE
PACIFIC PLATE
C
N
PPF
Southern Alps
AP
W
BP
SF
MB
CHATHAM RISE
HF
AF
WF
HMTFW
continental crust
oceanic crust
?
T

Despite the mechanics of the simplified slat model (Fig. 8.4B), the faults of the NMFZ do not link directly with the strike-slip faults on land in Marlborough, although they may be accommodating a minute component of the total dextral shear across the plate boundary, that has not been absorbed by the imbricate frontal wedge beneath the Marlborough slope (Lewis *et al.*, 1986; Van Dissen and Yeats, 1991; Lewis and Pettinga, in press), by oblique-slip on the Alpine Fault (Norris *et al.*, 1990), or transferred across Cook Strait to the southern North Island shear belt (Carter *et al.*, 1989) (Fig. 8.4A). Accommodation of a minute component of the dextral shear across the plate boundary by the NMFZ requires a component of strain to be transferred from the deforming crust over-riding the subducting slab (Marlborough), across the subduction interface to the continental Pacific Plate on the outer, southern edge of the subduction zone (western Chatham Rise). In the long term this seems incompatible with the large finite slip (> 200 km) that has occurred on the subduction zone beneath northern South Island during the last 8–6 Ma, which implies long-term decoupling of the NW Chatham Rise from Marlborough. However, in the short term, stress could be transferred across the subduction decollement beneath Marlborough during periods of time when it is locked. For example, geodetic and seismological data suggest that a large part of the subduction interface beneath the southern North Island and northern South Island regions is presently locked or very strongly coupled, resulting in large elastic strains in the overlying plate (Walcott, 1984a; Robinson, 1986). In fact, considering the thickness of the oceanic slab (c. 15 km beneath northern South Island and Cook Strait) and the buoyancy of the thick, continental Chatham Rise (c. 27 km thick; Reyners and Cowan, in press), one could argue that the subduction interface at the southern end of the Hikurangi margin would be locked for most of the time and only unlocked during the instant of large subduction earthquakes. Walcott (1987) considered that slip on the Hikurangi subduction zone diminishes to almost zero at it southern apex in the Kaikoura region.

8.3.2 FLEXURAL EXTENSION MODEL

An alternative model for extension in the NMFZ involves the edge of the continental Chatham Rise is being dragged downward into the southern end of the subduction zone along with the adjacent oceanic slab to the north (Lewis *et al.*, 1986). Extension resulting from the bending of a lithospheric plate, is referred to as flexural extension (Bradley and Kidd, 1991). Such extension may occur in collisional foreland basins or at subduction zones and differs from rifting in that it requires simultaneous extension (at the top) and contraction (at the base) of the lithosphere. The distribution of earthquakes beneath the Hikurangi margin defines the broad geometry of the subducting Pacific Plate, oceanic slab (e.g., Reyners, 1983; Robinson, 1991). The anomalously thick oceanic slab has several NW-SE oriented, down-dip 'tears' in it

(Figs 8.3 and 8.4C) (Robinson, 1986, 1991). Composite focal mechanisms of earthquakes within the upper part of the slab, have NW–SE orientated T-axes indicative of down-dip tension resulting from slab pull. The orientations of the tears and tension axes within the slab differ significantly from the direction of motion of the Pacific Plate. Continental extension of the NW Chatham Rise in a NW–SE direction, down the dip of the subducted slab and as a result of the weight of the subducted oceanic slab, could be accommodated on the unfavourably orientated, east-west trending normal faults in the NMFZ if the faults moved with left-lateral oblique slip (Fig. 8.4C). In contrast to the lateral-buckling model this would imply an overall component of left-lateral shear, not right-lateral shear, to be distributed across the extensional province and clockwise rotations of the fault bounded blocks would not be necessary (cf. Figs 6.8, 8.4A, 8.4B).

8.4 LATE CENOZOIC TECTONIC DEFORMATION OF NORTH CANTERBURY

8.4.1 REVIEW OF STRUCTURAL STYLES

Late Cenozoic (mostly Pleistocene) deformation throughout much of onshore north Canterbury is characterised by NE-trending, basement-cored hills and ranges, that are bounded locally by range-front thrust faults with structural relief typically of 1–3 km (Fig. 7.11) (Nicol, 1991; Mould, 1992). Range crests coincide closely with anticlinal axial traces and there is a close relationship between many of the range-bounding thrust faults and the folds. The folds deform both the cover sequence and the exposed basement rocks, and they represents a significant component of the total contractional strain imposed on the cover sequence and the upper few kilometres of basement by thrust faults in the upper crust. Shallow basins, underlain by Late Cretaceous and Cenozoic sedimentary strata, lie between the uplifted ranges. The largest are the Culverden and Cheviot basins, which at 40–60 km long and 10–15 km wide, have remarkably similar geometry to the offshore Conway Trough (Fig. 7.11). Between Mount Grey and Cheviot, the majority of the thrust faults are directed towards the northwest, whereas north of Cheviot and the Culverden Basin thrust faults are directed predominantly E–SE (Fig. 7.11 — top left diagram) (Nicol, 1991). This change in thrust vergence suggests the presence of one or more major, NW–SE oriented transfer structures in the upper crust in this region. From a 73 km-long, NW–SE cross-section between the coast and the foothills of the Southern Alps, Nicol estimated that north Canterbury has shortened by at least 15% (c. 11 km), mostly since the Early Pleistocene. This implies shortening at a rate of at least 6 ± 2 mm/yr. Furthermore, he showed that in both north Canterbury and Marlborough there is consistency between the NW–SE direction (c. 105–110°) of principal horizontal

compression and shortening determined by fault motion analyses and stylolites (e.g., Berryman, 1979; Nicol and Campbell, 1990; Nicol, 1991; Nicol and Wise, 1992), and by analysis of geodetic triangulation networks (e.g., Walcott, 1978; Bibby, 1981; Reilly, 1990) and earthquake focal mechanisms (e.g., Arabasz and Robinson, 1976; Walcott, 1978; Cowan, 1992) (Fig. 8.3 — bottom right).

Southwest of the Culverden Basin and west of Mount Grey (Fig. 7.11), the Porter's Pass-Amberley Fault Zone is characterised by a hybrid system of NE-trending, right-lateral strike-slip faults that splay upward into thrust faults in the eastern part of the zone (Cowan, 1992). This fault system is about 60 km south of the Hope Fault in Marlborough and represents the southernmost, major strike-slip element in northern South Island (Fig. 8.3). Focal mechanisms of microearthquakes west of Amberley and 7–10 km deep, including events beneath the Cust and Kowai anticlines (Fig. 7.11), are predominantly strike-slip (Cowan, 1992; Reyners and Cowan, in press). These observations led Cowan to argue that the thrust faults exposed in the eastern part of the Porter's Pass-Amberley Fault Zone (beneath Mounts Grey and Thomas, and beneath the the Cust and Kowai anticlines; Fig. 7.11) are convex-upward splays of a young and still developing zone of upper crustal transpression. The strike-slip surface displacements in the west of the zone (Berryman, 1979; Coyle, 1988) (Fig. 8.3 — top left) were interpreted by Cowan to reflect deeper structural levels of the strike-slip system, now exposed by greater tectonic uplift.

Cowan's (1992) data is new and significant, but the model of an evolving zone of transpression beneath the north Canterbury range front is not. Although significantly different in details both the previous models of Carter and Carter (1982) and Herzer and Bradshaw (1985) invoke an incipient zone of dextral shear extending beneath the north Canterbury range front and the Motunau coastal zone (Fig. 7.2). Sigmoidal, double-plunging folds in the Motunau coastal hills have been interpreted as classical wrench folds developing in the cover sequence in response to deeper-seated strike-slip faulting in the basement rocks (Yousif, 1987; Barrell, 1989; Campbell, 1991; Campbell and Nicol, 1992). In such models, fold hinges nucleate obliquely (c. 45°) to the orientation of the simple shear couple, parallel to the direction of maximum incremental extension (e.g., Wilcox *et al.*, 1973; Harding, 1976; Little, 1992). As simple shear deformation progresses and the folds develop contemporaneously with the strike-slip faults, the folds tighten, their axial surfaces rotate towards parallelism with the strike-slip faults, and the folds propagate longitudinally. Thrust faults that displace the northwestern limbs of several of the coastal folds (Fig. 7.11) were considered by Yousif (1987), Campbell (1991) and Campbell and Nicol, (1992) to be shallow, secondary structures accommodating a component of the NW-SE shortening that results from a NE–SW right-lateral simple-shear couple (see strain ellipse on Fig. 1.2).

The most detailed structural studies undertaken in the Motunau coastal hills and marine terraces (Barrell, 1989) show, in fact, that deformation is very complex, with imbricated thrust sheets and oblique-slip tear faults developed in the sedimentary cover sequence. Although Barrell considered that major episodes of NW–SE thrusting occurred in the Late Oligocene and Late Miocene, and that the major folds that now control the geomorphology of the coastal landscape (e.g., Yousif, 1987; Campbell and Nicol, 1992) are younger than Late Miocene, more recent interpretations suggests that most of the deformation in the region is < 1 million years old (Cowan, 1992). Barrell (1989) noted that by extrapolating the late Quaternary rates of coastal uplift and tilting back in time, the regional dips of the late Cenozoic strata on the flanks of major coastal folds could have been produced since c. 0.5 Ma.

The mapping undertaken in this thesis, of structures beneath the continental shelf, indicates that the deforming region in north Canterbury extends offshore for 20 km. A zone of NE-trending growth folds in the Pleistocene succession extends from central Pegasus Bay to the Conway Trough. Eleven major structures are recognised, including the Pegasus Bay Fault, 20 km from Christchurch, and fold J^c, which underlies the Conway Ridge (Fig. 7.11). All of the major folds, which range in length from 10–35 km, are asymmetric, landward verging structures that are interpreted here (Chapter 7) to be propagating above the tips of southeast-dipping thrust faults. Deformation of the Late Pliocene-Early Pleistocene seismic unit 12c beneath the inner shelf between Motunau and Point Gibson (Fig. 7.11) appears to be widespread and complex. Some of the major folds have deformed the Holocene seabed, implying rupture of the underlying thrust faults within the last 6500 years. Slow dip-slip rates of displacement of < 0.3 mm/yr are inferred by: (1) folding of Late Pleistocene unconformities; (2) the middle-Late Pleistocene displacement of middle Cenozoic strata by the Pegasus Bay Fault; and (3) possibly by the apparent structural elevation of the Conway Ridge above the floor of the Conway Trough. Although the Conway Trough is partly an erosional feature, it is inferred here to be structurally analogous to the thrust fault-fold Cheviot and Culverden basins (Nicol, 1991) onshore.

8.4.2 REGIONAL TECTONIC MODELS OF NORTH CANTERBURY

Any tectonic model of north Canterbury must account for the above observations and interpretations of the shallow structural styles in the region. The model must also account for the vertical partitioning of seismicity. Microearthquake data indicates that beneath north Canterbury there is a sub-horizontal upper crustal (< 12 km) seismic zone, a mid crustal aseismic (ductile) zone between 12 and 17 km depth and a lower crustal seismic zone below 17 km depth (Cowan, 1992; Reyners and Cowan, in press). The lower crustal seismic zone broadens vertically to the north and

northwest to a depth of c. 40 km, with a bottom edge dipping at 15° towards the northwest. This lower horizon is interpreted by Reyners and Cowan to be continental crust representing the southernmost part of the underthrust Pacific Plate beneath the northern South Island (Fig. 8.4C) (cf. Robinson, 1991). The lower crust must be contiguous with the lower crust of the adjacent NW Chatham Rise, beneath the NMFZ, which is still on the Pacific edge of the subduction zone. Differences in focal mechanisms and the trend of strain axes for microearthquake events above and below the mid crustal aseismic zone and north of the Porter's Pass-Amberley Fault Zone were interpreted by Cowan (1992) as evidence for decoupling of the upper and lower crust beneath north Canterbury. The structures mapped at the surface in north Canterbury and imaged in the shallow seismic reflection profiles offshore, are, therefore, inferred to be accommodating strain accumulating in the upper crust (< 12 km), which is detached from the underlying, southeastern edge of the subducted slab (Cowan, 1992; Reyners and Cowan, in press).

Although deformation beneath much of north Canterbury, including the continental shelf, appears to be dominated by thrust faulting and folding, strike-slip faulting is clearly taking place in the Porter's Pass-Amberley Fault Zone (Figs 7.11 and 8.3). How these two contrasting styles of upper crustal deformation interact kinematically is uncertain. No upper crustal microearthquakes were recorded east and north of Amberley during the 10-week survey by Cowan (1992) and despite several moderately large-magnitude historical events in this region there is no historical seismicity data that helps to constrain the kinematics of deformation there. The strike-slip displacement in the Porter's Pass-Amberley Fault Zone must either continue beneath the coastal hills towards the Hikurangi Trough, or it must be absorbed into other structures. If significant strike-slip faulting continues eastward of Mount Grey beneath the coast (Fig. 7.11), there are two possibilities: (1) the strike-slip displacement is pervasive across a very wide zone beneath the north Canterbury plains, range-front and coastal hills, and the structures at the surface are developing in response to this underlying dextral shear (Herzer and Bradshaw, 1985; Cowan, 1992); or (2) the easternmost strike-slip faulting is localised beneath folds in the Amberley to Motunau coastal region (Yousif, 1987; Barrell, 1989; Campbell, 1991; Campbell and Nicol, 1992; Cowan, 1992) and the major thrust faults beneath the flanks of the Culverden Basin and beneath the continental shelf (e.g., Pegasus Bay Fault), which lie up to 30 km from the axis of the coastal hills, are accommodating shortening outside of this strike-slip zone. The latter scenario (2) would imply a partitioning of strain into a strike-slip component which terminates downward into the brittle-ductile transition and is subparallel to the direction of relative plate motion, and a normal component of strain that is manifest as folds and thrusts which trend subparallel to the strike-slip zone and root in sub-horizontal detachments in the upper crust (Fig. 8.5A) (e.g., Namson and Davis, 1988). In such a laterally-

Fig. 8.5. Schematic block diagrams of two alternative upper crustal tectonic models for the north Canterbury coastal region. **A.** Strain is partitioned into two zones of NW-verging thrust faults lying to the northwest and southeast of a zone of strike-slip deformation that is localised beneath the Motunau coastal folds. The thrust faults beneath the continental shelf and the flanks of the Culverden Basin flatten out onto an upper crustal detachment (or more than one). The lower part of the upper crust, beneath the detachment, must be shortened by some other mechanism to balance the model. Folds and faults developed in the sedimentary cover sequence in the Motunau coastal region are secondary wrench structures lying above the zone of dextral shear. The diagram is based on section A–B (see location on Fig. 7.11). **B.** The entire north Canterbury region between the Hope Fault and the outer, southeastern edge of deformation beneath the continental shelf is shortening by a thin-skinned style of fold and thrust tectonics (modified from Nicol, 1991). Based on the transect C–D–E (see Fig. 7.11 for location), the thrust faults verge to the northwest and flatten out onto one or more upper crustal detachment faults. In both models the brittle-ductile transition lies at about 12 km depth (Cowan 1992; Reyners and Cowan, in press).

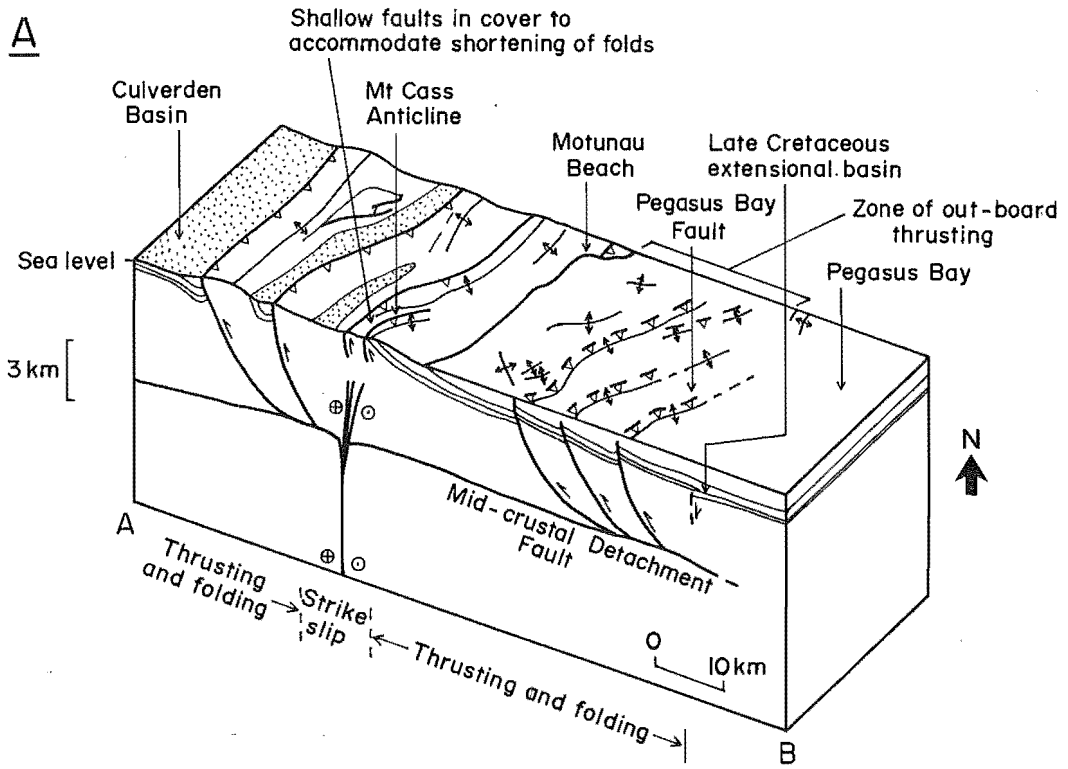
A
Shallow faults in cover to accommodate shortening of folds
Culverden Basin
Mt Cass Anticline
Motunau Beach
Late Cretaceous extensional basin
Pegasus Bay Fault
Zone of out-board thrusting
Pegasus Bay
Sea level
3 km
N
Mid-crustal Detachment Fault
A
Thrusting and folding
Strike slip
Thrusting and folding
0
10km
B

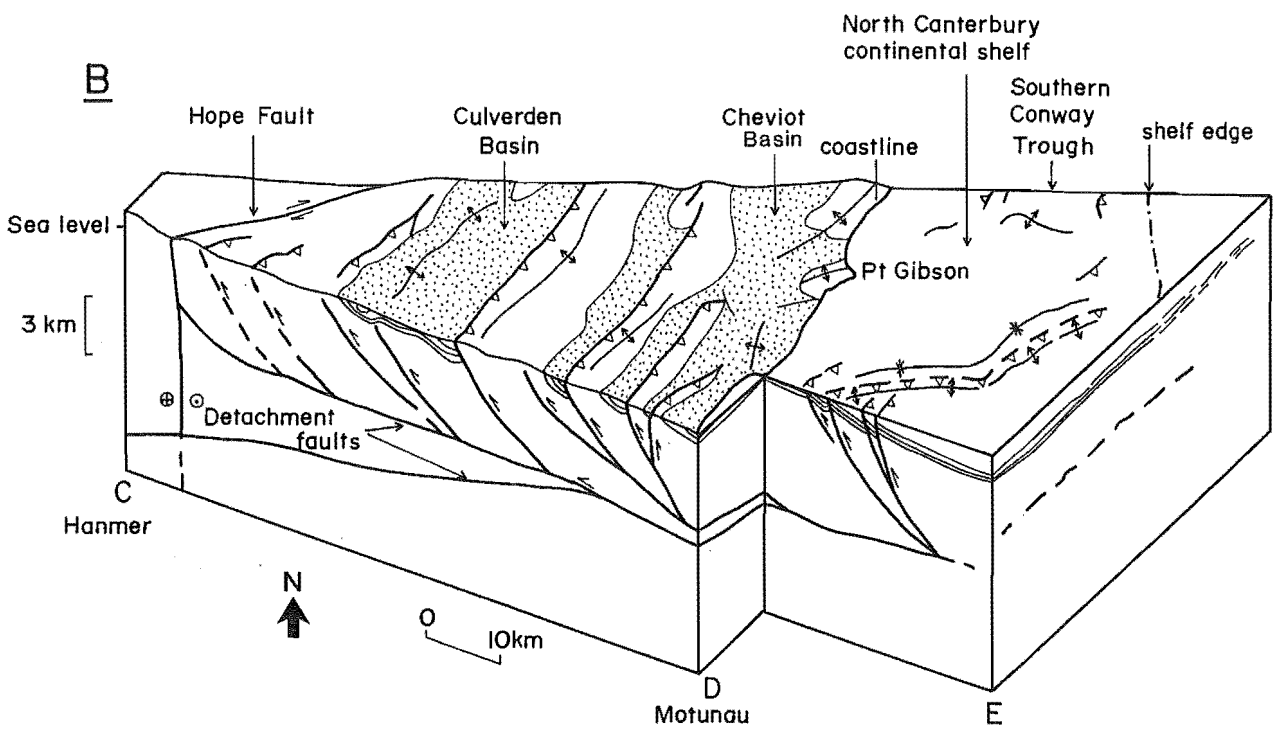
B
North Canterbury continental shelf
Southern Conway Trough
shelf edge
Hope Fault
Culverden Basin
Cheviot Basin
coastline
Sea level
3 km
Pt Gibson
Detachment faults
C
Hanmer
N
0
10km
D
Motunau
E

partitioned model, shortening beneath the brittle-ductile transition (c. 12 km) can be accommodated by mid-crustal ductile flow and by oblique underthrusting of the lower continental crust (> 17 km depth) beneath the Southern Alps (Reyners and Cowan, in press). However, if the thrust faults out-board of the strike-slip zone (e.g., Pegasus Bay Fault) root in sub-horizontal detachments in the upper crust, well above the brittle-ductile transition (Fig. 8.5A) (Nicol, 1991), then the laterally-sheared lower part of the upper crust (c. 8–12 km depth) beneath such detachment thrusts must also be shortened an equal amount by some unknown mechanism.

An alternative interpretation to the above model involving dextral shear in the basement beneath the north Canterbury coast is that the Porter's Pass-Amberley Fault Zone represents a separate upper crustal tectonic province to the coastal north Canterbury region, which is being mainly shortened by thrust faulting and folding. In this model, most of the right-lateral displacement within the Porter's Pass-Amberley Fault Zone is absorbed west of Amberley, by major, north-trending thrust faults and tight folds in the southwest corner of the Culverden Basin (e.g., Mt Arden thrust and MacDonald syncline) and by the hybrid system of oblique-slip, multi-directional thrust faults and folds in the Doctors Dome region (Fig. 7.11) (Nicol, 1991). Similar, northerly-trending transfer structures occur in coastal Marlborough and absorb a considerable component of the right-lateral motion on the Hope Fault (Fig. 7.11 — top left) (Van Dissen, 1991; Van Dissen and Yeats, 1991). The thrust faults and growing folds in the Motunau coastal region may, thus, be developing not above a deep seated zone of dextral shear, but as part of a northwest-verging fold and thrust zone that attains a combined width of about 60 km between the northwestern flank of the Culverden Basin and the southeastern edge of the deformation zone offshore (Figs 7.11 and 8.5B). This tectonic province contrasts with the Porter's Pass-Amberley Fault Zone and may involve a thin-skinned style of thrust tectonics with imbricated structures ramping upward from one or more sub-horizontal detachment surfaces in the upper crust (Nicol, 1991). Such detachments are common beneath fold and thrust belts elsewhere in the world and they commonly occur at multiple structural levels in association with thrust ramps, imbricates, fault-bend folds and fault-propagation folds (e.g., Boyer and Elliot, 1982; Yeats, 1983; Suppe, 1985; Jamison, 1987; Namson and Davis, 1988). If detachment faulting is occurring in the upper crust beneath north Canterbury at more than one structural level, then deformation is likely to be significantly more complex than what is expressed by the surface deformation and portrayed schematically in Figure 8.5B. Furthermore, the magnitude of total strain in the region is likely to be significantly greater than the 15% shortening estimated by Nicol (1991) from the structures exposed at the surface. For example, any estimates of shortening across the Motunau coastal area will be underestimated if measurements are based only on the major, geomorphologically-expressed structures (e.g., Yousif, 1987), and the imbricated thrust sheets mapped by Barrell (1989) are not reconstructed and balanced.

The local structural details obtained by Barrell (1989) from the Motunau coastal area suggest that more regional structural studies are required in the coastal zone to constrain the interactions between late Cenozoic growth folding and faulting. Furthermore, considerably improved earthquake data are required from north and east of Amberley, including offshore, to obtain focal mechanisms that would help to constrain the upper crustal fault kinematics. Although the sigmoidal axial traces and double-plunging hinges of the major folds in the Motunau coastal zone, together with their eastward alignment with the strike-slip Porter's Pass-Amberley Fault Zone have previously been cited as the key criteria for interpretation of these structures as wrench folds (e.g., Yousif, 1987; Campbell, 1991), the northwest-verging thrust faults that displace the western limbs of the folds are consistent with the style of NW–SE shortening throughout much of north Canterbury (Nicol, 1991). The double-plunging fold hinges may simply reflect the combined axial and upward propagation of the underlying thrust faults. Intuitively, I favour the second model discussed above, involving strike-slip deformation within the Porter's Pass-Amberley Fault Zone and predominantly fold and thrust faulting and NW-SE shortening beneath coastal north Canterbury, between the Culverden Basin and the southeastern edge of shelf deformation and between central Pegasus Bay and the Hope Fault (Figs 7.11 and 8.5B).

8.5 TECTONIC SYNTHESIS: PARTITIONED STRAIN WITHIN THE STRUCTURAL TRANSITION FROM HIKURANGI SUBDUCTION TO SOUTHERN ALPS COLLISION

In central New Zealand the Pacific and Australian plates are converging at about 42 mm/yr on an azimuth of 075° (De Mets *et al.,* 1990), whereas the orientation of the plate boundary zone in this region is c. 55 ± 5° (Fig. 8.3). In southern North Island the oblique plate convergence is accommodated by oblique subduction of anomalously thick (c. 11–15 km) Pacific Plate oceanic crust (Reyners, 1983, 1989; Robinson, 1986), and by dextral shear and shortening in the over-riding continental crust (e.g., Walcott, 1978; Smith *et al.,* 1989). In the South Island region, the c. 27 km-thick continental crust of the Chatham Rise is too buoyant for normal subduction to occur (Walcott, 1978; Anderson *et al.* in press; Reyners and Cowan, in press). This results in relative plate motion being transferred from the Hikurangi subduction margin to the Southern Alps continental collision zone, in which the major surface structure is the right-lateral, oblique-slip Alpine Fault (Norris *et al.*, 1990).

The crustal structure and kinematics within this mega-transfer zone in northern South Island are complex and strain is partitioned both vertically and laterally. The southern extent of deep (> 100 km) seismic activity within the subducted Pacific

Plate occurs along a line coinciding approximately with the onshore projection of the northern margin of the Chatham Rise (Robinson, 1991), the northwestern corner of which is extending by normal faulting at the edge of the subduction zone (Fig. 8.4C). South of this line, beneath north Canterbury, the underthrust slab is expressed by the lower seismicity zone (> 17 km depth) which dips gently to the northwest (Cowan *et al.*, 1991; Cowan, 1992). The line of southernmost deep seismic activity, therefore, appears to represent the change from oblique oceanic subduction beneath Marlborough to oblique continental collision.

Strain in the upper crust of northern South Island is partitioned laterally, into distinct tectonic provinces with contrasting styles and kinematics of deformation (Fig. 8.3) (e.g., Anderson *et al.*, in press). Late Quaternary fault-slip rates and geodetic shear strains indicate that the strike-slip Marlborough fault system and the Porter's Pass-Amberley Fault Zone together account for most of the slip predicted from the vector of relative plate motion (Bibby, 1981; Lamb, 1988; Campbell, 1991; Van Dissen, 1991; Van Dissen and Yeats, 1991; Knuepfer, 1992; Cowan, 1992). Focal mechanisms indicate that fault slip vectors are close to the predicted, Nuvel-1 plate motion vector (De Mets *et al.*, 1990) for strike-slip events in Marlborough and north Canterbury, and oblique for thrust events in northwestern South Island (northwest Nelson) and in north Canterbury (Arabasz and Robinson, 1976; Walcott, 1978; Cowan, 1992; Anderson *et al.*, in press). Although there are considerable local variations in the direction of principal compressive stress determined from fault motion data and stylolite analysis in parts of north Canterbury (Nicol, 1992), the combined geological, geodetic and seismological data indicate that in both the short (c. 10^2 yr) and long (c. 10^6 yr) term, the average azimuth of principal shortening across the plate-boundary zone in northern South Island is NW–SE, which is oblique to the relative plate motion direction and at a high angle to the major strike-slip faults (Fig. 8.3 — bottom right) (Walcott, 1978, 1984; Berryman, 1979; Reilly, 1990; Nicol and Wise, 1992; Anderson *et al.*, in press; Pettinga and Wise, in press). A similar relationship occurs in the San Andreas fault system in California (Zoback and Zoback, 1980; Mount and Suppe, 1987, 1992), although in that setting much of the plate motion is sub-parallel to the San Andreas Fault, not oblique to the faults as it is in northern South Island. Considering that the average orientation of the plate boundary in northern South Island is c. 055° and the Nuvel-1 relative plate motion vector is 42 mm/yr at an azimuth of about 075° (De Mets *et al.*, 1990), then c. 14 mm/yr of shortening normal to the plate boundary is required because of the obliquity of convergence. [Note that Nicol's (1992) calculation of 27 mm/yr for this shortening was based on the Chase (1978) vector of relative plate motion.] Nicol's estimate of 6 mm/yr shortening in the north Canterbury region since the Early Pleistocene, therefore, represents about 40% of the required total shortening across the northern South Island. This value of 40% is unlikely to be significantly increased by the new thrust

faults mapped beneath the continental shelf as part of this study, because these structures probably have accommodated only a very small amount of strain, at the very edge of the plate-boundary zone. However, as discussed in section 8.4.2, Nicol's estimate of shortening in north Canterbury could be underestimated if multiple upper crustal detachment faults are present beneath this region. The remainder of the required NW–SE shortening normal to the plate boundary must be accommodated by thrusting on the Alpine Fault, by oblique-slip faulting in northeastern Marlborough, and folding and thrust faulting in northwestern South Island (northwest Nelson) (Fig. 8.3) (Berryman, 1980; Bishop, 1992b; Anderson *et al.*, in press; Pettinga and Wise, in press).

In the North Island of New Zealand and at several other obliquely convergent plate boundaries around the Pacific rim, strain is partitioned into an axial zone of strike-slip faulting and a frontal zone of folding and thrusting, (e.g., Walcott, 1978; Melhuish, 1990; Cashman *et al.*, 1992; Ryan and Coleman, 1992). In contrast, the partitioning of strain across northern South Island appears to be more complex in a vertical and lateral sense, and it has evolved both spatially and temporally (Anderson *et al.*, in press; Pettinga and Wise, in press). Seismicity and geological data are consistent with a speculative model of continental collision involving: (1) vertical partitioning of strain by a mid-crustal ductile layer and crustal detachments beneath north Canterbury (Nicol, 1991; Nicol *et al.*, 1991; Cowan, 1992; Cowan and Reyners, in press) and possibly Marlborough (Nicol and Wise, 1992; Pettinga and Wise, in press); (2) southwestward telescoping of the mid-upper crust by the Alpine Fault, to produce the Southern Alps (e.g., Wellman, 1979; Sibson *et al.*, 1979; Kamp *et al.*, 1989; Norris *et al.*, 1990); and (3) oblique underthrusting of Pacific Plate lower continental crust beneath the Southern Alps (Wellman, 1979; Reyners, 1987; Reyners and Cowan, in press). Such detachment faulting within the mid-upper crust by a downward-flattening Alpine Fault and possibly other sub-horizontal structures beneath northern South Island may provide a means of partitioning deformation associated with the change from the east-dipping Alpine Fault to the west dipping subduction of the southern Hikurangi margin (Nicol and Wise, 1992; Pettinga and Wise, in press).

A surprising discovery made in this study of offshore data is the extraordinary tripartite arrangement of fault systems that merge to within 20 km of each other at the southern limit of oceanic subduction (Figs 8.3 and 8.4C). The three fault systems are distinct structural provinces that each play a different role in accommodating upper crustal strain within the Hikurangi margin to Alpine Fault transition. Two of the fault systems are shortening crust and the other is extending it. The east-verging thrust faults and folds beneath the Marlborough continental slope produce shortening within the southern part of the Hikurangi margin imbricate frontal wedge, above the southern part of oceanic subduction (Lewis *et al.*, 1986; Lewis and Pettinga, in

press). Furthermore, westward-dipping thrust faults off the Marlborough coast have been inferred to absorb some of the strike-slip displacement within the northeastern termination of the Hope Fault (Arabasz and Robinson, 1976; Lamb, 1988; Van Dissen, 1991; Van Dissen and Yeats, 1991). In contrast, SE-dipping thrust faults beneath the north Canterbury shelf and Conway Ridge are part of a fold and thrust belt, that is accommodating some of the NW-SE shortening normal to the plate boundary zone in northern South Island. If the inferred thrust faults beneath the north Canterbury shelf shallow out at depth into one or more upper crustal detachment faults, then the southeastern front of folding probably lies just inboard of the edge of crustal decoupling in the Pacific Plate (Fig. 8.5B), just as the Porter's Pass-Amberley Fault Zone is inferred to mark this feature onshore (Cowan, 1992).

It is considered to be very unlikely that either the Canterbury or offshore Marlborough fold and thrust belts are linked, in the sense of Gibbs (1990), to the normal faults within the NMFZ. That is, motion on one fault set is not linked kinematically to motion on the other set. Both the offshore Marlborough and north Canterbury thrust fault systems are developed in the upper crust above, and are detached from, the subducting slab, albeit the slab beneath Marlborough is oceanic (e.g., Robinson, 1986, 1991) and the slab underthrusting Canterbury is continental (Reyners and Cowan, in press). In contrast, the NMFZ is extending the upper crust on the Pacific edge of the subduction zone and is reflecting either: (1) flexural extension of the edge of the continental part of the slab as a result of it bending downwards into the subduction zone; or (2) exfoliation of crustal slivers as the rise moves past Marlborough towards the Southern Alps (Fig. 8.4) (Anderson *et al.*, in press). Whatever the kinematics of extension are in the NMFZ, the present east-west trend of the normal faults is strongly inherited from the basement fabric that was produced by a Mesozoic phase of imbricate-thrust tectonics and two older phases of normal faulting (Late Cretaceous and Eocene).

8.6 CONTINENTAL EXTENSION IN OTHER PARTS OF THE WORLD: ANY ANALOGUES TO THE NMFZ?

There are many different plate tectonic settings in other parts of the world where seismically active, continental, normal faulting is occurring today. Large regions of northeastern China, eastern Siberia, Mongolia and western Turkey are extending as a result of large-scale lateral movements of crust, resulting from Alpine-Himalayan collision-extrusion tectonics (e.g., Tapponnier and Molnar, 1979; McKenzie, 1978; Sengor, 1987). In some orogenic belts which have been overthickened by crustal underthrusting, for example, the Tibetan plateau (Molnar and Chen, 1982; Armijo *et al.*, 1986) and parts of the Peruvian-Andes (Cabrera *et al.*, 1991), normal faults

accommodate lateral crustal spreading and relaxation. Such faults may also occur in foreland regions in front of thrust belts (Hancock and Bevan, 1987).

Two highly seismic regions that are extending by normal faulting in complex subduction roll-back settings are the Basin and Range Province of the western USA and the Aegean region. The Basin and Range Province is a region of widespread continental extension that has received considerable attention focusing on seismotectonic hazard assessment and the development of fault segmentation models (e.g., de Polo *et al.*, 1991). This region lies between the San Andreas transpressive plate boundary and the cratonic interior of North America. Walcott (1993) showed that the considerable extension (> 200 km) that has occurred in the Basin and Range Province resulted from late Cenozoic stretching of continental lithosphere behind the anti-clockwise-rotating Juan de Fuca subduction zone and the northwestward migrating Sierra Nevada-Klamath crustal block. The Aegean region is extending between the Hellenic Trench, which is free to migrate southward, and Turkey, which is moving westward by major strike-slip faulting in response to continental collision of Arabia and Eurasia (Taymaz *et al.*, 1991).

In still other settings, extension and active normal faulting occur in arc regions in eastern Indonesia (Charlton, 1991) and southern Italy (Knott and Turco, 1991), and in back-arc regions such as northern North Island, New Zealand (Nairn and Beanland, 1989). Normal faults occur also in divergent plate boundaries such as in the Gulf of Suez and Red Sea (Jackson *et al.*, 1988), and in areas of intraplate rifting and crustal thinning like the East African Rift system (Shudofsky, 1985) and the complex Woodlark-D'Entrecasteau province near the Australia-Pacific plate-boundary zone northeast of Australia (Abers, 1991). Despite this vast range of plate tectonic settings in which regional scale, seismically active continental normal faulting is occurring, the following are seismotectonic features which are common to most systems (Jackson, 1987; Jackson and White, 1989): (1) The faults commonly occur in sets that bound tilted upper crustal blocks and they are not commonly continuous along strike for more than 25 km; (2) The faults commonly change strike and step over from one to the next in en echelon patterns, with segmentation lengths comparable to the thickness of the seismogenic layer; (3) Large seismically active normal faults appear to be approximately planar and to rotate 'domino-style' arrays of blocks about horizontal axes as they move; and (4) The majority of seismogenic faults dip in the range of 30–60° (Jackson, 1987) and dips of < 30° or > 70° are rare (e.g., Thatcher and Hill, 1991).

Irrespective of the kinematics of late Cenozoic extension of the NW Chatham Rise, the plate tectonic setting of the NMFZ is clear. The Chatham Rise continental plateau is too thick and buoyant for normal oceanic-type subduction to occur. The

western end of the rise, thus, constrains the southward termination of oblique oceanic subduction beneath the Hikurangi margin (e.g., Walcott, 1978; 1987; Lewis and Pettinga, in press; Reyners and Cowan, in press). The NMFZ lies at the outer edge of the transition zone from oceanic subduction to oblique continental collision. There are other locations in the southwest Pacific where oceanic subduction terminates at a thickened oceanic plateau and where plate motion is transferred to major zones of strike-slip faulting and collision. For example, the south Philippine Trench terminates at the intersection with the buoyant East Morotai Plateau and plate motion is transferred to a complex transpressional zone (Nichols *et al.*, 1990). The active tectonics in Taiwan also has similarities to New Zealand. Taiwan is formed by collision between the Luzon arc and sialic crust of the Asian continent and, like New Zealand, it links two opposite facing subduction zones which are marked by the Ryukyu and Manila trenches (Teng, 1990; Aubouin, 1990). An example of continental crust being extended as it enters a subduction zone occurs in the Timor Trough, where the Australian Plate is extending possibly by flexure, as a result of its northward subduction beneath the Banda Arc (e.g., Karig *et al.*, 1987). In contrast to the faults in the NMFZ, the normal faults on the outer slope of the Timor Trough displace a > 5 km thick shelf-slope sequence lying on cratonic basement and they trend roughly parallel to the subduction axis. Furthermore they are not located at a major structural transition in the plate-boundary zone. I have been unable to find reference to any area where continental crust is undergoing extension at the edge of a transition zone from oceanic subduction to continental collision. Thus, the tectonic setting of the North Mernoo Fault Zone is either unusual or similar features have yet to be recognised elsewhere.

8.7 COMMENTS ON FUTURE WORK

This thesis addresses many aspects of the sedimentology, paleoceanography, stratigraphy, structural evolution and late Cenozoic tectonics of the NW Chatham Rise and offshore north Canterbury regions. The results of the study significantly improve our geological understanding of this part of New Zealand and they also raise many new questions. There are several key areas of potential future research which could build on the results obtained in this thesis. The following such studies could be used to test models developed here, of the sedimentary and tectonic evolution of the region and of the active geological processes.

(1) Well positioned arrays of current meters and nephelometers in Mernoo Saddle and across the NW Chatham Rise slope would help constrain the present day physical oceanography and mid-bathyal sediment-water interactions. Such data might enable: (i) modeling of the bottom flow conditions during both interglacial

and glacial scenarios, and (ii) testing of the hypothesis developed here for a climatic control on the origin of the Plio-Pleistocene sedimentary units and erosion surfaces beneath the NW Chatham Rise slope.

(2) Basin analysis of the southern Hikurangi Trough would: (i) establish the relationships between the late Cenozoic evolution of the channel-levee turbidite system in the trough and the sediment drifts and current-controlled hemipelagic sedimentation on the adjacent NW Chatham Rise slope; and (ii) help constrain the timing of significant uplift and erosion of the Southern Alps.

(3) Acquisition of an improved, very high-resolution stratigraphy beneath the NW Chatham Rise slope could be used to test the hypothesis developed here for a climatic control on the bottom current system, on periods of seafloor erosion, sediment drift development and current-influenced hemipelagic sedimentation. The necessary stratigraphic resolution might only be achieved by detailed sedimentological, biostratigraphic and isotopic analysis of one or more well positioned deep-sea drilling cores.

(4) Swath side-scan sonar and bathymetric surveys could be used to test and refine the broad structural geometry of the middle slope part of the North Mernoo Fault Zone, where many faults have a surface expression. Resolution of < 5 m would be required to effectively image most surface traces. In addition, more closely spaced, intersecting seismic-reflection profiles in places could test the present inter-profile correlations.

(5) Further analysis of the existing seismic-reflection data on the north Canterbury shelf is necessary to interpret the seismic units established here in terms of the Vail/Exxon sequence stratigraphic model. This work is planned as part of on-going research at New Zealand Oceanographic Institute. If sea-level-cycle sequences can be established and if glacio-eustacy is assumed to be the dominant control on the cyclicity, then correlation of sequences with established marine oxygen isotope stratigraphy will enable a more detailed analysis of the rates and timing of deformation of the Late Pleistocene unconformities beneath the inner to middle shelf. Analysis of a well positioned, drilled core from the inner to middle shelf between Motunau and Point Gibson would greatly improve the resolution of the sequence stratigraphy.

(6) Good quality, processed, multichannel seismic reflection data with seismic penetration sufficient to image basement within the north Canterbury coastal province would help to constrain: (i) the geometry of the inferred thrust faults beneath the folds; (ii) the age of onset of thrusting in basement; (iii) the total

component of late Cenozoic fault displacement; and (iv) could be used to test for structural inversion of Late Cretaceous normal faults beneath the shelf. Deep crustal seismic-reflection profiles are required from both the NMFZ and the north Canterbury region to constrain the geometry of the faults in the upper crust and to test models of crustal detachment.

(7) Further detailed field studies are required in coastal north Canterbury between Waipara and Kaikoura to: (i) establish the style and kinematics of deformation including the relationships between faulting and folding, and (ii) test alternative models of strike-slip and thrust tectonics in the coastal region.

(8) Detailed micro-earthquake surveys in both coastal north Canterbury and offshore (using ocean-bottom seismographs) would help to constrain: (i) the kinematics of shallow and deep crustal deformation, and (ii) the structural relationships between the normal faults in the NMFZ and the folds and thrust faults in north Canterbury and offshore Marlborough.

8.8 FINAL COMMENTS

This thesis set out to address the late Cenozoic tectonic and sedimentation styles on the NW Chatham Rise slope and north Canterbury continental margin, and to establish the tectonic relationship between this region and the evolving New Zealand plate-boundary zone. The region studied is significant because it lies at the southern termination of the Hikurangi subduction zone and the NW Chatham Rise is actively extending by normal faulting on the edge of an obliquely convergent plate boundary.

In order to understand the evolution of the extensional North Mernoo Fault Zone the regional patterns of Quaternary sedimentation (Chapter 3) and a detailed late Cenozoic seismic stratigraphy (Chapter 4) had to be established. Mapping of the Quaternary sedimentation patterns on the NW Chatham Rise slope was extended northward into the southern part of the Hikurangi Trough, so that the inter-relationships between slope and trough sedimentation could be evaluated. The stratigraphic analysis of the sediments beneath the slope required careful and methodical mapping of a large collection of new seismic-reflection profiles. The seismic-stratigraphy was interpreted within a time framework provided by the bio-stratigraphy of cores recovered from the exposed parts of different sedimentary units. The results were surprising and significant. They showed that regional, unconformity-bounded sedimentary units can form in the deep-sea in response to bottom-current fluctuations that appear to be controlled by global climatic cycles and the unique physical oceanography of the region. The origin of the units is, thus, different from the origin of sequences in the Vail/Exxon sea-level model of sequence stratigraphy.

The structure of the NMFZ was mapped in detail for the first time by correlating faults between closely-spaced seismic profiles. The stratigraphy was used to constrain the timing, rates and amounts of dip-slip fault displacement during the late Cenozoic. In addition, analysis of two previous episodes of basement-involved normal faulting showed that many of the late Cenozoic faults in the NMFZ are reactivated structures and that the basement fabric produced during the older phases of deformation strongly influences the geometry of the late Cenozoic fault system, including the presently active faults.

A complementary study of the Quaternary deformation of the north Canterbury continental shelf was undertaken to constrain the relationship between the extensional faulting in the NMFZ and the major structural elements in the plate-boundary zone onshore in northern South Island. A fold and thrust zone extending from near Christchurch to Kaikoura and almost to the western end of the NMFZ was mapped in detail using a substantial amount of new seismic-reflection data. This style of inner-mid shelf deformation is shown to be similar to that characterising much of the onshore north Canterbury region. A preliminary high-resolution Pleistocene seismic stratigraphy was established beneath the inner to middle shelf. Following the method developed in the NMFZ, the north Canterbury seismic-stratigraphy was constrained by biostratigraphy of cores obtained from the exposed parts of different sedimentary units. In contrast to the NW Chatham Rise, the sedimentary units beneath the shelf result from base-level and shoreline changes caused by glacio-eustatic sea-level fluctuations.

Possible kinematic models of deformation of the NW Chatham Rise and the Canterbury regions are discussed in this thesis. Alternative tectonic models for the north Canterbury region build on the results and interpretations of several recent M.Sc. and Ph.D. studies of seismology and onshore geology, which were completed under the umbrella of the University of Canterbury Active Tectonics Programme. An attempt has been made to: (i) integrate the new data presented in this thesis with existing geological and seismological data from northern South Island; and (ii) relate the tectonics of both the coastal north Canterbury region and the NMFZ to the southern termination of the Hikurangi subduction zone and to the transfer of relative plate motion to the Southern Alps continental collision zone. After considering the many other plate tectonic settings in the world where active normal faulting is taking place at present, it is concluded that the North Mernoo Fault Zone is either a unique example of continental extension at the edge of a convergent plate boundary, or similar zones are yet to be recognised elsewhere.

REFERENCES

Abers, G.A. 1991: Possible seismogenic shallow-dipping normal faults in the Woodlark-d'Entrecasteaux extensional province, Papua New Guinea. *Geology 19* : 1205–1208.

Abbott, S.T.; Carter, R.M. (in press): The sequence architecture of mid-Pleistocene (c. 1.1–0.4 Ma) cyclothems from New Zealand : Facies development during a period of oribital control on sea-level cyclicity. *In* de Boer, P.L.; Smith, D.G. (eds) "Orbital Forcing and Cyclic Sequences". *International Association of Sedimentologists Special Publication.*

Adams, J. 1980: Contemporary uplift and erosion of the Southern Alps, New Zealand. *Bulletin of the Geological Society of America, part II, 91* : 11–44.

Allmendinger, R.W.; Hauge, T.A.; Hauser, E.C.; Potter, C.J.; Oliver, J. 1987: Tectonic heredity and the layered lower crust in the Basin and Range Province, western United States. *In* Coward, M.P.; Dewey J.F.; Hancock P.L. (eds) "Continental Extensional Tectonics". *Geological Society of London Special Publication 28* : 223–246.

Anderson H.; Webb, T.; Jackson, J. (in press): Focal mechanisms of large earthquakes in the South Island, New Zealand; implications for the accommodation of Pacific-Australia plate motion. *Geophysical Journal International.*

Arabasz, W.J.; Robinson, R. 1976: Microseismicity and geological structure in the northern South Island, New Zealand. *N.Z. Journal of Geology and Geophysics 19* : 569–601.

Armi, L. 1986: The hydraulics of two flowing layers with different densities. *Journal of Fluid Mechanics 163* : 27–58.

Armi, L.; Farmer, D. 1985: The internal hydraulics of the Strait of Gibraltar and associated sills and narrows. *Oceanologica Acta 8* : 37–46.

Armijo, R.; Tapponnier, P.; Mercier J.; Tong-Lin, H. 1986: Quaternary extension in southern Tibet : Field observations and tectonic implications. *Journal of Geophysical Research 91* : 13,803–13,872.

Aubouin, J. 1990: The west Pacific geodynamic model. *Tectonophysics 183* : 1–7.

Australian Gulf Oil Co., 1973: Basic geophysical data from M.V. Gulfrex cruises 94–98, October 1972–January 1973. *N.Z. Geological Survey Open File Petroleum Report 614.*

Bally, A.W.; Bernoulli, D.; Davis, G.A.; Montadert, L. 1981: Listric normal faults. *Oceanologica Acta 4* : 87–101.

Barnes, E.J. 1985: Eastern Cook Strait region circulation inferred from satellite-derived, sea-surface, temperature data. *N.Z. Journal of Marine and Freshwater Research 19* : 405–411.

Barnes, P.M.; Baldwin, R.P. 1993: Mernoo Bathymetry, 2nd edition. *N.Z. Oceanographic Institute Chart, Coastal Series, 1:200,000.*

Barnes, P.M.; Korsch, R.J. 1991: Melange and related structures in Torlesse accretionary wedge, Wairarapa, New Zealand. *N.Z. Journal of Geology and Geophysics 34* : 517–532.

Barrell, D. 1989: Geomorphic evolution and engineering geological studies of coastal Motunau, north Canterbury. Unpublished M.Sc. thesis, lodged in the library, University of Canterbury, Christchurch, N.Z.

Beanland, S.; Berryman, K. 1991: Neogene stratigraphy, structure, and evolution of the Eketahuna Basin, northern Wairarapa. *Field trip guide. Geological Society of N.Z. Miscellaneous Publication 59B* : 16–21.

Beggs, J.M. 1990: Seismic-stratigraphy of the Plio-Pleistocene Giant Forsets, Western Platform, Taranaki Basin. Pp 201–207 *in* Proceedings of the 1989 New Zealand Oil Exploration Conference, Energy and Resources Division, Ministry of Commerce, Wellington.

Berryman, K.R. 1979: Active faulting and derived PHS directions in the South Island, New Zealand. *In* Walcott, R.I.; Cresswell, M.M. (eds) "The Origin of the Southern Alps". *Bulletin of the Royal Society of N.Z. 18* : 29–34.

Berryman, K.R. 1980: Late Quaternary movement on the White Creek Fault, South Island, New Zealand. *N.Z. Journal of Geology and Geophysics 23* : 93–101.

Beu, A.G.; Edwards, A.R.; Pillans, B.J. 1987: A review of New Zealand Pleistocene stratigraphy, with emphasis on the marine rocks. Pp 250–269 *in* Itihara, M.; Kamei, T. (eds) Proceedings of the 1st International Colloquim on Quaternary Stratigraphy of Asia and the Pacific Area, Osaka, 1986.

Bibby, H.M. 1981: Geodetically determined strain across the southern end of the Tonga-Kermadec-Hikurangi subduction zone. *Geophysical Journal of the Royal Astronomical Society 66* : 513–533.

Bishop, D.J. 1991: Cretaceous and Cenozoic tectonics of the west coast region of South Island Pp 122–133 *in* Proceedings of the New Zealand Oil Exploration Conference, Christchurch. Ministry of Commerce, Wellington.

Bishop, D.J. 1992a: Extensional tectonism and magmatism during the middle Cretaceous to Paleocene, north Westland, New Zealand. *N.Z. Journal of Geology and Geophysics 35* : 81–91.

Bishop, D.J. 1992b: Neogene deformation in part of the Buller coalfield, Westland, South Island. *N.Z. Journal of Geology and Geophysics 35* : 249–258.

Bles, J.L.; Bonijoly, D.; Castaing, C.; Gros, Y. 1989: Sucessive post-Variscan stress fields in the French Massif Central and its borders (western European plate) : Comparison with geodynamic data. *Tectonophysics 169* : 79–111.

Borchardt, G.A.; Havard, M.E.; Schmitt, R.A. 1971: Correlation of volcanic ash deposits by activation analysis of glass separates. *Quaternary Research 1* : 247–260.

Boyer, S.E.; Elliot, D. 1982: Thrust systems. *Bulletin of the American Association of Petroleum Geologists 66* : 1196–1230.

Bradley, D.C.; Kidd, W.S.F. 1991: Flexural extension of the upper continental crust in collisional foredeeps. *Bulletin of the Geological Society of America 103* : 1416–1438.

Bradshaw, J.D. 1988: Cretaceous geotectonic patterns in the New Zealand region. *Tectonics 8* : 803–820.

Bradshaw, J.D. 1991: Cretaceous dispersion of Gondwana: continental and oceanic spreading in the southwest Pacific-Antarctic sector. Pp 581–585 *in* Thomson, M.R.A.; Crame J.A.; Thomson, J.W. (eds) "Continental Evolution of Antarctica". Cambridge University Press.

Briggs, R.M.; Fulton, B.W.J. 1990: Volcanism, structure and petrology of the Whiritoa-Whangamata coastal section, Coromandel Volcanic Zone, New Zealand : Facies model evidence for the Tunaiti caldera. *N.Z. Journal of Geology and Geophysics 33* : 623–633.

Browne, G.H. 1992: The northeastern portion of the Clarence Fault : Tectonic implications for the late Neogene evolution of Marlborough, New Zealand. *N.Z. Journal of Geology and Geophysics 35* : 437–445.

Bruce, C.H. 1973: Pressured shale and related sediment deformation : Mechanism for development of regional contemporaneous faults. *Bulletin of the American Association of Petroleum Geologists 57* : 878–886.

Burkle, L.H.; Abrams, N. 1987: Regional Late Pliocene-Early Pleistocene hiatuses of the southern ocean-diatom evidence. *Marine Geology 77* : 207–218.

Cabrera, J.; Sebrier, M.; Mercier, J.L. 1991: Plio-Quaternary geodynamic evolution of a segment of the Peruvian Andean Cordillera located above the change in the subduction geometry : the Cuzco region. *Tectonophysics 190* : 331–362.

Campbell, J.K. 1973: Displacement data from the Alpine Fault at Lake Rotoiti and its relevance to glacial chronology and the tempo of tectonism. Pp 57–58, Abstracts from the IXth INQUA Congress, Christchurch, N.Z.

Campbell, J.K. 1991: Styles of deformation associated with the Marlborough Fault System. *In* "Structural Transition from Alpine fault to Hikurangi Margin in Space and Time". Programme and Abstracts. *Geological Society of N.Z. Miscellaneous Publication 56* : 10–13.

Campbell, J.K.; Nicol, A. 1992: Holocene folding and rupture on the Bobys Creek Fault and related Quaternary deformation along the Waipara River. *Field trip guide. Geological Society of N.Z. Miscellaneous Publication 63B* : 137–152.

Cape, C.D.; Lamb, S.H.; Vella, P.; Wells, P.E.; Woodward, D.J. 1990: Geological structure of Wairarapa Valley, New Zealand, from seismic reflection profiling. *Journal of the Royal Society of N.Z. 20* : 85–105.

Carr, M.J. 1970: The stratigraphy and chronology of the Hawera series, marginal succession of the north Canterbury coast. Unpublished Ph.D. thesis, University of Canterbury Library, Christchurch, N.Z.

Carter, L.; Carter, R.M. 1985: Current modification of a mass failure deposit on the continental shelf, north Canterbury, New Zealand. *Marine Geology 62* : 193–211.

Carter, L.; Carter, R.M. 1988: Late Quaternary development of left-bank-dominant levees in the Bounty Trough, New Zealand. *Marine Geology 78* : 185–197.

Carter, L.; Carter, R.M.; Griggs, G.B. 1982: Sedimentation in the Conway Trough, a deep near-shore marine basin at the junction of the Alpine transform and Hikurangi subduction plate boundary, New Zealand. *Sedimentology 29* : 475–497.

Carter, L.; Carter, R.M.; Nelson, C.S.; Fulthorpe, C.S.; Neil, H.L. 1990: Evolution of Pliocene to Recent abyssal sediment waves on Bounty Fan levees, New Zealand. *Marine Geology 95* : 97–109.

Carter, L.; Herzer, R.H. 1979: The hydraulic regime and its potential to transport sediment on the Canterbury continental shelf. *Memoir. N.Z. Oceanographic Institute 83* : 33 p.

Carter, L.; Lewis, K.B.; Davey, F.J. 1989: Faults in Cook Strait and their bearing on the structure of central New Zealand. *N.Z. Journal of Geology and Geophysics 31* : 431–446.

Carter, L.; McCave, I.N. (under review): Structure of sediment drifts approaching an active plate margin under the SW Pacific Deep Western Boundary Current. *Paleoceanography.*

Carter, L.; Mitchell, J.S. 1987: Late Quaternary sediment pathways through the deep ocean, east of New Zealand. *Paleoceanography 2* : 409–422.

Carter, R.M. 1988: Plate boundary tectonics, global sea-level changes and the development of the eastern South Island continental margin, New Zealand, Southwest Pacific. *Marine and Petroleum Geology 5* : 90–107.

Carter, R.M.; Abbott, S.T.; Fulthorpe, C.S.; Haywick, D.W.; Henderson, R.A. 1991: Application of global sea level and sequence-stratigraphic models in southern hemisphere Neogene strata from New Zealand. *In* MacDonald, D.I.M. (ed.) "Sedimentation, Tectonics and Eustacy". *International Association of Sedimentologists Special Publication 12* : 41–65.

Carter, R.M.; Carter, L. 1982: The Motunau Fault and other structures at the southern edge of the Australian-Pacific plate boundary, offshore Marlborough, New Zealand. *Tectonophysics 88* : 133–159.

Carter, R.M.; Carter, L. 1985: The Motunau Fault revisited. *Tectonophysics 115* : 164–166.

Carter, R.M.; Carter, L.; Williams, J.J.; Landis, C.A. 1985: Modern and relict sedimentation on the Otago continental shelf, New Zealand. *Memoir. N.Z. Oceanographic Institute 93* : 43 p.

Carter, R.M.; Norris, R.J. 1976: Cainozoic history of southern New Zealand : An accord between geological observations and plate-tectonic predictions. *Earth and Planetary Science Letters 31* : 85–94.

Carver, G.A.; 1987: Geological criteria for recognition of individual paleoseismic events in compressional tectonic environments. *In* Crone, A.J.; Omdahl, E.M. (eds) "Directions in Paleoseismology". *U.S. Geological Survey Open File Report 87-673* : 115–128.

Cashman, S.M.; Kelsey, H.M.; Erdman, C.F.; Cutten, H,N,C,; Berryman, K.B. 1992: A structural transect and analysis of strain partitioning across the forearc of the Hikurangi subduction zone, Hawke's Bay, North Island, New Zealand. *Tectonics 11* : 242–257.

Chadwick, R.A. 1986: Extension tectonics in the Wessex Basin, southern England. *Journal of the Geological Society of London 43* : 465–488.

Chappell, J. 1974: Geology of coral terraces, Huon Peninsula, New Guinea : A study of Quaternary tectonic movements and sea-level changes. *Bulletin of the Geological Society of America 85* : 553–570.

Chappell, J.; Veeh, H.H. 1978: Late Quaternary tectonic movements and sea-level changes at Timor and Atauro Island. *Bulletin of the Geological Society of America 89* : 356–368.

Charlton, T.R. 1991: Postcollision extension in arc-continent collision zones, eastern Indonesia. *Geology 19* : 28–31.

Chase, C.G. 1978: Plate kinematics : The Americas, East Africa and the rest of the world. *Earth and Planetary Science Letters 37* : 353–368.

Christie-Blick, N. 1991: Onlap, offlap, and the origin of unconformity-bounded depositional sequences. *Marine Geology 97* : 35–56.

Cole, J.W. 1979: Structure, petrology, and genesis of Cenozoic volcanism, Taupo Volcanic Zone, New Zealand — a review. *N.Z. Journal of Geology and Geophysics 22* : 631–657.

Cooper, A.F.; Barreiro, B.A.; Kimbrough, D.L.; Mattinson, J.M. 1987: Lamprophyre dike intrusion and the age of the Alpine fault, New Zealand. *Geology 15* : 941–944.

Cowan, H.A. 1990: Late Quaternary displacements on the Hope Fault at Glynn Wye, north Canterbury. *N.Z. Journal of Geology and Geophysics 33* : 285–293.

Cowan, H.A. 1992: Structure, seismicity and tectonics of the Porter's Pass-Amberley Fault Zone, North Canterbury, New Zealand. Unpublished Ph.D. thesis, lodged in the library, University of Canterbury, Christchurch, N.Z.

Cowan, H.; Reyners, M.; Taber, J. 1991: Present tectonics of the east coast-Southern Alps plate boundary zone, north Canterbury, New Zealand : Inferences from seismicity. *In* "Structural Transition from Alpine fault to Hikurangi Margin in Space and Time". Programme and Abstracts. *Geological Society of New Zealand Miscellaneous Publication, 56* : 14.

Coyle, S. 1988: The Porter's Pass fault. Unpublished M.Sc thesis, lodged in the library, University of Canterbury, Christchurch, N.Z.

Crans, W.; Mandl, G.; Haremboure, J. 1880: On the theory of growth faulting : a geometrical delta model based on gravity sliding. *Journal of Petroleum Geology 2* : 265–307.

Crowell, J.C. 1986: Active tectonics along the western continental margin of the conterminous United States. Pp 10–29 *in* "Active Tectonics, Studies in Geophysics", National Academy Press, Washington, D.C.

Cullen, D.J. 1969: A tectonic analysis of the south-west Pacific. *N.Z. Journal of Geology and Geophysics 13* : 7–20.

Cullen, D.J. 1980: Distribution, composition and age of submarine phosphorite on Chatham Rise, east of New Zealand. *Special Publication, Society of Economic Paleontologists and Mineralogists 29* : 139–148.

Curray, 1961: Late Quaternary sea-level : a discussion. *Bulletin of the Geological Society of America 72* : 1707–1712.

Damuth, J.E. 1975: Echo-character of the western equatorial Atlantic floor and its relationship to the dispersal of terrigenous sediments. *Marine Geology 18* : 17–45.

Damuth, J.E. 1979: Migrating sediment waves created by turbidity currents in the northern South China Basin. *Geology 7* : 520–523.

Damuth, J.E. 1980: Use of high frequency (3.5–12 kHz) echograms in the study of near-bottom sedimentation processes in the deep-sea : a review. *Marine Geology 38* : 51–75.

Damuth, J.E.; Hayes, D.E. 1977: Echocharacter of the east Brazilian continental margin and its relationship to sedimentary processes. *Marine Geology 24* : M73–M95.

Damuth, J.E.; Kumar, N. 1975: Amazon cone: morphology, sediments, age and growth pattern. *Bulletin of the Geological Society of America 86* : 863–878.

Davey, F.J. 1977: Marine seismic measurements in the New Zealand region. *N.Z. Journal of Geology and Geophysics 20* : 719–777.

Davey, F.J.; Hampton, M.; Childs, J.; Fisher, M.A.; Lewis, K.B.; Pettinga, J.R. 1986: Structure of a growing accretionary prism, Hikurangi margin, New Zealand. *Geology 14* : 663–666.

Davies, T.W.; Ferrett, M.A. 1969: Marine seismic surveys, Canterbury Bight, April and December: B.P. Shell, Acquitaine and Todd Petroleum Development Ltd. *N.Z. Geological Survey Open File Petroleum Report 292.*

Davy, B.W. 1992: The influence of subducting plate buoyancy on subduction of the Hikurangi-Chatham Plateau beneath the North Island, New Zealand. Advances in the geology and geophysics of the continental margin. *Memoir of the American Association of Petroleum Geologists 53* : 75–92.

De Mets, C.; Gordon, R.G.; Argus, D.F.; Stein, S. 1990: Current plate motions. *Geophysical Journal International 101* : 425–478.

de Polo, C.M.; Clark, D.G.; Slemmons, D.B.; Ramelli, A.R. 1991: Historical surface faulting in the Basin and Range province, western North America : Implications for fault segmentation. *Journal of Structural Geology 13* : 123–136.

de Voogd, B.; Keen, C.E.; Kay, W.A. 1990: Fault reactivation during Mesozoic extension in eastern offshore Canada. *Tectonophysics 173* : 567–580.

Dingle, R.V.; Camden-Smith, F. 1979: Acoustic stratigraphy and current generated bedforms in deep ocean basins off southeastern Africa. *Marine Geology 33* : 239–260.

Dowrick, D.J. 1991: Magnitude reassessment of New Zealand earthquakes. *Earthquake Engineering and Structural Dynamics 20* : 577–596.

Doyle, L.J.; Orrin, H.P.; Woo, C.C. 1979: Sedimentation on the eastern United States continental slope. *In* Doyle, L.J.; Pilkey, O.H. (eds) "Geology of Continental Slopes". *Special Publication, Society of Economic Paleontologists and Mineralogists 27* : 119–129.

Duggan, M.B.; Reay, A. 1986: The Timaru Basalt. *In* Smith, I.E.M. (ed.) "Late Cenozoic Volcanism in New Zealand". *Bulletin of the Royal Society of N.Z. 23* : 264–277.

Eade, J.V. 1984: West Norfolk Ridge and the regional unconformity: products of Eocene-Oligocene plate collision?. *Geological Society of N.Z. Miscellaneous Publication 31A.*

Eade, J.V. 1988: The Norfolk Ridge System and its margins. Pp 303–324 *in* Nairn, A.E.M.; Stehli, F.G.; Uyeda, S. (eds) "The Ocean Basins and Margins". Vol. 7B. Plenum Publishing Corporation.

Edwards, A.R. 1987: An integrated biostratigraphy, magnetostratigraphy and oxygen isotope stratigraphy for the late Neogene of New Zealand. *N.Z. Geological Survey Record 23* : 80 p.

Edwards, A.R.; Hornibrook, N. de B.; Raine, J.I.; Scott, G.H.; Stevens, G.R.; Strong, C.P.; Wilson, G.J. 1988: A New Zealand Cretaceous-Cenozoic geological time scale. *N.Z. Geological Survey Record 35* : 135–149.

Elder, D.McG.; McCahon, I.F.; Yetton, M.D. 1991: The earthquake hazard in Christchurch: a detailed evaluation. Report to Earthquake and War Damages Commission.

Etheridge, M.A.; Branson, J.C.; Stuart-Smith, P.G. 1985: Extensional basin-forming structures in Bass Strait and their importance for hydrocarbon exploration. *Journal of the Australian Petroleum Exploration Association 25* : 344–361.

Field, B.D.; Browne, G.H. and others 1989: Cretaceous and Cenozoic sedimentary basins and geological evolution of the Canterbury region, South Island, New Zealand. *N.Z. Geological Survey Basins Studies 2* : 94 p.

Fitzgerald, M.G.; Mitchum, R.M.; Uliana, M.A.; Biddle, K.T. 1990: Evolution of the San Jorge Basin, Argentina. American *Bulletin of the American Association of Petroleum Geologists 74* : 879–920.

Fleming, C.A.; Reed, J.J. 1951: Mernoo Bank, east Canterbury, New Zealand. *N.Z. Journal of Science and Technology 6* : 17–30.

Freund, R. 1971: The Hope Fault: a strike-slip fault in New Zealand. *Bulletin of the N.Z. Geological Survey 86* : 49 p.

Froggatt, P.C. 1983: Toward a comprehensive upper Quaternary tephra and ignimbrite stratigraphy in New Zealand using electron microprobe analysis of glass shards. *Quaternary Research 19* : 188–200.

Froggatt, P.C.; Nelson, C.S.; Carter, L.; Griggs, G.; Black, K.P. 1986: An exceptionally large late Quaternary eruption from New Zealand. *Nature 319* : 578–582.

Fulthorpe, C.S.; Carter, R.M. 1989: Test of seismic sequence methodology on a Southern Hemisphere passive margin: the Canterbury Basin, New Zealand. *Marine and Petroleum Geology 6* : 348–359.

Fulthorpe, C.S.; Carter, R.M. 1991: Continental shelf progradation by sediment-drift accretion. *Bulletin of the Geological Society of America 103* : 300–309.

George, A.D. 1990: Deformation processes in an accretionary prism : a study from the Torlesse terrane of New Zealand. *Journal of Structural Geology 12* : 747–759.

Gibb, J.G. 1986: A New Zealand regional Holocene eustatic sea-level curve and its application to determination of vertical tectonic movements : a contribution to IGCP-Project 200. *Bulletin of the Royal Society of N.Z. 24* : 377–395.

Gibb, J.G.; Adams, J. 1982: A sediment budget for the east coast between Oamaru and Banks Peninsula, South Island, New Zealand. *N.Z. Journal of Geology and Geophysics 25* : 335–352.

Gibbs, A.D. 1984: Structural evolution of extensional basin margins. *Journal of the Geological Society of London 141* : 609–620.

Gibbs, A.D. 1990: Linked fault families in basin formation. *Journal of Structural Geology 12* : 795–803.

Gonthier, E.G.; Faugeres, J.C.; Stow, D.A. 1984: Contourite facies of the Faro drift, Gulf of Cadiz. *In* Stow, D.A.V.; Piper D.J.W. (eds) "Fine-grained Sediments: Deep-water Processes and Facies". *Geological Society of London Special Publication 15* : 275–292.

Gregg, D.R. 1964: Sheet 18 Hurunui (1st edition) *Geological Map of New Zealand 1:250 000.* DSIR, Wellington, N.Z.

Greig, M.J.; Gilmour, A.E. 1992: Flow through the Mernoo Saddle, New Zealand. *N.Z. Journal of Marine and Freshwater Research 26* : 155–165.

Greiling, R.O.; El Ramly, M.F.; Akhal, H. El; Stern, R.J. 1988: Tectonic evolution of the northwestern Red Sea margin as related to basement structure. *Tectonophysics 153* : 179–191.

Griggs, G.B.; Carter, L.; Kennett, J.P.; Carter, R.M. 1983: Late Quaternary marine stratigraphy southeast of New Zealand. *Bulletin of the Geological Society of America 94* : 791–797.

Grindley, G.W.; Adams, C.J.D.; Lumb, J.T.; Watters, W.A. 1977: Paleomagnetism, K-Ar dating and tectonic interpretation of upper Cretaceous and Cenozoic volcanic rocks of the Chatham Islands, New Zealand. *N.Z. Journal of Geology and Geophysics 20* : 425–468.

Grindley, G.W.; Davey, F.J. 1982: The reconstruction of New Zealand, Australia, and Antarctica : a review paper. Pp 315–329 *in* Craddock C. (ed.) "Antarctic Geoscience". University of Wisconson Press, Madison.

Grindley, G.W.; Oliver, P.J.; Seward, D. 1988: Stratigraphy, geochronology and paleomagnetism of ignimbrites in the Matahina Basin, Taupo Volcanic Zone. *Geological Society of N.Z. Miscellaneous Publication 41A* : 71.

Hamblin, W.K. 1965: Origin of "reverse drag" on the downthrown side of normal faults. *Bulletin of the Geological Society of America 76* : 1145–1164.

Hancock, P.L.; Bevan, T.G. 1987: Brittle modes of foreland extension. *In* Coward, M.P.; Dewey, J.F.; Hancock, P.L. (eds) "Continental Extensional Tectonics". *Geological Society of London Special Publication 28* : 127–137.

Harding, T.P. 1976: Tectonic significance and hydrocarbon trapping consequences of sequential folding synchronous with San Andreas faulting, San Joaquin Valley, California. *Bulletin of the American Association of Petroleum Geologists 60* : 356–378.

Harding, T.P. 1984: Graben hydrocarbon occurrences and structural style. *Bulletin of the American Association of Petroleum Geologists 68* : 333–363.

Harding, T.P.; Lowell, J.D. 1979: Structural styles, their plate tectonic habitats, and hydrocarbon traps in petroleum provinces. *Bulletin of the American Association of Petroleum Geologists 63* : 1016–1058.

Hayward, A.B.; Graham, R.H. 1989: Some geometrical characteristics of inversion. *In* Cooper M.A.; Williams, G.D. (eds) "Inversion Tectonics". *Geological Society of London Special Publication 44* : 17–39.

Hayward, B.W.; Brook, F.J.; Isaac, M.J. 1989: Cretaceous to middle Tertiary stratigraphy, paleogeography and tectonic history of Northland, New Zealand. *In* Spörli, B.; Kear, D. (eds) "Geology of Northland: Accretion, allochthons and arcs at the edge of the New Zealand micro-continent" *Bulletin of the Royal Society of N.Z. 26* : 47-64.

Heath, R.A. 1972a: The Southland Current. *N.Z. Journal of Marine and Freshwater Research 6* : 497–533.

Heath, R.A. 1972b: Choice of reference surface for geostrophic currents around New Zealand. *N.Z. Journal of Marine and Freshwater Research 6* : 148–177.

Heath, R.A. 1976: Oceanic circulation in the head of the Hikurangi Trench, east coast, New Zealand. *N.Z. Journal of Marine and Freshwater Research 10* : 651–674.

Heath, R.A. 1985: A review of the physical oceanography of the seas around New Zealand — 1982. *N.Z. Journal of Marine and Freshwater Research 19* : 79–124.

Heezen, B.C.; Johnson, G.L. 1969: Mediterranean undercurrent and microphysiography west of Gibaltar. *Bulletin de l'Institut Oceanographique de Monaco 67* : 51 p.

Herzer, R.H. 1977a: Mernoo Bathymetry. *N.Z. Oceanographic Institute Chart, Coastal Series 1:200 000.*

Herzer, R.H. 1977b: Late Quaternary geology of the Canterbury continental terrace. Unpublished Ph.D. thesis, lodged in the library, Victoria University of Wellington Wellington, N.Z.

Herzer, R.H. 1979: Submarine slides and submarine canyons on the continental slope off Canterbury, New Zealand. *N.Z. Journal of Geology and Geophysics 22* : 391–406.

Herzer, R.H. 1981: Late Quaternary stratigraphy and sedimentation of the Canterbury continental shelf, New Zealand. *Memoir, N.Z. Oceanographic Institute 89* : 71 p.

Herzer, R.H.; Bradshaw, J.D. 1985: The Motunau Fault and other structures at the southern edge of the Australian-Pacific plate boundary, offshore Marlborough, New Zealand — Discussion. *Tectonophysics 115* : 161–164.

Herzer, R.H.; Carter L. 1983: Pegasus Bathymetry, 2nd edition. *N.Z. Oceanographic Institute Chart, Coastal Series 1:200 000.*

Herzer, R.H.; Lewis, D.W. 1979: Growth and burial of a submarine canyon off Motunau, north Canterbury, New Zealand. *Sedimentary Geology 24* : 69–83.

Herzer, R.H.; Wood, R.A. 1988: The geology of Mernoo Bank and surrounding area, western Chatham Rise. *N.Z. Geological Survey Record 29* : 22 p.

Hollihan, K.; Yang, J. 1991: Eocene to Recent structural history of onshore Taranaki with references to the main play styles. Progamme and Abstract. P. 36 *in* Proceedings of the New Zealand Oil Exploration Conference, Christchurch. Ministry of Commerce, Wellington.

Hornibrook, N.de B. 1982: Late Miocene to Pleistocene *Globorotalia* (Foraminiferida) from the DSDP leg 29, site 284, Southwest Pacific. *N.Z. Journal of Geology and Geophysics 25* : 83–99.

Hornibrook, N.de B.; Brazier, R.C,; Strong, C.P. 1989: Manual of New Zealand Permian to Pleistocene foraminiferal biostratigraphy. *Palaeontological Bulletin, N.Z. Geological Survey 56* : 175 p.

Hull, A.G. 1987: Paleoseismic slip at reverse faults. Pp 262–270 in Crone, A.J.; Omdahl, E.M. (eds) "Directions in Paleoseismology". *U.S. Geological Survey Open File Report 87-673.*

Hunt Petroleum Company of New Zealand, 1971: Preliminary results of geophysical work in the offshore waters of South Island. October 1970 to June 1971. *N.Z. Geological Survey Open File Petroleum Report 558.*

Jackson, J.A. 1987: Active normal faulting and crustal extension. *In* Coward, M.P.; Dewey, J.F.; Hancock, P.L. (eds) "Continental Extensional Tectonics". *Geological Society of London Special Publication 28* : 3–17.

Jackson, J.A.; McKenzie, D.P. 1983: The geometrical evolution of normal fault systems. *Journal of Structural Geology 5* : 471–482.

Jackson, J.A.; White, N.J. 1989: Normal faulting in the upper continental crust: Observations from regions of active extension. *Journal of Structural Geology 11* : 15-36.

Jackson, J.A.; White, N.J.; Garfunkel, Z.; Anderson, H. 1988: Relations between normal fault geometry, tilting and vertical motions in extensional terrains : an example from the southern Gulf of Suez. *Journal of Structural Geology 10* : 155–170.

Jamison, W.R. 1987: Geometric analysis of fold development in overthrust terranes. *Journal of Structural Geology 9* : 207–219.

Jenkins, C.J. 1984: Erosion and deposition at abyssal depths in the Tasman Sea. A seismic stratigraphic study of the bottom-current patterns. *Ocean Science Institute report 4* : University of Sydney. 46 p.

Johnson, D.A.; Damuth, J.E. 1979: Deep thermohaline flow and current-controlled sedimentation in the Amirante Passage: western Indian Ocean. *Marine Geology 33* : 1–44.

Johnson, T.C.; Lynch, E.L.; Showers, W.J.; Nicholas, C.P. 1988: Pleistocene fluctuations in the western boundary undercurrent on the Blake Outer Ridge. *Paleoceanography 3* : 191–207.

Jolivet, L.; Daniel, J-M; Fournier, M. 1991: Geometry and kinematics of extension in Alpine Corsica. *Earth and Planetary Science Letters 104* : 278–291.

Joyce, J.E.; Tjalsma, L.R.C.; Prutzman, J.M. 1990: High-resolution planktic stable isotope record and spectral analysis for the last 5.35 M.Y. : Ocean drilling program site 625 northeast Gulf of Mexico. *Paleoceanography 5* : 507–529.

Kamp, P.J.J. 1986a: Late Cretaceous-Cenozoic tectonic development of the southwest Pacific region. *Tectonophysics 121* : 225–251.

Kamp, P.J.J. 1986b: The mid-Cenozoic Challenger Rift System in western New Zealand and its implications for the age of Alpine Fault inception. *Bulletin of the Geological Society of America 97* : 255–281.

Kamp, P.J.J.; Fitzgerald, P.G. 1987: Geological constraints on the Cenozoic Antarctica-Australia-Pacific plate motion circuit. *Geology 15* : 694–697.

Kamp, P.J.J.; Green, P.F.; White, S.H. 1989: Fission track analysis reveals character of collision tectonics in New Zealand. *Tectonics 8* : 169–195.

Karig, D.E.; Barber, A.J.; Charlton, T.R.; Klemperer, S.; Hussong, D.M. 1987: Nature and distribution of deformation across the Banda Arc-Australian collision zone at Timor. *Bulletin of the Geological Society of America 98* : 18–32.

Katz, H.R. 1974: Margins of the southwest Pacific. Pp 549–566 *in* Burke, C.A.; Drake, C.L. (eds) "The Geology of Continental Margins". Springer-Verlag, New York. 1009 p.

Kautz, S.A.; Sclater, J.G. 1988: Internal deformation in clay models of extension by block faulting. *Tectonics 7* : 823–832.

Kennard, L.; Schafer, C.; Carter, L. 1990: Late Cenozoic evolution of the Sackville Spur : a sediment drift on the New Foundland continental slope. *Canadian Journal of Earth Science 27* : 863–878.

Kennett, J.P. 1982: "Marine Geology". Prentice-Hall, Inc., New Jersey. 813 p.

Kennett, J.P.; von der Borch, C.C. 1986: Southwest Pacific paleoceanography. *In* Kennett, J.P.; von der Borch, C.C. *et al.* (eds) *Initial Reports of the Deep Sea Drilling Project 90* : 1493–1515.

Kennett, J.P.; von der Borch, C.C. *et al.* 1986: Site 594: Chatham Rise. *Initial Reports of the Deep Sea Drilling Project 90, part 1* : 653–744.

King, P.R. 1990: Polyphase evolution of the Taranaki Basin, New Zealand : Changes in sedimentary and structural style. Pp 134–150 *in* Proceedings of the New Zealand Oil Exploration Conference, Queenstown. Ministry of Commerce, Wellington.

King, P.R.; Thrasher, G.P. 1992: Post-Eocene development of the Taranaki Basin, New Zealand : convergent overprint of a passive margin. "Advances in the Geology and Geophysics of the Continental Margin". *Memoir of the American Association of Petroleum Geologists 53* : 93-118.

Kirk, P.A. 1991: Waipa Fault and the tectonic rotation of Hakarimmata-Taupiri Block. *N.Z. Geological Survey Record 43* : 81–84.

Klaus, A.; Ledbetter, M.T. 1988: Deep-sea sedimentary processes in the Argentine Basin revealed by high-resolution seismic records (3.5 kHz echograms). *Deep-Sea Research 35* : 899–917.

Knott, S.D.; Turco, E. 1991: Late Cenozoic kinematics of the Calabrian Arc, southern Italy. *Tectonics 10* : 1164–1172.

Knuepfer, P.L.K. 1992: Temporal variations in latest Quaternary slip across the Australian-Pacific plate boundary, northeastern South Island, New Zealand. *Tectonics 11* : 449–464.

Kolla, V.; Eittreim, S.; Sullivan, L.; Kostecki, J.A.; Burkle, L.H. 1980: Current-controlled, abyssal microtopography and sedimentation in Mozambique Basin, southwest Indian Ocean. *Marine Geology 34* : 171–206.

Kohn, B.P.; Pillans, B.; McGlone, M.S. 1992: Zircon fission track age for middle Pleistocene Rangitawa Tephra, New Zealand : Stratigraphic and paleoclimatic significance. *Paleogeography, Paleoclimatology, Paleoecology 95* : 73–94.

Korsch, R.J.; Lindsay, J.F. 1989: Relationships between deformation and basin evolution in the intracratonic Amedeus Basin, central Australia. *Tectonophysics 158* : 5–22.

Korsch, R.J.; Wellman, H.W. 1988: The geological evolution of New Zealand and the New Zealand region. Pp 411–481 *in* Nairn, A.E.M.; Stehli, F.G.; Uyeda, S. (eds) "The Ocean Basins and Margins". Vol. 7B. Plenum Publishing Corporation.

Krause, D.C.; Cullen, D.J. 1970: Bounty Bathymetry, 2nd ed. *N.Z. Oceanographic Institute Chart, Oceanic Series 1:1,000,000.*

Kroenke, L.W. 1984: A southwest Pacific regional synthesis : Migration of the Indo-Australia/Pacific Plate boundary during the Cenozoic era. Pp 111–122 *in* "Cenozoic Tectonic Development of the Southwest Pacific". *U.N. ESCAP, CCOP/SOPAC Technical Bulletin 6* : 122 p.

Laird, M.G. 1981: The late Mesozoic fragmentation of the New Zealand segment of Gondwana. Pp 311–318 *in* Cresswell, M.M.; Vella, P. (eds) "Gondwana Five". Balkema, Rotterdam.

Laird, M.G.; Nathan, S. 1988: The Eocene Torea Breccia, SW Nelson: redescription, sedimentology, and regional significance. Research Notes 1988, *N.Z. Geological Survey Record 35* : 104–108.

Lamb, S. 1988: Tectonic rotations about vertical axes during the last 4 Ma in part of the New Zealand plate-boundary zone. *Journal of Structural Geology 10* : 875–893.

Lamb, S.H.; Bibby, H.M. 1989: The last 25 Ma of rotation deformation in part of the New Zealand plate-boundary zone. *Journal of Structural Geology 11* : 473–492.

Larsen, P-H. 1988: Relay structures in a lower Permian basement-involved extensional system, East Greenland. *Journal of Structural Geology 10* : 3–8.

Lewis, D.W. 1976: Subaqueous debris flows of Early Pleistocene age at Motunau, north Canterbury, New Zealand. *N.Z. Journal of Geology and Geophysics 19* : 535–567.

Lewis, D.W. 1992: Anatomy of an unconformity on mid Oligocene Amuri Limestone, Canterbury, New Zealand. *N.Z. Journal of Geology and Geophysics 35* : 463–475.

Lewis, K.B. 1971: Growth rate of folds using tilted wave-planed surfaces : Coast and continental shelf, Hawke's Bay, New Zealand. *Bulletin of the Royal Society of N.Z. 9* : 225–231.

Lewis, K.B. 1973: Erosion and deposition on a tilting continental shelf during Quaternary oscillations of sea-level. *N.Z. Journal of Geology and Geophysics 16* : 281–301.

Lewis, K.B. 1980: Quaternary sedimentation on the oblique- subduction and transform margin, New Zealand. *In* Ballance, P.F.; Reading, H.G. (eds) "Sedimentation in oblique-slip mobile zones". *International Association of Sedimentologists Special Publication 4* : 171–189.

Lewis, K.B. 1985: New rock samples and cores from Hikurangi Margin geology cruise 1121. Pp 37–49 *in* Lewis, K.B. (Comp.) "New Seismic Profiles, Cores and Dated Rocks from the Hikurangi Margin, New Zealand. *N.Z. Oceanographic Institute Field Report 22* : 53 p.

Lewis, K.B. (under review): The 1500 km long Hikurangi Channel : an axial channel that leaves the trench. *Geo-Marine Letters.*

Lewis, K.B.; Bennett, D.J.; Herzer, R.H.; von der Borch, C.C. 1986: Seismic stratigraphy and structure adjacent to an evolving plate boundary, western Chatham Rise, New Zealand. *In* Kennett, J.P.; von der Borch, C.C. *et al.* (eds) *Initial Reports of the Deep Sea Drilling Project 90, part 2* : 1325–1327.

Lewis, K.B.; Pettinga, J.R. (in press): The emerging, imbricated frontal wedge of the Hikurangi margin. *In* Ballance, P.F. (ed.) "South Pacific Sedimentary Basins. Sedimentary Basins of the World". Elsevier.

Lister, G.S.; Etheridge, M.A.; Symonds, P.A. 1991: Detachment models for the formation of passive continental margins. *Tectonics 10* : 1038–1064.

Little, T.A. 1992: Development of wrench folds along the Border Ranges fault system, southern Alaska, USA. *Journal of Structural Geology 14* : 343–359.

Lowe, D.J.; Briggs, R.M.; Keane, A.J.; Itaya, T. 1988: Age of the Kauroa Ash Formation, western North Island. *Geological Society of N.Z. Miscellaneous Publication 41A* : 95.

MacKinnon, T.C. 1983: Origin of the Torlesse terrane and coeval rocks, South Island, New Zealand. *Bulletin of the Geological Society of America 94* : 967–985.

Magellan Petroleum New Zealand Ltd, 1969: Sparker reconnaissance survey of the North Bounty Basin and Chatham Rise, New Zealand. *N.Z. Geological Survey Open File Petroleum Report 650.*

Markl, R.G.; Bryan, G.M. 1983: Stratigraphic evolution of the Blake Outer Ridge. *Bulletin of the American Association of Petroleum Geologists 67* : 666–683.

Matos, R.M.D. 1991: Crustal structure and tectonic evolution of the Potiguar Basin - northeast Brazil. *Bulletin of the American Association of Petroleum Geologists 75* : 630.

McClay, K.R. 1990: Extensional fault systems in sedimentary basins : A review of analogue models. *Marine and Petroleum Geology 7* : 207–233.

McDougall, J.C. 1982: Bounty sediments. *N.Z. Oceanographic Institute Chart, Oceanic Series 1:1,000,000.*

McKenzie, D. 1978: Active tectonics of the Alpine-Himilayan belt: the Aegean Sea and surrounding regions. *Geophysical Journal of the Royal Astronomical Society 55* : 217–254.

McKenzie, D.; Jackson, J. 1986: A block model of distributed deformation by faulting. *Journal of the Geological Society of London 143* : 349–353.

Melhuish, A. 1990: Late Cenozoic deformation along the Pacific-Australian plate margin, Dannevirke region, New Zealand. Unpublished M.Sc thesis, lodged in the library, Victoria University of Wellington, Wellington, N.Z.

Mitchum, R.M.; Vail, P.R.; Thompson, S. 1977: Seismic stratigraphy and global changes of sea-level, part 2: the depositional sequence as a basic unit for stratigraphic analysis. *In* Payton, C.W. (ed.) "Seismic Stratigraphic Applications to Hydrocarbon Exploration". *Memoir of the American Association of Petroleum Geologists 26* : 53–62.

Mitchum, R.M.; van Wagoner, J.C. 1991: High frequency sequences and their stacking patterns : Sequence-stratigraphic evidence of high-frequency eustatic cycles. *Sedimentary Geology 70* : 131–160.

Mitra, S. 1990: Fault-propagation folds: geometry, kinematic evolution, and hydrocarbon traps. *Bulletin of the American Association of Petroleum Geologists 74* : 921–945.

Mobil International Oil Company, 1972: Geophysical reconnaissance survey, New Zealand region, 1972. *N.Z. Geological Survey Open File Petroleum Report 587.*

Molnar, P.: Atwater, T.; Mammerickx, J.; Smith, S.M. 1975: Magnetic anomalies, bathymetry and the tectonic evolution of the south Pacific since the Late Cretaceous. *Geophysical Journal of the Royal Astronomical Society 40* : 383–420.

Molnar, P.; Chen, W-P. 1982: Seismicity and mountain building. Pp 41–57 *in* Briegel, U.; Hsu, K.J. (eds) "Mountain Building Processes". Academic Press, London,

Montenat, C.: D'Estevou, P.O.; Purser, B.; Burollet, P-F.; Jarridge, J-J.; Orszag-Sperber, F.; Philobbos, E.; Plaziat, J-C.; Prat, P.; Richert, J-P.; Roussel, N.; Thiriet, J-P. 1988: Tectonic and sedimentary evolution of the Gulf of Suez and the northwestern Red Sea. *Tectonophysics 153* : 161–177.

Morley, C.K. Nelson, R.A.; Patton, T.L.; Munn, S.G. 1990: Transfer zones in the East African Rift System and their relevance to hydrocarbon exploration in rifts. *Bulletin of the American Association of Petroleum Geologists 74* : 1234–1253.

Mould, R.J. 1992: Structure and kinematics of late Cenozoic deformation along the western margin of the Culverden Basin, north Canterbury, New Zealand. Unpublished M.Sc. thesis, lodged in the library, University of Canterbury Christchurch, N.Z.

Mount, V.S.; Suppe, J. 1987: State of stress near the San Andreas fault : Implications for wrench tectonics. *Geology 15* : 1143–1146.

Mount, V.S.; Suppe, J. 1992: Present-day stress orientations adjacent to active strike-slip faults : California and Sumatra. *Journal of Geophysical Research 97* : 11995–12013.

Nairn, I.A.; Beanland, S. 1989: Geological setting of the 1987 Edgecumbe earthquake, New Zealand. *N.Z. Journal of Geology and Geophysics 32* : 1–13.

Namson, J.S.; Davis, T.L. 1988: Seismically active fold and thrust belt in the San Joaquin Valley, central California. *Bulletin of the Geological Society of America 100* : 257–273.

Nathan, S.; Anderson, H.G.; Cook, R.A.; Herzer, R.H.; Hoskins, R.H.; Raine, J.I.; Smale, D. 1986: Cretaceous and Cenozoic sedimentary basins of the west coast region, South Island. *N.Z. Geological Survey Basin Studies 1* : DSIR, Wellington. 89 p.

Nelson, C.S. 1986: Lithostratigraphy of deep sea drilling project leg 90 drill sites in the southwest Pacific: an overview. *In* Kennett, J.P.; von der Borch C.C. *et al.* (eds). *Initial Reports of the Deep Sea Drilling Project 90* : 1471–1489.

Nelson, C.S.; Froggatt, P.C.; Gossan, G.J. 1986a: Nature, chemistry, and origin of late Cenozoic megascopic tephras in leg 90 cores from the southwest Pacific. *Initial Reports of the Deep Sea Drilling Project 90 part 2* : 1161–1171.

Nelson, C.S.; Hendy, C.H.; Cuthbertson, A.M.; Jarret, G.R. 1986b: Late Cenozoic carbonate and isotope stratigraphy, subantarctic site 594, southwest Pacific. *In* Kennett, J.P.; von der Borch C.C. *et al.* (eds) *Initial Reports of the Deep Sea Drilling Project 90* : 1425–1436.

Nichols, G.; Hall. R.; Milsom, J.; Masson, D.; Parson, L.; Sikumbang, N.; Dwiyanto, B.; Kallagher, H. 1990: The southern termination of the Philippine trench. *Tectonophysics 183* : 289–303.

Nicol, A. 1991: Structural styles and kinematics of deformation on the edge of the New Zealand plate boundary zone, mid Waipara region, north Canterbury. Unpublished Ph.D. thesis, lodged in the library, University of Canterbury, Christchurch, N.Z.

Nicol, A. 1993: A Haumurian (c. 66–80 Ma) half-graben, mid-Waipara, north Canterbury, and its implications for late Cretaceous deformation in New Zealand. *N.Z. Journal of Geology and Geophysics 36* : 127–130.

Nicol, A.; Campbell, J.K. 1990: Late Cenozoic thrust tectonics, Picton, Marlborough Sounds, New Zealand. *N.Z. Journal of Geology and Geophysics 33* : 483-492.

Nicol, A.; Cowan, H.; Campbell, J.K; Pettinga, J. 1991: Styles and kinematics of deformation in Canterbury, at the southern limit of subduction. *In* "Structural Transition from Alpine fault to Hikurangi Margin in Space and Time". Programme and Abstracts. *Geological Society of N.Z. Miscellaneous Publication 56* : 35–36.

Nicol, A; Wise, D.U. 1992: Paleostress adjacent to the Alpine Fault of New Zealand : Vein and stylolite data from the Doctors Dome area. *Journal of Geophysical Research 97* : 17685–17692.

Ninkovich, D. 1968: Pleistocene volcanic eruptions in New Zealand recorded in deep sea sediments. *Earth and Planetary Science Letters 4* : 89–102.

Normark, W.R.; Hess, G.R.; Stow, D.A.V.; Bowen, A.J. 1980: Sediment waves on the Monterey Fan levee : a preliminary physical interpretation. *Marine Geology 37* : 1–17.

Norris, R.J.; Carter, R.M. 1980: Offshore sedimentary basins at the southern end of the Alpine Fault, New Zealand. *In* Ballance P.F.; Reading H.G. (eds) "Sedimentation in Oblique-slip Mobile Zones". *International Association of Sedimentologists Special Publication 4* : 237–265.

Norris, R.J.; Koons, P.O.; Cooper, A.F. 1990: The obliquely-convergent plate boundary in the South Island of New Zealand : Implications for ancient collision zones. *Journal of Structural Geology 12* : 715–725.

Norris, R.M. 1964: Sediments of the Chatham Rise. *Memoir. N.Z. Oceanographic Institute 26* : 39 p.

Northward, D. 1966: New Zealand-South Island east coast offshore seismic reconnaissance survey : Operation, data processing and interpretation report. *B.P. Shell Acquitaine and Todd Petroleum Development Ltd Technical Note 224. N.Z. Geological Survey Open File Petroleum Report 286.*

Osborn, N.I.; Ciesielski, P.F.; Ledbetter, M.T. 1983: Disconformities and paleoceanography in the southeast Indian Ocean during the past 5.4 million years. *Bulletin of the Geological Society of America 94* : 1345–1358.

Peacock, D.C.P.; Sanderson, D.J. 1991: Displacement, segment linkage and relay ramps in normal fault zones. *Journal of Structural Geology 13* : 721–733.

Pettinga, J.R. 1982: Upper Cenozoic structural history, coastal southern Hawke's Bay, New Zealand. *N.Z. Journal of Geology and Geophysics 25* : 149–191.

Pettinga, J.R.; Wise, D.U. (in press): Strain orientation adjacent to the Alpine Fault of New Zealand : Fault analysis near Nelson, South Island. *Journal of Geophysical Research.*

Pillans, B. 1990: Pleistocene marine terraces in New Zealand : a review. *N.Z. Journal of Geology and Geophysics 33* : 219–231.

Pinet, B.; Colletta, B. 1990: Probing into extensional sedimentary basins : Comparison of recent data and derivation of tentative models. *Tectonophysics 173* : 185–197.

Pratson, L.F.; Laine, E.P. 1989: The relative importance of gravity-induced versus current-controlled sedimentation during the Quaternary along the mideast U.S. outer continental margin revealed by 3.5 kHz echo character. *Marine Geology 89* : 87–126.

Prebble, W.M. 1980: Late Cenozoic sedimentation and tectonics of the east coast deformed belt in Marlborough, New Zealand. *In* Ballance, P.F.; Reading, H.G. (eds) "Sedimentation in oblique-slip mobile zones". *International Association of Sedimentologists Special Publication 4* : 217–228.

Prell, W.L.; Hutson, W.H; Williams, D.F. 1979: The subtropical convergence and Late Quaternary circulation in the southern Indian Ocean. *Marine Micropaleontology 4* : 225–234.

Rait, G.; Chanier, F.; Waters, D.W. 1991: Landward- and seaward-directed thrusting accompanying the onset of subduction beneath New Zealand. *Geology 19* : 230–233.

Ratcliffe, N.M.; Burton, W.C.; D'Angelo, R.M.; Costain, J.K. 1986: Low angle extensional faulting, reactivated mylonites, and seismic reflection geometry of the Newark basin margin in eastern Pennsylvania. *Geology 14* : 766–770.

Reed, D.L.; Meyer, A.W.; Silver, E.A.; Prasetyo, H. 1987: Contourite sedimentation in an intraoceanic forearc system : Eastern Sunda Arc, Indonesia. *Marine Geology 76* : 223–241.

Reed, J.J.; Hornibrook, N de B. 1952: Sediments from the Chatham Rise. Part 1, Petrology, Part 2, Recent and fossil macrofaunas. *N.Z. Journal of Science and Technology B34* : 173–188.

Regenauer-Lieb, K. 1992: Plastic plate tectonics in New Zealand : From the Gondwana margin to the present. Unpublished Ph.D. thesis, lodged in the library, University of Auckland, N.Z.

Reid, J.L.; Lonsdale, P.F. 1974: On the flow of water through the Samoan Passage. *Journal of Physical Oceanography 4* : 58–73.

Reilly, W.I. 1990: Horizontal crustal deformation on the Hikurangi margin. *N.Z. Journal of Geology and Geophysics 33* : 393–400.

Reyners, M. 1983: Lateral segmentation of the subducted plate at the Hikurangi Margin, New Zealand : Seismological evidence. *Tectonophysics 96* : 203–223.

Reyners, M. 1987: Subcrustal earthquakes in the central South Island, New Zealand, and the root of the Southern Alps. *Geology 15* : 1168–1171.

Reyners, M. 1989: New Zealand seismicity 1964-87 : an interpretation. *N.Z. Journal of Geology and Geophysics 32* : 307–315.

Reyners, M.; Cowan, H. (in press): The transition from subduction to continental collision: crustal structure in the north Canterbury region, New Zealand. *Geophysical Journal International.*

Robinson, R. 1986. Seismicity, structure and tectonics of the Wellington region, New Zealand. *Geophysical Journal of the Royal Astronomical Society 87* : 379–409.

Robinson, R. 1991: Extent and geometry of subduction in the northern South Island and Wellington regions. In: Structural transition from Alpine fault to Hikurangi Margin in space and time. Programme and Abstracts. *Geological Society of N.Z. Miscellaneous Publication 56* : 44–46.

Robinson, S.G.; McCave, I.N. (in press): Orbital forcing of bottom current enhanced sedimentation on Feni Drift, N.E. Atlantic, during the mid-Pleistocene. *Paleoceanography.*

Root, S.I. 1989: Basement control of structure in the Gettysburg rift basin, Pennsylvania and Maryland. *Tectonophysics 166* : 281–292.

Ruddiman, W.E.; Raymo, M.E.; Martinson, D.G.; Clement, B.M. and Backman, J. 1989: Pleistocene evolution: northern hemisphere ice sheets and north Atlantic ocean. *Paleoceanography 4* : 353–412.

Ryan, H.F.; Coleman, P.J. 1992: Composite transform-convergent plate boundaries : Description and discussion. *Marine and Petroleum Geology 9* : 89–97.

Scholz, C.H.; Rynn, J.M.W.; Weed, R.W.; Frolich, C. 1973: Detailed seismicity of the Alpine Fault zone and Fiordland region, New Zealand. *Bulletin of the Geological Society of America 84* : 3297–3316.

Scott, G.H.; Bishop, S.; Burt, B.J. 1990: Guide to some Neogene globorotalids (Foraminiferida) from New Zealand. *Palaeontological Bulletin, N.Z. Geological Survey 61* : 135 p.

Sengor, A.M.C. 1987: Cross faults and differential stretching of hangingwalls in regions of low-angle normal faulting: examples from western Turkey. *In* Coward, M.P.; Dewey, J.F.; Hancock, P.L. (eds) "Continental Extensional Tectonics". *Geological Society of London Special Publication 28* : 575–589.

Shackleton, N.J.; Opdyke, N.D. 1973: Oxygen isotope and paleomagnetic stratigraphy of equatorial Pacific core V28–238 : Oxygen isotope temperatures and ice volumes on a 10^5 year and 10^6 year scale. *Quaternary Research 3* : 39–55.

Shane, P.A.R. 1991: Remobilised silicic tuffs in middle Pleistocene fluvial sediments, southern North Island, New Zealand. *N.Z. Journal of Geology and Geophysics 34* : 489–499.

Shane, P.A.R.; Froggatt, P.C. 1991: Glass chemistry, paleomagnetism, and correlation of middle Pleistocene tuffs in southern North Island, New Zealand, and Western Pacific. *N.Z. Journal of Geology and Geophysics 34* : 203–211.

Shudofsky, G.N. 1985: Source mechanisms and focal depths of east African earthquakes using Rayleigh-wave inversion and body wave modelling. *Geophysical Journal of the Royal Astronomical Society 83* : 563–614.

Sibson, R.H. 1985: A note on fault reactivation. *Journal of Structural Geology 7* : 751–754.

Sibson, R.H.; White, S.H.; Atkinson, B.K. 1979: Fault rock distribution and structure within the Alpine Fault zone: a preliminary account. *In* Walcott, R.I.; Cresswell, M.M. (eds) "Origin of the Southern Alps". *Bulletin of the Royal Society of N.Z. 18* : 55–67.

Skinner, D.N. 1986: Neogene volcanism in the Hauraki Volcanic Region. *Bulletin of the Royal Society of N.Z. 23* : 21–47.

Smith, E.G.C.; Stern, T.; Reyners, M. 1989: Subduction and back-arc activity at the Hikurangi convergent margin, New Zealand. *Pure and Applied Geophysics 129* : 203–231.

Spörli, K.B. 1987: Development of the New Zealand microcontinent. *In* Monger J.W.H.; Francheteau, J. (eds) "Circum-Pacific Orogenic Belts and the Evolution of the Pacific Basin". *American Geophysical Union, Geodynamic Series 18* : 115–132.

Spörli, K.B. 1989: Tectonic framework of Northland, New Zealand. *In* Spörli, B.; Kear D. (eds) "Geology of Northland : Accretion, allochthons and arcs at the edge of the New Zealand micro-continent". *Bulletin of the Royal Society of N.Z. 26* : 3–14.

Spörli, K.B.; Ballance, P.F. 1989: Mesozoic-Cenozoic ocean floor/continent interaction and terrane configuration, southwest Pacific area around New Zealand. *In* Ben-Avraham, Z. (ed.) "The Evolution of the Pacific Ocean Margins". *Oxford Monograph, Geology and Geophysics 8* : 176–190.

Stearns, D.W.; Couples, G.D.; Jamison, W.R.; Morse, J.D. 1981: Understanding faulting in the shallow crust: contributions of selected experimental and theoretical studies. *In* Carter, N.L.; Friedman, M.; Logan, J.M.; Stearns, D.W. (eds) "Mechanical Behaviour of Crustal Rocks". The Handin Volume. *American Geophysical Union, Geophysical Monograph 24* : 215–229.

Stein, A.M.; Blundell, D.J. 1990: Geological inheritance and crustal dynamics of the northwest Scottish continental shelf. *Tectonophysics 173* : 455–467.

Stewart, R.B.; Neall, V.E. 1984: Chronology of paleoclimate change at the end of the last glaciation. *Nature 311* : 47–48.

Stock, J.M. 1989. Rigid plate reconstructions of New Zealand region since 68 Ma. Abstract, 28th International Geological Congress, Washington, D.C. Vol. 3 : 186.

Stock, J.; Molnar, P. 1982: Uncertainties in the relative positions of the Australia, Antarctica, Lord Howe, and Pacific plates since the Late Cretaceous. *Journal of Geophysical Research 87* : 4697–4714.

Stock, J.; Molnar, P. 1987: Revised history of early Tertiary plate motion in Southwest Pacific. *Nature 325* : 495–499.

Stow, D.A.V.; Holbrook, J.A. 1984: North Atlantic contourites : an overview. *In* Stow, D.A.V.; Piper, D.J.W. (eds) "Fine-grained Sediments : Deep-water processes and facies". *Geological Society of London Special Publication 15* : 245–256.

Suggate, R.P. 1990: Late Pliocene and Quaternary glaciations of New Zealand. *In* Clapperton C.M. (ed.) "Quaternary glaciations in the Southern Hemisphere". *Quaternary Science Reviews 9* : 175–197.

Suggate, R.P.; Stevens, G.R.; Te Punga, M.T. (eds) 1978: "The Geology of New Zealand". Government Printer, Wellington. 820 p.

Suppe, J. 1985: "Principles of Structural Geology". Englewood Cliffs, New Jersey, Prentice Hall, 537 p.

Tapponnier, P.; Molnar, P. 1979: Active faulting and Cenozoic tectonics of the Tien Shan, Mongolia, and Baykal regions. *Journal of Geophysical Research 84* : 3425–3459.

Taymaz, T.; Jackson J.; McKenzie, D. 1991: Active tectonics of the north and central Aegean Sea. *Geophysical Journal International 106* : 433–490.

Teng, L.S. 1990: Geotectonic evolution of late Cenozoic arc-continental collision in Taiwan. *Tectonophysics 183* : 57–76.

Thatcher, W.; Hill, D.P. 1991: Fault orientations in extensional and conjugate strike-slip environments and their implications. *Geology 19* : 1116–1120.

Tron, V.; Brun, J-P. 1991: Experiments on oblique rifting in brittle-ductile systems. *Tectonophysics 188* : 71–84.

Thrasher, G.P. 1990: Tectonics of the Taranaki Rift. Pp 124–133 *in* Proceedings of the New Zealand Oil Exploration Conference, Energy and Resources Division, Ministry of Commerce, Wellington.

Tulloch, A.J.; Kimbrough, D.L. 1989: The Paparoa metamorphic core complex, New Zealand : Cretaceous extension associated with the fragmentation of the Pacific margin of Gondwana. *Tectonics 8* : 1217–1234.

Uruski, C.I. 1992: Seismic evidence for dextral wrench faulting on the Moonlight Fault System. *N.Z. Geological Survey Record 44* : 69–75.

Uruski, C.I.; Turnbull, I.M. 1990: Stratigraphic and structural evolution of the western Southland sedimentary basins. Pp 225–240 *in* Proceedings of the New Zealand Oil Exploration Conference, Energy and Resources Division, Ministry of Commerce, Wellington.

Vail, P.R. 1987: Seismic stratigraphy interpretation using sequence stratigraphy, part 1 : Seismic stratigraphy interpretation procedure. *In* Bally, A.W. (ed.) "Atlas of Seismic Stratigraphy". *American Association of Petroleum Geologists, Studies in Geology 27* : 1-10.

Vail, P.R.; Mitchum, R.M. Jr.; Thompson, S. III. 1977: Seismic stratigraphy and global changes of sea-level. *In* Payton, C.W. (ed.) "Seismic Stratigraphic Applications to Hydrocarbon Exploration". *Memoir of the American Association of Petroleum Geologists 26* : 83–97.

Vail, P.R.; Audemard, F.; Bowman, S.A.; Eisner, P.N.; Perez- cruz, G. 1990: The stratigraphic signatures of tectonics, eustacy, and sedimentation. *American Association of Petroleum Geologists International Lecture* (version 2/15/90). Department Geology Geophysics, Rice University, Texas, 92 p.

Van Dissen, R.J. 1991: An evaluation of seismic hazard in the Kaikoura region, Southeastern Marlborough. *N.Z. Geological Survey Record 43* : 93–99.

Van Dissen, R.; Yeats, R.S. 1991: Hope Fault, Jordan Thrust, and uplift of the seaward Kaikoura Range, New Zealand. *Geology 19* : 393—396.

van Hoorn, B. 1987: The Celtic Sea/Bristol Channel Basin: origin, deformation and inversion history. *Tectonophysics 137* : 309–334.

Van Wagoner, J.C.; Posamentier, H.W.; Mitchum, R.M.; Vail, P.R.; Sarg, J.F.; Loutit, T.S.; Hardenbol, J. 1988: An overview of the fundamentals of sequence stratigraphy and key definitions. *In* Wilgus, C.K. *et al.* (eds) "Sea-level changes : An integrated approach". *Society of Economic Paleontologists and Mineralogists Special Publication 42* : 39–44.

Vella, P. 1963: Plio-Pleistocene cyclothems, Wairarapa, New Zealand. *Transactions of the Royal Society of N.Z. 2* : 15–49.

Vella, P. 1973: Ocean paleotemperatures and oscillations of the Subtropical Convergence Zone on the eastern side of New Zealand. Pp 315–318 *in* Fraser, R. (Comp.) "Oceanography of the South Pacific 1972". N.Z. National Commission for UNESCO, Wellington. 524 p.

Walcott, R.I. 1978: Present tectonics and late Cenozoic evolution of New Zealand. *Geophysical Journal of the Royal Astronomical Society 52* : 137–164.

Walcott, R.I. 1984a: The kinematics of the plate boundary zone through New Zealand: a comparison of short- and long-term deformations. *Geophysical Journal of the Royal Astronomical Society 79* : 613–633.

Walcott, R.I. 1984b: Reconstruction of the New Zealand region for the Neogene. *Paleogeography, Paleoclimatology, Paleoecology 46* : 217–231.

Walcott, R.I. 1987: Geodetic strain and the deformational history of the North Island of New Zealand during the late Cainozoic. *Philosophical Transactions of the Royal Society of London A321* : 163–181.

Walcott, R.I. 1989: The Paleogene plate boundary through New Zealand. *Geological Society of N.Z. Miscellaneous Publication 43* : 99.

Walcott, R.I. 1993: Neogene tectonics and kinematics of western North America. *Tectonics 12* : 326–333.

Walker, R.G.; Mutti, E. 1973: Turbidite facies and facies associations. Pp 119–158 *in* Middleton, G.V.; Bouma, A.H. (eds) "Turbidites and Deep-water Sedimentation". Society of Economic Paleontologists and Mineralogists, Pacific Short Course Notes, Anaheim.

Wang, H.; McCave, I.N. 1990: Distinguishing climatic and current effects in the mid-Pleistocene sediments of Hatton and Gardar Drifts, NE Atlantic. *Journal of the Geological Society of London 147* : 373–383.

Waters, D.W. 1988: The Flags Creek thrust. Unpublished B.Sc. (Hons) thesis, lodged in the library, Victoria University of Wellington, Wellington, N.Z.

Watkins, N.D.; Huang, T.C. 1977: Tephras in abyssal sediments east of the North Island, New Zealand : Chronology, paleowind velocity, and paleoexplosivity. *N.Z. Journal of Geology and Geophysics 20* : 179–198.

Watkins, N.D.; Kennett, J.P. 1971: Antarctic Bottom Water: major change in velocity during the Late Cenozoic between Australia and Antarctica. *Science 173* : 813–818.

Weissel. J.K.; Hayes, D.E; Herron, E.M. 1977: Plate tectonics synthesis: the displacements between Australia, New Zealand, and Antarctica since the late Cretaceous. *Marine Geology 25* : 231–277.

Wellman, H.W. 1979: An uplift map of the South Island of New Zealand and a model for the origin of the Southern Alps. *In* Walcott, R.I.; Cresswell, M.M. (eds) "Origin of the Southern Alps". *Bulletin of the Royal Society of N.Z. 18* : 13-20.

Wernicke, B.; Burchfiel, B.C. 1982: Modes of extensional tectonics. *Journal of Structural Geology 4* : 105–115.

White, N.J.; Jackson, J.A.; McKenzie, D.P. 1986: The relationship between the geometry of normal faults and that of the sedimentary layers in their hanging walls. *Journal of Structural Geology 8* : 897–909.

Wilcox, R.E.; Harding, T.P.; Seely, D.R. 1973: Basic wrench tectonics. *Bulletin of the American Association of Petroleum Geologists 57* : 74–96.

Willcox, J.B.; Stagg, H.M.J. 1990: Australia's southern margin : A product of oblique extension. *Tectonophysics 173* : 269–281.

Wilson, C.J.N.; Rogan, A.M.; Smith, I.E.M. 1984: Caldera volcanoes of the Taupo Volcanic Zone, New Zealand. *Journal of Geophysical Research 89* : 8463–8484.

Wilson, D.D. 1963: Geology of the Waipara subdivision. *Bulletin of the N.Z. Geological Survey 64.*

Winter, A.; Martin, K. 1990: Late Quaternary history of the Agulhas Current. *Paleoceanography 5* : 479–486.

Withjack, M.O.; Olson, J.; Peterson, E. 1990: Experimental models of extensional forced folds. *Bulletin of the American Association of Petroleum Geologists 74* : 1038–1054.

Wood, R.A. 1991: Structure and seismic stratigraphy of the western Challenger Plateau. *N.Z. Journal of Geology and Geophysics 34* : 1–9.

Wood, R.A.; Andrews, P.B.; Herzer, R.H. *et al.* 1989: Cretaceous-Cenozoic geology of the Chatham Rise region, South Island, *N.Z. Geological Survey Basins Studies 3* : DSIR, Wellington, 76 p.

Wood, R.A.; Herzer, R.H. (in press): The Chatham Rise, New Zealand. *In* Ballance P.F. (ed.) "South Pacific Sedimentary Basins. Sedimentary Basins of the World", Elsevier.

Wright, I.C.; Ashby, J.N.; Hoskins, R.H. 1985: An age for the sudden disappearance of *Globorotalia dehiscens* in Mangapoike River Valley, New Zealand. *N.Z. Geological Survey Record 9* : 102–104.

Yeats, R.S. 1983: Large scale Quaternary detachments in Ventura Basin, southern California. *Journal of Geophysical Research 88* : 569–583.

Yeats, R.S. 1987: Coseismic folding. *In* Crone, A.J.; Omdahl, E.M. (eds) "Directions in Paleoseismology". *U.S. Geological Survey Open File Report 87–673* : 163–172

Yousif, H.S. 1987: The applications of remote sensing to geomorphological neotectonic mapping in north Canterbury, New Zealand. Unpublished Ph.D. thesis, lodged in the library, University of Canterbury, Christchurch, N.Z.

Zhao, Z.Y.; Windley, B.F. 1990: Cenozoic tectonic extension and inversion of the Jizhong Basin, Hebei, northern China. *Tectonophysics 185* : 83–89.

Zoback, M.D.; Zoback, M. 1980: State of stress in the conterminous United States. *Journal of Geophysical Research 85* : 6113–6156.

APPENDIX 1

SUMMARY OF SEISMIC PROFILES referred to in this thesis.

Thesis Figure	Profile No. (Thesis)	Data Source (Cruise)	Profile Reference	Date Obtained	Time	Data Type
3.3	A	Cr. 2030	MC4	22.9.89	0320-0840	3.5 kHz
3.3	B	"	M6	20.9.89	1110-1205	"
3.3	C	"	MC8	26.9.89	0220-0450	"
3.3	D	"	TR20	2.10.89	1310-1430	"
3.3	E	"	TR1	25.9.89	2010-2040	"
3.3	F	"	M8	20.9.89	1810-1910	"
3.3	G	"	M6–M7	"	1230-1330	"
3.3	H	"	M3–M4	"	0210-0320	"
3.3	I	"	TA2	1.10.89	0330-0415	"
3.3	J	"	MC7	25.9.89	2240-2335	"
3.3	K	Cr 2019	28	10.6.88	2200-2245	"
3.3	L	Cr 2030	TR6	29.9.89	0635-0730	"
3.3	M	"	TA2	1.10.89	0450-0600	"
3.4	A	Cr. 2030	M1	19.9.89	1840-1930	3.5 kHz
3.4	B	"	M10	25.9.89	0220-0320	"
3.4	C	"	M12	"	1420-1540	"
3.4	D	"	MA3	26.9.89	0430-0520	"
3.5	A	Cr. 2030	M9	22.9.89	2330-0015	3.5 kHz
3.5	B	"	MC3	21.9.89	2240-0120	"
3.5	C	"	TA2	1.10.89	0230-0340	"
3.5	D	"	TR6	29.9.89	0710-0840	"
4.3	A	Cr. 2030	MA1	21-22.9.89	2230-0640	Airgun # 40
4.3	B	"	MA2	23-24.9.89	2320-0600	"
4.3	C	"	MA3	26-27.9.89	0430-0050	"
4.4		Cr. 2030	U645-U646	23.9.89	1250-1400	3.5 kHz
4.5	A	Cr. 2030	M5	20.9.89	0830-0910	3.5 kHz
4.5	B	"	M11	25.9.89	0840-1010	"
4.5	C	"	M6	20.9.89	1115-1205	"
4.5	D	"	M9	22.9.89	2320-0110	"
4.6	A	Cr. 2030	MC4	22.9.89	0300-0840	3.5 kHz
4.6	B	"	MC3	21.9.89	2110-0120	"

Thesis Figure	Profile No. (Thesis)	Data Source (Cruise)	Profile Reference	Date Obtained	Time	Data Type
5.2	1–1'	Cr. 2046	46/18	13.7.91	0540-0810	*Airgun # 120
5.2	2–2'	"	46/19	"	1110-1520	"
5.2	3–3'	*MIOC	72–7	17.2.72	2220-0110	Multichannel
5.4	4–4'	Cr. 2046	46/14	12.7.91	0250-0700	Airgun # 120
5.4	5–5'	"	46/18	13.7.91	0320-0630	"
5.6	6–6'	Cr. 2030	MA3	26-27.9.89	2210-0105	Airgun # 40
5.6	6–6'	"	MA3	"	2210-0200	3.5 kHz
5.6	7–7'	"	MA1	21-22.9.89	2310-0150	Airgun # 40
5.6	7–7'	"	MA1	"	2310-0240	3.5 kHz
6.1	1–1'	Cr. 2046	46/18	13.7.91	0150-0450	Airgun # 120
6.1	4–4'	"	46/18	"	0540-0810	"
6.2	2–2'	Cr. 2034	A23	11.9.90	1730-2200	Airgun # 40
6.2	3–3'	Cr. 2046	46/20	13.7.91	1950-2230	Airgun # 120
6.3	5–5'	Cr. 2040	M13	11.12.90	0250-0140	3.5 kHz
6.3	6–6'	Cr. 2030	MA3	26.9.89	2210-0105	"
6.3	6–6'	"	MA3	"	2220-0220	Airgun # 40
6.3	7–7'	"	MA2	23.9.89	2220-0140	3.5 kHz
6.3	7–7'	"	MA2	"	2010-0210	Airgun # 40
6.4	8–8'	Cr. 2046	46/14	12.7.91	0250-0500	Airgun # 120
6.4	9–9'	Cr. 2030	MA1	21-22.9.89	2310-0220	3.5 kHz
6.4	9–9'	"	MA1	"	2220-0230	Airgun # 40
6.4	10–10'	"	M3	20.9.89	0045-0200	3.5 kHz
6.4	11–11'	"	MC1	21.9.89	0110-0615	"
6.4	12–12'	"	MC6	24.9.89	2050-0000	"
7.3	1	*AGOC	NZ-76	1973	0500-1730	Multichannel
7.3	2	*MIOC	72-5	20.3.72	1240-1640	"
7.4	3	Cr. 2046	46/2	9.7.91	0650-0820	3.5 kHz
7.4	4	Cr. 2034	11	4.4.90	2220-2320	"
7.4	5	"	9	"	1700-1810	"
7.4	6	Cr. 2046	46/3	9.7.91	1000-1030	"
7.4	6	"	46/3	"	0850-1020	Airgun # 20
7.6	7	Cr 2046	46/1	19.7.91	0550-0635	3.5 kHz
7.6	7	"	46/1	"	0525-0630	Airgun # 20

Thesis Figure	Profile No. (Thesis)	Data Source (Cruise)	Profile Reference	Date Obtained	Time	Data Type
7.6	8	Cr. 2034	24	8.4.90	0020-0056	3.5 kHz
7.6	9	"	A12	9.4.90	2120-2230	"
7.6	9	"	A12	"	2120-2320	Airgun # 20
7.7	10	Cr. 2034	25	8.4.90	0120-0205	3.5 kHz
7.7	11	"	26	"	0325-0400	"
7.7	12	"	29	"	0700-0740	"
7.7	13	"	A7	"	0905-0945	"
7.7	13	"	A7	"	0855-1010	Airgun # 20
7.8	15	Cr. 2034	A3	8.4.90	1900-1950	3.5 kHz
7.8	15	"	A3	"	1800-1855	"
7.8	15	"	A3	"	1810-2000	Airgun # 20
7.8	16	"	AC12	"	2010-2230	"
7.8	14	*MIOC	72-6	17.2.72	1118-1410	Multichannel
7.8	17	Cr. 2046	46/6	9.7.91	1735-1950	Airgun # 20
7.9	18	Cr. 2046	46/1	9.7.91	0450-0520	3.5 kHz
7.9	19	Cr. 2034	8	4.4.90	1400-1420	"
7.9	20	"	A7	8.4.90	1115-1140	Airgun # 20
7.9	21	"	AC11	9.4.90	0230-0430	"
7.10	22	Cr. 2034	20	7.4.90	1220-1320	3.5 kHz
7.10	23	"	22	"	2110-2140	"
7.10	24	"	A21	10.4.90	0455-0630	"
7.10	25	"	S53	6.4.90	2040-2150	"
7.10	26	"	S54	6-7.4.90	2350-0030	"
7.10	27	"	AC10	10.4.90	0435-0550	"

* Airgun # 40 - Single channel airgun profile. Number refers to size of airgun chamber (cubic inches)

* MIOC - Mobil International Oil Co. (1972)

* AGOC - Australian Gulf Oil Co. (1973)

Cr. 2030 - NZOI Cruise number.

APPENDIX 2

SUMMARY OF PISTON CORES
referred to in this thesis.

Core	NZOI Cruise	Date Obtained	Latitude (° S)	Longitude (° E)	Depth (m)	Length (m)
S871	2019	12.6.88	42 57.0'	174 00'	1555	0.20
U640	2030	22.9.89	42 51.35'	174 13.97'	1480	1.10
U641	"	"	42 53.8'	174 12.38'	1332	1.90
U642	"	"	43 02.0'	174 27.0'	739	2.25
U643	"	"	43 54.22'	174 47.8'	828	2.55
U645	"	23.9.89	42 35.32'	174 43.05	1760	2.73
U646	"	"	42 37.23'	174 46.49'	1707	1.20
U647	"	"	43 00.33'	175 08.69'	411	1.78
U649	"	24.9.89	42 31.8'	174 25.34'	2284	2.30
U650	"	"	42 47.73'	174 32.8'	1300	3.15
U651	"	26.9.89	42 31.89'	175 17.54'	1885	2.97
U652	"	"	42 32.71'	175 25.05'	1801	1.20
U653	"	"	42 30.65'	175 47.30'	1713	2.40
U654	"	"	42 32.41'	175 48.17'	1260	1.80
U661	"	2.10.89	42 21.34'	176 23.31'	2830	1.77
U683	2034	9.4.90	42 48.4'	173 31.4'	95	0.44
U685	"	"	42 49.30'	173 33.9'	108	1.05
U686	"	"	42 51.3'	173 37.4'	111	0.80
U687	"	'	42 56.2'	173 30.8'	83	0.40
U689	"	"	43 01.2'	173 14.85'	36	0.75
U693	"	10.4.90	43 05.64'	173 20.03'	56	2.20
U694	"	"	43 02.1'	173 15.5'	44	0.30
U695	"	"	43 09.0'	173 03.9'	40	0.80
U698	"	"	43 06.95'	173 02.1'	24	0.35
U934	2046	10.7.91	43 01.2'	173 19.8'	57	0.25
U935	"	"	43 00.48'	173 20.74'	55	0.56
U937	"	11.7.91	43 00.3'	173 13.98'	29	0.35

APPENDIX 3

ANALYSIS AND INTERPRETATION OF TUFFACEOUS HORIZONS IN CHATHAM RISE SEDIMENT CORES

INTRODUCTION

Several cores of Pliocene-Pleistocene sediments from the NW Chatham Rise slope contain a significant amount of volcanic glass in tuffaceous horizons. The tuffaceous horizons are not megasopic and cannot be seen without microscopic examination. A joint study was undertaken with Philip Shane (Victoria University of Wellington) to examine the cores. The aims of the study were to: (i) locate and sample the glass-rich (tuffaceous) horizons; (ii) analyse the composition of the volcanic material and identify the likely source region of the eruptions; (iii) correlate the tuffaceous horizons (within the biostratigraphic framework) with tephra in other deep-sea cores and with onland sequences nearer the source; and (iv) account for the absence of megascopic ash in the cores.

The author was responsible for interpretation of the seismic stratigraphy and biostratigraphy, for locating the tuffaceous horizons by microscopic examination of samples, undertaking related sedimentological studies of the cores, including the textural and carbonate analyses and X-ray radiography, and for interpretation of the sedimentary processes responsible for deposition of the sediments. Philip Shane was responsible for identifying the volcanic mineralogy, analysing the chemistry of volcanic glass shards by electron microprobe, and for comparisons and correlations of the tuffaceous horizons with tephra in other deep-sea cores and in onland sequences in New Zealand.

METHODS

Sand fractions were extracted from all cores at 100–300 mm intervals and examined so that microscopic tuffaceous horizons could be identified for analysis. For comparisons with relevant tephras in other deep-sea cores and nearer the source, the glass chemistry of shards from 25 tuffaceous horizons in 8 cores was analysed by a Jeol 733 electron microprobe. Methods and standards for the Jeol 733 are described by Froggatt (1983). For microprobe operating conditions we used a 8 nA current at 15 kV and a 20 μm beam diameter.

VOLCANIC GLASS

Concentration and mineralogy

Megascopic tephra layers were not recognised in any core, but dispersed clear volcanic glass shards represent a dominant component of the sand fraction in many samples (Fig. 3.6). In some tuffaceous horizons, there are sparse euhedral ferromagnesian crystals, some of which have adhering glass indicating a volcanogenic origin. Hypersthene and green hornblende are identified, consistent with the rhyolitic composition for the glasses from electron microprobe analysis.

Considerable amounts of glass occur in eight cores of Late Opoitian to mid-late Haweran (late Early Pliocene to Late Pleistocene) age (Fig. 3.6). Those horizons in which glass shards are most abundant were analysed. These horizons are not evident on X-ray radiographs of core slices, which only reveal textural and structural features of the sediments (e.g., cf. Figs 3.6 and 3.8).

Glass chemistry

Over 230 shards were analysed by electron microprobe from 26 tuffaceous horizons. All shards have calc-alkaline rhyolitic compositions with SiO_2 content in the range 73.5–79.3 wt %, and total alkalis in the range 7.2–8.5 wt % (Table A3.1). Most have Na/K > 1. On Harker variation diagrams (e.g., Fig. A3.1) the shards form a unimodal grouping, indicating a single or closely related source provenance with similar petrogenetic origins. Their calc-alkaline composition and stratigraphic age indicate two possible source regions within New Zealand: Taupo Volcanic Zone (TVZ) (Cole, 1979; Froggatt, 1983; Wilson *et al.*, 1984; Shane and Froggatt, 1991) and the now extinct Coromandel Volcanic Zone (CVZ) (Skinner, 1986; Briggs and Fulton, 1990). No evidence is seen for eruptive products from contemporary, intraplate basaltic volcanic centres such as at Timaru (Duggan and Reay, 1986) and the Chatham Islands (Grindley *et al.*, 1977). It is not possible to differentiate a TVZ source from a CVZ source on the basis of glass composition.

Only seven of the tuffaceous horizons examined have homogeneous chemical populations of shards indicative of single eruptive events. The rest are heterogeneous with two or more populations of glass mixed together (Fig. A3.2). The glass shards in the tuffaceous horizons can be grouped into four broad classes (Shane, 1991): (1) single homogeneous glass populations representing single eruptive events (Fig.A3.2A); (2) a major glass population with a few anomalous shards, probably reworked (Fig. A3.2B); (3) two discrete populations of glass shards inferred to represent separate eruptive events (Fig. A3.2C); and (4) multiple and indistinguishable glass populations that indicate mixing of two or more eruptive events (Fig. A3.2D). The distribution of these classes in cores is shown on Figure 3.6.

Table A3.1

Electron microprobe analyses of glass shards in cores from the Chatham Rise. Analyses are recalculated to 100% on a volatile free basis and presented as a mean and standard deviation (in parentheses). Water by difference. n = number of shards analysed.

	642/31A	642/31B	642/103	642/131	642/161	642/181	650/91
SiO_2	77.74 (.21)	78.19 (.25)	77.42 (.97)	78.04 (.25)	77.98 (.55)	78.02 (.02)	77.64 (.32)
Al_2O_3	12.34 (.12)	12.35 (.17)	12.44 (.42)	12.17 (.16)	12.20 (.14)	12.21 (.11)	11.92 (.11)
TiO_2	0.17 (.05)	0.11 (.01)	0.17 (.09)	0.15 (.03)	0.13 (.05)	0.13 (.03)	0.15 (.04)
FeO	1.43 (.10)	1.14 (.06)	1.41 (.35)	1.26 (.14)	1.41 (.42)	1.11 (.10)	1.03 (.12)
MgO	0.14 (.02)	0.11 (.03)	0.16 (.05)	0.12 (.02)	0.11 (.03)	0.12 (.04)	0.12 (.03)
CaO	1.11 (.11)	1.02 (.13)	1.15 (.12)	1.07 (.05)	1.07 (.06)	1.08 (.08)	0.84 (.10)
Na_2O	3.95 (.08)	3.88 (.16)	3.93 (.12)	3.92 (.08)	3.82 (.07)	3.87 (.09)	3.60 (.08)
K_2O	3.00 (.12)	3.07 (.09)	3.16 (.21)	3.08 (.09)	3.09 (.13)	3.24 (.11)	4.47 (.22)
Cl	0.18 (.04)	0.17 (.04)	0.19 (.06)	0.20 (.04)	0.19 (.05)	0.22 (.06)	0.24 (.08)
H_2O	5.85 (.99)	5.70 (.97)	6.29 (.98)	4.70 (.99)	5.95 (2.06)	5.61 (1.14)	4.04 (.94)
n	8	3	8	10	8	10	10

	650/181	650/210	646/91	646/111	640/82	654/03	654/21
SiO_2	78.01 (.33)	77.31 (.79)	76.19 (.20)	76.20 (.46)	77.19 (.90)	77.60 (.19)	76.69 (.72)
Al_2O_3	11.92 (.06)	12.03 (.25)	12.75 (.12)	12.81 (.17)	12.31 (.35)	12.27 (.17)	12.57 (.26)
TiO_2	0.13 (.04)	0.15 (.05)	0.24 (.06)	0.23 (.06)	0.15 (.05)	0.14 (.02)	0.16 (.05)
FeO	0.93 (.18)	0.98 (.05)	1.76 (.07)	1.67 (.20)	1.24 (.28)	1.24 (.18)	1.43 (.25)
MgO	0.10 (.03)	0.13 (.03)	0.16 (.02)	0.16 (.04)	0.12 (.04)	0.13 (.04)	0.13 (.03)
CaO	0.79 (.23)	1.11 (.61)	1.04 (.07)	1.09 (.11)	0.98 (.19)	1.08 (.11)	0.98 (.13)
Na_2O	3.56 (.09)	3.55 (.15)	4.39 (.09)	4.29 (.15)	4.06 (.28)	3.95 (.20)	4.23 (.23)
K_2O	4.32 (.34)	4.47 (.11)	3.23 (.07)	3.34 (.13)	3.75 (.26)	3.44 (.52)	3.62 (.10)
Cl	0.24 (.04)	0.27 (.02)	0.24 (.09)	0.20 (.05)	0.21 (.04)	0.21 (.03)	0.21 (.05)
H_2O	6.10(2.45)	4.36 (1.36)	6.19 (1.56)	5.45 (.95)	5.53 (1.18)	5.79 (1.84)	6.14 (1.43)
n	6	7	7	10	10	10	10

	654/77	652/04	652/11	652/20	652/23	661/21	661/33
SiO_2	77.10 (.38)	75.71 (1.18)	75.22 (.49)	75.02 (.38)	74.99 (.44)	77.57 (.12)	76.65 (1.16)
Al_2O_3	12.68 (.19)	12.88 (.52)	13.02 (.25)	12.98 (.21)	12.91 (.28)	12.06 (.11)	12.44 (.49)
TiO_2	0.14 (.03)	0.15 (.04)	0.15 (.04)	0.17 (.03)	0.18 (.05)	0.12 (.03)	0.17 (.07)
FeO	1.35 (.19)	1.58 (.52)	1.84 (.25)	1.85 (.13)	1.95 (.21)	1.23 (.09)	1.47 (.38)
MgO	0.15 (.03)	0.12 (.03)	0.09 (.02)	0.11 (.02)	0.10 (.02)	0.10 (.01)	0.13 (.06)
CaO	1.36 (.08)	1.01 (.12)	0.92 (.13)	0.92 (.06)	0.97 (.14)	0.96 (.03)	1.08 (.25)
Na_2O	4.04 (.15)	4.20 (.34)	4.22 (.22)	4.07 (.14)	4.10 (.19)	3.91 (.12)	4.08 (.24)
K_2O	3.02 (.09)	4.07 (.36)	4.37 (.40)	4.62 (.23)	4.56 (.38)	3.83 (.04)	3.79 (.38)
Cl	0.18 (.06)	0.28 (.04)	0.23 (.05)	0.27 (.04)	0.24 (.03)	0.23 (.02)	0.22 (.05)
H_2O	7.90 (.88)	8.18 (1.15)	6.15(1.12)	6.15 (.88)	6.13 (1.28)	3.91 (.95)	3.99 (.67)
n	9	9	10	10	10	10	8

	661/41	661/76	661/103	661/131	661/133
SiO_2	77.03 (1.25)	76.36 (1.50)	75.74 (1.24)	75.35 (1.32)	76.65(1.16)
Al_2O_3	12.31 (.43)	12.62 (.50)	12.90 (.47)	12.94 (.44)	12.44 (.49)
TiO_2	0.15 (.08)	0.20 (.09)	0.23 (.08)	0.27 (.09)	0.17 (.07)
FeO	1.53 (.52)	1.70 (.54)	1.79 (.35)	1.93 (.33)	1.47 (.38)
MgO	0.13 (.07)	0.21 (.12)	0.20 (.09)	0.27 (.06)	0.13 (.06)
CaO	1.09 (.23)	1.21 (.37)	1.57 (.25)	1.58 (.28)	1.08 (.25)
Na_2O	3.98 (.21)	4.13 (.23)	4.15 (.23)	4.23 (.15)	4.08 (.24)
K_2O	3.58 (.25)	3.50 (.37)	3.27 (.34)	3.30 (.17)	3.79 (.38)
Cl	0.20 (.03)	0.18 (.05)	0.15 (.05)	0.16 (.03)	0.22 (.05)
H_2O	4.64 (1.01)	4.05 (.54)	5.73 (1.48)	6.03 (.03)	3.99 (.67)
n	8	10	12	9	8

Sample names = U core number/depth from top in centimetres.
Analyses with large standard deviations (e.g., FeO > 0.15 wt%, TiO_2 and MgO > 0.04 wt%) represent the means of two or more compositional populations within the sample.
Sample 642/31 has been separated into two glass populations (A and B).

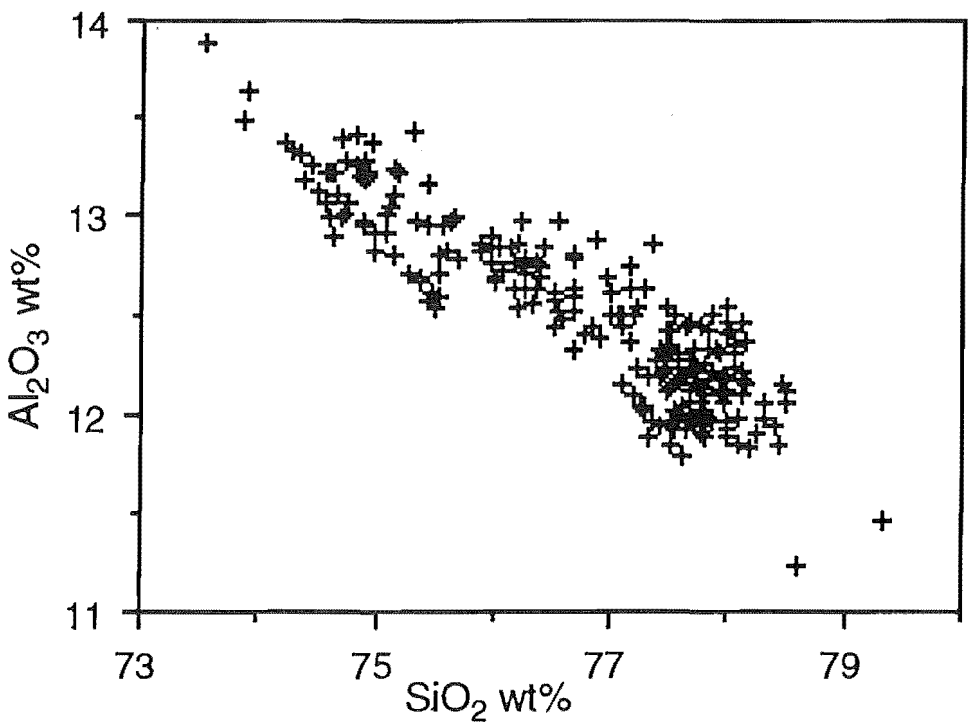

Fig. A3.1. Compositional range displayed by 230 glass shards from Chatham Rise cores.

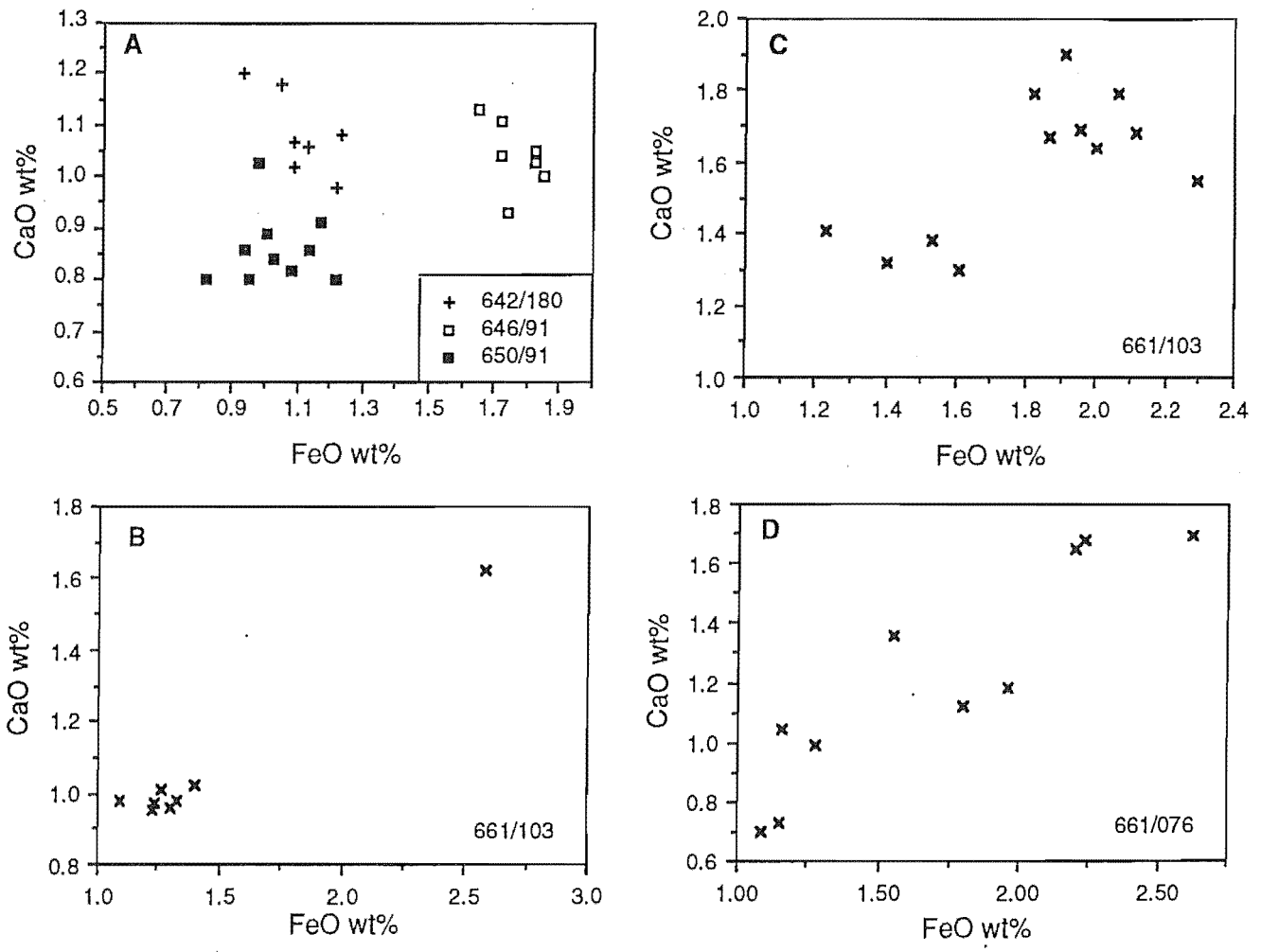

Fig. A3.2. Characteristics of tuffaceous horizons in Chatham Rise cores as shown by individual shard analyses. **A.** Three horizons, each consisting of a single, discrete, compositional population. **B.** Horizon consisting of a large population and containing a chemically anomalous shard. **C.** Horizon consisting of two compositional populations. **D.** Multiple populations or a near-continuum within a tuffaceous horizon.

Because of the degree of mixing of different eruptive products in the cores, it is uncertain how many eruptive events are recorded. For Pleistocene-aged sediments, five chemically distinctive horizons or zones are recognised based on a dominant glass population within the samples. Three chemically distinctive horizons occur in core U642 at (1) 0.31 m depth; (2) 1.31 m depth; and (3) at 1.81 m depth. A fourth chemically distinctive horizon occurs at depths of 0.91 m and 1.11 m in core U646, and a fifth horizon occurs at 0.91 m in core U650. Because each horizon is chemically and stratigraphically different, five major eruptive events are recorded. In addition, a number of smaller eruptive events are recorded as anomalous shards within and between these horizons.

Correlations

Volcanic ash (tephra) is common in Pliocene-Pleistocene deep-sea sediments elsewhere in the southwest Pacific Ocean, at sites up to 1100 km east and southeast of volcanic centres in central New Zealand (Ninkovich, 1968; Watkins and Huang, 1977; Froggatt *et al.,* 1986). Several authors have attempted to correlate Pleistocene tephra exposed in onshore sequences in New Zealand with deep-sea cores up to about 1000 km away in the Southwest Pacific using magnetostratigraphy, biostratigraphy, fission-track ages, and more recently by chemical fingerprinting of glass shards (Watkins and Huang, 1977; Froggatt, 1983; Froggatt *et al.*, 1986; Nelson *et al.*, 1986a; Shane and Froggatt, 1991). Using the seismic-stratigraphy established for the North Chatham Rise slope (Fig. 4.2) and comparing the glass chemistry of tuffaceous horizons in cores from this region with tephra in other deep- sea cores and in onshore sequences in New Zealand, two tentative correlations can be made. These are (1) the Late Pleistocene core U650, 0.91 m depth, can be correlated with the widespread Mt Curl Tephra (referred to as Rangitawa Tephra by Kohn *et al.*, 1992, variously dated at 0.23–0.38 Ma (Froggatt *et al.,* 1986) but which is probably close to 0.35 Ma old (Kohn *et al.,* 1992); and (2) the Late Pleistocene core U642, 1.80 m depth, with the c. 0.27 Ma Layer E tephra of Ninkovich (1968) and Watkins and Huang (1977).

Glass compositions have been compared for correlation purposes using similarity coefficients (SC) (Borchardt *et al.,* 1971), based on all oxides except Cl which is often invariant. High values of SC (> 0.92) are obtained for correlative samples. The compositions of tephras from elsewhere that were used for correlation purposes are shown in Table A3.2. An SC of 0.96 was obtained for the match between glass at 0.91 m in core U650 and the Mt Curl Tephra at its type section in the Manawatu-Wanganui area (Table A3.2). This tephra is distinctive in its high K_2O content and Na/K < 1 compared to other Late Pleistocene tephras (Froggatt *et al.,* 1986). The Haweran biostratigraphic age of core U650 supports this chemical correlation. Mt Curl Tephra, the co-eruptive airfall equivalent of the Whakamaru Ignimbrite, has been recognised

Table A3.2

Composition of tephras used in correlations to samples from Chatham Rise cores.
Analyses presented as in Table A3.1.
Grid references from the metrid NZMS 260 map series.

	Layer E[1]	Matahina Ignimbrite[2]	Layer D[3]	Mt Curl Tephra[4]
SiO_2	78.11 (.33)	77.38 (.45)	77.93 (.28)	78.09 (.30)
Al_2O_3	12.45 (.24)	12.54 (.27)	12.26 (.17)	12.33 (.21)
TiO_2	0.13 (.03)	0.12 (.02)	0.12 (.03)	0.14 (.03)
FeO	1.13 (.12)	1.07 (.07)	0.87 (.11)	1.01 (.08)
MgO	0.11 (.03)	0.11 (.02)	0.12 (.02)	0.12 (.02)
CaO	0.88 (.07)	0.88 (.05)	0.78 (.05)	0.79 (.04)
Na_2O	3.76 (.17)	3.91 (.15)	3.53 (.14)	3.30 (.16)
K_2O	3.37 (.18)	3.83 (.17)	4.38 (.18)	4.33 (.15)
Cl	-	0.18 (.02)	-	-
H_2O	4.35 (.69)	5.04 (1.95)	4.38 (1.03)	4.55 (.13)
n	21	10	18	132

[1] Core RC12–215, western Pacific lat. 35°28', long. 167°53.5' (Froggatt, unpubl. data)
[2] State Highway 38, Murupara, V17/305993.
[3] Core RC12–215 (Froggatt *et al.*, 1986).
[4] Mt Curl Road, Manawatu, S22/195345 (Froggatt *et al.*, 1986).

in Tasman Sea DSDP core 591 and Southwest Pacific cores (Watkins and Huang, 1977; Froggatt, 1983; Froggatt *et al.*, 1986; Nelson *et al.*, 1986a). In the southwestern Pacific the correlative of the Mt Curl Tephra is known as Layer D. An SC of 0.94 was obtained for comparison of glass in core U650 with Layer D in core RC 12-215.

Core U642 is inferred to be stratigraphically younger than U650 (Fig. 4.2). Glass shards in core U642 at a depth of 1.81 m represent a chemically distinctive single population similar to Layer E found in several deep-sea cores in the western Pacific, including RC12–215 (Table 2; SC = 0.95). An age of c. 0.27 Ma for Layer E (Ninkovich 1968) is consistent with the stratigraphic position of core U642. Froggatt (1983) suggested the correlation of Layer E to the Matahina Ignimbrite in the Bay of Plenty region of North Island. An SC of 0.93 was obtained for the comparison between glass at 1.81 m in core U642 and this ignimbrite.

DISCUSSION

Eruptive Source and Ash Accumulation on a Current-swept Seafloor

The rhyolitic tephra deposited on the NW Chatham Rise slope is inferred to be the airfall product of eruptions from two closely related source provences within the late Cenozoic, North Island, calc-alkaline arc. The upper, late Opoitian (c. 4.0–3.6 Ma) part of sequence 13 (cores U652, U653 and U654), and the late Opoitian-Waipipian core U661 (Fig. 3.6) probably predate the onset of volcanism within the TVZ about 2.3–2.0 Ma (Lowe *et al.*, 1988; Grindley *et al.*, 1988) and hence, the shards are inferred to be products of now-extinct rhyolitic centres (Fig. 2.1) on the Coromandel Peninsula (Skinner, 1986; Nelson *et al.*, 1986). The number of discrete eruptions recorded in the Early Pliocene cores is uncertain because mixing of separate eruptive products is common (Fig. 9.2) and because the detailed stratigraphic relationships between the cores is not known (they may or may not be chronostratigraphically synchronous).

In contrast to the Early Pliocene cores, the Late Pliocene-Late Pleistocene (c. 1.6–0.25 Ma) cores from seismic unit 10 to 6 (Fig. 4.2) contain the distal airfall products of at least five eruptions from the TVZ. These include possible co-eruptive correlatives of the Late Pleistocene Whakamaru and Matahina Ignimbrites. Rare to very minor amounts of glass occur throughout the post last-glacial age seismic unit 1 cores U645, U651, and U653 (Figs 3.6 and 4.2). Some of this glass in unit 1 is reworked from older sequences, and some may be airfall sprinklings from TVZ eruptions.

Distances of 460–600 km between the volcanic source areas and the core sites imply that very explosive eruptions have occurred since the Early Pliocene. As the present prevailing winds in the region are westerlies, the presence of glass shards at

these distances to the south of the sources suggest the ejection of material high into the atmosphere (e.g., Nelson *et al.*, 1986a). Large, explosive, silicic eruptions are often associated with caldera formation. Such calderas are known from the TVZ (Wilson *et al.*, 1984) and have recently been found in the CVZ (Briggs and Fulton, 1990). Rock compositions from these areas are broadly similar to glasses found in the Chatham Rise cores and, thus, we consider the latter to be distal products of these large eruptions.

An important feature of volcanic glass occurrence on the NW Chatham Rise slope is the absence of megascopic tephra in all cores. This is unusual for deep-sea cores from east of New Zealand spanning the interval from late Early Pliocene to late Quaternary. For example, of the 17 tephras identified by Watkins and Huang (1977) in South Pacific cores, 8 are megascopic and include the 5 five tephras recognised by Ninkovich (1968). Elsewhere, in DSDP Leg 90 cores from the southwest Pacific and Tasman Sea, 15 late Cenozoic, silicic, megascopic tephras have been recorded (Nelson *et al.*, 1986a).

One explanation for the absence of megascopic tephra in cores from the NW Chatham Rise slope is that the combined physical oceanographic and sedimentary processes made this region unfavourable for developing thick concentrations of ash on the seafloor, irrespective of the rates of airfall transport of glass to the area. The sediments are inferred to have accumulated at low rates and bioturbation is extensive, producing predominantly homogenous and mottled sedimentary textures (Chapter 3). In addition, significant bottom-current activity is clear from the multiple, regional-scale erosion surfaces and sediment drifts evident in seismic profiles, from the sedimentary textures in cores, and from the presence of corroded and reworked microflora (Chapter 4). These combined processes have the effect of disseminating and reworking the glass shards into the terrigenous and biogenic components of the sediments, enabling multiple tephra deposits to be mixed. Furthermore, the NW Chatham Rise slope lies due south of the inferred volcanic sources, which is probably not favourable for maximum fallout, considering the prevailing westerly winds. Some of the eruptions recorded simply may not have been of sufficient magnitude to produce visible ash at the site, although this clearly does not account for the microscopic occurrence of Mt Curl Tephra, which is 100 mm thick at DSDP site 594 to the south (Fig. 4.1) (Froggatt *et al.*, 1986).

CONCLUSIONS

1. No megascopic tephra occur in any cores from the NW Chatham Rise slope, but the relative down-core concentrations of glass indicate prominent fluctuations in the rate of tephra accumulation during the Pliocene-Pleistocene. Individual tuffaceous horizons may contain the airfall deposits of one or two eruptions, or of multiple eruptions mixed together. The physical oceanography, slow sedimentation and extensive bioturbation in the region produced unfavourable conditions for preserving megascopic Pliocene-Pleistocene tephra.

2. Early Pliocene (late Opoitian) glass shards originated from the now-extinct Coromandel Volcanic Zone, whereas Pleistocene ash, including probable co-eruptive correlatives of the Whakamaru Ignimbrite (Mt Curl Tephra; c. 0.35 Ma) and Matahina Ignimbrite (Layer E; c. 0.27 Ma) originated from the Taupo Volcanic Zone.